

THE HALOGEN GROUP IN SUPRAMOLECULAR CHEMISTRY

**A Thesis
Submitted for the Degree of
Doctor of Philosophy**

By

BINOY KRISHNA SAHA



**School of Chemistry
University of Hyderabad
Hyderabad 500 046
India**

April 2006

I dedicate this thesis

To

ম্মাওবাবা

STATEMENT

I hereby declare that the matter embodied in this thesis entitled **“THE HALOGEN GROUP IN SUPRAMOLECULAR CHEMISTRY”** is the result of investigations carried out by me in the School of Chemistry, University of Hyderabad under the supervision of Prof. Ashwini Nangia.

In keeping with the general practice of reporting scientific observations due acknowledgements have been made wherever the work described is based on the findings of other investigators.

Hyderabad
April 2006

Binoy Krishna Saha

CERTIFICATE

Certified that the work **“THE HALOGEN GROUP IN SUPRAMOLECULAR CHEMISTRY”** has been carried out by **Binoy Krishna Saha** under my supervision and that the same has not been submitted elsewhere for a degree.

Dean
School of Chemistry

Prof. Ashwini Nangia
Thesis Supervisor

ACKNOWLEDGEMENT

With deep sense of gratitude and profound respect, I express my sincere thanks to my mentor, **Prof. Ashwini Nangia** for his inspiring guidance and constant encouragement throughout my Ph.D. He has been my source of inspiration. I have been able to learn a great deal from him and consider my association with him a rewarding experience.

I thank Prof. M. Periasamy, Dean, School of Chemistry and former Deans of the School for their co-operation in providing facilities in the School. I extend my sincere thanks to each and every faculty member of the School for help on various occasions.

I would like to thank Prof. M. Jaskólski, A. Mickiewicz University, Poland, Prof. R. Boese, Institut für Anorganische Chemie der Universität Essen, Germany and T. C. W. Mak, The Chinese University of Hong Kong, China, for their assistance with X-ray diffraction data on some of the compounds studied in this thesis.

I am thankful to all the teachers and lecturers who taught me throughout my career. My sincere thanks to Mr. Bhabesh Mondal, my first teacher who ignited my interest in science in the early stage.

I am grateful to CSIR, New Delhi for fellowship support. I thank DST for providing single crystal X-ray diffractometer facility and UPE programme of UGC for infrastructure facilities.

I thank all the non-teaching staff of the School of Chemistry, COSIST building and the Computer Centre for their assistance on various occasions. I thank Mr. Raghavaiah for his help with X-ray data collection.

I wish to thank my cooperative seniors Drs. V. R. Vangala, S. George, R. K. R. Jetti, S. S. Kuduva, R. Thaimattam, V. S. S. Kumar, P. Vishweshwar, P. K. Thallapally, V. R. Vangala and Mrs. Sairam and friendly labmates Archan, Srinivasulu, L. S. Reddy, Dinu, Rahul, Malla Reddy, Bala Krishna Reddy, S. Basavoju, Saikat, Prashant, Sreekanth, Jagadeesh, Sunil, Tejendar, Aparna, Pati, Sandip, Bipul, Ranjit, Nabakama and Sanjeeb for creating a cheerful working atmosphere in the lab. My stay on this campus has been pleasant with the association of all the research scholars at the School

of Chemistry, Sunirban, Abhijit, Abhik, Manab, Moloy, Subhas, Tamalda, Sandy, Bhaswati, Aniruddha, Shatabdi, Ullas, Prasun, Ghana, Ghata, Arindam, Tanmay, Tapta, Rumpa, Anindita, Rakesh, Anindita, Sreeparna, Gupta, Pavan, Venkatesh, Balaraman, Madhu.

I thank my M.Sc. classmates, Manoj, Doyel, Mukul, Chayan, Sujit and all others for their timely help and encouragement.

It would be too formal to thank my bosom friends and well wishers Dulal, Kuntal, Somnath, Rajuda, Samar kaku, Prasanna, Ashok kaku, Raju, Sambhu for their unreserved encouragement.

I thank my sisters, Bakul and Bubu for their support and encouragement. I thank my cousin brothers, nieces, nephews and all the children in my family for their smiles and wishes.

The blessings and best wishes of my parents keep me active throughout my life. They made me what I am and I owe everything to them. Dedicating this thesis to them is a minor recognition for their invaluable support and encouragement.

Binoy Krishna Saha

SYNOPSIS

This thesis entitled “**THE HALOGEN GROUP IN SUPRAMOLECULAR CHEMISTRY**” consists of eight chapters.

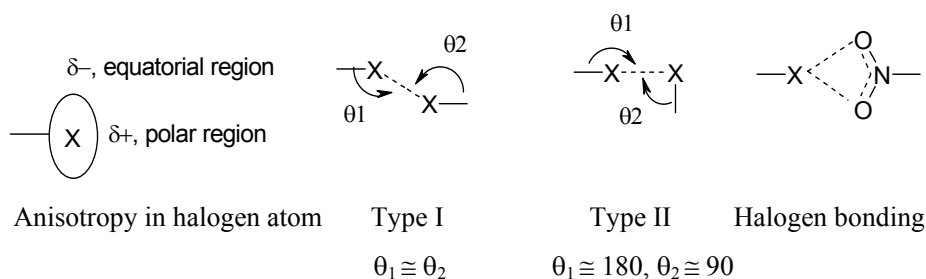
CHAPTER 1

INTRODUCTION

Crystal engineering is a subset of the grand supramolecular chemistry paradigm. It deals with “*the understanding of intermolecular interactions in the context of crystal packing and in the utilization of such understanding in the design of new solids with desired physical and chemical property.*” Supramolecular synthons, or small recurring structural units in crystals, and the identification of crystal structures as network, namely as nodes and node connectors, simplifies our understanding of complex crystal packing and assists in rational design. On the other hand polymorphism is one of the challenges in crystal engineering, and its proper analysis can give an insight into the complex crystallization process.

Halogen atoms have been used in crystal engineering for over two decades now. The gradual change in size and electronic property makes it a tailored functional group for designing organic solids. The heavier halogens are believed to be elliptical in shape (scheme 1). The polar C–X region is electro positive and the equatorial region is negatively polarized. Halogen···halogen interactions are of two types, type I ($\theta_1 \cong \theta_2$) and type II ($\theta_1 \cong 180^\circ$, $\theta_2 \cong 90^\circ$). The tendency to form type II interaction increases in the order $\text{Cl} < \text{Br} < \text{I}$. Type I geometry is generally a consequence of close packing whereas type II interaction is due to polarization induced electrophile-nucleophile pairing. Halogen bonding of donor halogens with acceptors containing lone pairs, e.g. N, O, P, S, Br^- , I^- is strong and directional, similar to traditional hydrogen bonds. In halogen bonding the lone pair is directed to the polar halogen region of partial electro positive character. The interaction becomes stronger as electron-withdrawing capacity of the halogen and electron-donating capacity around the lone pair group increases. Halogen

bonding has been used in clathrates, polymorphs, NLO materials, electronic devices and network structures. The halogen atom is important not only in crystal engineering and molecular devices but also in biological systems.

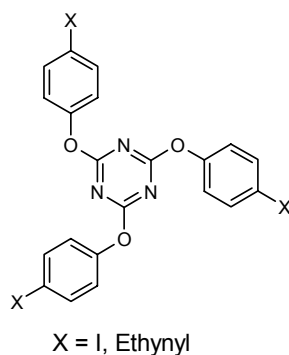


Scheme 1. Polar flattening of halogen atom, halogen...halogen interactions and halogen bonding.

CHAPTER 2

HALOGEN TRIMER-MEDIATED HEXAGONAL HOST FRAMEWORK AND ARCHITECTURAL ISOMERISM IN 2,4,6-TRIS(4-HALOPHENOXY)-1,3,5-TRIAZINE

Host-guest inclusion compounds form a significant contribution to the growing field of crystal engineering and supramolecular chemistry because they are important for both fundamental and utilitarian reasons. The strategy to design a host framework is such that the building block alone cannot pack efficiently. Proper shape, size and functional groups are needed for the discovery of a new host material. When halogen is used as sticky functional group, trigonal tecton 2,4,6-tris(4-halophenoxy)-1,3,5-triazine (4-XPOT) (scheme 2) self-assemble in hexagonal network via halogen trimer synthon which include guest molecules in its cavities. The corresponding methyl derivative adopts a close-packed structure with no voids, indicating the importance of directional halogen...halogen interaction in generating the open network structure.



Scheme 2. Compounds studied in this chapter

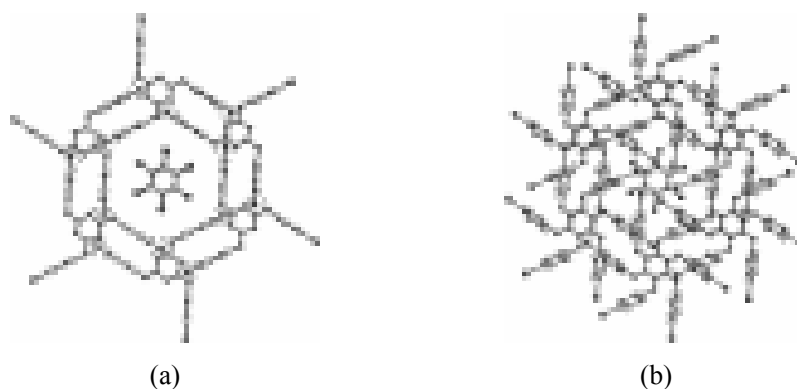


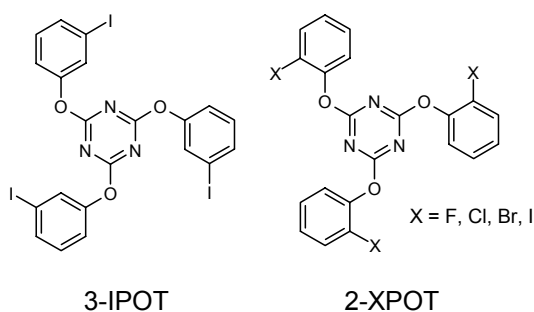
Figure 1. (a) Channel structure of 4-CIPOT•HCB. (b) Cage structure of 4-IPOT•HCB.

4-CIPOT and 4-BrPOT have been reported previously from our group. 4-CIPOT forms channel structure (Figure 1a) and 4-BrPOT forms both channel and cage structure, depending upon the guest molecule. The iodo (4-IPOT) derivative is discussed in my thesis. It self-assembles via the expected halogen trimer synthon of type II to generate open framework with cage type cavities (Figure 1b) for the inclusion of guest (e.g. CH_2Cl_2 , 1-methylnaphthalene, mesitylene, tribromomesitylene, hexachlorobenzene, etc). As the halogen size and polarizability increases ($\text{Cl} \rightarrow \text{Br} \rightarrow \text{I}$) the system undergoes architectural isomerism from channel to cage structure. This is explained through a number of intra and inter-layer halogen \cdots halogen, C–H \cdots halogen, C–H \cdots N and C–H \cdots O interactions. Variable temperature PXRD shows both host frameworks convert to the

same close packed structure after guest release. The ethynyl group ($\text{C}\equiv\text{C}-\text{H}$) behaves like halogen in organic supramolecular chemistry. Replacing halogens by ethynyl group (4-EPOT) gives similar result like 4-IPOT. When CCl_4 , a non-accommodateable guest in the cage, is used as solvent to crystallize 4-EPOT, it generates different host architecture. CSD search has been carried out to check the presence of cooperativity in ethynyl...ethynyl interaction via $\text{C}-\text{H}\cdots\pi$ interaction. Thermal analysis proves that the cage type clathrate is more stable than channel structure. A CSD search highlights the unique feature of this trigonal tecton family to carry-over trigonal symmetry from molecule to the solid state.

CHAPTER 3

Halophenoxytriazine, Halogen Exchange and Isostructurality



Scheme 3. Compounds studied in this chapter



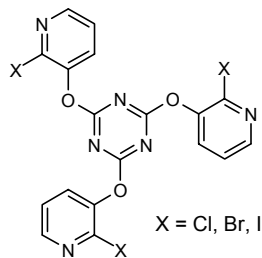
Figure 2. Piedfort Unit observed in 2-IPOT crystal structure. It is similar in all four 2-XPOT structures and 3-IPOT structure.

4-XPOT and 3-XPOT crystallize in high symmetry hexagonal system ($P6_3/m$, $R\bar{3}$, $R3c$, $P\bar{3}c1$). In both cases the structures are close-packed and the molecules stack in continuous Piedfort Unit (PU) to form columnar architecture. However 2-XPOT molecules (scheme 3) crystallize in triclinic system ($P\bar{1}$ space group). The bromo and iodo derivatives are isostructural and different from chloro and fluoro structures. All the structures contain PU dimer (Figure 2) of approximate C_{3i} symmetry. The halogen group at 2 position makes it difficult to stack these PUs further in columns. In 4-halophenoxytriazine series iodo and chloro derivatives crystallize in different framework and bromo derivative follows one of them depending upon guest molecule. In 3-halophenoxytriazine series the bromo derivative is similar to the chloro structure. However the 3-IPOT Structure is different from Cl and Br compounds. In 2-XPyOT series, 2-BrPyOT is isostructural to 2-IPyOT but chloro derivative is different. Thus halogen exchange does not guarantee isostructurality. CSD search has been performed to analyze the effect of halogen exchange on crystal packing.

CHAPTER 4

VAN DER WAALS GUEST INCLUSION HOST ASSEMBLE VIA WEAK HYDROGEN BONDS

With proper size and shape of tecton, interactions like van der Waals, C–H \cdots X (X=halogen, N, O) have been used to design inclusion compounds. Even though the interactions between host \cdots host and host \cdots guest are weak in nature, the systems are quite stable. 2,4,6-Tris(2-halo-3-pyridinoxy)-1,3,5-triazine (2-XPyOT) molecules form open framework via weak H bonds and the halogens mainly play space filling role.



Scheme 4. Compounds studied in this chapter.

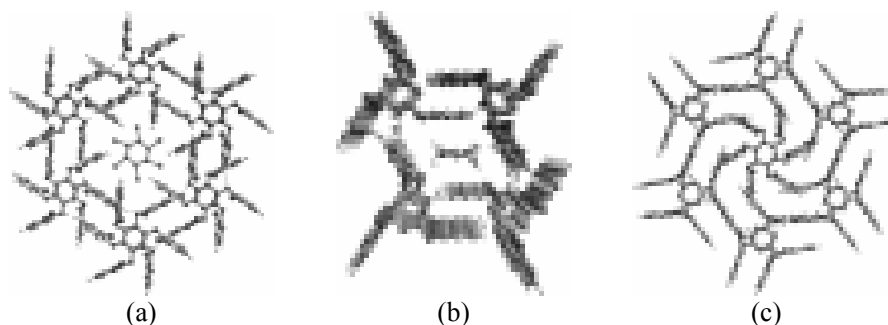


Figure 3. (a) Cage structure of 2-IPyOT•collidine. (b) Channel structure of 2-ClPyOT•ethylmethylketone (c) Guest free structure of 2-ClPyOT.

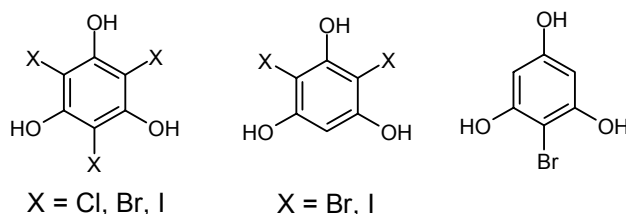
2,4,6-Tris(2-halophenoxy)-1,3,5-triazine (2-XPOT) molecules crystallize in triclinic crystal system. When 2-halophenoxy ring is replaced by 2-halo-3-pyridinoxy ring to explore C–H···N interaction parallel to aryl ring the closed packed structure converts to open framework. 2-BrPyOT and 2-IPyOT (Scheme 4) crystallize in hexagonal system ($R\bar{3}$) (Figure 3a) and isostructural to 4-IPOT. Interestingly 2-ClPyOT crystallizes in low symmetric triclinic system and forms channel (Figure 3b) to include linear guest (nitromethane, acetone, ethylmethylketone, ethylacetate, acetylacetone etc.) molecules. It shows partial zeolite like behavior and reversible guest uptake of solvent vapour. The diameter is suitable for inclusion of methane sized gas molecules. Gradual structural change with the amount of guest loss has been analyzed by PXRD. This molecule exists in two other guest free phases namely, hexagonal self-inclusion type and amorphous form. According to PXRD the apohost is different from these two phases. Thermal analyses have been performed to analyze the stability of the systems with respect to temperature.

CHAPTER 5

WATER CLUSTERS IN HALOGENATED PHLOROGLUCINOL HOST

Water is the most studied single natural chemical entity, yet its mystery has not been uncovered fully. In spite of the simple molecular structure it shows a lot of anomalous behavior like, high melting and boiling point, low density in solid phase, H

bonding, high dielectric constant etc. Entrapment of water into small molecular host systems to understand its nature in solid ice and liquid phase as well as structural and functional properties in biology has become a hot topic in supramolecular chemistry. Different halogenated phloroglucinol molecules (Scheme 5) have been crystallized to trap various motifs of water clusters in the organic host lattice. Interestingly here also inter halogen interaction influences the handedness of strong H bonded water helices.



Scheme 5. Compounds studied in this chapter



Figure 4. (a) Helical water chain trapped in TCPG and TBPG host lattices. (b) 1-D water boat hexamer tape trapped in DBPG host lattice.

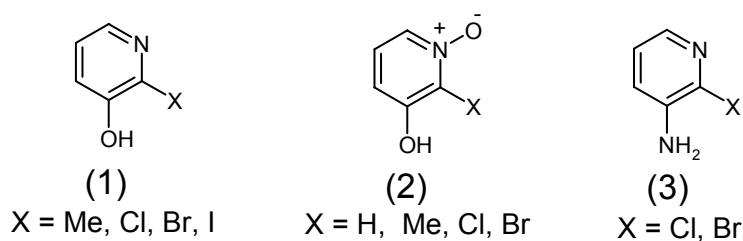
The idea of halogenating phloroglucinol was to alter the steric and electronic environment around the phenolic OH group so that they do not interact themselves efficiently but hydrogen bond to small guest (e.g. water, alcohol etc.) molecules. Trichlorophloroglucinol (TCPG), tribromophloroglucinol (TBPG) and dibromophloroglucinol (DBPG) include water in the lattice whereas triiodophloroglucinol (TIPG), diiodophloroglucinol (DIPG) and monobromophloroglucinol (MBPG) are obtained in anhydrous form. TCPG and TBPG trap helical chains of H bonded water molecules. The halogen...halogen (Cl...Cl vs

Br \cdots Br) interactions control the handedness of helices. DBPG includes ice (I_h) like 1-D water tape made of cyclic hexamer in high-energy boat conformation as well as in anhydrous form. The Br \cdots Br interactions are different in two structures, being type I in hydrated structure and type II in anhydrous form. Thermal and PXRD analyses show that TCPG behaves like an organic zeolite whereas TBPG and DBPG are not stable after complete guest loss.

CHAPTER 6

HALOGEN \cdots HALOGEN INTERACTION TO INDUCE SUPRAMOLECULAR NON-CENTROSYMMETRY

Controlling the frequency, phase, polarization and path of electromagnetic radiation has great technological importance in the area of tunable laser and optical data storage devices. Interest is growing in NLO active material for frequency doubling in SHG devices. Though it is possible to control the dipole moment and polarizability at the molecular level, a proper control over the crystal packing is still challenging. A necessary condition for SHG activity is that the material should crystallize in non-centrosymmetric space group. The only guaranteed method to direct non-centric crystallization is to use chiral compounds. Thus it is a challenge to crystal engineers to search for new materials or strategies to generate non-centrosymmetric materials from achiral molecules. Non-centrosymmetry induced in the bulk solid by directed inter-halogen interaction is presented herein.



Scheme 6. Compounds studied in this chapter



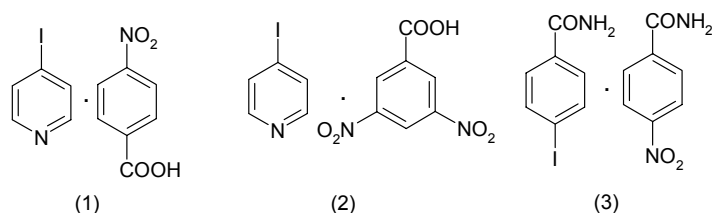
Figure 5. (a) Non-centrosymmetric structure of 1I guided by I...I interaction. (b) Centrosymmetric structure of 1Me.

Three series of systems have been examined here, 2-halo-3-pyridinol (1), 2-halo-3-pyridinol *N*-oxide (2) and 3-amino-2-halopyridine (3) (Scheme 6). The O–H...N, O–H...O or N–H...N strong hydrogen bond chains run antiparallel as expected. Significantly the ‘L’ or ‘V’ shape halogen...halogen interactions direct non-centrosymmetry in the crystal structure (Figure 5a). When halogen is replaced by isosteric methyl group the structures adopt inversion center (Figure 5b) retaining the strong H bonded chains antiparallel. There is no halogen...halogen interaction in 3-amino-2-chloropyridine and it crystallizes in a centrosymmetric space group.

CHAPTER 7

HALOGEN BONDING AND HYDROGEN BONDING IN CRYSTAL PACKING

Understanding the robust synthons and its proper combination can give various new desired solid materials with useful properties. Carboxylic acid and amide groups form O–H...O or N–H...O homosynthon and heterosynthon with pyridine and pyridine *N*-oxide groups. Similarly iodo...nitro is another robust synthon¹³ has been successfully used in crystal engineering. Halogen bonds can be stronger than conventional H bonds. We use here some combinations of H bonds and halogen bonds to control the 1-D and 2-D architectures of cocrystals.



Scheme 7. Compounds studied in this chapter



Figure 6. (a) 1-D tape made of heterosynthon acid...pyridine and iodo...nitro synthon in crystal structure of 1. (b) 2-D layer made of homosynthon amide...amide and heterosynthon iodo...nitro in crystal structure of 3.

Cocrystallization of 4-iodopyridine•4-nitrobenzoic acid, 4-iodopyridine•3,5-dinitrobenzoic acid and 4-iodobenzamide•4-nitrobenzamide are studied (Scheme 7). The iodo group is more specific towards nitro group to form short halogen bond and acid prefers pyridine to form strong heterosynthon in complex 1 (Figure 6a) and 2 to generate 1-D tape structure. The amide group form usual tape of homosynthon along with similar iodo...nitro halogen bond produce 2-D layer structure in complex 3 (Figure 6b).

CHAPTER 8

CONCLUSIONS AND FUTURE PROSPECTS

From the above studies the following conclusions and future implications can be drawn.

4-XPOT self-assemble via halogen trimer synthon to produce hexagonal network in 2-D and the difference in size as well as electronegativity of the halogen may be utilized to control the third direction. Placing halogen at meta position of 4-halophenoxy ring in 4-XPOT will be interesting to see whether it can modify the cavity or produce guest free structure with similar packing.

In halophenoxytriazine the *o*-hydrogens are important for making PU dimer. These PU stack infinitely and forms cylindrical molecular rod, which could be the reason for high symmetry crystal packing. Interruption of PU stack results in low symmetry crystal structure. Halogen exchange does not guarantee isostructurality but the probability that bromo derivative follows either chloro or iodo structure is very high.

In 2-XPOT the host molecules self-assemble via weak H-bonds. Halogens mainly play space-filling role. Larger halogen causes transformation in the structure from channel to cage open framework. Thermal analysis shows the stability of the clathrates and the importance of weak interactions. Replacing pyridyl group by pyridine *N*-oxide may produce another interesting host framework.

Halogen in proper place with respect to hydrophilic group can be used to trap water of various topologies and exchange can change the geometry of water cluster as it is observed in halophloroglucinol. A mix-halogenated phloroglucinol is expected to be an interesting system to modify the aqua pores.

Weak inter halogen interaction is responsible for non-centrosymmetry in the crystalline architecture even as the strong H bonds run antiparallel. In the absence of inter halogen interactions the structure adopts centrosymmetric packing. Thus halogen...halogen interaction can be used to produce SHG materials. A conjugated spacer between halogen and aryl group may increase the SHG activity in 2-halo-3-pyridinol and related systems.

Halogen bonding can be used along with H bonding to produce new molecular solids and architectures. Proper selection of the groups forming halogen bond and H bond will generally not interfere with each other and so crystal packing can be controlled in different regions of the structure. A similar strategy can be used to prepare higher order, like ternary cocrystal when proper selection of halogen bonding functional groups with hydrogen bonding functional groups at suitable places of the molecules are used.

Size, polarizability and electronegativity are important for the halogen group. The gradual change in both the properties and ease in synthesis has made halogens an

interesting group for structural control in supramolecular chemistry of organic and metal-organic systems.

Salient crystallographic details of the crystal structures discussed in this thesis have been given in an appendix at the end of the thesis. A full list of atomic coordinates has been deposited with the University of Hyderabad and is available upon request from Prof. Ashwini Nangia (ashwini_nangia@rediffmail.com).

CONTENTS

Statement	v
Certificate	vii
Acknowledgement	ix
Synopsis	xi
 CHAPTER ONE	 1–20
INTRODUCTION	
1.1 Crystal engineering	1
1.2 Intermolecular interactions and supramolecular synthons	3
1.3 Interactions involving halogens	4
1.3.1 Inter-halogen interactions	5
1.3.2 Halogen bonding	7
1.3.3 Halogens in hydrogen bonding	8
1.4 Host-guest compounds	9
1.5 NLO materials	11
1.6 Polymorphism	13
1.7 Hydrates	14
1.8 Theme of the present work	14
1.9 References	15
 CHAPTER TWO	 21–65
HALOGEN TRIMER-MEDIATED HEXAGONAL HOST FRAMEWORK AND ARCHITECTURAL ISOMERISM IN 2,4,6-TRIS(4-HALOPHENOXY)-1,3,5-TRIAZINE	
2.1 Introduction	21
2.2 Results and discussion	26
2.2.1 4-IPOT•guest crystal structures	28

2.2.2	Ethynyl group: A supramolecular pseudo halogen	32
2.2.3	4-EPOT•guest crystal structures	34
2.2.3.1	Cage-I structure	35
2.2.3.2	Cage-II structure	38
2.2.4	IR measurements	39
2.2.5	Cooperativity in C–H $\cdots\pi$ interaction	41
2.2.6	Computational study	44
2.2.7	Halogen and guest mediated architectural isomerism	45
2.2.8	Hexagonal crystal system	49
2.2.9	Thermal analysis	52
2.3	Conclusions	56
2.4	Experimental section	58
2.5	References	60
CHAPTER THREE		67–86
HALOPHENOXYTRIAZINE, HALOGEN EXCHANGE AND ISOSTRUCTURALITY		
3.1	Introduction	67
3.2	Crystal structures of 4-XPOT	71
3.3	Crystal structures of 3-XPOT	71
3.4	Crystal structures of 2-XPOT	73
3.4.1	2D isostructural 2-FPOT and 2-CIPOT	74
3.4.2	Isostructural 2-BrPOT and 2-IPOT	76
3.5	Conformation of phenoxytriazine	77
3.6	CSD search	78
3.7	Conclusions	82
3.8	Experimental Section	84
3.9	References	85

CHAPTER FOUR 87–112

VAN DER WAALS GUEST INCLUSION HOST ASSEMBLE VIA WEAK HYDROGEN BONDS

4.1	Introduction	87
4.2	Channel structure	91
4.3	Self host–guest structure	94
4.4	High Z' and examples of self-inclusion systems	95
4.5	Guest exchange and PXRD experiments	97
4.6	Cage structure	98
4.7	Isostructurality between $1X \cdot \text{guest}$ and $3X \cdot \text{guest}$	102
4.8	Thermal Analysis	104
4.9	Conclusions	107
4.10	Experimental	107
4.11	References	109

CHAPTER FIVE 113–140

WATER CLUSTERS IN HALOGENATED PHLOROGLUCINOL HOST

5.1	Introduction	113
5.2	Results and Discussion	117
5.2.1	TCPG•3H ₂ O and TBPG•3H ₂ O	118
5.2.2	DBPG•4H ₂ O and DBPG (anhydrous)	122
5.2.3	TIPG	126
5.2.4	DIPG	127
5.2.5	BPG	127
5.2.6	Thermal Analysis	130
5.2.7	PXRD and IR Analysis	131
5.3	Conclusions	133
5.4	Experimental	135

5.5	References	137
-----	------------	-----

CHAPTER SIX	141–161
-------------	---------

HALOGEN...HALOGEN INTERACTION TO INDUCE SUPRAMOLECULAR NON-CENTROSYMMETRY

6.1	Introduction	141
6.2.	Crystal Structures of 1X	145
6.2.1	3-Hydroxypyridine	145
6.2.2	2-Chloro-3-hydroxypyridine, 1Cl	146
6.2.3	2-Bromo-3-hydroxypyridine, 1Br and 2-Iodo-3-hydroxypyridine, 1I	147
6.2.4	2-Methyl-3-hydroxypyridine, 1Me	148
6.3	Crystal Structures of 2X	149
6.3.1	3-hydroxypyridine <i>N</i> -oxide, 2H	149
6.3.2	2-Chloro-3-hydroxypyridine <i>N</i> -oxide, 2Cl	150
6.3.3	2-Bromo-3-hydroxypyridine <i>N</i> -oxide, 2Br	150
6.3.4	2-Methyl-3-hydroxypyridine <i>N</i> -oxide, 2Me	151
6.4	Crystal structures of 3X	152
6.4.1	2-Chloro-3-aminopyridine, 3Cl	152
6.4.2	2-Bromo-3-aminopyridine, 3Br	153
6.5	Discussion	154
6.6	Dipole Moment Comparison	156
6.7	Conclusions	157
6.8	Experimental Section	158
6.9	References	159

CHAPTER SEVEN	163–175
---------------	---------

HALOGEN BONDING AND HYDROGEN BONDING IN CRYSTAL PACKING

7.1	Introduction	163
7.2	Results and Discussions	166
7.2.1	4-Nitrobenzoic Acid•4-Iodopyridine, 1	166
7.2.2	3,5-Dinitrobenzoic Acid•4-Iodopyridine, 2	167
7.2.3	4-Nitrobenzamide•4-Iodobenzamide, 3	168
7.3	Conclusions	172
7.4	Experimental Section	172
7.5	References	173

CHAPTER EIGHT 177–184**CONCLUSIONS AND FUTURE PROSPECTS**

8.1	Halogen is a Sticky Group	177
8.2	Halogen Exchange and Isostructurality	179
8.3	Weak Interactions are Important in Crystal Packing	181
8.4	Halogen and Hydration	182

APPENDIX 185–203

Salient crystallographic details	185
About the Author	201
List of Publications	203

CHAPTER 1

INTRODUCTION

1.1 Crystal engineering

Molecules are a collection of atoms connected by strong covalent bonds (50–120 kcal/mol) that result from partial overlap between atomic orbitals. For more than a century organic chemists have been studying chemical reactions in a systematic way, leading ultimately to the development of a wealth of synthetic methods. In chemical reactions, different molecules react with one another by the stepwise breaking and making of covalent bonds. Protection–deprotection protocol is widely used in the sequential process of molecular synthesis, especially in the field of polypeptide synthesis. This renders the total synthesis of very complex molecules with molecular weights < 1000 Da, such as taxol, epothilone, palytoxin, calichearubicins and brevetoxin, a herculean exercise.^{1–5} But the chemistry of the covalent bond has its own conceptual limits. The synthesis of molecular structures with molecular weight > 1000 Da through the traditional covalent bond stepwise methods poses a difficult challenge. The field of covalent synthesis has perhaps reached the limit of what is synthetically achievable in terms of time requirements and yields. Therefore, chemists were in search for novel concepts and new approaches for efficient methods of generating extended structures of various dimensions. The consequence is the birth of a new field namely, ‘*Supramolecular Chemistry*’⁶ which has emerged as a new discipline that deals with complex super structures. This branch of chemistry, also referred as "Non-covalent synthesis or synthetic supramolecular chemistry" includes the self-assembly of supermolecules using non-covalent interactions.

Supermolecules are synthesized through the self-assembly of a large number of intermolecular interactions in a single step whereas covalent synthesis of complex molecules requires many sequential steps. According to Lehn's analogy^{6a} "*supramolecules are to molecules and the intermolecular bond what molecules are to*

atoms and the covalent bond". Molecular recognition relies upon complementary of size, shape, and the chemical functionalities. Lehn's definition of supramolecular chemistry is "*chemistry beyond the molecule*", while Dunitz has explained a crystal as "*a supermolecule par excellence*".⁷ The ultimate aim of supramolecular chemistry is to become the "science of informed matter". Some of the important discoveries in this field are mentioned in table 1.⁸

Table 1.

1811	Sir Humphrey Davy prepared chlorine hydrate.
1823	Michael Faraday confirmed Davy's observation and determined the composition of chlorine hydrate.
1849	F. Wohler prepared a β -qionol•H ₂ S molecular complex.
1947	D. E. Palin and H. M. Powell published the crystal structures of β -qionol•H ₂ S compound.
1948	H. M. Powell introduced the term "clathrate."
1967	C. J. Pedersen prepares crown ethers.
1969	J. -M. Lehn and coworkers synthesized cryptands.
1974	D. J. Cram and J. M. Cram introduced the terms "host," "guest," and "host-guest complexation."
1987	The Noble prize for Chemistry was awarded to D. J. Cram, J.-M. Lehn, and C. J. Pedersen for their contribution to the field of supramolecular chemistry.

Crystal engineering was evolved to understand and control supramolecular organization in the solid state. The term "*Crystal engineering*" was introduced by Pepinsky⁹ in 1955 but conceptualized and elaborated by Schmidt during the period 1950–1971 in the context of organic solid-state photochemical reactions of cinnamic acids and amides.¹⁰ A broad and more meaningful definition of crystal engineering was provided by Desiraju in 1989 as "*the understanding of intermolecular interactions in the context of crystal packing and in the utilization of such understanding in the design of new solids with desired physical and chemical properties*".¹¹ The realization that a

crystal is one of the best examples of a supermolecule, with atoms and covalent bonds being replaced by molecules and intermolecular interactions, led to the recognition of crystal engineering as a supramolecular equivalent of organic synthesis.¹² Therefore crystal engineering has become an integral part of supramolecular chemistry, the chemistry of 21st century.

1.2 Intermolecular interactions and Supramolecular Synthons

It is well known that attractive forces between molecules are responsible for many interesting phenomena in chemical and biological sciences. The physical state of a compound i.e. solid, liquid or gas depends upon the strength of intermolecular forces. Crystal structure of a compound is the result of balance between attractive forces and repulsive contacts between the molecules. Intermolecular forces can be divided into two categories—isotropic or non-directional and anisotropic or directional.¹¹ Long range dispersion forces and short range repulsive forces are isotropic. On the other hand hydrogen bond, charge transfer interactions are considered as directional in nature. These interactions vary with r^{-n} , where r is the distance between relevant non-bonded atoms and n is a positive integer. The attractive forces vary from r^{-1} to r^{-6} depending upon the interaction type and short range exchange repulsion varies with r^{-12} . Dispersion forces and exchange repulsions together constitute the universal van der Waals glue.

Table 2. Some properties of very strong, strong and weak H-bonds.

Properties	Very strong	Strong	Weak
Bond energy (-kcal/mol)	15–40	4–15	<4
Examples	[F...H...F] ⁻ [N...H...N] ⁺ P-OH...O=P	O-H...O=C O-H...O=C O-H...O-H	C-H...O O-H... π Os-H...O
Red shift in IR	>25%	5–25%	<5%
$D(X\cdots A)$ (Å)	2.2–2.5	2.5–3.2	3.0–4.0
$D(H\cdots A)$ (Å)	1.2–1.5	1.5–2.2	2.0–3.0
$\theta(X-H\cdots A)$ (°)	175–180	130–180	90–180

Covalency	Pronounced	Weak	Vanishing
Electrostatic	Significant	Dominant	Moderate

Among these interactions H-bonds or similar directional interactions are very important in crystal packing. It is likely that H-bonded aggregates can exist in solution state and hence can direct the arrangement of molecules in crystal nucleation and the final solid-state structure. Short range forces perhaps come into play in the late stage of crystallization. H-bonds vary in their strengths depending upon the donor and acceptor capabilities of the concerned atoms in D–H···A interaction. Some of the properties of strong and weak H-bonds are listed in table 2.¹³ From crystal engineering point of view the strong, directional forces are more helpful to design target crystal structures. These interaction motifs are termed as supramolecular synthons because crystallization can be considered as supramolecular reaction. The term synthon was first introduced by Corey in 1967 to represent key structural features in a target molecule organic synthesis.¹⁴ In supramolecular chemistry this term is used as supramolecular synthon and Desiraju defined it as “*supramolecular synthons are structural units within supermolecules which can be formed and/or assembled by known or conceivable synthetic operations involving intermolecular interactions.*”¹⁵ Some of the well known homosynthons are COOH···COOH, CONH₂···CONH₂, OH···OH, NH₂···NH₂, halogen···halogen, etc. which are between similar functional groups and heterosynthons i.e. between different functional groups, are COOH···pyridine, CONH₂···pyridine, COOH···CONH₂, OH···NH₂, CONH₂···N-oxide, halogen bonds, etc.

1.3 Interactions Involving Halogens

Kitaigorodskii proposed the close-packing model to explain organic crystal packing where he considered that the volume of a molecule in a crystal is defined by a system of intersecting spheres. Each sphere represents an atom with van der Waals radius equal to the sphere radius. According to his close-packing model the contacts between two adjacent molecules are tangential on spherical surfaces of the atoms. In course of time it has been realized that there are many exceptions to this over simplified

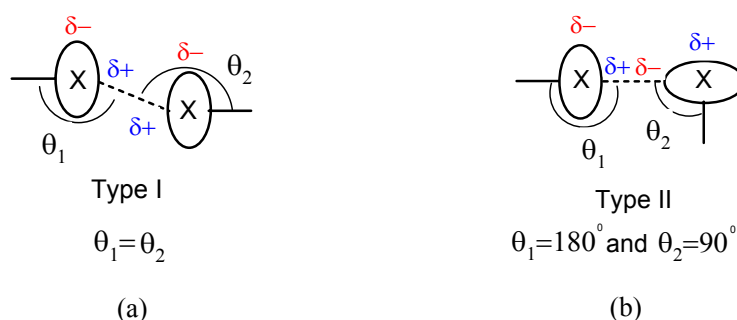
rule. Crystallographers recognized the chemical factors associated with atoms or group of atoms, which are capable of controlling the crystal structures. In short, a crystal structure is a subtle balance between geometrical and chemical factors.

There has been a lot of debate about the nature of the halogens and the interactions made by this group of atoms. Halogens are involved in halogen bonding¹⁶ ($D\cdots X-Y$) with weak to very strong interaction energy where halogen (X) is electron acceptor (Lewis acid, halogen bond donor) and the other atom (D) donates electrons (Lewis base, halogen bond acceptor). Recently inter-halogen interactions also are included in this category. Halogens also can make very weak hydrogen bonds.

1.3.1 Inter-halogen Interactions

Halogens can make short contact with respect to their spherical van der Waals radii sum, as it has been seen in several crystal structures. The Cl_2 , Br_2 and I_2 molecules make side on contact in their orthorhombic crystal structures (*Cmca*).¹¹ Sakurai et al. noticed that there are some directional preferences in $Cl\cdots Cl$ contacts while studying 2,5-dichloroaniline crystal structures.¹⁷ According to spherical atomic shape there is considerable overlap between the atoms but spherical atom-atom potential is inadequate to explain many of the features shown by halogens. It was Bondi, who observed that the effective shapes of some atoms might not be truly spherical but rather ellipsoid or 'pear-shaped' especially for heavier elements.¹⁸ Nyburg and Faerman showed the atomic radii of the non-spherical halogen atoms along C-X bond vector are shorter than the distance perpendicular to it.¹⁹ The polar flattening of the organic chlorine atoms has led to considerable speculation whether the short contacts in certain directions are due to orientation dependent specific attractive force or anisotropy in the short range repulsive potential. Halogen \cdots halogen contacts have two preferred geometries, type I ($\theta_1 \cong \theta_2$) and type II ($\theta_1 \cong 180^\circ$ and ($\theta_2 \cong 90^\circ$) shown in scheme 1. Desiraju and Parthasarathy emphasized on specific attractive forces between halogens based on gas phase result of 'L' shaped geometry taken by X_2 and statistical analysis on halogenated hydrocarbons considering the halogen \cdots halogen contact area with respect to total area.²⁰ On the other hand Price et al. discarded the chance of any specific contacts between organic chlorine

atoms. They explained the directional contacts based on anisotropic electrostatic forces and anisotropic exchange repulsion without any significant contribution from charge transfer. They showed by theoretical calculation that $\text{Cl}\cdots\text{Cl}$ interactions are quite normal, with the repulsion, dispersion and electrostatic contributions being the most important, but the non-sphericity of the chlorine charge distribution has a significant effect on these contributions.²¹



Scheme 1. (a) Type I geometry of halogen \cdots halogen interaction. (b) Type II geometry of halogen \cdots halogen interaction.

It is believed that the halogens are polarized positively in polar region and negatively in equatorial region (Scheme 1). The size and polarization increases in the order $\text{Cl} < \text{Br} < \text{I}$, where as electronegativity change is in the reverse direction. Thus in the cases of unsymmetrical inter halogen interactions the negative equatorial part of the lighter-halogen approaches to the positive axial region of heavier halogen.²² Anionic halides also show strong preference to interact with the polar region of organic halogens.²³ Brammer *et al.* showed that the role of inorganic halogens ($\text{M}-\text{Cl}$) and organic halogens ($\text{C}-\text{X}$) are distinct and different. The $\text{C}-\text{X}\cdots\text{Cl}$ angle is markedly linear and $\text{M}-\text{Cl}\cdots\text{X}$ angle is markedly angular ($120\text{--}130^\circ$) in $\text{C}-\text{X}\cdots\text{Cl}-\text{M}$ interaction, because inorganic halogens are more negatively charged.²⁴ F behaves quite differently than other three halogens due to its hardness, small size and very high electronegativity. Thus various researches described the short inter halogen contacts as a result of close packing due to elliptical shape of the halogen atoms or electrophile \cdots nucleophile interaction type

due to polarization. It appears that inter-halogen type I is van der Waals interaction and type II is polarization induced.²⁵

1.3.2 Halogen Bonding

The term “halogen bonding” was introduced by Dumas et al. for describing the attractive donor–acceptor interactions that involve halogen atoms functioning as Lewis acids and another atom containing lone pair of electrons functioning as Lewis base (Figure 1).²⁶ Prout and Kamenar described the resulting complexes as $n \rightarrow \sigma^*$ type.²⁷ In halogen bond with $D \cdots X-Y$ geometry the angle around X (halogen) tends to be linear. Hassel first demonstrated halogen bonding as a powerful tool in driving the self-assembly of chains of alternating donor and acceptor modules.²⁸ The halogen atoms that are involved in halogen bonding can be bound to other halogen or to carbon or to nitrogen atoms and the electron pair donor can be neutral or anionic (N, O, S, Se, I^- , Br^- , Cl^- , F^- , etc.). The interaction energy of halogen bonding spans over a very wide range, from 10 to 200 kJ/mol.²⁹ Theoretical and experimental data prove that all four halogens can act as halogen bond donor and the bond strength order is $F < Cl < Br < I$ (Scheme 1). Though F_2 is a strong donor but organic F hardly participate in halogen bond as donor.³⁰ The donating capacity also depends on the remaining molecular part containing the halogen atom. For a particular halogen the order of donor strength is observed as $X-X > X-C(sp) > X-C(sp^2) > X-C(sp^3)$. With increase in electron donating capacity of the halogen bond acceptor the interaction becomes stronger. The halogen bond accepting strength of halide ions increases as $F^- < Cl^- < Br^- < I^-$ and nitrogen is better acceptor than oxygen and sulfur.³¹ The relative effectiveness of oxygen and sulfur depends on the donor nature and follows HSAB theory. Taking the advantage of high electronegativity of F Resnati and co-workers engineered several desired crystal structures using haloperfluoroalkanes as strong donor in halogen bonding. They showed controlled photochemical reaction in the crystal structure mediated via halogen bonding and $\pi \cdots \pi$ stacking³² and preference of halogen bonding over strong H-bonding in a series of competition experiments where the donor compounds were diiodoperfluorocarbon.³³ Halogen bonding can play a crucial role in some biological systems. Short $I \cdots O$

interactions play important roles in the recognition of some hormones by their cognate proteins. A very large number of short $I\cdots O$ contacts from thyroxine and thyroxine derivatives to their associated proteins were identified.³⁴ Thus halogen bonding is another route other than robust H-bonding synthons through which crystal engineering can be studied.

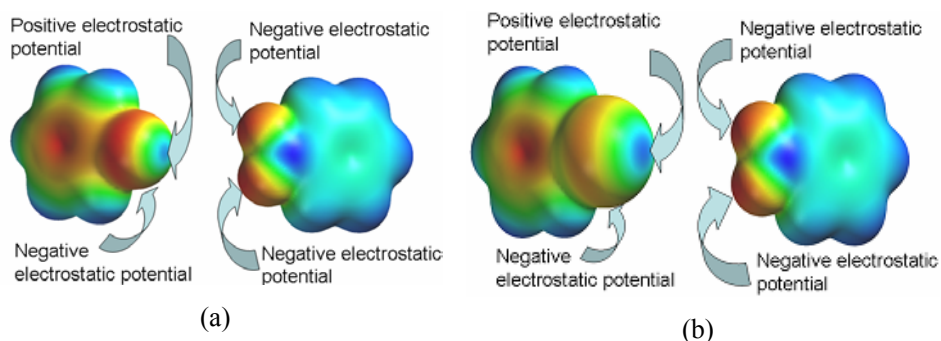


Figure 1. Electrostatic surface potential (ESP) calculated in Spartan (AM1). (a) The electronegative surface (red) of Cl atom is available to hydrogen bond donor groups in the weaker $Cl\cdots O_2N$ interaction. (b) The electrostatic origin of $I\cdots O_2N$ interaction is evident in the blue (dark) lobe pointing towards the oxygen atoms, $I^{\delta+}\cdots O^{\delta-}$.

1.3.3 Halogens in Hydrogen Bonding

Organic halogens can participate in hydrogen bond but energetically very weak because of the weakness in acceptor property. Especially C–F is most surprising because F poses high electronegativity and yet weak accepting capacity. It is interesting that strong donors/acceptors O and N are also electronegative atoms and in H-bonding electronegativity of donor and acceptors play an active role. So it was thought that organic F also should be capable of making strong H-bonds. Dunitz and Taylor concluded after CSD and protein data base study along with theoretical energy calculations that organic fluorine hardly ever accepts hydrogen bonds. They reasoned the less contribution from polarizability, charge transfer, dispersion interactions and inability to withdraw electron density via resonance made the hard, monovalent fluorine a weak acceptor.³⁵ Desiraju, Nangia and co-workers³⁶ as well as Guru Row *et al.*³⁷ independently concluded after studying some fluorinated aromatics that in the absence of other

competing acceptor organic fluorine also can accept H-bonds, but they agreed about the weakness of the interactions. The H-bonding capability is not very different for other three halogens Cl, Br and I. Though the organic halogens are weak acceptors but the metal bound halogens and halide ions are strong H-bond acceptors and the order of acceptor strength is $X^- > M-X > C-X$.¹³

Several researchers have used halogens as design element in host–guest compounds, NLO materials, polymorphism, photo chemical reactions etc.

1.4 Host–guest Compounds

The concept of supramolecular chemistry originated from host–guest compounds which dates back to 1811 when Davy discovered chlorine hydrate by bubbling chlorine into cool water.³⁸ But the field flourished two decades ago with host–guest compounds in which the metal ions are trapped into the cavity of crown ethers and the discovery of urea inclusion complexes. The rational construction of novel open-framework organic solids has received particular interest because of their diverse applications such as chemical separation, reactions and catalysis in a microcavity, and for electrooptic, nonlinear and magnetic materials.³⁹ Two broad approaches are being pursued in this direction. Metal–ligand coordination bonding is extensively used in the modular assembly of extended porous solids and low density frameworks⁴⁰ and hydrogen bond or other weak interactions mediated self-assembly is another contemporary topic.

These compounds are divided into two major categories based on the nature of the host. Cavitands, or molecular host compounds with intra-molecular cavities; the cavity is an intrinsic property of the molecule and exists in solution and in the solid state. Clathrands are hosts with extra-molecular cavities that result from the aggregation of more than one molecule; lattice inclusion hosts exists only in the solid state. The corresponding inclusion adducts are referred to as cavitates and clathrates.^{39a} Based on the size of porosity, open frameworks are divided into three categories, such as nanoporous or microporous (<15 Å), mesoporous (15–500 Å) and macroporous (>500 Å) materials.⁴¹ The guest cavities surrounded by host molecules can be zero dimensional (cage), one dimensional (channel) or two dimensional (layered).⁴²

Various methods have been developed to design microporous solids. The design of porous solids is based on crystal engineering strategies, molecular symmetry carry-over through rigid directional forces, hydrogen bonds or metal coordination bonds such that open porous networks may result. One of the main challenges in these approaches is to prevent interpenetration to obtain open frameworks. Weber proposed some rules for designing host framework after studying several aromatic molecules. A typical host molecule should have some of these characteristics: (1) bulky and awkward shape; (2) rigid framework which can survive upon guest loss; (3) high affinity functional groups for strong and directional synthon and (4) an overall balanced shape to achieve close-packing in the host-guest crystal.^{39a,43} Desiraju has suggested that crystal engineering principles can be used to construct host architectures by considering molecular and crystal symmetry, synthon and solvation phenomena.¹⁵ Wheel-and-axle or dumb-bell shaped molecules are a typical example of open frameworks, where mismatched size of wheel (rigid, bulky) and axle (long, linear) groups prevent interpenetration or close-packing, resulting small guest inclusion in the voids.⁴⁴ Bishop *et al.* showed a series of halogenated 'V' shaped diquinoline derivatives which are potentially capable of forming inclusion adducts.⁴⁵ The non-halogenated parent compound (1H) close-packed without inclusion of guest molecules, but the dibromo compound (1Br) is unable to pack efficiently. So 1Br forms square molecular pens which include guest molecules where the host molecules assemble via inter halogen interaction and other weak H-bonds (Figure 2).

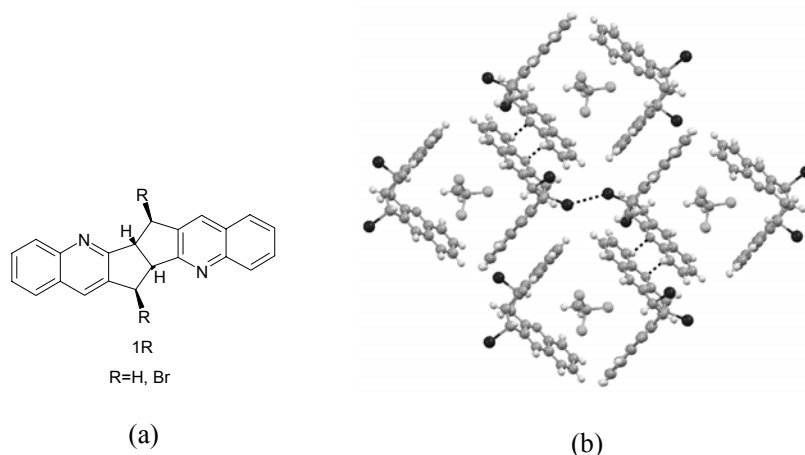


Figure 2. (a) Diquinoline derivative. (b) Molecular pen of dibrominated host (R=Br) include trichloroethane guest molecules.

1.5 NLO Materials

NLO (non linear optics) property of a material originates when the molecule is subjected to very intense fields, as in laser light, the material become so polarized that its polarizability can change and hence the induced polarization is a nonlinear function of the field strength. Currently a great deal of effort is being devoted in NLO research of both organic and inorganic compounds, specially second harmonic generation (SHG), which causes a doubling in frequency of incident beam. Interest in this subject stems from the potential utility of NLO active materials in the development of high intensity laser, optical memory and switching devices and telecommunication industry. Two fundamental requirements for SHG activity in a solid are bulk non-centrosymmetry and molecular polarizability.⁴⁶ The second requirement can be easily achieved by choosing appropriate push-pull system in the molecular level, but the first condition deals in supramolecular level and difficult to control. Furthermore with increase in molecular dipole moment the tendency to crystallize in centric alignment increases. According to the Cambridge Structural Database only 10–15% of the achiral compounds crystallize in non-centrosymmetric space group.⁴⁷ Though non-centrosymmetry can be generated by choosing chiral compound, it does not guarantee an optimum alignment of the molecules

which is another important condition for effective SHG activity.

There are several strategies have been tried to overcome these problems. Diamondoid networks,⁴⁸ strong H-bonded ionic building blocks,⁴⁹ octupolar molecules⁵⁰ and pyridine *N*-oxide (POM)⁵¹ to avoid antiparallel alignment of molecules due to dipole moment effect have been used to design NLO materials. Halogens also played an important role in this field. Zhao et al. showed that bromo group can be used effectively in improving the properties of organic optical materials. It is highly polarizable and less electronegative to be able to donate electrons, which minimizes ground state dipole moment of the molecule. It also can improve the transparency and melting point of the materials.⁵² Hulliger and co-workers showed that *p*-BrC₆F₄CN and *p*-IC₆F₄CN crystallize in non-centrosymmetric space group (*Pna*2₁)⁵³ where the molecular chains via halogen bonding (CN...X) run parallel in a plane and there is no inter-chain contact within van der Waals radii range. 4-iodo-4'-nitrobiphenyl self-assemble into parallel-oriented ribbons mediated by NO₂...I halogen bonds.⁵⁴ In this crystal structure overall non-centrosymmetry arises due to the combination of helical shape of the molecules for twisting of phenyl rings and the polar alignment of chains. Tetrahedral molecule 4,4'-diiodo-4'',4'''-dinitrotetraphenylmethane forms diamondoid network via NO₂...I halogen bonds in non-centrosymmetric spacegroup (*Fdd*2).⁵⁵ 2,4-dibromo-1,3,5-trinitrobenzene crystallize in *C*₂ space group. It forms pseudo hexagonal planar structure mediated via NO₂...Br halogen bonds and perfect polar alignment of NO₂...H-C hydrogen bonds, which makes the bulk SHG very high (Figure 3).⁵⁶

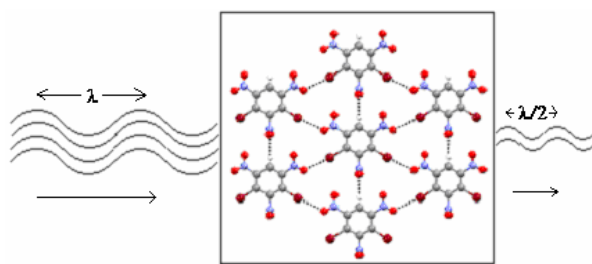


Figure 3. Polar alignment of 2,4-dibromo-1,3,5-trinitrobenzene in hexagonal layer. Schematic representation shows that the resultant beam is with double frequency (half wave length) of incident beam. SHG appears equal to POM.⁵⁶

1.6 Polymorphism

Polymorphism is the ability of a chemical entity to exist in more than one distinct crystalline form as a result of differences in the packing arrangement and/or molecular conformation.⁵⁷ Mitscherlich recognized the phenomenon of polymorphism in 1822.⁵⁸ In principle a molecule can have several local minima in different arrangements of close energies in crystallization process which is believed a kinetic phenomena.⁵⁹ As a result polymorphism can occurs for different substances and at different conditions or even in same condition (concomitant polymorphism). The existence of polymorphism implies that free energy differences between different crystalline forms are small (<10 kJ/mol).⁶⁰ McCrone statement “*the number of forms known for a given compound is proportional to the time and money spent in research on that compound*” is quite important in this issue.⁶¹ A survey of CSD showed that only 5% of compounds are classified as polymorphic.⁶² Polymorphic forms of a substance can have different chemical and physical properties, including melting point, chemical reactivity, solubility, dissolution rate, optical and mechanical properties, vapor pressure, and density.⁶³ These properties can have a direct effect on the ability to process and/or manufacture the drug substance and the drug product, as well as on stability, dissolution, and bioavailability which make polymorphism is so important in drug industries.

There are some reports where halogens have participated in active role on polymorphic transformations. Bhadbhade et al. showed single crystal to single crystal transformation in a dimorphic system of tri-*O*-[*p*-halobenzoyl]-*myo*-inositol-1,3,5-orthoformate compound where halogen bonding play a crucial role in the transition process ($\text{C}-\text{Br}\cdots\text{O}-\text{C}$ to $\text{C}-\text{Br}\cdots\text{O}=\text{C}$).⁶⁴ Desiraju et al. recently demonstrated isostructurality, polymorphism and mechanical properties of some hexahalogenated benzenes. They explained the polymorphism of 1,3,5-tribromo-2,4,6-triiodobenzene based on the size difference between the halogens after analyzing the other hexahalogenated benzene crystal structures.²⁵ Polymorphism is a major hurdle in crystal engineering and is a not fully understood phenomenon at the fundamental level. A better understanding of this phenomenon will certainly improve crystal engineering design strategies.

1.7 Hydrates

Hydration of molecules in the crystal structure is an important phenomena, specially in pharmaceutical industry. Because the anhydrous and hydrated crystals have different physical and chemical properties. Hydrated forms of pharmaceutical solids are also more common than solvates because of the presence of large number of functional groups, abundance of water in the atmosphere, flexibility of water molecules due to small size and ability to act as both a hydrogen bond donor and acceptor.⁶⁵ The study of different water clusters is also important to understand the bulk properties of water and its role in different biological processes, such as protein–DNA binding, ion transport, protein folding–defolding, structure determination of the fibrous proteins, etc. Due to the difficulties in studying the role of water molecules in macromolecular systems, entrapment of water in small molecular environment and then study has become an interesting topic in recent solid state supramolecular chemistry. Henry *et al.* showed that the water can act also as templating nanoporous material.⁶⁶ From a statistical analysis Infantes and Motherwell showed the influence of different chemical groups on hydration of molecular crystals. They showed that with increase in the number of halogen atoms the hydration possibility decreases.⁶⁷

1.8 Theme of the Present Work

This thesis deals with the X-ray structural analysis of different halogenated compounds and highlights the role of halogens in directing crystal packing. The compounds are selected so as to test some of the existing models of halogen bonds and the nature of inter-halogen interactions.

The importance of inter-halogen interaction in designing hexagonal host framework from trigonal molecule 2,4,6-tris(4-halophenoxy)-1,3,5-triazine via halogen trimer synthon is illustrated in chapter 2. Halogen mediated and guest induced architectural isomerism of channel to cage structure also have been demonstrated. The similarity between halogens and terminal alkyne group along with the cooperativity in C–H $\cdots\pi$ hydrogen bonds in ethynyl \cdots ethynyl interaction are discussed.

Chapter 3 shows the isostructurality in halogen exchange in haloaryloxytriazine

group of structures as well as other halogenated derivatives in the Cambridge Structural Database. The high probability of isostructurality upon halogen exchange is a unique characteristic of this group of atoms. The reasons of this capability of halogen atoms are discussed.

Weak hydrogen bond mediated channel and cage host frameworks for van der Waals guest inclusion and desolvation of the channel to the apohost are discussed in chapter 4. This chapter shows the importance of weak interactions such as van der Waals interactions between host and guest molecules and host...host C-H...O and C-H...N interactions. Self inclusion with higher Z' values is also discussed.

Chapter 5 is about water clusters of different topologies trapped in the host lattice of halogenated phloroglucinol derivatives and the influence of halogen atoms in directing the overall crystal structure. The influence of halogen atoms on hydration of the molecules is illustrated.

A crystal engineering strategy to induce non-centrosymmetry in polar crystals using inter-halogen interactions is discussed in chapter 6. In the absence of inter-halogen interaction the system adopts centrosymmetric structure, which has been tested by replacing halogen atoms by methyl group.

Chapter 7 illustrates the simultaneous use of halogen bond optimization with hydrogen bond in the synthesis of targeted cocrystals. This chapter illustrates the selectivity between halogen bond and hydrogen bond, which is comparable to Etter's rule on hydrogen bond hierarchy.

Chapter 8 outlines the significant results presented in this thesis and conclusions based on the studies. Their implications for future studies to understand the nature of halogens and their use in more systematic ways to achieve target materials are mentioned.

1.9 References

1. E. J. Corey and X.-M. Cheng, in *The Logic of Chemical Synthesis*; Wiley: New York, **1989**.

2. K. C. Nicolaou and E. J. Sorensen, in *Classics in Total Synthesis*; VCH: Weinheim, **1995**.
3. K. C. Nicolaou, D. Vourloumis, N. Winssinger and P. S. Baran, *Angew. Chem. Int. Ed.*, **2000**, 39, 44.
4. S. J. Danishefsky and J. R. Allen, *Angew. Chem. Int. Ed.*, **2000**, 39, 836.
5. R. W. Armstrong, J.-M. Beau, S. H. Cheon, W. J. Christ, H. Fujioka, W.-H. Ham, L. D. Hawkins, H. Jin, S. H. Kang, Y. Kishi, M. J. Martinelli, W. W. McWhorter, M. Mizuno, M. Nakata, A. E. Stutz, F. X. Talamas, M. Taniguchi, J. A. Tino, K. Ueda, J. Uenishi, J. B. White and M. Yonaga, *J. Am. Chem. Soc.*, **1989**, 111, 7530.
6. (a) J.-M. Lehn, *Supramolecular Chemistry, Concepts and Perspectives*, VCH, Weinheim: Germany, **1995**. (b) *Supramolecular Chemistry*; Eds. J. W. Steed and J. L. Atwood, Wiley: Chichester, **2000**.
7. J. D. Dunitz, in *Perspectives in Supramolecular Chemistry. The Crystal as a Supramolecular Entity*; ed. G.R. Desiraju, Wiley: Chichester, **1995**, vol. 2, pp. 1.
8. L. R. Nassimbeni, in *Inclusion Compounds: Selectivity, Thermal Stability, and Kinetics*; Encyclopedia of Supramolecular Chemistry, **2004**, 696.
9. R. Pepinsky, *Phys. Rev.*, **1955**, 100, 52.
10. G. M.J. Schmidt, *Pure Appl. Chem.*, **1971**, 27, 647.
11. G. R. Desiraju, in *Crystal Engineering: The Design of Organic Solids*; Elsevier: Amsterdam, **1989**.
12. J. F. Stoddart, *Acc. Chem. Res.*, **1997**, 30, 393.
13. G. R. Desiraju, T. Steiner, in *The Weak Hydrogen Bond In Structural Chemistry and Biology*; Oxford University Press: New York, **1999**.
14. E. J. Corey, *Pure Appl. Chem.*, **1967**, 14, 19.
15. G. R. Desiraju, *Angew. Chem. Int. Ed.*, **1995**, 34, 2311.
16. (a) P. Metrangolo and G. Resnati, *Chem. Eur. J.*, **2001**, 7, 2511. (b) J. P. M. Lommerse, A. J. Stone, R. Taylor and F. H. Allen, *J. Am. Chem. Soc.*, **1996**, 118, 3108. (c) P. Metrangolo and G. Resnati, in *Halogen Bonding*; Encyclopedia of Supramolecular Chemistry, **2004**.
17. T. Sakurai, M. Sundaralingam and G. A. Jeffrey, *Acta Crystallogr.*, **1963**, 16, 354.

18. A. Bondi, *J. Phys. Chem.*, **1964**, 68, 441.
19. S. C. Nyburg and C. H. Faerman, *Acta Cryst.*, **1987**, B43, 106.
20. G. R. Desiraju and R. Parthasarathy, *J. Am. Chem. Soc.*, **1989**, 111, 8725.
21. (a) S. L. Price, A. J. Stone, J. Lucas, R. S. Rowland and A. E. Thornley, *J. Am. Chem. Soc.*, **1994**, 116, 4910. (b) J. B. O. Mitchell and S. L. Price, *J. Phys. Chem.*, **2001**, A105, 9961. (c) G. M. Day and S. L. Price, *J. Am. Chem. Soc.*, **2003**, 125, 16434.
22. V. R. Pedireddi, D. S. Reddy, B. S. Goud, D. C. Craig, A. D. Rae and G. R. Desiraju, *J. Chem. Soc. Perkin Trans. 2*, **1994**, 2353.
23. M. Freytag, P. G. Jones, B. Ahrens and A. K. Fischer, *New J. Chem.*, **1999**, 23, 1137.
24. (a) F. Zordan, L. Brammer and P. Sherwood, *J. Am. Chem. Soc.*, **2005**, 127, 5979. (b) G. M. Espallargas, L. Brammer and P. Sherwood, *Angew. Chem. Int. Ed.*, **2006**, 45, 435.
25. C. M. Reddy, M. T. Kirchner, R. C. Gundakaram, K. A. Padmanavan and G. R. Desiraju, *Chem. Eur. J.*, **2005**, 12, 2222.
26. J. M. Dumas, L. Gomel and M. Guerin, in *The Chemistry of functional group, Supplement D*; Eds. S. Patai and Z. Rappoport, Wiley: New York, **1983**, pp 985.
27. C. K. Prout and B. Kamenar, in *Molecular Complexes*; Elek Science: London, **1973**, vol. 1, pp. 151.
28. O. Hassel, *Science*, **1970**, 170, 497.
29. G. A. Landrum, N. Goldberg and R. Hoffmann, *J. Chem. Soc., Dalton Trans.*, **1997**, 19, 3605.
30. (a) A. C. Legon, *Angew. Chem. Int. Ed.*, **1999**, 38, 2686. (b) I. Alkorta, I. Rozas and J. Elguero, *J. Phys. Chem.*, **1998**, A102, 9278.
31. P. Metrangolo, H. Neukirchi, T. Pilati and G. Resnati, *Acc. Chem. Res.*, **2005**, 38, 386.
32. T. Caronna, R. Liantonio, T. A. Logothetis, P. Metrangolo, T. Pilati and G. Resnati, *J. Am. Chem. Soc.*, **2004**, 126, 4500.
33. E. Corradi, S. V. Meille, M. T. Messina, P. Metrangolo and G. Resnati, *Angew. Chem. Int. Ed.*, **2000**, 39, 1782.

34. P. Auffinger, F. A. Hays, E. Westhof and P. S. Ho, *Proc. Natl. Acad. Sci. USA*, **2004**, *101*, 16789.
35. J. K. Dunitz and R. Taylor, *Chem. Eur. J.*, **1997**, *3*, 89.
36. (a) V. R. thalladi, H.-C. Weiss, D. Bläser, R. Boese, A. Nangia and G. R. Desiraju, *J. Am. Chem. Soc.*, **1998**, *120*, 8702. (b) G. R. Desiraju, *Acc. Chem Res.*, **2002**, *35*, 565.
37. A. R. Choudhury and T. N. Guru Row, *Cryst. Growth Des.*, **2004**, *4*, 47.
38. H. Davey, *Philos. Trans. R. Soc. Lond.*, **1811**, *101*, 155.
39. (a) A. Nangia in *Nanoporous Materials: Science and Engineering*, eds. G.Q. Lu and X.S. Zhao, Imperial College Press, London, **2004**, pp. 165. (b) L.R. MacGillivray and J.L. Atwood, *Angew. Chem., Int. Ed.*, **1999**, *38*, 1018. (c) P.J. Langley and J. Hulliger, *Chem. Soc. Rev.*, **1999**, *28*, 279. (d) Y. Aoyama, *Top. Curr. Chem.*, **1998**, *198*, 131. (e) M.D. Hollingsworth, *Science*, **2002**, *295*, 2410.
40. (a) S.L. James, *Chem. Soc. Rev.*, **2003**, *32*, 276. (b) K. Biradha, *CrystEngComm*, **2003**, *5*, 374. (c) S.A. Barnett and N.R. Champness, *Coord. Chem. Rev.*, **2003**, *246*, 145. (d) S. Kitagawa, R. Kitaura and S. Noro, *Angew. Chem. Int. Ed.*, **2004**, *43*, 2334. (e) N.W. Ockwig, O. Delgado-Friedrichs, M. O’Keeffe and O.M. Yaghi, *Acc. Chem. Res.*, **2005**, *38*, 176. (f) S. Kitagawa and K. Uemura, *Chem. Soc. Rev.*, **2005**, *34*, 109.
41. A. Nangia, *Curr. Opin. Solid State Mater. Sci.*, **2001**, *5*, 115.
42. Y. A. Dyadin and I. S. Terekhova, in *Classical descriptions of Inclusion compounds*; Encyclopedia of Supra Molecular Chemistry, **2004**.
43. E. Weber, in *Comprehensive Supramolecular Chemistry*; Eds. D. D. macNicol, F. Toda and R. Bishop, Pergamon: Oxford, **1996**, vol. 6.
44. (a) C. M. Reddy, S. Basavoju and G. R. Desiraju, *CrystEngComm*, **2005**, *7*, 44. (b) C. M. Reddy, A. Nangia, C.-K. Lam and T. C. W. Mak, *CrystEngComm*, **2002**, *4*, 323.
45. (a) A. N. M. M. Rahman, R. Bishop, D. C. Craig and M. L. Scudder, *Eur. J. Org. Chem.*, **2003**, *72*. (b) A. N. M. M. Rahman, R. Bishop, D. C. Craig and M. L. Scudder, *Org. Biomol. Chem.*, **2004**, *2*, 175. (c) A. N. M. M. Rahman, R. Bishop, D. C. Craig and M. L. Scudder, *Org. Biomol. Chem.*, **2003**, *1*, 1435. (d) A. N. M. M.

- Rahman, R. Bishop, D. C. Craig and M. L. Scudder, *J. Supramol. Chem.*, **2002**, *2*, 409. (e) A. N. M. M. Rahman, R. Bishop, D. C. Craig and M. L. Scudder, *Chem. Commun.*, **1999**, 2389.
46. (a) J. Zyss and I. Ledoux, *Chem. Rev.* **1994**, *94*, 77. (b) N. J. Long, *Angew. Chem., Int. Ed.*, **1995**, *34*, 21. (c) J. J. Wolff, F. Siegler, R. Matschiner and R. Wortmann, *Angew. Chem. Int. Ed.*, **2000**, *39*, 1436.
47. (a) E. Pidcock, *Chem. Commun.*, **2005**, 3457. (b) M. C. Etter and K.-S. Huang, *Chem. Mater.*, **1992**, *4*, 824. (c) C. P. Brock and J. D. Dunitz, *Chem. Mater.*, **1994**, *6*, 1118.
48. O. R. Evans and W. Lin, *Chem. Mater.*, **2001**, *13*, 2705.
49. (a) S. R. Marder, J. W. Perry and W. P. Schaefer, *Science*, **1989**, *245*, 626. (b) Y. L. Fur, M. Bagieu-Bucher, R. Masse, J.-F. Nicoud and J.-V. Levy, *Chem. Mater.*, **1996**, *8*, 68.
50. B. Traber, J. J. Wolff, F. Rominger, T. Oeser, R. Gleiter, M. Goebel and R. Wortmann, *Chem. Eur. J.*, **2004**, *10*, 1227.
51. J. Zyss, D. S. Chemla and J. F. Nicoud, *J. Chem. Phys.*, **1981**, *74*, 4800.
52. B. Zhao, W.-Q. Lu, Z.-H. Zhou and Y. Wu, *J. Mater. Chem.*, **2000**, *10*, 1513.
53. A. D. Bond, J. Griffiths, J. M. Rawson and J. Hulliger, *Chem. Commun.*, **2001**, 2488.
54. N. Masciocchi, M. Bergamo and A. Sironi, *Chem. Commun.*, **1998**, 1347.
55. R. Thaimattam, C. V. K. Sharma, A. Clearfield and G. R. Desiraju, *Cryst. Growth Des.*, **2001**, *1*, 103.
56. P. K. Thallapally, G. R. Desiraju, M. Bagieu-Bucher, R. Masse, C. Bourgogne and J.-F. Nicoud, *Chem. Commun.*, **2002**, 1052.
57. (a) J. Bernstein, R. J. Davey and J. O. Henck, *Angew. Chem., Int. Ed.*, **1999**, *38*, 3441. (b) J. Bernstein, in *Polymorphism in Molecular Crystals*; Clarendon: Oxford, **2002**. (c) A. Kálmán, L. Fábián, G. Argay, G. Bernáth and Z. C. Gyarmati, *J. Am. Chem. Soc.*, **2003**, *125*, 34. (d) V. S. S. Kumar, C. F. Pigge and N. P. Rath, *CrystEngComm*, **2004**, *6*, 102. (e) K. E. Holmes, P. F. Kelly and M. R. J. Elsegood, *CrystEngComm*, **2004**, *6*, 56. (f) L. Fábián, A. Kálmán, G. Argay, G. Bernáth and Z.

- C. Gyarmati, *Chem. Commun.*, **2004**, 18, 2114. (g) S. Aitipamula and A. Nangia, *Chem. Commun.*, **2005**, 3159.
58. E. Mitscherlich, *Ann. Chim. Phys.*, **1822**, 19, 350.
59. M.R. Caira, *Top. Curr. Chem.*, **1998**, 198, 164.
60. A. Gavezzotti and G. Fillippini, *J. Am. Chem. Soc.*, **1995**, 117, 12299.
61. W.C. McCrone, in *Polymorphism in Physics and Chemistry of the Organic Solid State*; Eds. D. Fox, M.M. Labes and A. Weisemberg, Interscience: New York, **1965**, pp. 726.
62. J. A. R. P. Sarma and G.R. Desiraju, in *Crystal Engineering: The Design and Application of Functional Solids*; Eds., M. J. Zaworotko and K. R. Seddon, Kluwer: Dordrecht, **1999**, pp. 325.
63. T. Siegrist, C. Kloc, J. H. Schön, B. Batlogg, R. C. Haddon, S. Berg and G. A. Thomas, *Angew. Chem. Int. Ed.*, **2001**, 40, 1732.
64. R. G. Gonnade, M. M. Bhadbhade, M. S. Shashidhar and A. K. Sanki, *Chem. Commun.*, **2005**, 5870.
65. (a) R. K. Khankari and D. J. W. Grant, *Thermochim. Acta*, **1995**, 61. (b) A. L. Gillon, N. Feeder, R. J. Davey and R. Storey, *Cryst. Growth Des.*, **2003**, 3, 663. (c) L. Infantes and W. D. S. Motherwell, *CrystEngComm*, **2004**, 4, 454.
66. M. Henry, F. Taulelle, T. Loiseau, L. Beitone and G. Férey, *Chem. Eur. J.*, **2004**, 10, 1366.
67. L. Infantes, J. Chisholm and S. Motherwell, *CrystEngComm*, **2003**, 5, 480.

CHAPTER 2

HALOGEN TRIMER-MEDIATED HEXAGONAL HOST FRAMEWORK AND ARCHITECTURAL ISOMERISM IN 2,4,6-TRIS(4-HALOPHENOXY) -1,3,5-TRIAZINE

2.1 Introduction

Host–guest inclusion compounds form a significant contribution to the growing field of crystal engineering and supramolecular chemistry because they are important for both fundamental and utilitarian reasons.¹ They can serve as models to understand complex phenomenon such as chirality evolution, nucleation, crystallization, and ligand–receptor binding. These hollow, porous materials have applications in tailored catalysts, magnetism, electrooptic, nonlinear optical materials, chemical separation, gas storage devices and targeted drug delivery.² The history of inclusion compounds is about 200 years old when Sir Humphrey Davy discovered chlorine hydrate in 1811.³ Despite over two centuries of research and knowledge, discovery of host–guest systems is still largely a matter of chance and prediction before experiment is quite difficult even at the present time. A few strategies have appeared in recent years for the planned construction of host–guest architectures with reasonable success.⁴ Trigonal⁵ and tetrahedral⁶ molecules have been used in the crystal engineering of honeycomb and diamondoid host networks respectively. In previous work from our group,⁷ the versatility of 2,4,6-tris(4-halophenoxy)-1,3,5-triazine, abbreviated as 4-XPOT hereafter, in building hexagonal host frameworks is demonstrated. The 4-XPOT molecule is a trigonal tecton⁸ with halogen sticky groups that reproducibly assemble via the X···X trimer supramolecular synthon⁹ **I** to form hexagonal host–guest structures.⁷ The triazine molecular scaffold is an excellent system to understand and validate the tecton → synthon → crystal self-assembly model for trigonal molecules, analogous to the tetrahedral tecton → diamond network relation.⁶ In inorganic supramolecular chemistry Yaghi *et al.* decorated diamondoid nets using porous metal sulfide materials where C vertices of the diamond

network were replaced alternately by $\text{Ge}_4\text{S}_{10}^{4-}$ cages and Mn(II) centers in the crystal structure of $\text{MnGe}_4\text{S}_{10} \cdot 2(\text{CH}_3)_4\text{N}$.¹⁰ Wuest and co-workers have designed several diamondoid networks using tectons with four sticky sites tetrahedrally oriented to the central C or Si atoms. One such tetrahedral tecton is tetrakis(1,2-dihydro-2-oxo-5-pyridyl)silane in which the nodes contain Si atoms and the four sticky groups are pyridone moieties. This compound forms doubly interpenetrated diamondoid network which include solvent molecules in the remaining space as guests.^{6b} Another classical host molecule is 1,3,5,7-adamantanetetracarboxylic acid.¹¹ Apart from these strong H-bonded sticky functional groups, Desiraju has reported diamondoid solid made of tetrahedral tecton, such as tetrakis(4-bromophenyl)methane and tetrahedrally oriented Br_4 synthon.¹² There are several examples of trigonal tectons form hexagonal network in organic and metal–organic systems. Banfi *et al.* reported a (6,3) net in metal–organic coordination polymers where they have used tritopic ligand 1,3,5-tris(4-cyanophenoxymethyl)-2,4,6-trimethylbenzene and silver(I) as three-connected node. The three nitrile groups act as donors to the silver metal node.¹³ Trimesic acid is one of them where interpenetrated hexagons as well as non-interpenetrated hexagonal inclusion structure with suitable guest have been reported.^{14a,b} Coppens *et al.* have reported hexagonal channel made of TMA and 2,4,6-tris(4-pyridyl)-1,3,5-triazine complex which include nano rods of pyrene as guest molecules.^{14c} In a recent thesis from our group Balakrishna Reddy reported several hexagonal networks in cocrystals of 1,3*cis*,5*cis*-cyclohexanetricarboxylic acid and dipyridyl derivatives. Halogen trimer mediated hexagonal framework from trigonal trihalomesitylene was reported by Bosch.¹⁵ This approach to crystal design and synthesis was recently termed the tecton–synthon model for synthetic crystallography by Orpen.¹⁶

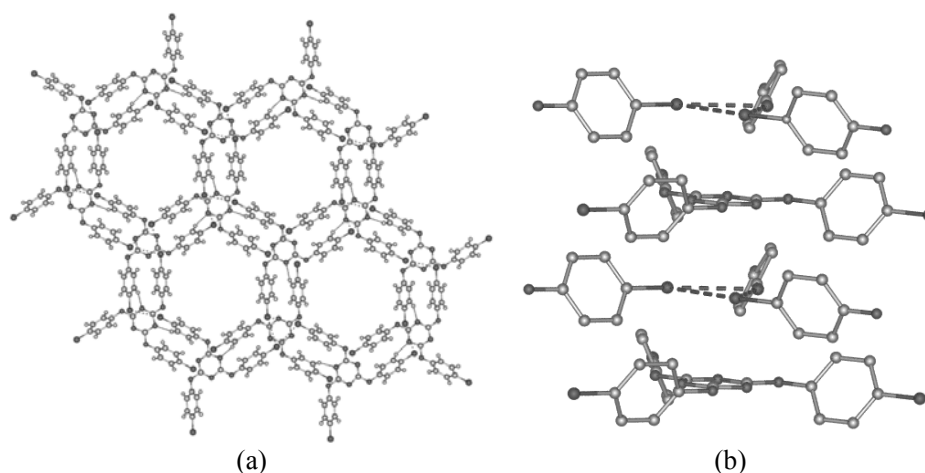
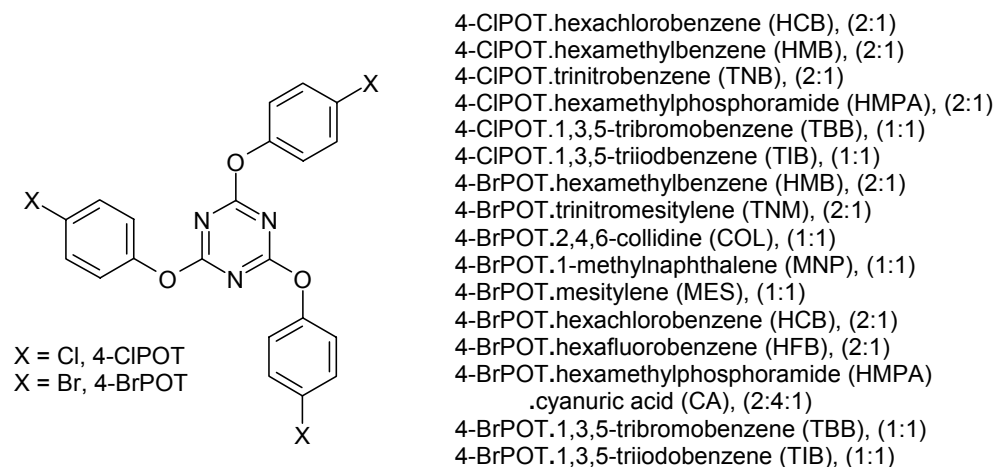


Figure 1. (a) Honeycomb layer of 4-CIPOT in the *ab*-plane to show alternating triazine molecule and halogen trimer synthon at the nodes of the hexagon. The hexagonal cavities have diameter of ~ 12 Å. (b) Stacking of triazine molecule and trimer synthon along the *c*-axis produces the channel host structure. Guest molecules and H atoms are removed for clarity.

A prototype hexagonal channel type structure of 4-XPOT ($X = \text{Cl}, \text{Br}$; Scheme 1) in $P6_3/m$ space group is illustrated in figure 1. The honeycomb layer is assembled by triazine ring of 4-CIPOT molecules and halogen trimer synthon **I** (Scheme 2) alternating at the nodes of the hexagon in the *ab*-plane. Alternate stacking of the same structural units along the *c*-axis leads to channels of 12 Å uniform pore diameter and area ca. 105 Å². Analysis of host–guest complexes studied so far show that the adduct structure is controlled by the nature of the halogen *X* on the triazine ring and the functional groups on the guest molecule. For example, hexachlorobenzene (HCB) gives channel type host network with chloro-phenoxytriazine (4-CIPOT:HCB = 2:1, $P6_3/m$),^{7b} whereas 4-BrPOT forms a cage type lattice (clathrate) with the same guest (2:1, $R\bar{3}$).^{7a} The $\text{halogen}_{\text{guest}} \cdots \pi(\text{phenyl})_{\text{host}}$ synthon guides the self-assembly of 4-XPOT host with 1,3,5-trihalobenzene guests to polar host–guest crystals in $P6_3$ space group.^{7c} From over fifteen 4-XPOT•guest inclusion crystals we concluded that the structure is fully ordered when weak host⋯guest interactions are present (e.g. $\text{Br} \cdots \text{O}$, $\text{Cl} \cdots \text{O}$, $\text{Br} \cdots \pi$) whereas the guest molecule is disordered when such stabilizing interactions are absent (e.g. halogen \rightarrow

methyl replacement).^{7b} A summary of 4-XPOT host–guest structures, stoichiometry, space group, X...X interaction, architecture type (channel or cage), cavity size and guest order/disorder is tabulated (Table 1).



Scheme 1. Channel and cage inclusion adducts of host molecules 4-CIPOT and 4-BrPOT.

Table 1. Selected crystallographic and host framework data on halo-phenoxytriazines 4-CIPOT and 4-BrPOT.

4-XPOT•guest	Space group	Architecture	X...X (Å)	Cavity size (Å)	Guest atoms
4-CIPOT•HCB	<i>P</i> 6 ₃ / <i>m</i>	channel	3.45	12.1	disordered
4-CIPOT•HMB	<i>P</i> 6 ₃ / <i>m</i>	channel	3.48	12.1	disordered
4-CIPOT•TNB	<i>P</i> 6 ₃ / <i>m</i>	channel	3.42	11.8	ordered
4-CIPOT•HMPA	<i>P</i> 6 ₃ / <i>m</i>	channel	3.44	11.6	disordered
4-CIPOT•TBB	<i>P</i> 6 ₃	channel	3.44	11.7	ordered
4-CIPOT•TIB	<i>P</i> 6 ₃	channel	3.56	12.1	ordered
4-BrPOT•HMB	<i>P</i> 6 ₃ / <i>m</i>	channel	3.47	12.2	disordered
4-BrPOT•TNM	<i>P</i> 6 ₃ / <i>m</i>	channel	3.50	12.8	disordered
4-BrPOT•COL	<i>P</i> 6 ₃ / <i>m</i>	channel	3.50	11.9	disordered
4-BrPOT•MNP	<i>P</i> 6 ₃ / <i>m</i>	channel	3.51	12.2	disordered
4-BrPOT•MES	<i>P</i> 6 ₃ / <i>m</i>	channel	3.53	12.1	disordered

4-BrPOT•TBB	$P6_3$	channel	3.51	11.9	ordered
4-BrPOT•TIB	$P6_3$	channel	3.55	12.1	ordered
4-BrPOT•HCB	$R\bar{3}$	cage	3.79	12.7	ordered

A perusal of table 1 shows that 4-ClPOT always gives channel type host architecture whereas this is generally true for bromophenoxytriazines. Hexachlorobenzene (HCB) and hexafluorobenzene (HFB, reported in this thesis) guests result in the cage type host lattice of 4-BrPOT. Second, the X...X distance in the halogen trimer synthon correlates with the type of the host framework. An inter halogen distance of ca. 3.5 Å gives the channel structure whereas a longer distance of ~3.8 Å produces the cage lattice. Third, architectural isomerism from channel to cage structure does not disrupt the hexagonal symmetry of the crystal system because crystallization routinely occurs in $P6_3/m$, $P6_3$ and $R\bar{3}$ space groups. In channel type structures Cl...Cl distance in the trimer synthon is at the van der Waals sum ($\Sigma_{vdW} = 3.50$ Å) whereas Br...Br distance is less than Σ_{vdW} (= 3.70 Å). However, the Br...Br distance is slightly longer than Σ_{vdW} in the cage structures of 4-BrPOT•HCB. The larger, more polarizable and softer iodine atom is able to participate in I...I contacts shorter than Σ_{vdW} (= 3.96 Å) compared to Br and Cl in relation to their atomic radii. Based on the inter halogen distances in Table 1 we reasoned that the penetration of one iodine atom into the van der Waals sphere of an adjacent iodine to the extent of 5% will give I...I ~3.8 Å¹⁷ which is the X...X distance in the 4-BrPOT•HCB cage structures. The anticipated hexagonal cage structures of 4-IPOT•guest through the iodo trimer synthon **I** (Scheme 2) is a result of continuous change in the size and polarizability of halogens from Cl to I. The tuning of host framework through functional group modification on the molecular scaffold will expand the supramolecular diversity of 4-XPOT lattice inclusion adducts. We describe in this chapter ten isostructural inclusion clathrates of 4-IPOT with mesitylene, collidine, tribromomesitylene, triiodomesitylene, hexachlorobenzene, hexafluorobenzene, 1-methylnaphthalene, dichloromethane, dibromomethane, and diiodomethane guests in $R\bar{3}$ space group (Scheme 2). The release of guest molecule from the channel or cage type framework of 4-XPOT host is measured by thermal gravimetric analysis (TGA) and the

phase purity of the solid is confirmed by differential scanning calorimetry (DSC).

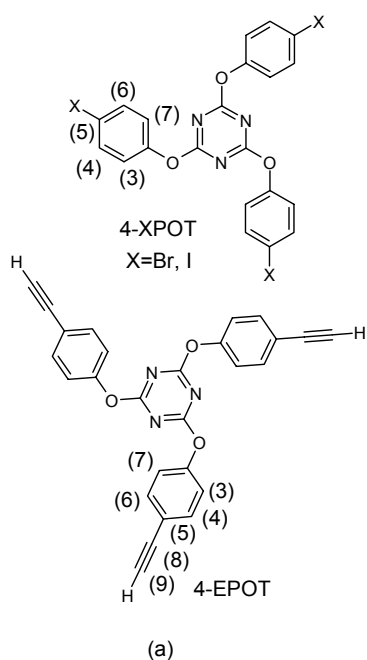
In addition to describing new 4-IPOT•guest cage structures, we explain why crystallization of trigonal 4-XPOT molecules occurs in high symmetry hexagonal crystal system. This is not so common, in general, as shown by statistics from CSD Symmetry,¹⁸ a relational database of point group and space group symmetry in small molecule crystal structures. The high frequency of crystallization in hexagonal crystal systems for C_3 symmetry 4-XPOT molecules is ascribed to two recurring aggregation motifs. (1) The halogen trimer synthon has 3-fold symmetry in 4-ClPOT, 4-BrPOT and 4-IPOT structures. (2) The triazine molecules aggregate via the inversion-related Piedfort Unit¹⁹ dimer, C_{3i} -PU in 4-IPOT structures. To summarize, it is shown that the tecton \rightarrow synthon \rightarrow crystal supramolecular hierarchy model can lead to persistent architectures even with weak intermolecular interactions if molecular and synthon symmetry are properly incorporated as design elements.

2.2 Results and Discussion

The host molecule 4-IPOT was crystallized from several guest/solvent molecules of different size, shape and symmetry. Diffraction quality single crystals of 4-IPOT•guest appeared after a week at room temperature, which were characterized by X-ray diffraction. $^1\text{H-NMR}$ of the crystal and TGA confirmed the host:guest stoichiometry and the temperature of guest release from the host framework.

Halogen...halogen and halogen...oxygen interactions have been the subject of intense debate for over a decade.²⁰ The exact nature of $\text{X}\cdots\text{X}$ interactions is still not fully understood, though it can be said that they arise due to electrostatic interaction along with contribution from charge transfer, polarization and dispersion–repulsion. Desiraju and Parhasarathy^{20a} suggested that halogen...halogen contacts are attractive in nature, which was challenged by Price *et al.*^{20b} who argued that the directional and short $\text{Cl}\cdots\text{Cl}$ contacts are a result of the close packing of pear shaped halogen atom. There is spherical to elliptical shape change with increase in the size and polarization of the halogen atom, from F to Cl to Br to I. Lommerse *et al.*^{20c} have shown that the directional and attractive halogen...oxygen contact is of the charge-transfer or electrophile–nucleophile pairing

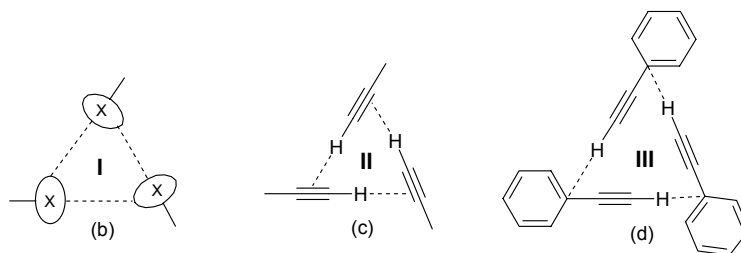
type. The angular preferences in halogen...halogen and halogen...oxygen attractive interactions are of two types: nucleophiles approach the polar δ^+ region of the C–X bond head on while electrophiles prefer attack in the equatorial δ^- region. Type I halogen...halogen geometries is a consequence of close packing while the type II generally is polarization-induced and stabilized by electrostatic forces. The halogen trimer synthon in halophenoxy triazine and trihalomesitylene crystal structures is stabilized by the cooperative array of three halogen atoms in the attractive electrophile–nucleophile type II approach.^{15,7} The polar δ^+ region of one elliptical halogen atom points towards the equatorial δ^- region of an adjacent halogen, with each halogen behaving both as a donor and as an acceptor, leading to stabilization of the halogen trimer synthon by electrostatics as well as cooperative effects. Halogen bonding has emerged as a new cohesive force in supramolecular organization²¹ and a recent paper on the crystal engineering of short inter halogen contacts^{21c} adds further support to these interactions being of the Lewis acid–base type, at least for the heavier halogens.



4-BrPOT.hexafluorobenzene (HFB), (2:1)

4-IPOT.mesitylene (MES), (2:1)
 4-IPOT.collidine (COL), (2:1)
 4-IPOT.tribromomesitylene (TBM), (2:1)
 4-IPOT.triiodomesitylene (TIM), (2:1)
 4-IPOT.hexachlorobenzene (HCB), (2:1)
 4-IPOT.hexafluorobenzene (HFB), (2:1)
 4-IPOT.1-methylnaphthalene (MNP), (2:1)
 4-IPOT.dichloromethane (DCM), (1:1)
 4-IPOT.dibromomethane (DBM), (1:1)
 4-IPOT.diiodomethane (DIM), (1:1)

4-EPOT.mesitylene (MES), (2:1)
 4-EPOT.collidine (COL), (2:1)
 4-EPOT.hexamethylbenzene (HMB), (2:1)
 4-EPOT.benzene (BEN), (2:1)
 4-EPOT.hexachlorobenzene (HCB), (2:1)
 4-EPOT.hexafluorobenzene (HFB), (2:1)
 4-EPOT.diethylether (DEE), (1:1)
 4-EPOT.dichloromethane (DCM), (1:1)
 4-EPOT.dibromomethane (DBM), (1:1)
 4-EPOT.diiodomethane (DIM), (1:1)
 4-EPOT.tetrachloromethane (TCM), (1:1)



Scheme 2. (a) Host molecules 4-XPOT (X=Br, I) and 4-EPOT are studied in this chapter. (b) Halogen trimer synthon (I) observed in 4-Cl/Br/IPOT hexagonal host architectures. Ethynyl trimer synthon (c, d) observed in the host architecture of 4-EPOT molecule. C–H donor points towards the phenyl carbon atom in (d).

2.2.1 4-IPOT•guest Crystal Structures

The I⋯I distance, C–H⋯O, C–H⋯N, C–H⋯X interactions, tilt of the phenyl ring with the *c*-axis, and the guest order/disorder in 4-IPOT•guest clathrates are listed in Tables 2. Self-assembly of the host molecule in 4-IPOT•HCB to the honeycomb layer structure with hexagonal voids of cross-sectional area 110 Å² is mediated by the iodo trimer synthon with I⋯I distance of 3.85 Å (Figure 2a). Hexachlorobenzene guest is included in the cavity, which is capped by iodo trimer synthon and triazine molecule. The ordered HCB guest resides at the inversion center in a cavity of $\bar{3}$ symmetry and is bonded to the host via six Cl⋯O interactions of 3.64 Å (Figure 2a). In contrast to the perpendicular orientation of the phenoxy group in the channel structure of 4-ClPOT and 4-BrPOT, the phenyl ring is tilted by 81° with respect to the *c*-axis, which results in the cage structure of 4-IPOT. This clathrate structure is identical to 4-BrPOT•HCB and 4-BrPOT•HFB with ordered guest molecules. Inversion-related triazine molecules stack at a separation of 3.43 Å to form the C_{3i}-PU. Such dimers of triazine molecules and iodo trimer synthons close the host cavity on both sides. The final result is a penta-decker sandwich^{19d} of host and guest molecules with HCB forming the middle layer (Figure 2b).

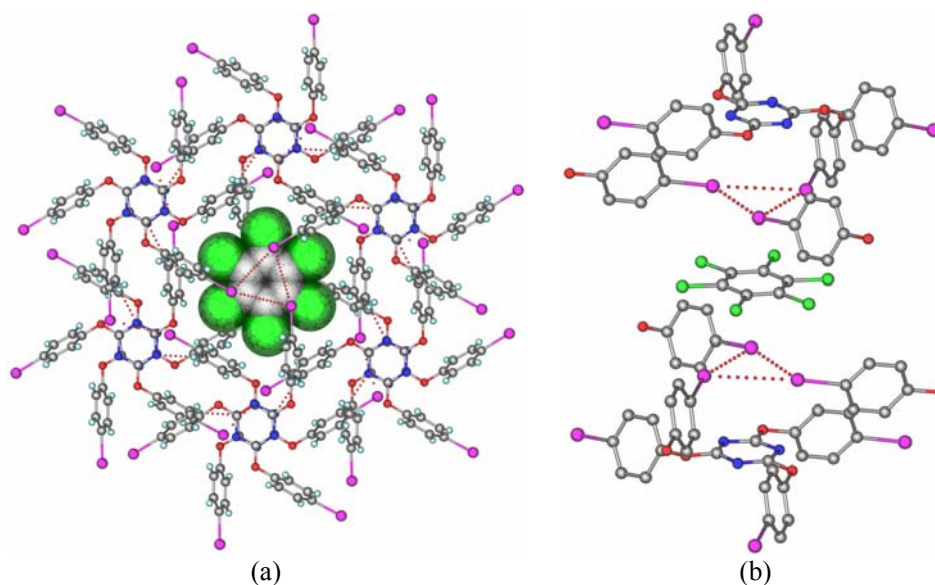


Figure 2. (a) Perspective view of the host•guest structure viewed down the *c*-axis. The 2D layer arrangement is similar to the channel structure of Figure 1a. In third dimension these layers stack with offset to form cage. The other structures are identical except in the arrangement of guest molecules. (b) Viewed perpendicular to *c*-axis. Penta-decker sandwich of triazine–trimer–guest–trimer–triazine along the *c*-axis. The guest molecule occupies the $\bar{3}$ special position in the crystal.

4-IPOT adducts with several other guest molecules are isostructural in $R\bar{3}$ space group, albeit the guest molecules are disordered in several structures (Table 2). Guest disorder is due to the lack of specific host···guest interactions and/or because the point group symmetry of the guest is lower than the site symmetry of the hexagonal void. The arrangement of host atoms is fully ordered and identical to 4-IPOT•HCB. The I···I distances in these structures (3.82–3.91 Å) are comparable to the 4-BrPOT•HCB crystal structures because iodine, being more polarizable than bromine, can participate in short interactions relative to its van der Waals sum. The present family of structures illustrates supramolecular isomerism based on the halogen atom as the anchor group.

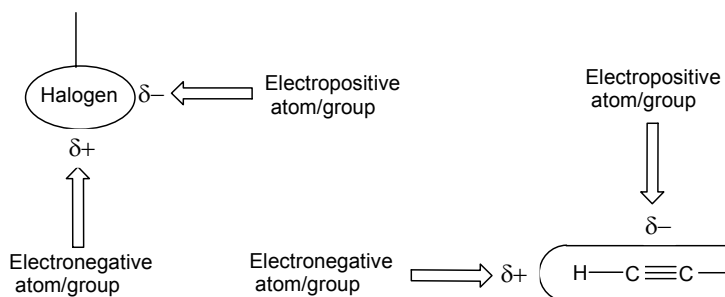
Table 2. Geometry of X...X and C–H...O/N interactions, π ... π stacking distance, tilt of the phenyl ring, hexagonal cavity size, and guest order/disorder in cage structures of 4-IPOT•guest, 4-BrPOT•HFB and 4-BrPOT•HCB. Atom numbering is given in scheme 2.

Complex	Interaction	d (Å)	D (Å)	θ (°)
4-IPOT•MES Guest disordered	C(3)–H...N	2.72	3.461(6)	125.5
	C(6)–H...N	2.65	3.691(5)	161.5
	C(6)–H...O	2.76	3.643(6)	138.6
	C(7)–H...I	3.23	4.148(4)	142.9
	I...I (trimer)		3.886(1)	162.5, 105.3
	π ... π (C_{3I} -PU)		3.426	
	phenyl tilt			80
	cavity size		12.9	
4-IPOT•COL Guest disordered	C(3)–H...N	2.71	3.447(5)	124.7
	C(6)–H...N	2.63	3.669(5)	161.0
	C(6)–H...O	2.73	3.618(6)	138.6
	C(7)–H...I	3.21	4.122(4)	142.4
	I...I (trimer)		3.857(1)	162.5, 105.2
	π ... π (C_{3I} -PU)		3.395	
	phenyl tilt			81
	cavity size		12.8	
4-IPOT•TBM Guest disordered	C(3)–H...N	2.74	3.454(9)	123.2
	C(6)–H...N	2.63	3.677(7)	162.0
	C(6)–H...O	2.81	3.678(8)	137.3
	C(7)–H...I	3.25	4.152	141.3
	I...I (trimer)		3.862(6)	163.2, 105.8
	Br...O		3.517(4)	154.8
	π ... π (C_{3I} -PU)		3.379	
	phenyl tilt			81
	cavity size		13.1	
4-IPOT•TIM Guest disordered	C(3)–H...N	2.73	3.458(4)	124.0
	C(6)–H...N	2.69	3.732(4)	162.2
	C(6)–H...O	2.96	3.815(4)	135.9
	C(7)–H...I	3.32	4.210(3)	140.0
	I...I (trimer)		3.913(1)	164.4, 106.9
	I...O		3.446(3)	155.8
	π ... π (C_{3I} -PU)		3.35	
	phenyl tilt			81
	cavity size		13.3	

4-IPOT•HCB Guest ordered	C(3)–H...N	2.74	3.470(6)	124.5
	C(6)–H...N	2.64	3.688(5)	162.5
	C(6)–H...O	2.79	3.668(5)	138.4
	C(7)–H...I	3.25	4.168(4)	143.0
	I...I (trimer)		3.851(1)	162.3, 105.0
	Cl...O		3.641(4)	156.1
	$\pi\cdots\pi$ (C_{3I} -PU)		3.426	
	phenyl tilt			81
	cavity size		12.9	
4-IPOT•HFB Guest ordered	C(3)–H...N	2.66	3.399(4)	125.0
	C(6)–H...N	2.60	3.636(4)	160.1
	C(6)–H...O	2.66	3.557(3)	140.2
	C(7)–H...I	3.20	4.121(3)	143.2
	I...I (trimer)		3.829(4)	161.6, 104.4
	$\pi\cdots\pi$ (C_{3I} -PU)		3.378	
	phenyl tilt			80
	cavity size		12.7	
4-IPOT•MNP Guest disordered	C(3)–H...N	2.66	3.450(5)	129.3
	C(6)–H...N	2.60	3.654(5)	164.3
	C(6)–H...O	2.75	3.604(4)	135.8
	C(7)–H...I	3.20	4.093(3)	140.0
	I...I (trimer)		3.821(5)	162.2, 104.7
	$\pi\cdots\pi$ (C_{3I} -PU)		3.374	
	phenyl tilt			80
	cavity size		13.0	
4-IPOT•DCM Guest disordered	C(3)–H...N	2.68	3.470(10)	129.1
	C(6)–H...N	2.68	3.723(9)	161.6
	C(6)–H...O	2.81	3.712(10)	140.5
	C(7)–H...I	3.24	4.160(7)	143.6
	I...I (trimer)		3.909(1)	161.7, 103.9
	$\pi\cdots\pi$ (C_{3I} -PU)		3.487	
	phenyl tilt			81
	cavity size		12.9	
4-IPOT•DBM Guest disordered	C(3)–H...N	2.70	3.453(10)	126.1
	C(6)–H...N	2.65	3.692(10)	160.1
	C(6)–H...O	2.76	3.655(9)	140.0
	C(7)–H...I	3.21	4.132(7)	143.9
	I...I (trimer)		3.869(1)	161.8, 104.0
	$\pi\cdots\pi$ (C_{3I} -PU)		3.432	

	phenyl tilt cavity size		12.8	81
4-IPOT•DIM Guest disordered	C(3)–H···N	2.72	3.472(11)	126.1
	C(6)–H···N	2.72	3.760(10)	161.9
	C(6)–H···O	2.84	3.736(10)	139.6
	C(7)–H···I	3.19	4.113(8)	143.4
	I···I (trimer)		3.844(1)	163.1, 104.8
	$\pi\cdots\pi$		3.391	
	phenyl tilt cavity size		12.9	82
4-BrPOT•HFB Guest ordered	C(3)–H···N	2.68	3.379(3)	121.8
	C(6)–H···N	2.42	3.464(3)	162.4
	C(6)–H···O	2.54	3.417(3)	137.2
	C(7)–H···Br	3.11	4.045(2)	144.4
	Br···Br		3.646(1)	162.9, 105.1
	$\pi\cdots\pi$ (C_{3I} -PU)		3.232	
	phenyl tilt cavity size		12.4	81.2
4-BrPOT•HCB Guest ordered	C(3)–H···N	2.73	3.454(5)	124.2
	C(6)–H···N	2.48	3.535(4)	163.6
	C(6)–H···O	2.71	3.572(4)	136.4
	C(7)–H···Br	3.23	4.136(4)	142.3
	Br···Br		3.278(1)	163.5, 105.8
	Cl···O		3.531(3)	152.8
	$\pi\cdots\pi$ (C_{3I} -PU)		3.239	
	phenyl tilt cavity size		12.7	81.2

2.2.2 Ethynyl Group: A Supramolecular Pseudo Halogen



Scheme 2. Similar charge distribution in heavier halogens and terminal ethynyl groups. Halogen groups are elliptical shape and ethynyl group is cylindrical shape.

There are several examples where halogens have been replaced by terminal ethynyl groups successfully to build similar supramolecular structures. This is because they have similar kind of polarizability (Scheme 2). Both the groups contain partial positive charge along the covalent bond vector (polar region) and partial negative charge perpendicular to it (equatorial region). As a result the electropositive atom or group approaches towards equatorial region and electronegative atom or group approaches towards polar region. The volume of ethynyl group (28.8 \AA^3) is in between Br (24.4 \AA^3) and I (32.96 \AA^3)²² and the main difference between ethynyl and halogens is in their shape, halogens are elliptical and terminal ethynyl is cylindrical in shape. It has been seen that the simple molecule 4-ethynyl aniline is isostructural to its Cl and Br analogue.²² The halogens and the ethynyl triple bond accept hydrogen from N–H and also participate in halogen $\cdots\pi$ and ethynyl C–H $\cdots\pi$ interactions. Dey *et al.* have reported the isostructurality among *para*-substituted 4-phenoxyaniline, where substituents are Cl, Br, I and ethynyl groups.²³ Harris and co-workers documented the interchangeability of halogen and ethynyl substituents in di- and tri-substituted benzenes.²⁴ They have shown the structural similarities in 1,4-dichlorobenzene, 1,4-dibromobenzene, 1-bromo-4-ethynylbenzene and 1,4-diethynylbenzene. The ethynyl groups or halogens in these structures interact via type II geometry. They have also explained isostructurality among 1,3,5-trichlorobenzene, 1,3,5-tribromobenzene, 1,3-dibromo-5-ethynylbenzene and 1-bromo-3,5-diethynylbenzene crystal structures. Galoppini *et al.* have exemplified the halo–ethynyl mimicry in tetrahedral geometrical molecule.²⁵ They showed that crystal structures of tetrakis(4-bromophenyl)methane and corresponding tetraiodo, dibromodiethynyl, monobromotriethynyl and tetraethynyl derivatives are similar. The halogens and ethynyl groups form tetramer halogen synthon. Thus, we see that ethynyl group can replace halo groups in organic supramolecular chemistry quite often to produce similar crystal structure. In this context this is important to note that very often I does not follow Cl and Br e.g. 1,4-diiodobenzene^{24a} and 4-iodoaniline.²² Recently Nangia and co-workers have shown ethynyl–iodo exchange in urea derivatives to induce non-centrosymmetry in isostructural crystal²⁶ where both iodo group and ethynyl groups interact with the nitro group in similar fashion (Figure 3). We argue based on the results

in this chapter and previous papers that due to the overwhelming similarity with halogens in organic supramolecular chemistry, the ethynyl group may be termed as *supramolecular pseudo halogen*.

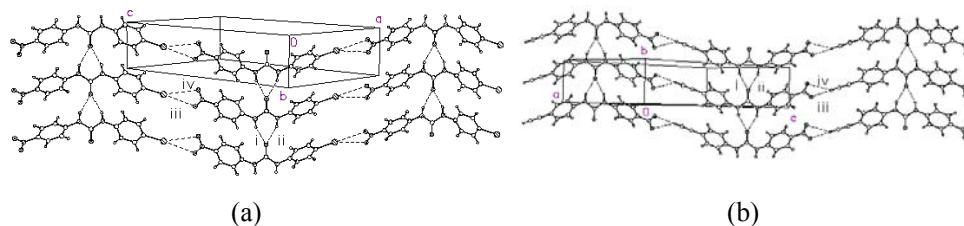


Figure 3. The α -network observed in isostructural *N*-4-(iodo)phenyl-*N'*-4'-nitrophenylurea (a) and *N*-4-(ethynyl)phenyl-*N'*-4'-nitrophenylurea (b) compounds which are supported by the similar $\text{I}\cdots\text{NO}_2$ and $\text{C}\equiv\text{C}\cdots\text{H}\cdots\text{NO}_2$ interactions respectively.

Interestingly the crystal structure of 1,3,5-triethynylbenzene a simple trigonal molecule, is not similar to its halogenated derivative. We present in this thesis ten isostructural inclusion clathrates of trigonal tecton 4-EPOT with hexachlorobenzene (HCB), hexafluorobenzene (HFB), hexamethylbenzene (HMB), mesitylene (MES), collidine (COL), benzene (BEN), diethylether (DEE), dichloromethane (DCM), dibromomethane (DBM), and diiodomethane (DIM) guests in $R\bar{3}$ space group (Scheme 2). They are in turn isostructural to halogenated counterpart (4-IPOT) but it forms different kind of cage structure with CCl_4 guest in $P6_3/m$ space group. There are only two examples (refcodes RICCOV and YUXJEG) in CSD where ethynyl trimer synthon is present in hexagonal crystal system.

2.2.3 4-EPOT•guest Crystal Structures

The 4-EPOT host molecule forms two kinds of cage structures depending upon guest molecules—one in $R\bar{3}$ space group (cage-I), which is isostructural to 4-IPOT and the second is in $P6_3/m$ space group (cage-II).

2.2.3.1 Cage-I Structure

Benzene was used as crystallizing solvent for HCB, HFB and HMB guests inclusion. For benzene guest, pentane was used as co solvent, but benzene has been included selectively as proved by $^1\text{H-NMR}$. Only HCB, HFB, HMB are ordered and others are disordered due to mismatch of size and/or symmetry of the guest molecules with host cavity. There is 1/3 host molecule in the asymmetric unit. The host molecules form hexagonal layer in *ab*-plane mediated via ethynyl trimer synthon (synthon II; Scheme 2) where the ethynyl C–H is directed to the mid point of the triple bond. The hexagonal layers are interconnected via weak C–H \cdots N interactions in the third dimension. The guest molecules are surrounded by 12 host molecules in the cavity. Along *c*-axis the repeating unit is triazine–ethynyl trimer synthon–guest–inversion-related ethynyl trimer synthon–inversion-related triazine. Thus a pair of triazines stacks to form Piedfort unit of C_{3i} symmetry mimicking a hexahost. The 4-EPOT•guest are packed more efficiently than the corresponding 4-IPOT•guest due to the larger spherical shape of iodo group. The packing coefficient of 4-EPOT•HFB (68.6%) is 1% higher than 4-IPOT•HFB (67.6%) at the same temperature (100 K).

Table 3. Geometry of C–H \cdots O/N and C–H $\cdots\pi$ interactions, $\pi\cdots\pi$ stacking distance, hexagonal cavity size, packing coefficient (without guest) and red shift in IR of ethynyl C–H stretching frequency in cage structures of 4-EPOT•guest. Atom numbering is given in scheme 2. π_m is the mid point of triple bond.

Complex	Interaction	d (Å)	D (Å)	θ (°)	$\Delta\nu$ cm $^{-1}$
4-EPOT•HCB	C(4)–H \cdots O	2.67	3.518(6)	134.6	21
	C(4)–H \cdots N	2.51	3.552(5)	161.2	
	C(7)–H \cdots N	2.75	3.444(6)	121.4	
	C(9)–H $\cdots\pi_m$	2.64	3.559	141.9	
	C(3)–H $\cdots\pi$	2.82	3.790	149.3	
	$\pi\cdots\pi$		3.327(2)		
	Cavity size		12.8		
4-EPOT•HFB	C(4)–H \cdots O	2.60	3.474(3)	137.7	15
	C(4)–H \cdots N	2.54	3.569(3)	159.1	
	C(7)–H \cdots N	2.72	3.431(3)	123.0	
	C(9)–H $\cdots\pi_m$	2.62	3.535	141.4	

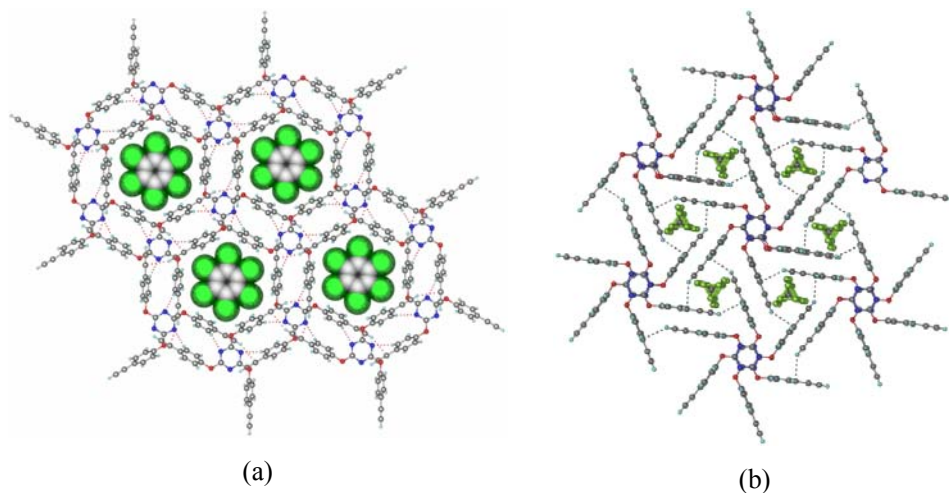
	C(3)–H $\cdots\pi$	2.78	3.773	151.0	
	$\pi\cdots\pi$		3.322(1)		
	Cavity size		12.6		
4-EPOT•HMB (100K)	C(4)–H \cdots O	2.69	3.531(3)	134.5	
	C(4)–H \cdots N	2.55	3.584(4)	159.4	
	C(7)–H \cdots N	2.78	3.467(3)	121.0	
	C(9)–H $\cdots\pi_m$	2.67	3.606	144.7	25
	C(3)–H $\cdots\pi$	2.84	3.803	147.7	
	$\pi\cdots\pi$		3.347(1)		
	Cavity size		12.9		
4-EPOT•HMB (200K)	C(4)–H \cdots O	2.71	3.569(4)	136.3	
	C(4)–H \cdots N	2.60	3.628(5)	158.9	
	C(7)–H \cdots N	2.79	3.493(4)	122.8	
	C(9)–H $\cdots\pi_m$	2.70	3.632	144.5	
	C(3)–H $\cdots\pi$	2.88	3.841	148.0	
	$\pi\cdots\pi$		3.398(1)		
	Cavity size		12.8		
4-EPOT•HMB (298K)	C(4)–H \cdots O	2.73	3.604(5)	137.4	
	C(4)–H \cdots N	2.63	3.660(6)	159.0	
	C(7)–H \cdots N	2.77	3.509(6)	124.9	
	C(9)–H $\cdots\pi_m$	2.73	3.664	144.8	
	C(3)–H $\cdots\pi$	2.91	3.878	148.5	
	$\pi\cdots\pi$		3.447(2)		
	Cavity size		12.8		
4-EPOT•MES	C(4)–H \cdots O	2.67	3.520(3)	134.9	
	C(4)–H \cdots N	2.56	3.592(3)	159.4	
	C(7)–H \cdots N	2.79	3.480(2)	121.5	
	C(9)–H $\cdots\pi_m$	2.74	3.689	146.4	21
	C(3)–H $\cdots\pi$	2.87	3.821	146.3	
	$\pi\cdots\pi$		3.357(1)		
	Cavity size		12.8		
4-EPOT•COL	C(4)–H \cdots O	2.65	3.503(4)	135.2	
	C(4)–H \cdots N	2.54	3.578(5)	159.3	
	C(7)–H \cdots N	2.78	3.466(4)	121.4	
	C(9)–H $\cdots\pi_m$	2.65	3.586	143.9	21
	C(3)–H $\cdots\pi$	2.82	3.782	148.6	
	$\pi\cdots\pi$		3.352(1)		
	Cavity size		12.8		
4-EPOT•DCM	C(4)–H \cdots O	2.63	3.509(3)	137.4	

	C(4)–H \cdots N	2.54	3.578(3)	159.2	
	C(7)–H \cdots N	2.72	3.445(4)	123.8	
	C(9)–H $\cdots\pi_m$	2.70	3.635	144.1	17
	C(3)–H $\cdots\pi$	2.83	3.793	148.6	
	$\pi\cdots\pi$		3.340(1)		
	Cavity size		12.6		
4-EPOT•DBM	C(4)–H \cdots O	2.64	3.525(5)	138.8	
	C(4)–H \cdots N	2.57	3.604(5)	158.3	
	C(7)–H \cdots N	2.73	3.461(5)	124.7	
	C(9)–H $\cdots\pi_m$	2.64	3.584	144.7	17
	C(3)–H $\cdots\pi$	2.78	3.755	149.7	
	$\pi\cdots\pi$		3.348(2)		
	Cavity size		12.6		
4-EPOT•DIM	C(4)–H \cdots O	2.66	3.553(4)	139.3	
	C(4)–H \cdots N	2.60	3.636(3)	158.9	
	C(7)–H \cdots N	2.74	3.484(4)	126.3	
	C(9)–H $\cdots\pi_m$	2.66	3.595	144.4	21
	C(3)–H $\cdots\pi$	2.83	3.809	151.0	
	$\pi\cdots\pi$		3.407(1)		
	Cavity size		12.6		
4-EPOT•BEN	C(4)–H \cdots O	2.60	3.476(3)	136.9	
	C(4)–H \cdots N	2.55	3.583(3)	158.2	
	C(7)–H \cdots N	2.75	3.464(3)	123.2	
	C(9)–H $\cdots\pi_m$	2.64	3.563	143.0	14
	C(3)–H $\cdots\pi$	2.78	3.759	150.0	
	$\pi\cdots\pi$		3.349		
	Cavity size		12.6		
4-EPOT•DEE	C(4)–H \cdots O	2.63	3.499(3)	136.9	
	C(4)–H \cdots N	2.54	3.573(3)	158.9	
	C(7)–H \cdots N	2.72	3.443(3)	123.6	
	C(9)–H $\cdots\pi_m$	2.64	3.557	141.5	17
	C(3)–H $\cdots\pi$	2.78	3.759	150.8	
	$\pi\cdots\pi$		3.336(1)		
	Cavity size		12.6		
4-EPOT•TCM	C(3)–H \cdots O	2.92	3.688(6)	127.8	
	C(3)–H \cdots N	2.99	3.992	154.1	
	C(7)–H $\cdots\pi$	2.80	3.719(6)	142.4	10
	$\pi\cdots\pi$		3.959(0)		
	Cavity size		8.9		

2.2.3.2 Cage-II Structure

Ethynyl C–H is known as one of the strongest donor among all C–H donors but as an acceptor it is not significantly good. In fact there is no strong preference for C–H towards the mid point of C≡C acceptor. Philp and co-workers showed that the accepting capacity is almost equal all over the triple bond.²⁷ Even it has been seen that one ethynyl C–H is interacting with π bond of ethynyl and another with π bond of aromatic ring in the same crystal structure and the later is stronger.²⁸

When we chose CCl₄ as a crystallizing solvent, which is not suitable as a guest for the former cavity ($R\bar{3}$, cage-I) due to its size and shape, the host framework of 4-EPOT have been adjusted to accommodate CCl₄ into a different kind of cavity and hence form different crystal structure ($P6_3/m$, cage-II). The disordered guest molecules and trimer synthons alternately stack along c -axis. Here the ethynyl C–H is not directed to triple bond but to the phenyl ring carbon (synthon III; Scheme 2). Unlike the cage-I structures, there are columns of continuous C_{3i}-PUs made of stacked triazine ring along the c -axis and guest molecules are sandwiched between trimer synthons III (Figure 4). Interaction geometries are given in table 3.



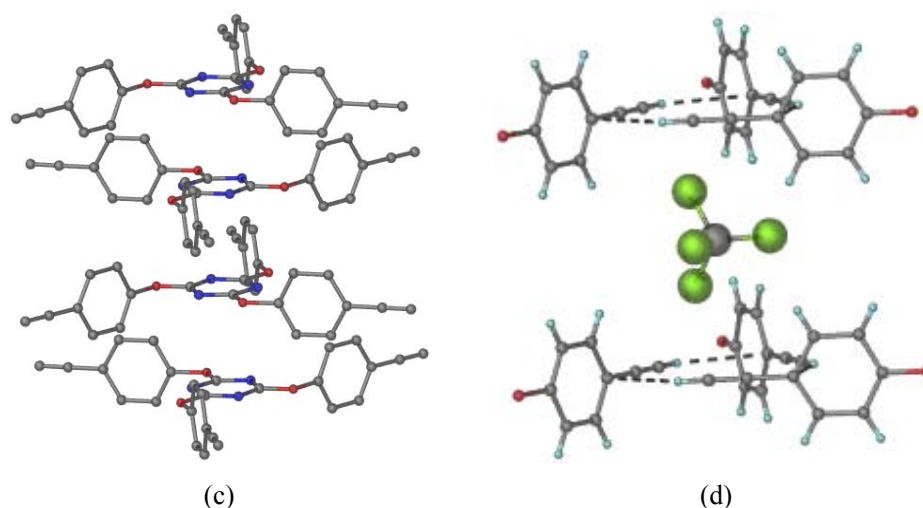


Figure 4. (a) Guest HCB is enclathrated by 4-EPOT in $R\bar{3}$ cage structure. (b) CCl_4 guest molecules are caged by $P6_3/m$ lattice of 4-EPOT host molecules. (c) The columnar structure of 4-EPOT made of stacked triazine molecules along c -axis. (d) The CCl_4 guest molecule is sandwiched by ethynyl trimer synthon.

2.2.4 IR Measurements

The thermal stability of 4-EPOT•guest is higher than the corresponding isostructural 4-IPOT•guest system as observed in DSC/TGA. Here the I_3 trimer synthon has been replaced by ethynyl trimer synthon. One valuable tool for checking the strength of $\text{C-H}\cdots\pi$ interaction is its stretching frequency shift in IR spectrum. The larger the red shift in solid state with respect to dilute solution in non-polar solvent the stronger is the interaction. Thus it can give a quantitative idea about the strength of the interaction.

For very strong H-bonds such as $\text{O-H}\cdots\text{O}$, bathochromic shifts can be up to 1950 cm^{-1} for 0.15 \AA lengthening of the O-H bond.²⁹ There are several attempts to correlate stretching frequency with bond length.³⁰ The relation was found linear only for strong H-bonds and starts curving for weaker interactions. At longer distance the shift becomes insensitive to change in distance.²⁹ Naturally for weak H-bonds this shift is less. In the crystal structure of 3-phenylpenta-1,4-diyn-3-ol the hydroxyl group form cyclic tetramer and the ethynyl groups interact with themselves. The red shift in O-H stretching frequency is -443 cm^{-1} and for $\equiv\text{C-H}$ the value is only -23 to -44 cm^{-1} (Figure 5).³¹

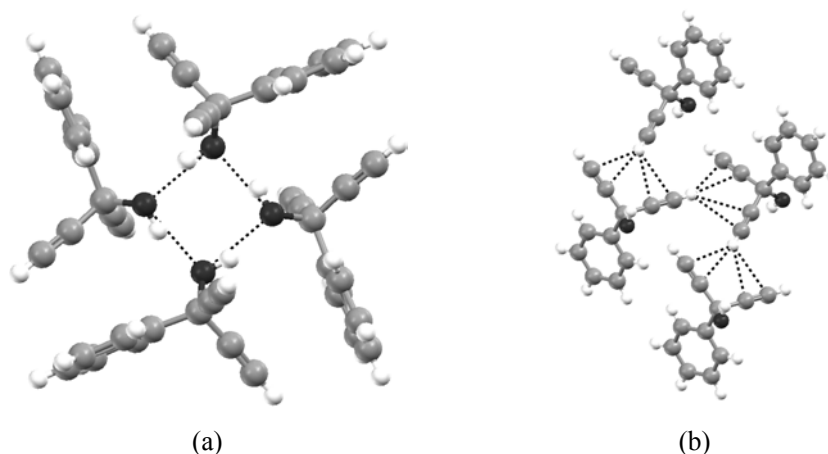


Figure 5. (a) O–H···O tetramer and (b) alkynyl···alkynyl interactions in the crystal structure of 3-phenylpenta-1,4-diyne-3-ol.

Due to the low solubility of the compound in CCl_4 , dilute solution in CH_2Cl_2 was used for solid state IR to check the strength of $\text{C-H}\cdots\pi$ interaction in cooperative stabilized ethynyl trimer synthon. The moderate $\Delta\nu$ ($14\text{--}25\text{ cm}^{-1}$) value (Table 3) alone cannot explain the high stability of the host lattice. The IR spectrum in THF solution has also been checked, which shows a higher red shift (58 cm^{-1}) due to $\equiv\text{C-H}\cdots\text{O}$ interaction with THF oxygen.³² However, 4-EPOT does not make complex with triphenylphosphineoxide via $\text{C-H}\cdots\text{O}$ hydrogen bond when crystallized from CH_2Cl_2 . The IR spectrum of a mixture of TPPO and 4-EPOT shows similar red shift to 4-EPOT•DCM complex. A dramatic red shift (202 cm^{-1}) of ethynyl C–H stretching band due to strong $\text{C-H}\cdots\text{O}$ hydrogen bond with water in the presence of triphenylphosphineoxide is reported (Figure 6).³³ Thus the cumulative effect of denser packing and comparatively stronger $\text{C-H}\cdots\text{N}$ and $\text{C-H}\cdots\text{O}$ hydrogen bonds are responsible for the high stability of 4-EPOT clathrates.

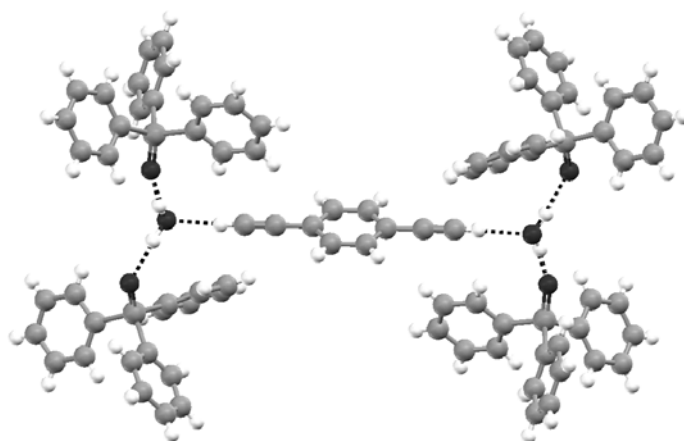
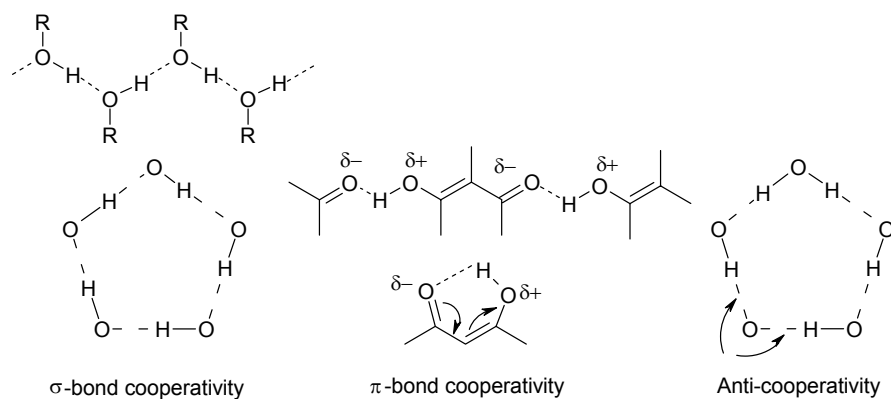


Figure 6. Crystal structure of hydrated triphenylphospheneoxide and 1,4-diethynylbenzene. Cooperative C–H...O interaction occurs due to the presence of strong O–H...O H-bonds.

2.2.5 Cooperativity in C–H... π Interaction

Some properties of H-bonds are more than additive. This means that if there are n number of interconnected hydrogen bonds, then the total energy of the array is not just a sum of n isolated H-bonds. Two mechanisms, namely cooperativity and anti-cooperativity are responsible for the extra and non-additivity in H-bond strength.^{29,34}

Cooperativity is of two types— σ -bond cooperativity and π -bond cooperativity (Scheme 3). If a $X^{\delta-}-H^{\delta+}$ group participates in hydrogen bonding as a donor or acceptor then the polarity of the σ -bond increases, which in turn strengthens the H-bond and weakens the covalent bond. Thus in a chain of H-bonds the charges flow through out the X–H σ -bonds and hence is called σ -bond cooperativity. On the other hand π -bond cooperativity involves hydrogen bonding between molecules with conjugated π -bonds, where the charge flows through π -bond and so it is termed also as RAHB (resonance assisted hydrogen bond).³⁵ Due to cooperativity the H-bond strength increases, because both donor and acceptor strengths are enhanced compared to the isolated H-bond.



Scheme 3. Examples of σ -bond cooperativity, π -bond cooperativity and anti-cooperativity.

In anti-cooperativity the effect is opposite and the occurrence of H-bonds reduces the strengths of each other (Scheme 3). When a single acceptor or a single donor forms more than one H-bonds, one bond polarity discourages other bonds to form and at the same time the parallel bond dipoles repel each other.

Cooperativity strength in moderately strong H-bonds is ca. 20% of its isolated interaction energy.³⁶ Harris *et al.* presented an example which shows an exceptionally short C-H \cdots O (1.96 Å, 3.02 Å) hydrogen bond with as much as 202 cm⁻¹ red shift in \equiv C-H stretching frequency.³⁷ Here ethynyl C-H is hydrogen-bonded to water oxygen which in turn donates two H-bonds to oxygens of two Ph₃P=O molecules (Figure 6). Similar situation has been observed by Nangia and co-workers in the case of strong H-bond. They have noticed very short O-H \cdots O H-bond (1.50 Å, 2.479 Å, 170.3°) in 2,3,5,6-pyrazinetetracarboxylic acid dihydrate.³⁸ Here water is donating two H-bonds to pyridine N and acid O. As a result it strongly accept one H-bond from carboxylic acid and makes the short contact. Steiner *et al.* have documented the importance of cooperativity in terminal alkynyl \equiv C-H $\cdots\pi$ interaction in (\pm)-3-phenylbut-1-yn-3-ol, pent-4-ynoic acid and DL-prop-2-ynylglycine.^{29,39} In the crystal structure of the first compound, there are two molecules in asymmetric unit. One ethynyl group donate H-bond to phenyl ring and accepts from another ethynyl group. It has been ascribed that due to cooperativity the \equiv C-H \cdots Ar hydrogen bond is stronger. In the crystal structures of

last two cases, the molecules aggregate via infinite zig-zag chain of $\text{C}\equiv\text{C}-\text{H}\cdots\text{C}\equiv\text{C}-\text{H}\cdots\text{C}\equiv\text{C}-\text{H}$ interactions stabilized by cooperativity. Whereas Steiner emphasized the cooperativity in H-bonds of ethynyl group, Philp believes that the cooperativity is insignificant for ethynyl H-bonds due to its low polarizability and weakness in nature.²⁷

We have used the Cambridge Structural Database (CSD) to understand the nature of cooperativity or lack of it in extended $\text{C}-\text{H}\cdots\pi$ arrays. We expect that $\text{C}-\text{H}\cdots\pi$ interaction will be shorter and linear for extended array compared to shorter motif. Is the interaction is stabilized by cooperativity?

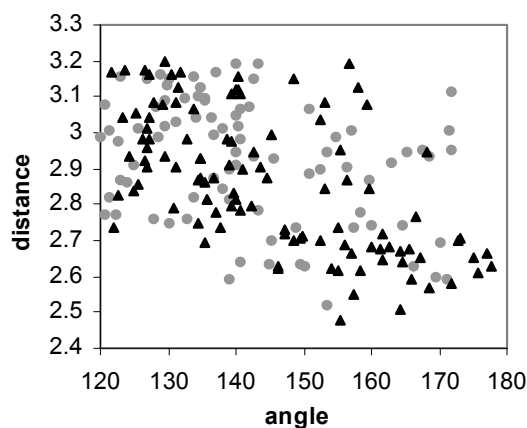


Figure 7. Distribution of distance with respect to angle of dimer (•) and infinite (▲) ethynyl...ethynyl ($\text{C}-\text{H}\cdots\pi_m$) interaction (π_m is the mid point of triple bond).

Distance-angle scatter plots are displayed in figure 7. There are 107 hits for infinite ethynyl...ethynyl interactions. Among them 27 % hits are within the high angle ($150-180^\circ$) and low distance ($2.4-2.8 \text{ \AA}$) range, where as this value is only 13 % in 85 dimer motifs (Table 4). The numbers are not statistically significant for the trimer motif. This analysis show that the region of linear angle and short distance, which is a general criteria for strong hydrogen bonds, is more populated in infinite ethynyl...ethynyl interaction than the dimer. This might indicates that infinite interactions in this weak

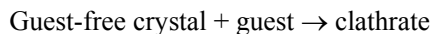
hydrogen bond are stronger due to cooperativity, analogous to strong hydrogen bonds.

Table 4. Summary of CSD search result for the geometry of infinite and dimer ethynyl...ethynyl interactions.

Ethynyl...ethynyl interaction type	120–150°		150–180°		Total
	2.4–2.8 Å	2.8–3.2 Å	2.4–2.8 Å	2.8–3.2 Å	
Infinite	16 (15%)	52 (49%)	29 (27%)	10 (9%)	107
Dimer	12 (14%)	47 (55%)	11 (13%)	15 (18%)	85

2.2.6 Computational Study

It is interesting to know why some compounds form clathrates while others do not. If the free energy change due to clathration is negative then guest inclusion is favored.⁴⁰ As a rough guide we use enthalpy as a guiding energy assuming that the entropy factors are of similar magnitudes.



$$\Delta E_{\text{clathration}} = E_{\text{clathrate}} - (E_{\text{guest-free}} + E_{\text{guest}})$$

The greater the negative value of $\Delta E_{\text{clathration}}$, the higher the stability of host-guest system. Facile guest inclusion in the triazine family of structures is explained by the much higher lattice energy gain due to inclusion. We have calculated the lattice energies of ordered 4-BrPOT•HCB, guest-free 4-BrPOT and HCB crystal structures and compared to show that clathration is thermodynamically favorable (Table 5). Single point lattice energy calculations show that inclusion is favorable by 5.85 kcal/mol and the optimized value is 7.76 kcal/mol in this family.

Table 5. Lattice energy comparison shows inclusion lattice is more favorable.

Compound	$E_{\text{single point}}$ (kcal/mol)	$E_{\text{optimized}}$ (kcal/mol)
4-BrPOT•0.5 HCB	−67.00	−70.33
4-BrPOT (guest-free)	−48.67	−49.50
HCB	−24.95	−26.13
ΔE (4-BrPOT•0.5 HCB– 4-BrPOT–0.5 HCB)	−5.85	−7.76

Lattice energy calculations similarly support that the 4-EPOT•guest architectures are 7.5–8.7 kcal (per 1:0.5 host•guest) more stable than the corresponding 4-IPOT•guest lattices. The main contribution to the additional stabilization in 4-EPOT arises from van der Waals interactions (Table 6). This is also reflected in TGA results where the same guest molecules evolve at higher temperature for 4-EPOT compared to 4-IPOT.

Table 6. Lattice energy calculations on 4-EPOT•guest and 4-IPOT•guest structures.

Compounds	Single point energy (kcal/mol)			Optimized energy (kcal/mol)		
	V.W.	E.S.	Total	V.W.	E.S.	Total
4-EPOT•HCB	−66.18	−5.70	−71.88	−67.40	−6.45	−73.85
4-IPOT•HCB	−59.74	−3.27	−63.01	−62.38	−3.17	−65.55
ΔE (4-EPOT– 4-IPOT)	−6.44	−2.43	−8.87	−5.02	−3.28	−8.30
4-EPOT•HFB	−54.63	−5.95	−60.59	−55.72	−6.71	−62.43
4-IPOT•HFB	−49.01	−3.43	−52.44	−51.73	−3.16	−54.89
ΔE (4-EPOT– 4-IPOT)	−5.62	−2.52	−8.15	−3.99	−3.55	−7.54
4-EPOT•MES	−57.49	−5.17	−62.66	−58.95	−5.79	−64.74
4-IPOT•MES	−51.53	−2.47	−54.00	−53.64	−2.33	−55.97
ΔE (4-EPOT– 4-IPOT)	−5.96	−2.70	−8.66	−5.11	−3.46	−8.77
4-EPOT•COL	−56.96	−5.55	−62.51	−58.10	−5.99	−64.09
4-IPOT•COL	−51.35	−2.51	−53.85	−53.85	−2.35	−56.20
ΔE (4-EPOT– 4-IPOT)	−5.61	−3.04	−8.66	−4.25	−3.64	−7.89

2.2.7 Halogen and Guest Mediated Architectural Isomerism

Supramolecular isomerism⁴¹ is the existence of more than one type of superstructure for the same molecular building block. When a molecule forms different supramolecular synthon, supramolecular isomerism is synonymous to polymorphism and if different architectures are responsible for the supramolecular isomerism, then it is called architectural isomerism.⁴² This can be achieved by the influence of different guest molecules in inclusion compounds. In some cases guest mediated structural change occurs with very little change in the host framework. Urea⁴³ and TPP⁴⁴ systems

experience this perturbation due to different guest inclusion. They crystallize in hexagonal and monoclinic system with hexagonal and pseudo hexagonal crystal packing. There are examples where guest exchange causes severe structural change. TOT clathrates exhibit cage-like cavities with small guest molecules but adopt channel-type cavity with long chain guest molecules.⁴⁵ Recently Aitipamula and Nangia reported supramolecular isomerism in crystal structures of a T-shaped molecule, 4,4-bis(4'-hydroxyphenyl)cyclohexanone. It forms ladder open framework with phenol and aniline guest molecules, but inclusion of *o/m*-fluorophenol changes the structure to brick wall framework.⁴⁶ Ward and co-workers have demonstrated the bilayer-to-brick architectural isomerism in their well-studied guanidium–organodisulfonate system.⁴² Conformational flexibility of the ligand leads to supramolecular isomerism in metal–organic coordination polymer. Zaworotko and co-workers reported supramolecular isomerism due to the different conformations of the ligand 1,2-bis(4-pyridyl)ethane in $\text{Co}(\text{NO}_3)_2$ complex.⁴⁷

Table 8. Some properties of halogen atoms.

Halogen	van der Walls radius (Å)			Electronegativity (Pauling scale)	Polarizability (halomethane)
	Bondi	Nyburg			
		major axis	minor axis		
F	1.47	1.38	1.30	4.0	2.62
Cl	1.76	1.78	1.58	3.0	4.55
Br	1.85	1.84	1.54	2.8	5.61
I	1.98	2.13	1.76	2.5	7.59

The reasons for the organization of 4-XPOT to a channel or cage type lattice depending on the host halogen atom were analyzed from several crystal structures. Since all interactions in the host···host and host···guest supramolecular assembly are weak, our arguments are based on differences in C–H···O, C–H···N, C–H···X and X···X interactions in the chloro and bromo channel structures reported previously compared to the iodo and ethynyl series reported in this thesis. The van der Waals radius, electronegativity, and polarizability of the halogen atoms are summarized in table 8.⁴⁸ The 2D layer assembly of 4-XPOT molecules, stabilized by the X_3 trimer synthon, has hexagonal symmetry in

all cases. The channel wall of 4-ClPOT and 4-BrPOT structures have weak C-H \cdots O/N interactions from the phenyl donor to the triazine ring of the next layer (Figure 8). The C-H \cdots O/N interactions become longer (weaker) from Cl to Br derivatives (Table 9) because the molecular layers are pushed apart by the larger Br atom compared to Cl. These interactions for the channel wall become too long (weak) for X = I, C \equiv C-H that the channel architecture can no longer be sustained by weak interactions. The weakening of the channel wall due to the longer interaction consistently drives crystallization of 4-IPOT and 4-EPOT towards the cage type lattice irrespective of the guest species. The reorganization of layers from channel to cage framework results in the wrapping of the guest by the cage type architecture, i.e. a more efficient close packing in the crystal. The difference between the channel and cage architecture is translation by ~ 6.0 Å, the radius of the hexagon, such that the stacked column along the *c*-axis changes from the infinite stack of triazine-X₃-trimer-triazine-X₃-trimer (Figure 1b) to the penta-decker sandwich of triazine-X₃-trimer-guest-X₃ trimer-triazine (Figure 2b) with the C_{3i}-PU connecting such supramolecular sandwiches. The C-H \cdots O/N interactions have normal distances because of the phenyl ring tilt in cage structures (Table 3). We surmise that the C_{3i}-PU, Br₃/I₃ trimer and C-H \cdots O/N interactions of the cage architecture are comparable in strength to the Cl₃/Br₃ trimer and C-H \cdots O/N interactions of the channel structures.

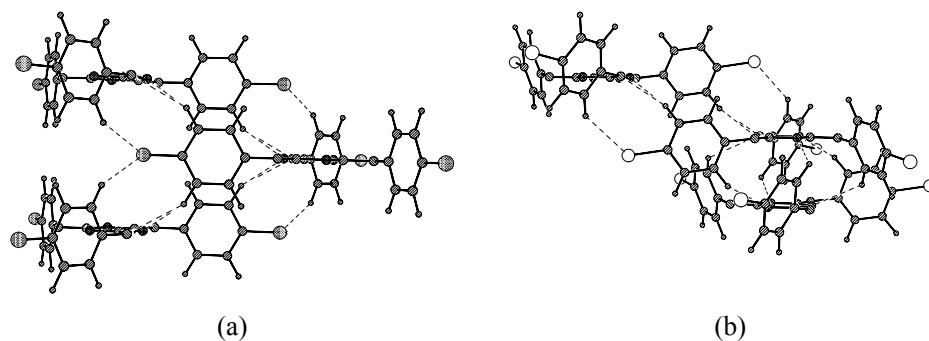
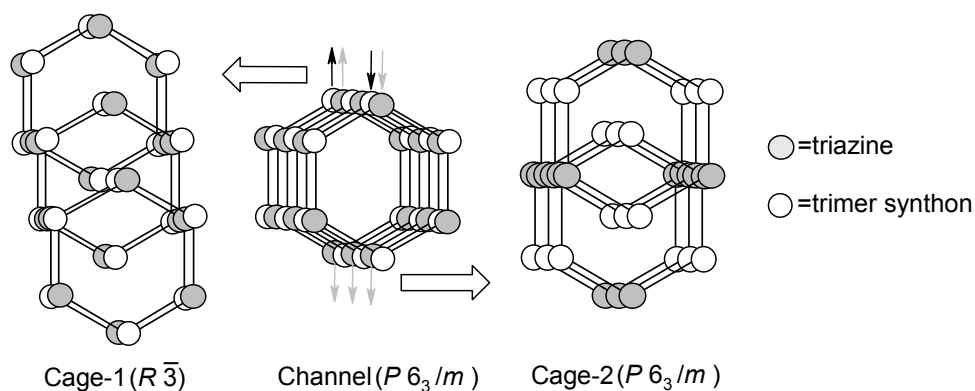


Figure 8. (a) Channel wall structure of 4-ClPOT to show the inter-layer C-H \cdots O/N and C-H \cdots X interactions. The phenyl ring is bisected by the central triazine plane. (c) The tilt of the phenyl ring in 4-IPOT cage structures optimizes C-H \cdots O/N interactions.

In the 4-EPOT•guest clathrate system there is further guest mediated architectural isomerism. In the CCl_4 inclusion structure every alternate hexagonal layer moves forward from its original positions in the channel structure such that triazine rings stack one above the other to form continuous C_{3i} -PU (Scheme 4). The ethynyl C–H interacts with phenyl π electron cloud rather than triple bond and forms continuous PU stack along the c -axis stabilized by $\pi\cdots\pi$ stacking and weak C–H \cdots N, C–H \cdots O interactions. It is important to note that 4-BrPOT host architecture also undergoes isomerisation depending upon the nature of the guest molecule. Hexagonal guest molecules such as HFB, HCB inclusions occur in cage framework whereas HMB is included in channel framework of 4-BrPOT. Thus, supramolecular isomerism of the host architecture is controlled by the numerous weak interactions in these crystal structures. The facile formation of both channel and cage type 4-XPOT adduct structures under near identical crystallization conditions means that the energy of these structures must be comparable.

Table 9. C–H \cdots N and C–H \cdots O hydrogen bonds in some channel structures of 4-CIPOT and 4-BrPOT (Scheme 1).

Compound	Space group	d (Å), θ (°) of C–H \cdots N	d (Å), θ (°) of C–H \cdots O
4-CIPOT•TIB	$P6_3$	2.58, 155.7	2.82, 148.9
4-CIPOT•TBB	$P6_3$	2.40, 158.1	2.55, 150.1
4-CIPOT•TNB	$P6_3/m$	2.71, 144.0	2.74, 146.2
4-CIPOT•HCB	$P6_3/m$	2.67, 145.4	2.81, 142.9
4-BrPOT•TIB	$P6_3$	2.68, 155.0	2.92, 146.2
4-BrPOT•TBB	$P6_3$	2.60, 157.3	2.79, 148.6
4-BrPOT•HMB	$P6_3/m$	2.84, 143.0	2.91, 145.7
4-BrPOT•TNM	$P6_3/m$	2.88, 143.7	2.98, 143.9
4-BrPOT•COL	$P6_3/m$	2.64, 160.2	2.83, 149.9
4-BrPOT•MNP	$P6_3/m$	2.68, 158.9	2.82, 153.4



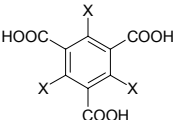
Scheme 4. The schematic diagram shows how architectural isomerism occurs by the translations of hexagonal layers from channel framework to two different types of cage structures. Top arrows direct channel to cage-1 ($R\bar{3}$) framework transformation and bottom arrows indicate the movement of hexagons from channel to cage-2 framework in 4-EPOT•CCl₄ crystal structure.

2.2.8 Hexagonal Crystal System

A recurring theme in over forty 4-XPOT•guest ($X = \text{Cl}, \text{Br}, \text{I}, \text{C}\equiv\text{C}-\text{H}, \text{NO}_2$) structures is that all these trigonal tectons crystallize in high symmetry space groups, e.g. $P6_3/m$, $R\bar{3}$, $P6_3$, $P-3$. In general, trigonal molecules do not reside on the Wyckoff position in crystal structures ($Z' > 1/3$), as shown by statistics from CSD search (Table 10).⁴⁹ According to the close packing ideas of Kitaigorodskii,⁵⁰ the only molecular symmetry element that is routinely carried over into the crystal is the inversion center. A recent database study shows that there is a hierarchy in the retention of molecular symmetry elements during crystallization: C_i (99%), S_4 (73%), S_6 (67%), C_3 (66%), C_2 (59%), C_s (26%).⁴⁹ These statistics mean that it is relatively easier to predict the location of a molecule in its crystal structure on a point-acting symmetry operation (C_i , S_4 , S_6) compared to rotation axes (C_2 , C_3). In the high symmetry crystal structures of 4-XPOT, the hexagonal layer of alternating triazine molecule and halogen trimer synthon is the building block for further crystal growth in the third dimension. The stacking of these layers in the channel (without offset, eclipsed) and cage (with offset, staggered) structures occurs without a loss of the hexagonal symmetry in all cases. This is because

in 4-Cl/BrPOT channel structures: (1) the size of the halogen trimer synthon and the stacked triazine ring along the column is about the same to facilitate C–H···O/N interactions (Figure 1b), (2) the weak C–H···O/N interactions (Table 9) between adjacent host molecules maintain inter-layer registry and transmit the symmetry information to the third dimension. In the 4-IPOT cage crystal structures, the triazine rings aggregate via the point-acting C_{3i} -PU because: (1) the dipole-assisted anti-parallel stacking of octupolar triazine rings is favored, (2) the centrosymmetric PU is additionally stabilized by six mutual C–H···N interactions (2.66–2.73 Å; Table 2; Figure 8b). In summary, it is the C_{3i} -PU structural unit, or the symmetry retaining S_6 dimer, which carries over the trigonal molecular symmetry to the rhombohedral crystal system. A survey of the recent literature shows that triphenylphosphonium salts are an example of trigonal molecules that routinely crystallize in the cubic lattice.⁵¹ Here, the triphenyl groups engage in the sextuple phenyl embrace, stabilized by the edge-to-face and vertex-to-face interactions, to form a S_6 dimer motif, which resides on the special position in the crystal. Lastly, we note that even though the above-mentioned factors are all weak in nature they are nonetheless collectively significant for the structural and functional behavior of the 4-XPOT host. The closely related molecule, 2,4,6-tris(4-bromotetrafluorophenoxy)-1,3,5-triazine,⁵² in which C–H···X type interactions are not possible, crystallizes in the triclinic space group $P\bar{1}$ and does not exhibit guest inclusion behavior. Similarly, fluorophenoxytriazine⁵³ (4-FPOT, space group $P2_1/c$) also does not form inclusion crystals because fluorine is too hard and electronegative to participate in cohesive F···F interactions through the F_3 trimer synthon.

Table 10. Frequency of some C_3 molecules crystallizing in high symmetry space groups. Data extracted using CSD search.

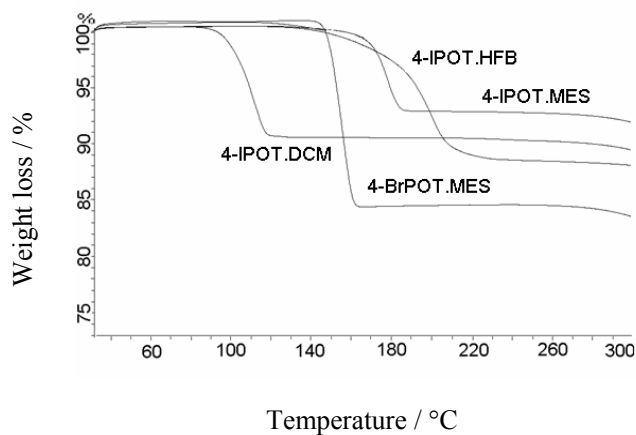
Compound Type	Crystal structures containing C_3 axis	Number of trigonal molecules
	1	19

	6	71
	2	14
	8	71
	61	89
	5	28

Trigonal molecules do not always crystallize in high symmetry space groups. For example, molecular layers are assembled via the appropriate X_3 synthon of (pseudo) hexagonal symmetry in trihalomesitylenes¹⁵ (halo = Cl, Br, I) but crystallization occurs in the triclinic space group $P\bar{1}$ because there are no specific inter-layer interactions (e.g. C–H \cdots O/N in triazines) to control growth in the third dimension. Similarly, the hexagonal layer network in 2,4,6-triethynyl-1,3,5-triazine⁵⁴ does not have perfect D_{3h} symmetry, but instead is C_2 symmetric, with two types of short C–H \cdots N interactions in the monoclinic crystal system C_2/c . This structure is similar to the interaction network in cyanuric chloride,⁵⁵ a prototype trigonal molecule assembled via Cl \cdots N interactions. Although these C_3 molecules have hexagonal 2D layer structures with triangular arrays of molecules and synthons they lack the high crystal symmetry characteristic of the

phenoxy triazines. The CSD contains five organic crystal structures with iodo trimer synthon in I...I distance of 3.5-4.0 Å but these motifs are pseudo trigonal in lower symmetry space groups (CSD refcodes and space group (April 2004 update): QODRUW, $P2_1/c$; QODSAD, $C2/c$; SAQZOY, $P\bar{1}$; SAQZOY01, $P\bar{1}$; EJERAM, $P\bar{1}$). We present here new examples of high symmetry iodo trimer synthon for crystal engineering. Trigonal tectons such as 1,3,5-benzenetricarboxylic acid (trimesic acid) and 1,3,5-cyclohexanetricarboxylic acid⁵⁶ are expected to produce robust hexagonal networks but these structures usually crystallize in monoclinic space groups like $P2_1/c$, $C2/c$. The frequent interpenetration in the hydrogen bond networks of these tricarboxylic acids prompts us to note that we have thus far not found any example of catenation in the 4-XPOT family; perhaps the 12 Å diameter cavities are too small to permit interweaving of identical networks and the specific interlayer interaction also prevent interpenetration.

2.2.9 Thermal Analysis



(a)

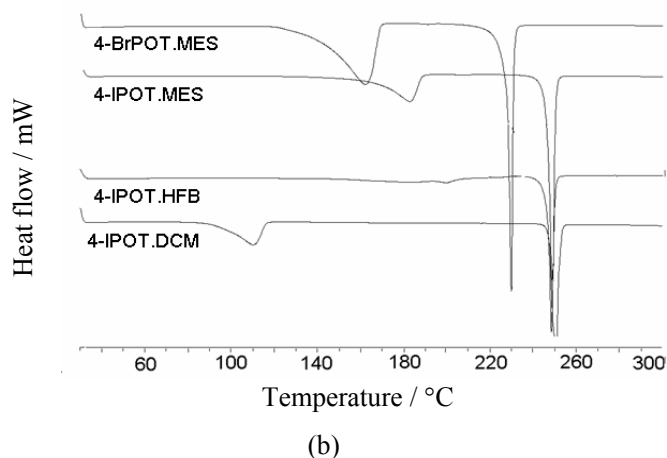


Figure 9. (a) TG and (b) DSC of 4-BrPOT•mesitylene, 4-IPOT•mesitylene 4-IPOT•dichloromethane and 4-IPOT•hexafluorobenzene. Guest release occurs at a higher temperature from the cage lattice compared to the channel framework for the same guest (MES). Volatile guest (CH_2Cl_2 , HFB) escape from the clathrate at a much higher temperature than the boiling point of the pure solvent.

Of the ten 4-IPOT•guest crystal structures described in this thesis, the guest molecules are ordered in two structures (HCB, HFB) whereas they are disordered in other eight clathrates. Thermal gravimetric analysis (TGA) of host–guest compounds provides valuable data about the stability of the host framework, the nature of guest enclathration in the cavity, and the strength of host–guest interactions.^{1c} An added motivation for TGA measurements in the present case was to confirm the host:guest stoichiometry. Some times it is difficult to locate and assign highly disordered guest atoms from the difference Fourier maps in the crystal structure refinement cycle. While the nature of the guest species can be inferred from the solvents and components used during cocrystallization, the exact host:guest stoichiometry is difficult to determine in cases of heavy guest disorder. Differential scanning calorimetry (DSC) confirms the phase purity of these 4-IPOT inclusion solids. TGA shows that the solvent/guest is released at a temperature that corresponds to the first endotherm in the DSC. Melting of the host compound occurs at the second endotherm at 250–300 °C in all 4-IPOT•guest compounds. The difference in guest evolution from the 4-BrPOT channel and 4-IPOT

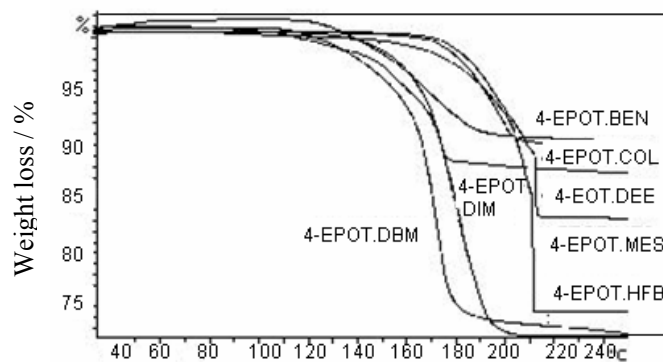
cage lattice is shown in figure 9. Evolution of mesitylene and collidine occurs at 20–40 °C higher temperatures from the cage framework compared to the channel inclusion structure because the host framework surrounds the solvent in the former structure. Variable temperature PXRD experiments show that both the structures (cage and channel) transforms to the same close packed structure⁵² (*R3c*). The difference in temperature between the release of solvent from the clathrate and the normal boiling point of that solvent, $T_{\text{onset}} - T_{\text{bp}}$, is a measure of the strength of host–guest interactions and the physical robustness of the lattice. Comparison of T_{onset} for CH_2Cl_2 (96 °C) and hexafluorobenzene (160 °C) with their $T_{\text{onset}} - T_{\text{bp}}$ values (56 °C, 78 °C; Figure 9) shows that the guest is able to vaporize and escape from the host only after the framework starts to disintegrate. The T_{onset} values for CH_2Cl_2 , CH_2Br_2 and CH_2I_2 guest release increase progressively (96, 116, 152°C), though the difference, $T_{\text{onset}} - T_{\text{bp}}$ decreases for the higher boiling guest. Further the host:guest stoichiometry of 2:1 determined from the X-ray data matches with the guest weight loss in all cases except the CH_2X_2 solvents (Table 11). The 1:1 stoichiometry from the TGA measurement for 4-IPOT• CH_2X_2 is used here.

Table 11. Relevant thermal analysis (TG/DSC) data for the inclusion compounds.

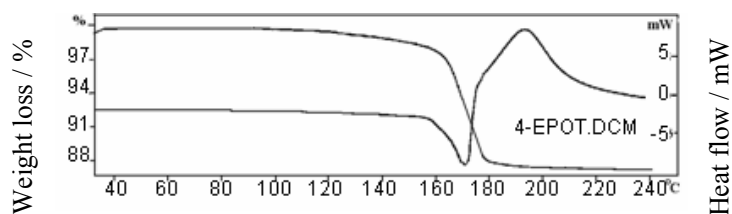
Inclusion compounds	Observed weight loss from TG (%)	Calculated weight loss (%) (host:guest ratio)	Guest release $T_{\text{on}} / ^\circ\text{C}$	Boiling point of the guest ($^\circ\text{C}$)
4-IPOT•MES	7.6	7.6 (2:1)	169	164
4-IPOT•COL	7.7	7.6 (2:1)	155	168
4-IPOT•DCM	9.9	10.4 (1:1)	96	40
4-IPOT•DBM	19.1	19.1 (1:1)	116	97
4-IPOT•DIM	26.9	26.7 (1:1)	152	181
4-IPOT•MNP	9.1	8.8 (2:1)	228	243
4-IPOT•HFB	12.0	11.2 (2:1)	160	81
4-BrPOT•HFB	13.3	13.5 (2:1)	155	81
4-BrPOT•MES	16.6	20.2 (1:1)	139	164

The isostructural 4-EPOT•guest clathrates are more stable than the corresponding 4-IPOT•guest systems. Comparison of T_{onset} for CH_2Cl_2 (163 °C), diethylether (156 °C) and hexafluorobenzene (189 °C) with their $T_{\text{onset}} - T_{\text{bp}}$ values (123,

121 and 109 °C respectively; Figure 10; Table 12) shows that the guest is able to vaporize and escape from the host only after the framework starts to disintegrate. After melting the material solidifies immediately and becomes red in colour. DSC experiment also shows a large exotherm after the endotherm corresponding to guest release and melting. This is probably due to polymerization along with decomposition of the compound. For this reason the host–guest ratios are not possible to calculate accurately from TG analysis for $R\bar{3}$ structures in which guest molecules are released during melting. The ratios are therefore determined by $^1\text{H-NMR}$ integrations. This is further supported in isostructural 4-IPOT series with similar guest molecules and were determined by TG as well as $^1\text{H-NMR}$. The $P6_3/m$ cage structures are calculated to have a 1:1 host–guest ratio by TG. The above thermochemical measurements and the ready formation of inclusion crystals suggest that the physical strength of 4-EPOT lattice could be exploited for the entrapment of volatile liquids and gases.



(a)



(b)

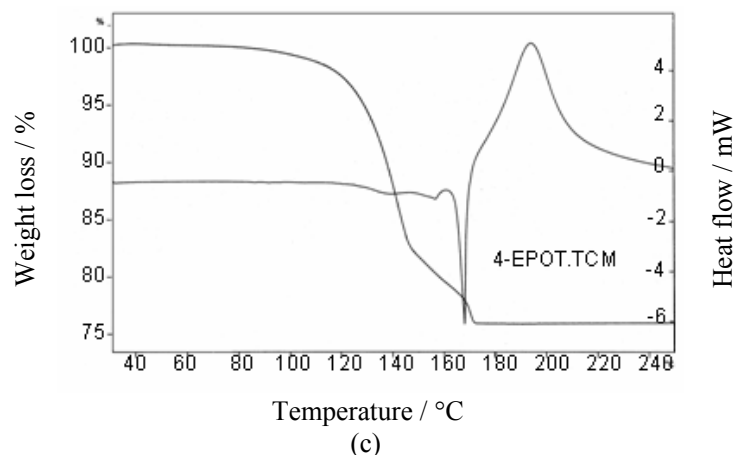


Figure 10. (a) TGA plot of 4-EPOT with guests mesitylene, collidine, dibromomethane, diiodomethane, benzene, hexafluorobenzene and diethyl ether. (b) TGA and DSC plot of 4-EPOT•dichloromethane. (c) TGA and DSC plot of 4-EPOT•tetrachloromethane.

Table 12. Relevant thermal analysis data on 4-EPOT•guest inclusion compounds.

Inclusion compounds	Host•guest ratio ^a	Guest release T_{onset} (°C)	Boiling point of the guest (T_{bp} , °C)	$T_{\text{onset}} - T_{\text{bp}}$
4-EPOT•DCM	1:1	162.9	40	122.9
4-EPOT•DBM	1:1	147.7	97	50.7
4-EPOT•DIM	1:1	162.0	181	-19.0
4-EPOT•MES	2:1	177.5	164	13.5
4-EPOT•COL	2:1	177.7	168	9.7
4-EPOT•HFB	2:1	184.3	81	103.3
4-EPOT•BEN	2:1	137.8	80	57.8
4-EPOT•DEE	1:1	119.5	36	83.5
4-EPOT•TCM	1:1	125.6	76	49.6

^a Host:guest ratio calculated based on ¹H-NMR.

2.3 Conclusions

Crystal engineering of robust, high symmetry host architecture through a joint consideration of molecular trigonal symmetry, weak halogen···halogen trimer synthon, and C_{3v} -PU aggregate is described. We show that the halogen atom may be used as the steering group to control the type of the host architecture whereas the nature of the guest

species determines the order/disorder of the included species. 4-CIPOT routinely gives channel type architectures and 4-IPOT favors the cage lattice, while 4-BrPOT forms either types of structures guided by the nature of the guest molecule. The channel structures have stronger C–H \cdots O/N interactions along the *c*-axis but slightly weaker chloro trimer synthon in the *ab*-plane whereas the cage structures have stabilization from the stronger iodo trimer synthon and Piedfort Unit. Both channel and cage type host–guest architectures have comparable stability and this explains why 4-BrPOT, which is intermediate between chlorine and iodine, gives both types of crystal structures. The persistent crystallization of 4-XPOT host molecules via the halogen trimer synthon underscores the significance of this cooperative recognition motif in designing robust host frameworks. The importance of these halogen trimer synthon can be realized by the different crystal structure of 2,4,6-tris(4-methylphenoxy)-1,3,5-triazine, where the trimer synthon is absent due to substitution of halogens by methyl group.⁵⁷ The hexagonal layer of triazine molecules and halogen trimers at the nodes is shown to be the structural building unit for self-assembly to the channel and cage frameworks. The weak interlayer interactions permit slipping of 2D sheets to induce supramolecular isomerization from channel to cage host architecture. The 4-XPOT tecton fulfils the criteria of a good host framework: it forms strong and robust isostructural frameworks and yet the lattice is flexible enough to breath. These results are an elegant illustration of the tecton \rightarrow synthon \rightarrow crystal design paradigm with weak intermolecular interactions. Because of larger size and high polarizability of iodine, the iodo compounds differ from corresponding bromo and chloro compounds in several cases, where the interactions of the halogens are different. In 4-XPOT series halogen \cdots halogen interactions are retained in all cases but it differs slightly in other regions to give architectural isomerism.

The ethynyl group acts as a supramolecular pseudo halogen. It produces isostructural crystal structure on exchange with iodo group in 4-XPOT tecton. 4-EPOT exhibits architectural isomerism by the inclusion of tetrahedral symmetry guest molecule, CCl₄. In this structure the ethynyl H donates to the phenyl ring π -cloud, indicates that there is little selectivity between ethynyl triple bond and phenyl π electron

cloud as acceptor. Statistical survey of the CSD shows that C–H $\cdots\pi$ interactions in infinite chains are stronger than these in dimers due to stabilization by cooperativity.

Thermal experiments as well as theoretical calculations show that the cage structure is stable compared to channel framework because desolvation requires severe fragmentation of the host network in cage structure compared to channel structure. Ethynyl trimer mediated cage host–guest system is more stable to temperature than the iodo trimer mediated cage architecture. Theoretical lattice energy calculation indicates that the main contribution to stabilization comes from van der Waals interactions.

2.4 Experimental Section

Synthesis

2,4,6-Tris(4-iodophenoxy)-1,3,5-triazine (4-IPOT): 4-Iodophenol and KOH (4.0 equiv.) were dissolved in acetone (40 mL) and stirred for half an hour. Cyanuric chloride (1.0 equiv.) was added to the reaction mixture at 0 °C and stirred for one hour. The reaction mixture was allowed to stir for another 48 hours at room temperature, and then poured into crushed ice and the resulting white precipitate was suction filtered and washed with methanol. Drying and column purification gave the product with satisfactory NMR and IR spectra.

2,4,6-Tris(4-ethynylphenoxy)-1,3,5-triazine (4-EPOT): 4-EPOT has been synthesized from 4-IPOT (1.0 mmol, 735 mg) by sonogashira coupling using trimethylsilylacetylene (4.5 mmol, 0.7 mL), CuI (20 mg), dichlorotriphenylphosphine Pd(II) catalyst (50 mg) in triethylamine and THF solvent mixture (1:1, 20 mL). Dry solvents were used and the reaction was performed under inert atmosphere of N₂. All reagents were added at 0°C and stirred for 1 hour at that temperature then stirred at room temperature over night and the solvent were removed by vacuum from the reaction mixture. Solid was washed by methanol and dissolved in CH₂Cl₂ (10 mL). Five equivalent of Bu₄N⁺F[−] trihydrate (5 mmol, 1.575 g) was added and stirred for half an hour to deprotect the trimethylsilyl group. Solvent was evaporated using vacuum and the solid was washed by methanol and purified by column chromatography.

2,4,6-Tris(4-iodophenoxy)-1,3,5-triazine (4-IPOT): $^1\text{H-NMR}$ (CDCl_3 , 200 MHz) δ 7.68 (d, J 8Hz, 6H), 6.88 (d, J 8Hz, 6H).

IR (KBr) 3082, 3057, 1591, 1564, 1481, 1205 cm^{-1} .

2,4,6-Tris(4-ethynylphenoxy)-1,3,5-triazine (4-EPOT): $^1\text{H-NMR}$ (CDCl_3 , 400 MHz) δ 7.49 (d, J 8Hz, 6H), 7.10 (d, J 8Hz, 6H), 3.08 (s, 3H).

IR (KBr): 3275, 1564, 1503, 1368, 1209 cm^{-1} .

Computational Lattice Energy Calculation

The lattice energy was calculated using Cerius² software (Accelrys, San Diego, CA, USA) using the following sequence. The unit cell structure was uploaded and molecules were corrected for the bond type. The space group was converted to *P1* keeping the structure unchanged to avoid fractional molecule in the asymmetric unit. Then force field (Compass) was loaded, followed by atom type correction using appropriate typing rules, the rigid body option was used to fix the conformation of the molecules. Ewald energy term was used for van der Waals and Coulombic force. The charge was assigned for each atom using the charge-equilibration method. Then single point and optimized energies were calculated.

X-ray Crystallography

Reflections were collected for single crystal of 4-IPOT with mesitylene, collidine, tribromomesitylene, hexachlorobenzene, dibromomethane and diiodomethane guest molecules on a Siemens SMART CCD area detector system using Mo- $K\alpha$ radiation ($\lambda = 0.71073 \text{ \AA}$). Empirical absorption corrections using SADABS⁵⁸ were applied. Data for 4-IPOT•dichloromethane were collected on a Bruker SMART CCD 1K area detector (Mo- $K\alpha$ radiation). Structure solution and refinement were performed with SHELX-97 packages.⁵⁹ X-ray intensity for 4-IPOT with hexafluorobenzene, triiodomesitylene, 1-methylnaphthalene guest molecules, Br-POT•hexafluorobenzene and all 4-EPOT•guest were measured on a Bruker SMART APEX CCD area detector system equipped with graphite monochromator and a Mo- $K\alpha$ fine-focus sealed tube ($\lambda = 0.71073 \text{ \AA}$). The intensities were corrected for absorption effects using the multi-scan

technique (SADABS).⁵⁸ The structures were solved and refined using the Bruker SHELXTL⁵⁹ (version 6.14) Software Package. Hydrogen atoms were generated with idealized geometries and isotropically refined using the Riding model. Refinement of coordinates and anisotropic thermal parameters of non-hydrogen atoms were carried out by the full-matrix least-squares method. The final *R* indices are acceptable in all crystal structures. All C–H distances are neutron normalized to 1.083 Å for the weak hydrogen bonds listed in tables 2 and 3.

Thermal Analysis

Differential scanning calorimetry (DSC) was performed on Mettler Toledo DSC 822e module and thermal gravimetry (TG) was performed on Mettler Toledo TGA/SDTA 851e module. Crystals taken from the mother liquor were blotted dry on filter paper and placed in open alumina pans for TG experiment and in crimped but vented aluminum sample pans for DSC experiment. Sample size in each case was 5–7 mg. The sample was heated from 30–300 °C at a rate of 10 °C/min. The samples were purged with a flow of dry nitrogen at 150 ml/min for DSC and 50 mL/min for TG runs.

2.5 References

1. (a) *Comprehensive Supramolecular Chemistry, Solid-State Supramolecular Chemistry, Crystal Engineering*; Eds. D. D. MacNicol, F. Toda and R. Bishop, Oxford: Pergamon, **1996**, vol. 6. (b) Y. Aoyama, *Top. Curr. Chem.*, **1998**, 198, 131. (c) A. Nangia, *Curr. Opin. Solid State Mater. Sci.*, **2001**, 5, 115. (d) K. T. Holman, A. M. Pivovar, J. A. Swift and M. D. Ward, *Acc. Chem. Res.*, **2001**, 34, 107. (e) L. R. Nassimbeni, *Acc. Chem. Res.*, **2003**, 36, 631.
2. (a) M. D. Hollingsworth, *Science*, **2002**, 295, 2410. (b) J. L. Atwood, L. J. Barbour and A. Jerga, *Science*, **2002**, 296, 2367.
3. H. Davy, *Philos. Trans. R. Soc. Lond.*, **1811**, 101, 1.
4. (a) A. Nangia, *Nanoporous materials: Science and Engineering*; Eds. G. Q. Lu and X. S. Zhao, Imperial College Press: London, **2004**, pp.165.

5. (a) S. V. Kolotuchin, E. E. Fenlon, S. R. Wilson, C. J. Loweth and S. C. Zimmerman, *Angew. Chem., Int. Ed. Engl.*, **1995**, *34*, 2654. (b) C. V. K. Sharma, and A. Clearfield, *J. Am. Chem. Soc.*, **2000**, *122*, 4394. (c) D. J. Plaut, K. M. Lund and M. D. Ward, *Chem. Commun.*, **2000**, 769. (d) M. J. Zaworotko, *Chem. Commun.*, **2001**, 1. (e) T. Hertzsch, F. Budde, E. Weber and J. Hulliger, *Angew. Chem., Int. Ed.*, **2002**, *41*, 2282. (f) C.-Y. Su, Y.-P. Cai, C.-L. Chen, F. Lissner, B.-S. Kang and W. Kaim, *Angew. Chem., Int. Ed.*, **2002**, *41*, 3371. (g) B.-Q. Ma and P. Coppens, *Chem. Commun.*, **2003**, 2290.
6. (a) M. Simard, D. Su and J. D. Wuest, *J. Am. Chem. Soc.* **1991**, *113*, 4696. (b) X. Wang, M. Simard and J. D. Wuest, *J. Am. Chem. Soc.*, **1994**, *116*, 12119. (c) W. Guo, E. Galoppini, R. Gilardi, G. I. Rydja and Y.-H. Chen, *Cryst. Growth Des.*, **2001**, *1*, 231. (d) R. Thaimattam, F. Xue, J. A. R. P. Sarma, T. C. W. Mak and G. R. Desiraju, *J. Am. Chem. Soc.*, **2001**, *123*, 4432. (e) J. H. Fournier, T. Maris, J. D. Wuest, W. Z. Guo and E. Galoppini, *J. Am. Chem. Soc.*, **2003**, *125*, 1002. (f) J.-H. Fournier, T. Maris and J. D. Wuest, *J. Org. Chem.*, **2004**, *69*, 1762.
7. (a) R. K. R. Jetti, F. Xue, T. C. W. Mak and A. Nangia, *Cryst. Eng.*, **1999**, *2*, 215. (b) R. K. R. Jetti, P. K. Thallapally, F. Xue, T. C. W. Mak and A. Nangia, *Tetrahedron*, **2000**, *56*, 6707. (c) R. K. R. Jetti, A. Nangia, F. Xue and T. C. W. Mak, *Chem. Commun.*, **2001**, 919. (d) C. K. Broder, J. A. K. H. Howard, D. A. Keen, C. C. Wilson, F. H. Allen, R. K. R. Jetti, A. Nangia and G. R. Desiraju, *Acta Crystallogr.*, **2000**, *B56*, 1080. (e) R. K. R. Jetti, P. K. Thallapally, A. Nangia, C.-K. Lam and T. C. W. Mak, *Chem. Commun.*, **2002**, 952.
8. (a) S. Mann, *Nature*, **1993**, *365*, 499. (b) A. Jouaiti, M. W. Hosseini and N. Kyritsakas, *Chem. Commun.*, **2003**, 472.
9. (a) G. R. Desiraju, *Angew. Chem. Int. Ed.*, **1995**, *34*, 2311. (b) A. Nangia and G. R. Desiraju, *Top. Curr. Chem.*, **1998**, *98*, 57.
10. O. M. Yaghi, H. Li, C. Davis, D. Richardson and T. L. Groy, *Acc. Chem. Res.*, **1998**, *31*, 474.
11. O. Ermer, *J. Am. Chem. Soc.*, **1988**, *110*, 3747.
12. D. S. Reddy, D. C. Craig and G. R. Desiraju, *J. Am. Chem. Soc.*, **1996**, *118*, 4090.

13. S. Banfi, L. Carlucci, E. Caruso, G. Ciani and D. M. Proserpio, *Cryst. Growth Des.*, **2004**, *4*, 29.
14. (a) D. J. Duchamp and R. E. Marsh, *Acta Crystallogr.*, **1969**, *B25*, 5. (b) O. Ermer and J. Neudorfi, *Helv. Chim. Acta.*, **2001**, *84*, 1268. (c) B.-Q. Ma and P. Coppens, *Chem. Commun.*, **2003**, 2290.
15. E. Bosch, *Cryst. Growth Des.*, **2002**, *2*, 299.
16. A. Angeloni, P. C. Crawford, A. G. Orpen, T. J. Podesta and B. J. Shore, *Chem. Eur. J.*, **2004**, *10*, 3783.
17. L. Brammer, G. M. Espallargas and H. Adams, *CrystEngComm*, **2003**, *5*, 343.
18. J. W. Yao, J. C. Cole, E. Pidcock, F. H. Allen, J. A. K. Howard and W. D. S. Motherwell, *Acta Crystallogr.*, **1985**, *B58*, 640.
19. (a) The Piedfort Unit (PU) concept in hexahost design was first introduced by MacNicol. A. S. Jessiman, D. D. MacNicol, P. R. Malinson and I. Vallance, *J. Chem. Soc., Chem. Commun.*, **1990**, 1619. For recent examples, see: (b) L. Fábíán, P. Bombicz, M. Czugler, A. Kálmán, E. Weber and M. Hecker, *Supramol. Chem.*, **1999**, *11*, 151. (c) V. R. Thalladi, S. Brasselet, H.-C. Weiss, D. Blaser, A. K. Katz, H. L. Carrell, R. Boese, J. Zyss, A. Nangia and G. R. Desiraju, *J. Am. Chem. Soc.*, **1998**, *120*, 2563. (d) M. Czugler, E. Weber, L. Párkányi, P. P. Korkas and P. Bombicz, *Chem. Eur. J.*, **2003**, *9*, 3741.
20. (a) G. R. Desiraju and R. Parthasarathy, *J. Am. Chem. Soc.*, **1989**, *111*, 8725. (b) S. L. Price, A. J. Stone, J. Lucas, R. L. Rowland and A. E. Thornley, *J. Am. Chem. Soc.*, **1994**, *116*, 4910. (c) J. P. M. Lommerse, A. J. Stone, R. Taylor and F. H. Allen, *J. Am. Chem. Soc.*, **1996**, *118*, 3108.
21. (a) P. Metrangolo and G. Resnati, *Chem. Eur. J.*, **2001**, *7*, 2511. (b) T. Caronna, R. Liantonio, T. A. Logothetis, P. Metrangolo, T. Pilati and G. Resnati, *J. Am. Chem. Soc.*, **2004**, *126*, 4500. (c) T. A. Logothetis, F. Meyer, P. Metrangolo, T. Pilati and G. Resnati, *New J. Chem.*, **2004**, *28*, 760.
22. A. Dey, R. K. R. Jetti, R. Boese and G. R. Desiraju, *CrystEngComm*, **2003**, *5*, 248.
23. A. Dey and G. R. Desiraju, *CrystEngComm*, **2004**, *6*, 642.

24. (a) J. M. A. Robinson, B. M. Kariuki, K. D. M. Harris and D. Philp, *J. Chem. Soc., Perkin Trans. 2*, **1998**, 2459. (b) H.-C. Weiss, D. Bläser, R. Boese, B. M. Doughan and M. M. Haley, *Chem. Commun.*, **1997**, 1703. (c) H.-C. Weiss, R. Boese, H. L. Smith and M. M. Haley, *Chem. Commun.*, **1997**, 2403.
25. (a) E. Galoppini and R. Gilardi, *Chem. Commun.*, **1999**, 173. (b) W. Guo, E. Galoppini, R. Gilardi, G. I. Rydja and Y.-H. Chen, *Cryst. Growth Des.*, **2001**, *1*, 231. (c) D. S. Reddy, D. C. Craig and G. R. Desiraju, *J. Am. Chem. Soc.*, **1996**, *118*, 4090.
26. S. George, A. Nangia, C.-K. Lam, T. C. W. Mak and J.-F. Nicoud, *Chem. Commun.*, **2004**, 1202.
27. D. Philp and J. M. A. Robinson, *J. Chem. Soc., Perkin Trans. 2*, **1998**, 1643.
28. T. Steiner, E. B. Starikov, A. M. Amado and J. J. C. Teixeira-Dias, *J. Chem. Soc., Perkin Trans. 2*, **1995**, 1321.
29. G. A. Jeffrey, *An Introduction to Hydrogen Bonding*; OUP: Oxford, **1997**.
30. (a) R. M. Badger, *J. Chem. Phys.*, **1940**, *8*, 288. (b) R. M. Badger and S. H. Bauer, *J. Chem. Phys.*, **1937**, *5*, 839. (c) L. J. Bellami and R. J. Pace, *Spectrochim Acta.*, **1969**, *A25*, 319.
31. T. Steiner, M. Tamm, A. Grzegorzewski, N. Schulte, N. Veldman, A. M. M. Schreurs, J. A. Kanters, J. Kroon, J. V. D. Maas and B. Lutz, *J. Chem. Soc., Perkin Trans. 2*, **1996**, 2441.
32. A. J. Matzger, M. Shim and K. P. C. Vollhardt, *Chem. Commun.*, **1999**, 1871.
33. B. M. Kariuki, K. D. M. Harris, D. Philp and J. M. A. Robinson, *J. Am. Chem. Soc.*, **1997**, *119*, 12679.
34. (a) T. Steiner, *Angew. Chem. Int. Ed.*, **2002**, *41*, 48, (b) G. R. Desiraju and T. Steiner, in *The Weak Hydrogen Bond In Structural Chemistry and Biology*; Oxford University Press: New York, **1999**.
35. G. Gilli, F. Bellucci, F. Ferretti and P. Gilli, *J. Am. Chem. Soc.*, **1989**, *111*, 1023.
36. S. Scheiner, *Hydrogen Bonding. A Theoretical Perspective*; Oxford University Press: Oxford, **1997**.
37. B. M. Kariuki, K. D. M. Harris, D. Philp and J. M. A. Robinson, *J. Am. Chem. Soc.*, **1997**, *119*, 12679.

38. P. Vishweshwar, N. J. Babu, A. Nangia, S. A. Mason, H. Puschmann, R. Mondal and J. A. K. Howard, *J. Phys. Chem.*, **2004**, *A108*, 9406.
39. T. Steiner, *J. Chem. Soc., Chem. Commun.*, **1995**, 95.
40. T. Hosokawa, S. Datta, A. R. Sheth and D. J. W. Grant, *CrystEngComm*, **2004**, *6*, 243.
41. B. Moulton and M. J. Zaworotko, *Chem. Rev.*, **2001**, *101*, 1629.
42. (a) J. A. Swift, A. M. Pivovar, A. M. Reynolds and M. D. Ward, *J. Am. Chem. Soc.*, **1998**, *120*, 5887. (b) V. A. Russell, C. C. Evans, W. Li and M. D. Ward, *Science*, **1997**, *276*, 575. (c) K. T. Holman, A. M. Pivovar, J. A. Swift and M. D. Ward, *Acc. Chem. Res.*, **2001**, *34*, 107.
43. K. D. M. Harris, *Chem. Soc. Rev.*, **1997**, *26*, 279.
44. (a) H. R. Allcock, M. L. Levin and R. R. Whittle, *Inorg. Chem.*, **1986**, *25*, 41. (b) P. Sozzani, S. Bracco, A. Comotti, L. Ferretti and R. Simonutti, *Angew. Chem. Int. Ed.*, **2005**, *44*, 1816.
45. R. Gerdil, *Top. Curr. Chem.*, **1987**, *140*, 72.
46. S. Aitipamula and A. Nangia, *Chem. Eur. J.*, **2005**, *11*, 6727.
47. T. L. Hennigar, D. C. MacQuarrie, P. Losier, R. D. Rogers and M. J. Zaworotko, *Angew. Chem. Int. Ed.*, **1997**, *36*, 972.
48. (a) A. Bondi, *J. Phys. Chem.*, **1964**, *68*, 441. (b) S. C. Nyburg and C. H. Faerman, *Acta Crystallogr.*, **1985**, *B41*, 274. (c) L. Pogliani, *New J. Chem.*, **2003**, *27*, 919.
49. E. Pidcock, W. D. S. Motherwell and J. C. Cole, *Acta Crystallogr.*, **2003**, *59*, 634.
50. A. I. Kitaigorodskii in *Molecular Crystals and Molecules*; Academic Press: New York, **1973**.
51. I. Dance and M. Scudder, *New. J. Chem.*, **2001**, *25*, 1500.
52. K. Reichenbacher, H. I. Süss, H. Stoeckli-Evans, S. Bracco, P. Sozzani, E. Weber and J. Hulliger, *New. J. Chem.*, **2004**, *28*, 393.
53. R. Boese, G. R. Desiraju, R. K. R. Jetti, M. T. Kirchner, I. Ledoux, V. R. Thalladi and J. Zyss, *Struct. Chem.*, **2002**, *13*, 321.
54. M. Ohkita, M. Kawano, T. Suzuki and T. Tsuji, *Chem. Commun.*, **2002**, 3054.
55. K. Xu, D. M. Ho and R. A. Pascal, *J. Am. Chem. Soc.*, **1994**, *116*, 105.

- 56. B. R. Bhogala, P. Vishweshwar and A. Nangia, *Cryst. Growth Des.*, **2002**, 2, 325.
- 57. V. R. Thalladi, R. Boese, S. Brasselet, I. Ledoux, J. Zyss, R. K. R. Jetti and G. R. Desiraju, *Chem. Commun.*, **1999**, 1639.
- 58. G. M. Sheldrick, SADABS: (a) Program for Empirical Absorption Correction of Area Detector Data; University of Göttingen, Germany, **1996**. (b) Program for Multi-Scan Absorption Correction of Area Detector Data; Version 2.10. University of Göttingen, Germany, **2003**.
- 59. (a) Sheldrick, G. M. SHELXS-97, Program for the Solution of Crystal Structures, University of Göttingen, Germany, **1997**. (b) Sheldrick, G. M. SHELXL-97, Program for Crystal Structure Refinement, University of Göttingen, Germany, **1997**.

CHAPTER 3

HALOPHENOXYTRIAZINE, HALOGEN EXCHANGE AND ISOSTRUCTURALITY

3.1 Introduction

A functional group has a great impact on crystal packing. It has a definite shape, size and electronegativity, i.e. geometrical property and also electrostatic character. It is not always easy to distinguish and separate chemical and geometric effects on crystal packing. Kitaigorodskii has given importance to the volume and shape of functional groups in crystal packing. But the electronic nature of functional groups also cannot be over looked.¹ Desiraju distinguishes anisotropic long range forces (hydrogen bonds) from the equally important isotropic van der Waals forces.² In spite of their small sizes, –OH, –NH₂ groups are able to control supramolecular organization due to their strong H-bonding capability and electronic nature, however, as the size of the molecule increases the significance of geometric effects becomes important. From the examples published in the literature it has been noticed that a given packing motif may be able to tolerate small changes in the molecular structure without a considerable change in the already established close-packed crystal structure. These changes are minor alterations in substitution and/or epimerization. The tolerance may be ascribed to the presence of ~30% free space in close-packed structures because the packing coefficients of organic crystals are generally about 70%.³ This phenomenon where different molecules pack in a similar fashion to produce similar crystal structures, is called isostructurality.⁴ Kitaigorodskii was the first to summaries isostructurality in organic molecular crystals. Kálmán et al. have divided isostructurality into two categories—isostructural crystals or main-part isostructuralism of related molecules and homeostructural crystals.⁴ When isometric molecules (molecules with small differences on their surface) pack in similar motif it is called isostructural crystal and when the related molecules differing by substitutions on more than one atomic site have similar packing, it is called

homeostructural crystals. Kálmán has proposed two parameters to quantify isostructurality—unit-cell similarity index Π and isostructurality index $I_i(n)$.⁴

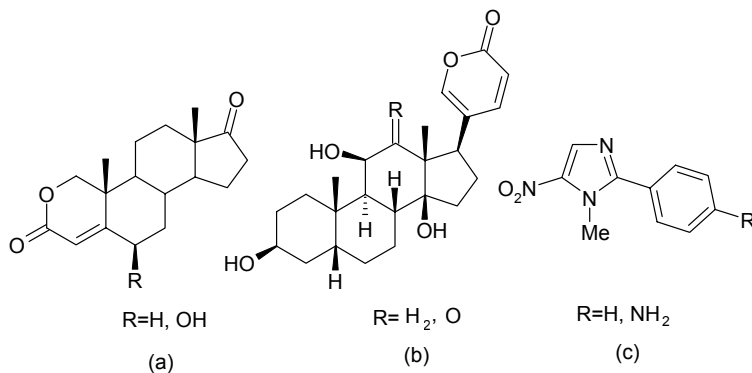
$$\Pi = \left| \frac{a + b + c}{a' + b' + c'} \right| - 1$$

Where a, b, c and a', b', c' are orthogonalized lattice parameters of the two crystals being compared and $(a + b + c) > (a' + b' + c')$. With increase in similarity of the related crystal structures the value of Π reaches zero.

$$I_i(n) = \left[1 - \left(\frac{\sum \Delta R_i^2}{n} \right)^{1/2} \right] \times 100$$

ΔR_i is the distance differences of identical n number of non-H atom coordinates in the two crystal structures within the same section of asymmetric units. The value of $I_i(n)$ approaches 100 as the two structures become similar.

From the crystal engineering point of view, it is important to have some knowledge about which groups are interchangeable and under which circumstances. Kitaigorodskii has ranked them as follows, (1) the halogens Cl, Br and I, (2) then O and S, (3) followed by C, quadrivalent Si, Ge, Sn and Pb.⁵ These latter ranked atoms are generally inner core atoms and so their sizes are important in crystal packing. There are some examples where strong hydrogen bonding functional groups, such as $-\text{OH}$, $-\text{NH}_2$, $=\text{O}$, can also replace hydrogen to produce isostructural crystals (Scheme 1).



Scheme 1. (a) H/OH exchange produces isostructural crystals. (b) H₂/O exchange

generates isostructurality and (c) H/NH₂ exchange forms isostructural crystals. One hydrogen in 2-oxa-4-androstene-3,17-dione is replaced by –OH in 6 α -hydroxy-2-oxa-4-androstene-3,17-dione.⁶ The weak C–H \cdots O hydrogen bond has been replaced by strong O–H \cdots O hydrogen bond keeping the overall crystal structure nearly unchanged (Figure 1). Keto–methylene exchange is observed in isostructural arenobufagin and gamabofotalin where keto group is prevented from H-bonding.⁷ Surprisingly, 1-methyl-5-nitro-2-phenylimidazole and its 4-amino derivative are isostructural in spite of the presence of strong N–H \cdots O H-bonds.⁸ Quite interestingly, naphthalene is isostructural to

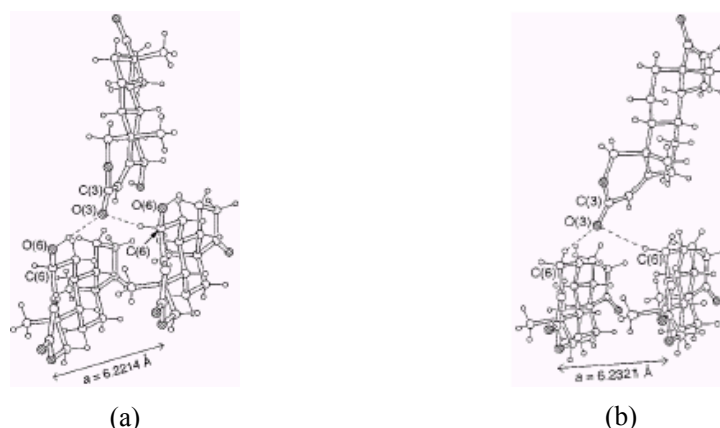
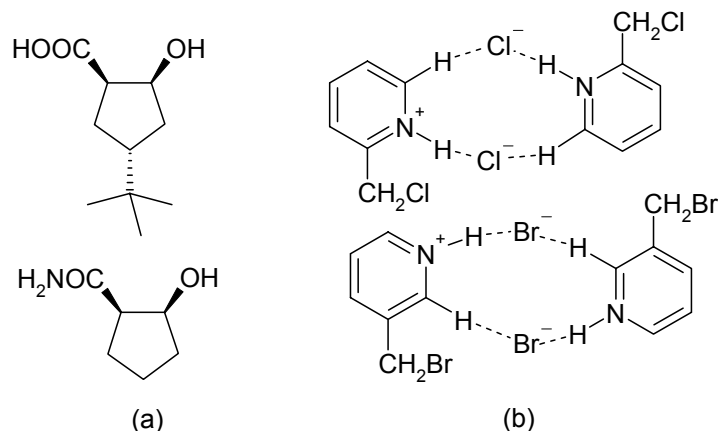


Figure 1. (a) Strong O–H \cdots O hydrogen bond in hydroxy lactone. (b) Weak C–H \cdots O hydrogen bond in non-hydroxy lactone, mimicking (a).

its β -substituted derivatives where the functional groups are –OH, –NH₂, –Me.⁴ Some other isometric replacements are hydrogen–methyl in digitoxigenin and (21*R*)- and (21*S*)-methyldigitoxigenins,⁹ methyl–ethyl in C₁₃H₁₁NS and C₁₄H₁₃NS.¹⁰ There is enough space around the methyl group and thus it can easily accommodate the ethyl group without considerable change in the structure. Oxygen and lone pair on phosphorous exchange has been published recently,¹¹ where it was concluded that P=O does not play a structure directing role. Due to close similarity in size and to some extent in shape, the phenyl–thiophene exchange also has been possible on a few occasions.¹² There are reports on isostructurality based on strong hydrogen bond in spite of the large difference in

volume,^{1a} and combination of weak and strong hydrogen bond (Scheme 2).¹³



Scheme 2. (a) Strong H-bonding functional groups direct the molecules to produce isostructural crystals. One molecule contains bulky *tert*-butyl group and it is absent in other molecule. (b) Combination of strong $N^+-H\cdots X^-$ and weak $C-H\cdots X^-$ hydrogen bonds produces isostructural crystals.

Chloro–methyl exchange is well known and this rule states that when the geometry of the groups governs the crystal packing they produce isostructural crystals due to their similar size and shape ($Cl\ 20\ \text{\AA}^3$ and $Me\ 24\ \text{\AA}^3$).¹⁴ There is a report on bromide and nitrate exchange in isostructural crystals in spite of their different shapes where both of the anions make strong H-bonds with the cation counter part.¹⁵ Above all these groups, the halogen exchange, specially Cl, Br and I to produce isostructurality, are more frequent. Isostructurality due to exchange of halides has also been reported by Steiner.¹⁶ Propargylammonium halides (Cl^- , Br^- , I^-) are isostructural where halide ions accept three H-bonds from ammonium group and one from terminal alkyne group. Another interesting isostructurality has been reported by Bar et al.¹⁷ in *para* substituted $X-C_6H_4-CH=N-C_6H_4-X'$ molecules. When $X = X' = Cl$ or Br , the molecules are not isostructural, but molecule with $X = Cl$ and $X' = Br$ is isostructural to the dichloro compound. On the other hand $X = Br$ and $X' = Cl$ substituted molecule is isostructural to dibromo derivative. It indicates the importance of halogens as well as the position of substitution in the molecules.

3.2 Crystal Structures of 4-XPOT

4-XPOT clathrate structures have been discussed in chapter 2. Except fluoro-derivative¹⁸ all other three halo-derivatives (Cl, Br, I) self assemble via halogen trimer synthon.²⁹ 4-ClPOT crystallizes in $P6_3/m$ and $P6_3$ space group and forms channel structure whereas 4-IPOT crystallizes in $R\bar{3}$ space group and forms cage lattice. The intermediate 4-BrPOT is isostructural to its chloro or iodo counterpart, depending upon guest molecules. Hulliger and co-workers reported the guest-free form of 4-BrPOT in $R3c$ space group²⁰ where the molecules form D_3 -PU and are stacked in column along the c -axis. There is no Br...Br interaction, rather bromo group is involved in Br... π interaction with the phenyl ring. Interestingly the parent phenoxytriazine compound and the corresponding methyl derivative²¹ are isostructural to 4-BrPOT (Figure 2), though the parent compound cannot maintain the crystallographic 3-fold symmetry due to slight distortion in the crystal structure from hexagonal symmetry and crystallizes in Ia space group, the structures are quite similar.²²

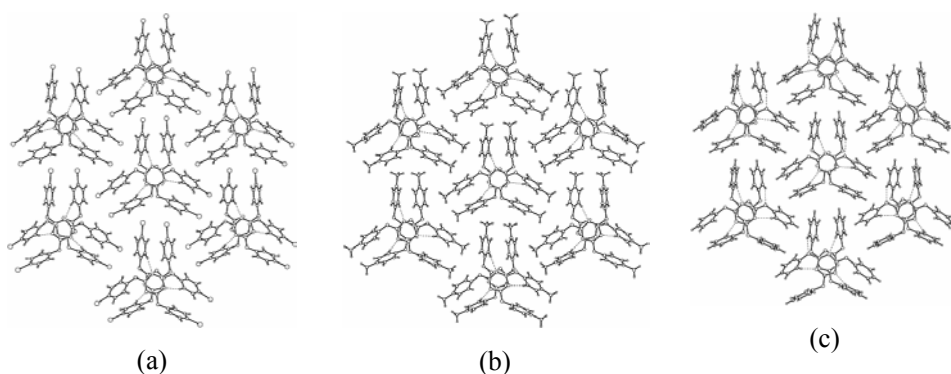


Figure 2. (a) Guest-free 4-BrPOT crystallizes in $R3c$ space group. (b) 4-MePOT is isostructural to the 4-BrPOT and (c) parent compound 4-HPOT crystallizes in Ia space group with slight distortion but similar packing.

3.3 Crystal Structures of 3-XPOT

Crystal structure of *meta*-chloro/bromo/methyl-phenoxytriazine have been reported previously by Nangia, Desiraju, Boese and their co-workers.²³ 3-ClPOT and 3-

BrPOT are isostructural and crystallize in $P\bar{3}c1$ space group, also isostructural to the corresponding Me derivative. It indicates that the halogens are playing more like a space filling role here. Similar to 4-BrPOT these structures have continuous Piedfort Unit in hexagonal packing (Fig 3). PUs of C_{3i} and D_3 symmetry (Scheme 3) are stabilized by $\pi\cdots\pi$ stacking between the central triazine rings, C-H \cdots N, C-H \cdots O interactions via *ortho*-hydrogens and herringbone C-H $\cdots\pi$ interactions.

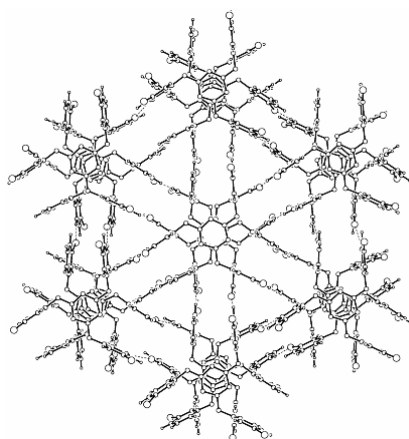
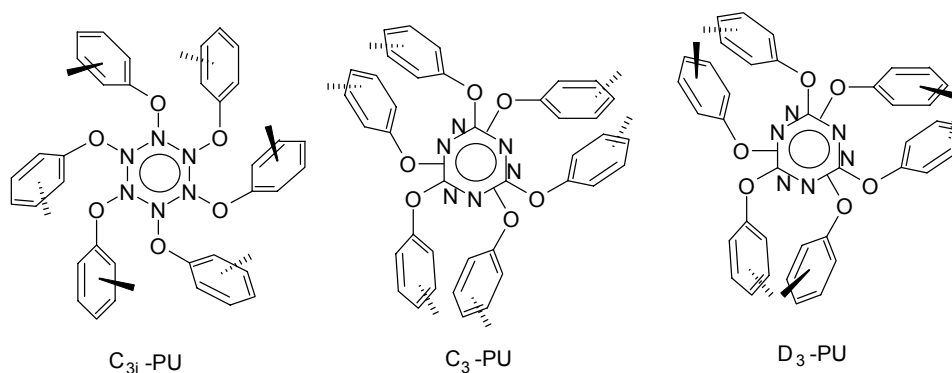


Figure 3. Hexagonal ($P\bar{3}c1$) crystal structure of 3-BrPOT. 3-MePOT and 3-CIPOT crystals are isostructural to it.



Scheme 3. Piedfort Unit of different symmetry.

In continuation of this work, the crystal structure of 3-IPOT is reported in this thesis. Contrary to chloro and bromo derivative it crystallizes in $R\bar{3}$ space group with 1/3 molecule in the asymmetric unit, the molecules are stacked in column made of only C_{3i} -PU and polarisation-induced helical I \cdots I interactions (type II, 3.85 Å, 169.9°, 83.0°) along the c -axis aggregate these columns (Figure 4). Again these columns pack in hexagonal array resulting in high symmetry crystal packing. The more polarisable iodine atom compared to chlorine and bromine²⁴ is responsible for this halogen-directed crystal structure. Triazine rings are separated by 3.42 and 3.87 Å in the PU and connected via C–H \cdots O and C–H \cdots N interactions using the *ortho*-H donors of phenyl ring where as the *meta*-H atoms participate in C–H \cdots I interaction. The interaction geometries are listed in table 1.

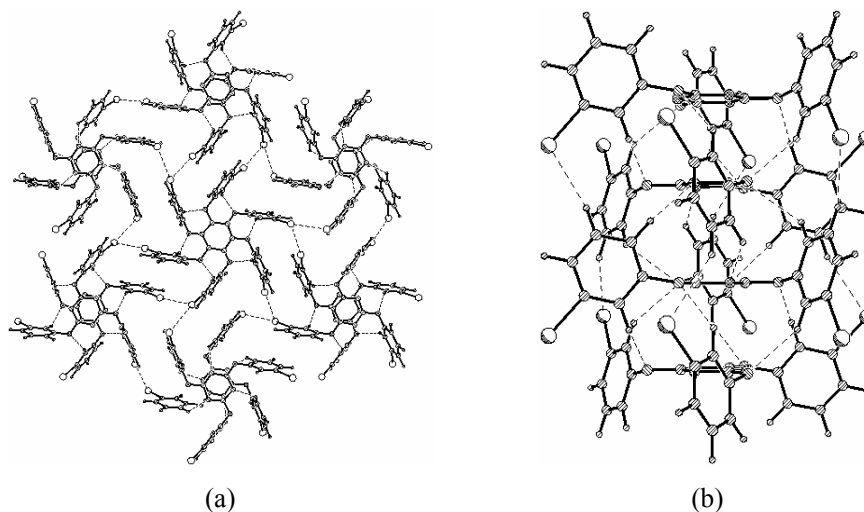


Figure 4. Crystal structure of 3-IPOT. (a) Helical iodo trimer motif. (b) Columnar structure along the c -axis stabilised by C–H \cdots O/N/I interactions.

3.4 Crystal Structures of 2-XPOT

In continuation of this series, crystal structures of 2-XPOT (X = F, Cl, Br, I) were determined. Unlike 4-XPOT and 3-XPOT, all the compounds crystallize in triclinic system. The molecules maintain approximate trigonal symmetry and form PU dimer of

approximate C_{3i} symmetry. The Piedfort Unit dimer forms on the opposite side of halogen, i.e. from the side of *ortho*-hydrogen to stabilize via C–H \cdots N and C–H \cdots O interactions along with $\pi\cdots\pi$ interaction. From the halogen side the PU stacking cannot propagate due to the absence of *ortho*-hydrogen and steric crowding by the halogen. Propagation is terminated by the *ortho*-halogen atoms and so molecules are unable to stack in trigonal symmetric column similar to 3-XPOT. Thus the presence of *ortho*-hydrogen is important in forming PU. When 2,4,6-tris(pentafluorophenoxy)-1,3,5-triazine (PF POT) or 2,4,6-tris(4-bromotetrafluorophenoxy)-1,3,5-triazine (4-BrTF POT) is crystallized, they do not form PU due to the absence of *ortho*-hydrogen and also can not maintain trigonal symmetry in the molecular conformation (Figure 5).²⁰

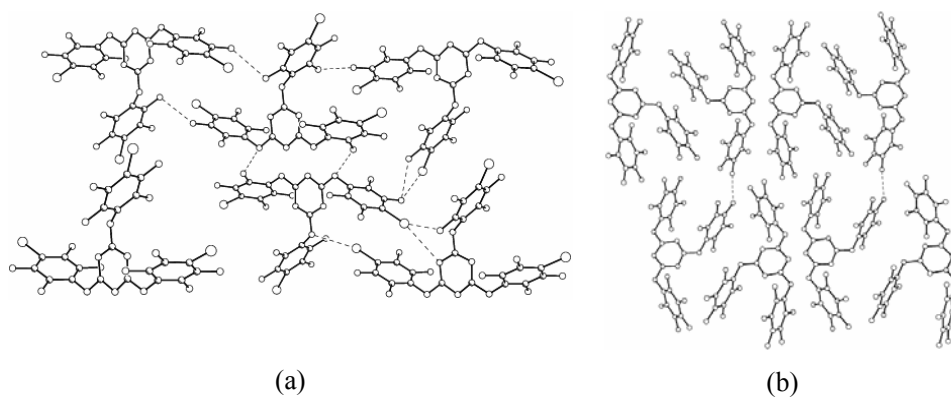


Figure 5. Crystal structures of (a) 4-BrTFPOT and (b) PF POT. The molecules are not trigonal symmetric in crystal structure and do not form PU.

3.4.1 2D Isostructural 2-FPOT and 2-CIPOT

2-FPOT crystallizes in $P\bar{1}$ space group and contains one molecule in asymmetric unit. It forms pseudo C_{3i} -PU dimers, stabilized via *ortho*-C–H \cdots O and *ortho*-C–H \cdots N interactions as well as $\pi\cdots\pi$ interaction. The $\pi\cdots\pi$ stacking distance between the triazine rings within a PU is 3.34 Å. Due to the obstacle of halogens on both sides of PU, they can not stack infinitely along PU axis but align with slight offset. One F atom from a PU sits on the top of the intramolecular fluoro trimer of the next PU dimer in the column. The closest F to F distance for this packing is 3.26 Å.²⁵ The stacking axis is

inclined by 26.6° angle with PU axis unlike hexagonal packing with 0° (Figure 6). These tilted columns pack parallelly to generate 3-D structure.

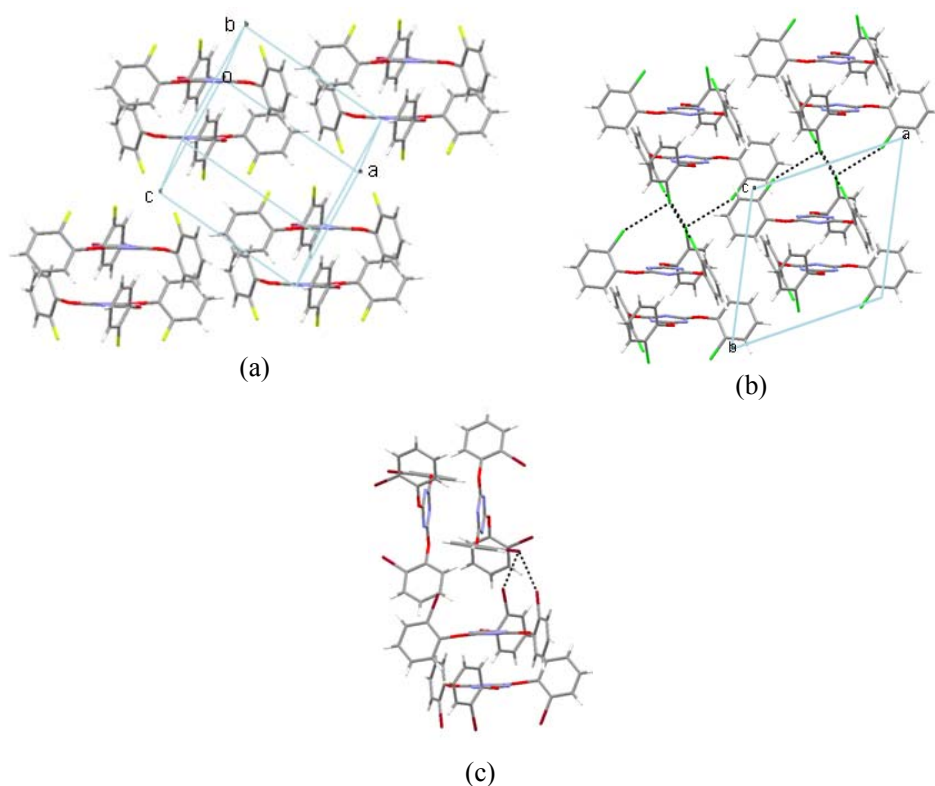


Figure 6. 2D layers of stacked PU dimers with offset in the crystal structures of (a) 2-FPOT and (b) 2-CIPOT. One halogen atom from a PU sits on the top of the intramolecular halogen trimer of the next PU dimer in the column. (c) Perpendicular PU dimers made of symmetry independent molecules interact via type II Br \cdots Br interaction.

2-CIPOT crystallizes in $P\bar{1}$ space group and contains two molecules in asymmetric unit. These molecules form PU dimers within symmetry related molecules in pseudo C_{3i} symmetry and stack similarly like 2-FPOT to form tilted columns. These parallel columns form alternate layers made of symmetry independent molecules. The $\pi\cdots\pi$ stacking distances between the triazine rings in PUs are 3.23 Å and 3.44 Å. The columns are tilted by 20.2° and 20.9° with respect to PU axes and the skew angle

between the symmetry independent column axes is 56.7° . Thus 2-FPOT and 2-CIPOT are two dimensionally isostructural. 4-XPOT clathrates are also two dimensional isostructural where the hexagonal layers are assembled via halogen trimer synthon. Recently Kálmán et al. have exemplified some polymorphic crystal structures with one, two and three dimensional isostructurality.²⁶ The Cl...Cl contacts arises when one Cl fill the space among three intramolecular chloro groups around inversion center. The interaction geometries are listed in table 1.

3.4.2 Isostructural 2-BrPOT and 2-IPOT

2-BrPOT crystallizes in $P\bar{1}$ space group with two molecules in the asymmetric unit. Here also similar PUs are observed and PUs are formed by symmetry related molecules only and the distances between the triazine planes within PUs are 3.46 Å and 3.62 Å. Two symmetry independent PUs are aligned almost perpendicular (87.2°) because bromo groups form type II contact 3.73 Å, 157.6° , 91.9° and 3.75 Å, 147.3° , 99.3° (Figure 6). The bromo groups are also involved in C-Br...O and C-Br... π contacts.

2-IPOT is isostructural to 2-BrPOT and the unit-cell similarity index $\Pi = 0.008$. The triazine planes are 3.34 Å and 3.49 Å apart in the PUs and the symmetry independent PUs are inclined by 87.1° angle with each other. The type II geometry of I...I interaction is 3.90 Å, 147.4° , 94.3° and 3.82 Å, 162.7° , 87.5° . The iodo group also makes C-I...O and C-I... π interactions in the structure. The interaction geometries are listed in table 1.

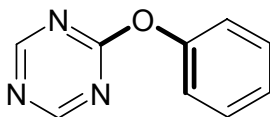
Table 1. Interaction geometries of 3-IPOT and 2-XPOT crystal structures.

Compound	Interaction	d (Å)	D (Å)	θ°
3-IPOT	C(7)-H...N	2.69	3.563(8)	137.6
	C(3)-H...O	2.58	3.497(6)	142.4
	C(6)-H...I	3.05	4.021(6)	149.0
	I...I		3.852(1)	169.9, 82.9
2-FPOT	C(9)-H...N(3)	2.60	3.560(2)	147.7
	C(14)-H...N(1)	2.74	3.527(3)	129.6
	C(17)-H...O(1)	2.75	3.604(3)	135.0

	C(18)–H...F(1)	2.39	3.310(4)	141.9
2-ClPOT	C(10)–H...N(2)	2.66	3.554(2)	140.0
	C(27)–H...N(3)	2.63	3.701(2)	169.9
	C(32)–H...O(4)	2.37	3.406(3)	159.8
	C(18)–H...O(3)	2.75	3.767(2)	155.9
	C(19)–H...Cl(5)	2.87	3.626(2)	127.2
	Cl(5)...Cl(5)		3.773(0)	150.8, 150.8
	Cl(5)...Cl(6)		3.708(1)	154.5, 106.5
	Cl(1)...Cl(3)		3.459(1)	160.5, 107.2
	Cl(2)...Cl(3)		3.611(1)	154.3, 105.9
2-BrPOT	C(15)–H...N(1)	2.62	3.596(8)	150.1
	C(36)–H...N(6)	2.65	3.630(8)	150.4
	C(8)–H...O(4)	2.59	3.542(8)	146.1
	C(35)–H...O(2)	2.64	3.635(8)	152.7
	Br(3)...Br(5)		3.729(1)	157.6, 92.0
	Br(1)...Br(5)		3.754(1)	147.3, 99.3
	C–Br(1)...O(6)		3.514(4)	160.3
2-IPOT	C(10)–H...N(5)	2.65	3.511(4)	135.6
	C(10)–H...N(5)	2.56	3.522(5)	147.7
	C(5)–H...O(3)	2.56	3.513(4)	146.0
	C(35)–H...O(4)	2.69	3.721(4)	158.5
	I(3)...I(2)		3.899(0)	147.4, 94.3
	I(5)...I(2)		3.823(0)	162.6, 87.5
	C–I(3)...O(2)		3.544(2)	160.1

3.5 Conformation of Phenoxytriazine

The conformation (shape) of flexible aryloxytriazine molecule is quite important in directing the crystal packing. The aryl groups are always perpendicular or nearly perpendicular to the central triazine core, which causes some free space on both sides of the triazine ring. This space can be filled up by the formation of PU through $\pi\cdots\pi$ stacking and it is also stabilized via C–H...N and C–H...O interactions. The potential energy surface scan of the torsion angle of C–O–C=C around phenoxy O–C bond of 2-phenoxy-1,3,5-triazine (Scheme 4) was carried out using B3LYP method with 6-31G** basis set in Gaussian 03 program.²⁷



Scheme 4. Torsion angles of C–O–C=C (bold) about phenoxy O–C bond are scanned.

The energy profile as a function of torsion angle (τ°) about O–C bond of phenoxy group is plotted in the range 0–180° (Figure 7). There is energy minimum around $\tau = 90^\circ$, which is the conformation of molecules observed in the crystal structures of different aryloxytriazine molecules. The co-planar conformation ($\tau = 180^\circ$) is 27 kcal/mol higher in energy and impossible to adopt by the molecules under normal P/T condition. The reason may be repulsion between *ortho*-C–H and N atoms.

In a previous thesis from this group, Sumod George examined the conformation of 1,2-dihydro-*N*-aryl-4,6-dimethylpyrimidin-2-one is in global minimum when the aryl groups are perpendicular to each other and this conformation is more stable by ~18 kcal/mol than the planar conformation.²⁸

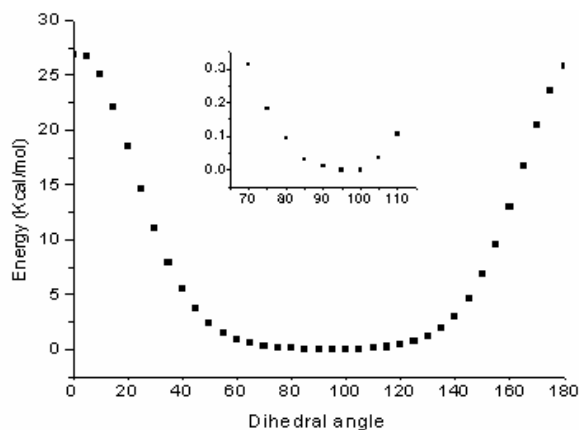


Figure 7. B3LYP/6-31G** energy vs. (triazine)C–O–C=C(phenyl) torsion angle in phenoxytriazine calculated using Gaussion 03 program. The perpendicular conformation is the most stable.

3.6 CSD Search

Recently Allen and co-workers have developed a program GRX (GRoup eXchange) to find all crystal structures of compounds related by functional group

exchange. It has been used to search the crystal structures related by a methyl–chlorine substitution and likewise for methyl–bromine substitution. The simulated powder patterns are then compared for pairs of crystal structures to check their isostructurality. The exchange resulted isostructurality for chlorine and bromine cases is 26% and 25% cases respectively, indicating that both halogens are equally effective in replacing a methyl group without changing the crystal structure.²⁹

CSD search was carried out to check how many halo derivatives show isostructurality after halogen (Cl, Br and I) exchange and how many times bromo follows chloro or iodo compounds crystal structure. So those families hits were considered where all three halo derivatives are present. If corresponding fluoro compounds are available then those also have been considered. The search criteria used for monovalent iodo compound is as follows—(i) CSD version 5.26 updates (Feb 2005), (ii) 3-D coordinate available, (iii) single component, (iv) not disordered, (v) not polymeric, (vi) no powder structure, (vii) R factor<0.1, (viii) no errors, (ix) no ions, (x) only organics. The hits obtained from this search were subjected to further search if corresponding bromo and chloro derivatives were present and listed in table 2 along with the unit-cell similarity index values for isostructural pairs.

Table 2. Results of the CSD search for molecules having crystal structures of at least Cl, Br, and I derivatives. Unit-cell similarity index is given for isostructural pairs.

No.	Fluoro	Chloro	Bromo	Iodo	Π
1	HUFVEJ	ACOKAE	ACOKEI	ACOKIM	I/Br=0.029
2		BAXTUQ	BAXVAY	BAXVIG	I/Cl=0.008
3	BEFSOV	SUHSET	JUKVIU	BEFSUB	I/Br=0.023 Br/F=0.068 I/F=0.093
4	PFBZAD01	CLBZAP01	BRBZAP	BENMOW01	I/Br=0.074 Br/F=0.026 I/F=0.103
5		UGIGEW	BROPOS	BENXAT	Nil
6		TECLPH01	TBPHAN	BOPDOZ	Br/Cl=0.020
7		CCBCBT	CBBCBT	CIBCBT	I/Br=0.032

8	VAXLUB	SEGWUW	SEGXAD	DIHRIV	Br/Cl=0.005
9		DCLMET10	DBRMET10	DIMETH01	I/Br=0.058
10	BENAFM10	NABRAJ	BRBZAM	DUMNUU	I/Br=0.017 Br/Cl=0.010 I/Cl=0.027
11		CLANIC05	PBRANL01	EJAYET	Br/Cl=0.026
12	KIFXIG	BENCLN02	BENBRN02	ENIGIR	Br/Cl=0.0003
13		FABDIW	FABDOC	FABDUI	I/Br=0.037 Br/Cl=0.015
14	GOGXOP	GOGXEF	PALWOO	GIHTIA	I/Br=0.035 Br/Cl=0.032 I/Cl=0.068
15	HIRNEB	TIYJEQ01	TIYJIU01	HIRPAZ01	I/Cl=0.032
16	BIGSUF	CLBZAM10	BRBZAO	IBNZAM	I/Br=0.017
17		CCACEN	BCACEN	ICACEN	I/Br=0.057 Br/Cl=0.029 I/Cl=0.087
18	FDOURD	CLDOUR	BROXUR10	IDOXUR	Br/Cl=0.007
19	DFPSLO	CLPSUL01	BPHSUL01	IPSULO	I/Br=0.018 Br/Cl=0.022
20		CPPTLM01	BPPHIM	IPTHIM10	I/Br=0.025 Br/Cl=0.003 I/Cl=0.022
21		CUNWIR	UNASOR	IQITIL	Nil
22	FURACL	CLURAC10	BRURAC10	IURACL10	Br/Cl=0.019
23		CLURID10	BRURID10	IURIDN10	Br/Cl=0.009
24	TAPSEI	JENHIV	JIKCAH	KEYNUX	Br/Cl=0.001
25		SINVOA	SINVIU10	KICRET	Br/Cl=0.009
26		MUTZOQ	MUTZIK	LALMEQ	Br/Cl=0.003
27		MUVBAG	MUTZUW	LALNUH	Br/Cl=0.004
28	LIKHOC	LIKHUI	LIKJEU	LIZNEN	Nil
29		LUSNAO	VIXHAL01	LUSNUI	I/Br=0.023 Br/Cl=0.031 I/Cl=0.055
30	NACBUO	NACCEZ	NACCAV	NACBOI	I/Br=0.019 Cl/F=0.046
31		NEGJAK	NEGKIT	NEGLEQ	I/Br=0.021

					Br/Cl=0.009 I/Cl=0.030
32		NEGJEO	NEGKOZ	NEGLIU	Br/Cl=0.005
33		NOTZAX	NOTZEB	NOTZIF	I/Br=0.009 Br/Cl=0.005 I/Cl=0.009
34		WIKKUW	WERBAW	NUZNOL	I/Br=0.009 Br/Cl=0.005 I/Cl=0.014
35		IHARAK	QUDHEC	OCOQIG	I/Br=0.021 Br/Cl=0.007 I/Cl=0.028
36		ODAHOQ	QODQUV01	ODAHUW	Br/Cl=0.003
37	FBENZA	CLBZAC	BRBZAC	OIBZAC	Br/Cl=0.006
38	PUGPIQ	DCLBIP	HIQQON	PIPROV	I/Br=0.021 Cl/F=0.046
39		ZIVLIZ	QOMYIA	QOMYOG	Br/Cl=0.003
40		CHLSAN	BSALAN	RAVTIR	I/Br=0.005 Br/Cl=0.008
41		YICFAR	YICFEV	RIWTOG	Br/Cl=0.017
42	FLUANA	CLANAC10	VAGTUS	SANZUC	Br/Cl=0.001 Cl/F=0.058
43		ZEPDAZ	PUZHIB	SAQZOY	I/Br=0.052 Br/Cl=0.020 I/Cl=0.074
44		DCLANT01	DBANTH01	TECWUT	I/Br=0.0003
45		ZZZVTY12	TPHMBR01	TEWWEX	Br/Cl=0.001
46	HEVLAV	VOYMUR	VOYNAY	VOYNEC	I/Br=0.009 Br/Cl=0.003 I/Cl=0.012
47		VICXOU	VUCHAC	VUCHEG	I/Br=0.012 Br/Cl=0.006 I/Cl=0.018
48		WOJXUO	WOJXIC	WOJXOI	Nil
49		CLNIBZ	BRNIBZ	WURTOS	Br/Cl=0.001
50		XALBER	MALGOV	XALBIV	Br/Cl=0.019
51		XAXQIW	XAXQOC	XAXQUI	I/Br=0.007 Br/Cl=0.013 I/Cl=0.006

52		YIHQAH	YIHQUB	YIJQAJ	I/Br=0.015 Br/Cl=0.006 I/Cl=0.021
53		CARBTC	CTBROM	ZZZKDW01	Nil
54	HATXIJ	CBENPH	CUZKUD	ZZZOVY01	Cl/F=0.028 I/Br=0.043
55	EBICUO	EBIDAV	EBIDEZ	EBIDID	I/Br=0.009
56		EYISIO	BRACPH02	EYITAH01	I/Br=0.028

The CSD analysis shows some interesting results. There are total 56 examples where crystal structures of chloro, bromo and iodo derivatives of a compound have been reported and 21 cases fluoro derivatives are also present. There is no example where all the four halo derivatives (F, Cl, Br, I) are isostructural. Interestingly 17 hits out of 56 are present where chloro, bromo and iodo derivatives are isostructural which is a quite large number for organic compounds. In the series more polarisable I and Br derivatives display similar packing motif in 28 cases i.e. 50%. More surprisingly Br and Cl derivatives shows maximum isostructurality, 37 examples i.e. 66%, in spite of the dispute about the nature of Cl \cdots Cl interaction.²⁶ Quite expectedly there are only 4 examples where chloro and fluoro compounds are isostructural (entries 30, 38, 42 and 54). There are two entries (38 and 54) where Cl is isostructural to F and I is isostructural to Br analog. Another new finding from the search is that there are at least three examples (entries 2, 3 and 4), wherein terminal members are isostructural but not the middle ones. Though Kitaigorodskii stated that “*if the end members of a series are isomorphous, the middle ones are always so as well.*”⁵ Is there a possibility of polymorphism in these cases?

3.7 Conclusions

The phenomenon of isostructurality is more common in inorganic crystals, because there is exchange of ions of spherical symmetry in general and hence does not change the overall structure. But in the case of organic crystals, molecules may undergo considerable change in shape due to the exchange of functional group. As a result isostructurality is not so common phenomenon in organic molecular crystals.

There are some examples where strong hydrogen bonding group exchange does not alter the overall structure, but these are special cases and rare observations. With increase in size of the rest of the molecule the geometric effect starts dominating and small functional group becomes less important. In periodic table only the halogen group, namely Cl, Br and I with van der Waals radii 1.75 Å, 1.85 Å and 1.98 Å respectively, are exchangeable more frequently to produce isostructural crystals. The electronegativity of the three atoms are 3.16, 2.96 and 2.66 on the Pauling scale. Thus the steric and electronic property changes gradually. Moreover they are monovalent and hence the geometry, like bond angle remains constant. In the previous column in periodic table i.e. chalcogens, there is a sudden jump in the size from O to S (van der Waals radii 1.52 Å and 1.80 Å respectively) and electronegativity changes from 3.44 to 2.58 for these two atoms. Moreover they differ considerably in the divalent geometry: the C–O–C angle in ether is $\sim 120^\circ$ and for C–S–C is $\sim 100^\circ$ in thioether as shown by Desiraju, Howard and co-workers.³⁰ For these reasons the halogen groups are different from other groups in organic isostructural supramolecular chemistry.

CSD analysis shows Cl/Br/I exchange is possible to produce similar packing in 30% cases and Cl/Br exchange frequency (66%) is higher than the Br/I (50%) exchange. F behaves quite differently as reflected by the low exchange probability (F/Cl 19%), because of small size (1.47 Å) and high electronegativity (3.98) of F.

In halophenoxytriazine series 4-XPOT and 3-XPOT retains their molecular trigonal symmetry in crystal structures. In the cases of guest-free close-packed structures the molecules stack in continuous PU columns. The cross sections of these columns are circular, naturally the overall crystal structures are of hexagonal symmetry. For 2-XPOT the molecules pair up from the side of *ortho*-hydrogen in PU. Since these PUs cannot stack infinitely without offset due to the presence of *ortho*-halogen, crystal packing occurs in low symmetry instead of hexagonal setting. In 2-FPOT and 2-CIPOT crystal structures the inter halogen interactions are mainly driven by close packing but for isostructural 2-BrPOT and 2-IPOT the polarizability factor comes into play and type II interaction is formed. There is no example so far in X-POT series where Cl/I or F/X (X=Cl, Br, I) exchange produces isostructural crystal structure. Polarizability as well as

volume both play a key role for this observation and bromo compounds have followed either Cl or I derivatives, as expected.

3.8 Experimental Section

Synthesis

4 equiv. of ArOH and 4 equiv. of KOH were dissolved in THF and stirred for 30 min at room temperature. The reaction mixture was cooled to 0°C and then slowly one equiv. of cyanuric chloride was added and stirred for 1 h at 0°C. After continuing for 48 hours at room temperature, the reaction mixture was poured into crushed ice. The heavy white precipitate was filtered by vacuum suction and washed with methanol, dried and purified by column chromatography. All compounds showed satisfactory NMR spectra.

3-IPOT: ¹H-NMR (CDCl₃, 200 MHz) δ 7.59 (m, 3H), 7.48 (s, 3H), 7.12 (m, 6H).

2-FPOT: ¹H-NMR (CDCl₃, 400 MHz) δ 7.09 (m, 6H), 7.17 (m, 6H).

2-CIPOT: ¹H-NMR (CDCl₃, 400 MHz) δ 7.39 (d, J 8 Hz, 3H), 7.26 (m, 6H), 7.17 (d, J 8 Hz, 3H), 7.17 (t, J 8 Hz, 3H).

2-BrPOT: ¹H-NMR (CDCl₃, 400 MHz) δ 7.56 (d, J 8 Hz, 3H), 7.29 (t, J 8 Hz, 3H), 7.17 (d, J 8 Hz, 3H), 7.10 (t, J 8 Hz, 3H).

2-IPOT: ¹H-NMR (CDCl₃, 400 MHz) δ 7.78 (d, J 8 Hz, 3H), 7.32 (t, J 8 Hz, 3H), 7.13 (d, J 8 Hz, 3H), 6.96 (t, J 8 Hz, 3H).

Crystallization Experiments

3-IPOT was dissolved in 50:50 mixture of THF and mesitylene solvents. Diffraction quality single crystals were obtained after a week. All four 2-XPOT diffraction quality single crystals were obtained from chloroform solution within a week.

X-Ray Crystallography

Reflections were collected for the single crystal of 3-IPOT on a Siemens SMART CCD area detector system at 223(2) K and for 4-FPOT, 2-CIPOT, 2-BrPOT, 2-

IPOT on a Bruker SMART APEX CCD area detector system at 298, 100, 298, 100 K respectively (Mo-K α radiation, $\lambda = 0.71073$ Å). Empirical absorption correction was applied for 3-IPOT and multi-scan absorption correction was applied for 4-XPOT using SADABS. Structure solution and refinement were performed with SHELXS-97 and SHELXL-97 packages. Hydrogen atoms were generated with idealised geometries and isotropically refined using Riding model. Refinement of coordinates and anisotropic thermal parameters of non-hydrogen atoms was carried out by the full-matrix least-squares method.

3.9 References

1. (a) A. Kálmán, L. Fábián and G. Argay, *Chem. Commun.*, **2000**, 2255. (b) A. Nangia and G. R. Desiraju, *Acta Crystallogr.*, **1998**, *A54*, 934.
2. (a) G. R. Desiraju, *Angew. Chem. Int. Ed. Engl.*, **1995**, *34*, 2311. (b) G. R. Desiraju, *Chem. Commun.*, **1997**, 1475.
3. L. Fábián and A. Kálmán, *Acta Crystallogr.*, **1999**, *B55*, 1099.
4. A. Kálmán, L. Párkányi and Gy. Argay, *Acta Crystallogr.*, **1993**, *B49*, 1039.
5. A. I. Kitaigorodskii, *Organic Chemical Crsytallography*, New York, **1961**.
6. A. Anthony, M. Jaskólski, A. Nangia and G. R. Desiraju, *Chem. Commun.*, **1998**, 2537.
7. Gy. Argay, A. Kálmán, B. Ribar, S. Vladimirov and D. –S. Zivanov, *Acta Crystallogr.*, **1987**, *C43*, 922.
8. T. A. Olszak, O. M. Peeters, N. M. Blaton and C. J. de Ranter, *Acta Crystallogr.*, **1994**, *C50*, 761.
9. L. Prasad and E. J. Gabe, *Acta Crystallogr.*, **1983**, *C39*, 273.
10. S. S. C. Chu, V. Napoleone, A. I. Jr. Ternay and S. Chang, *Acta Crystallogr.*, **1982**, *B38*, 2508.
11. M. Chakravarty, P. Kommana and K. C. K. Swamy, *Chem. Commun.*, **2005**, 5396.
12. P. K. Thallapally, K. Chakraborty, H. L. Carrell, S. Kotha and G. R. Desiraju, *Tetrahedron*, **2000**, *56*, 6721.
13. P. G. Jones and F. Vancea, *CrystEngComm*, **2003**, *5*, 303.

14. G. R. Desiraju and J. A. R. P. Sarma, *Proc. Ind. Acad. Sci., Chem. Sci.*, **1986**, 96, 599.
15. L.-P. Zhang and T. C. W. Mak, *J. Mol. Struct.*, **2004**, 693, 1.
16. T. Steiner, *J. Mol. Struct.*, **1998**, 443, 149.
17. I. Bar and J. Bernstein, *Tetrahedron*, **1987**, 43, 1299.
18. R. Boese, G. R. Desiraju, R. K. R. Jetti, M. T. Kirchner, I. Ledoux, V. R. Thalladi and J. Zyss, *Struct. Chem.*, **2002**, 13, 321.
19. (a) R. K. R. Jetti, F. Xue, T. C. W. Mak and A. Nangia, *Cryst. Eng.*, **1999**, 2, 215. (b) R. K. R. Jetti, P. K. Thallapally, F. Xue, T. C. W. Mak and A. Nangia, *Tetrahedron*, **2000**, 56, 6707. (c) R. K. R. Jetti, A. Nangia, F. Xue and T. C. W. Mak, *Chem. Commun.*, **2001**, 919.
20. K. Reichenbacher, H. I. Süss, H. Stoeckli-Evans, S. Bracco, P. Sozzani, E. Weber and J. Hulliger, *New J. Chem.*, **2004**, 28, 393.
21. V. R. Thalladi, R. Boese, Sophie, I. Ledoux, J. Zyss, R. K. R. Jetti and G. R. Desiraju, *Chem. Commun.*, **1999**, 1639.
22. V. R. Thalladi, S. Brasselet, H. -C .Weiss, D. Blaser, A. K. Katz, H. L. Carrell, R. Boese, J. Zyss, A. Nangia and G. R. Desiraju, *J. Am. Chem. Soc.*, **1998**, 120, 2563.
23. L. Pogliani, *New J. Chem.*, **2003**, 27, 919.
24. L. Fábán and A. Kálmán, *Acta Crystallogr.*, **2004**, B60, 547.
25. A. R. Choudhury and T. N. Guru Row, *Cryst. Growth Des.*, **2003**, 4, 47.
26. (a) G. R. Desiraju and R. Parthasarathy, *J. Am. Chem. Soc.*, **1989**, 111, 8725. (b) S. L. Price, A. J. Stone, J. Lucas, R. S. Rowland and A. E. Thornley, *J. Am. Chem. Soc.*, **1994**, 116, 4910.
27. M. J. Frisch *et al.*, Gaussion03, Revision B05, Gaussion Inc, Pittsburgh, PA, **2004**.
28. S. George, A. Nangia, M. Muthuraman, M. Bagieu-Bucher, R. Masse and J.-F. Nicoud, *New J. Chem.*, **2001**, 25, 1520.
29. J. Chisholm, E. Pidcock, J. van de Streek, L. Infantes, S. Motherwell and F. H. Allen, *CrystEngComm*, **2006**, 8, 11.
30. V. R. Vangala, B. R. Bhogala, A. Dey, G. R. Desiraju, C. K. Broder, P. S. Smith, R. Mondal, J. A. K. Howard and C. C. Wilson, *J. Am. Chem. Soc.*, **2003**, 125, 14495.

Halophenoxytriazine... 87

CHAPTER 4

VAN DER WAALS GUEST INCLUSION HOST ASSEMBLY VIA WEAK HYDROGEN BONDS

4.1 Introduction

An exciting research challenge in supramolecular chemistry is to design, synthesize and characterize porous materials with applications in biology, chemistry and materials science.¹ But designing a nanoporous material is not easy because Nature abhors a vacuum. Another problem is interpenetration among the well-defined networks to fill up the porosity. The goal is more difficult to achieve when the interactions are weak H-bonds or similar less specific van der Waals interactions.² On the other side, the frameworks are not very rigid when the interactions are weak in nature. The lability allows them to incorporate different guest molecules in adjustable cavities.³ Pigge et al. have reported several inclusion clathrates based on 1,3,5-triarylbenzenes. In the absence of strong H-bonding donor, the molecules self assemble via weak C–H \cdots O and van der Waals interactions. The *tris*-1,3,5-(4-nitrobenzoyl)benzene host compound forms isostructural clathrates with dichloromethane, acetone and nitromethane guests, but the DMSO clathrate crystal structure is different.⁴ Porphyrin sponges are one of the most studied systems where the host architectures differ due to change in central metal ion as well as change in guest molecules. Over 200 structures have been examined. The host molecules assemble via C–H \cdots π and van der Waals interactions to form different kind of channel and sheet structures. One essential feature of these tetraphenylporphyrin (TPP)-based clathrate structures is their ability to pack efficiently in one or two but not all three dimensions. The rigidity of the molecules due to high degree of conjugation has been ascribed for its effectiveness in enclathration.⁵ Tris(5-acetyl-3-thienyl)methane (TATM) is one of the most studied tripodal host molecule, because of flexibility in host–guest stoichiometries, diversity in structural motifs⁶ and polymorphism.⁷ The host–guest interactions are mainly of the van der Waals type and the host–host molecules also

interact weakly. In the absence of guest TATM has tendency to form low melting amorphous solid. Only after a long time the guest-free form crystal has been observed where $C-H\cdots O$ and $\pi\cdots\pi$ interactions are present.⁸ In the course of their work with fascinating molecule calix[4]arene, Atwood and co-workers have noted that large, unoccupied lattice voids are stabilized by van der Waals forces. They have shown the capability of these voids to entrap volatile guest molecules like methane, freons, etc. The host molecules form trimer and become spherical in shape, which makes the 3D structure as symmetric hexagonal close-packed assembly.⁹ Nangia and co-workers have reported isostructural inclusion clathrate of 4,4-(4'-biphenyl)cyclohexa-2,5-dienone with dimethoxyethane and hexane. The host molecules aggregate via benzoquinone like $C-H\cdots O$ tape (Figure 1).¹⁰

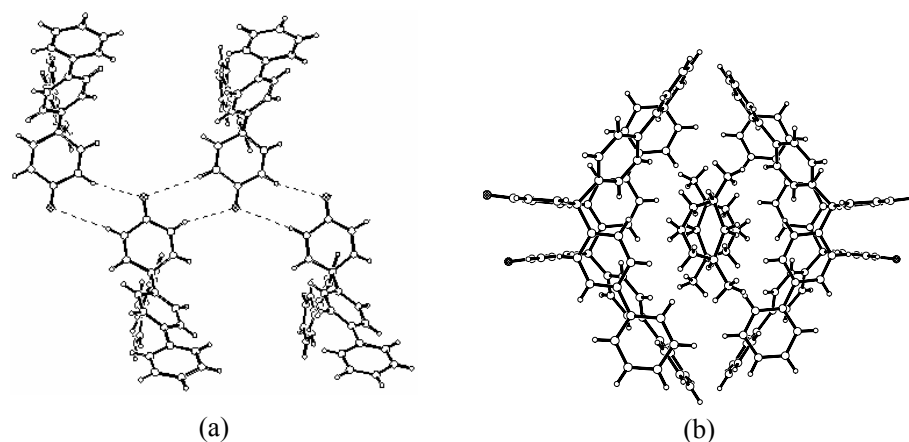
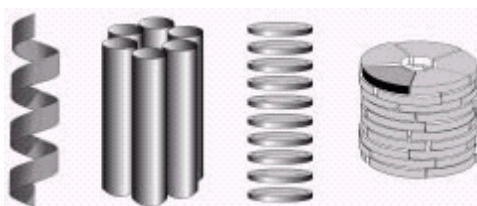


Figure 1. (a) Weak $C-H\cdots O$ hydrogen-bonded tape motif of host molecules. (b) Inversion-related biphenyl groups form parallelepiped-shaped channels that are filled with ordered 1,2-dimethoxyethane molecules.

The occurrence of channels in inclusion compounds is encountered more frequently for a wide range of host architectures. Different terms like “channel,” “tunnel,” “canal,” “cylinder” and “tube” are used to describe the cavities in one dimension without restriction in the host framework. There are four possible ways to form channel, a) helical molecules can form cavity along its axis, b) rod-like molecules self-

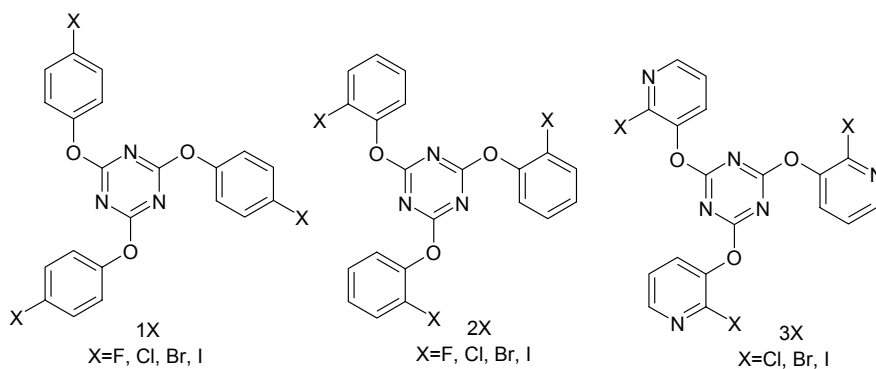
assemble in a barrel-stave fashion to form channel inside the molecular bundle, c) macrocycles can be stacked without off-set to form cylinder, d) sector or wedge-shaped molecules can assemble to form macrocycle like cavity and further stack to generate tube (Scheme 1).¹¹ The organic channel structures are more attractive than the cage framework due to its fascinating applications, many of which are evident in biological systems.^{11a} For example, water transport in gramicidin A channel¹² and transmembrane ion channels are believed to be responsible for chemical information,¹³ protein folding¹⁴ and protein degradation enzymes.¹⁵ The internal surfaces of these protein tubes are enhancing the enzyme activity through functional group complementarity and chemical catalysis. Inspired by the remarkable functions of tubular structures in biology, a large number of tubular structures have been constructed for desired applications. Apart from carbon nanotubes,¹⁶ among well known organic host materials form channel type cavity are cyclic oligosaccharides,¹⁷ cyclic peptides,¹⁸ bile acids,¹⁹ alicyclic diols,²⁰ cyclodextrins,²¹ urea,²² thiourea,²² perhydropyrene (PHTP),²³ tri-o-thymotide (TOT),²⁴ triphenylphosphazene (TPP)²⁶ and 2,4,6-tris(4-halophenoxy)-1,3,5-triazine (4-XPOT),²⁶ discussed in chapter 2. Urea has been employed successfully in industry and by research chemists for the selective inclusion of long chain alkanes over their small-branched analogues.²² Discriminating enantiomers from a racemic mixture has been possible by inclusion in the chiral channels of host molecules, such as cyclodextrins, TOT and bile acids.²⁷ Organized self-assembly of these tailored building units as nanotubular structures are mediated by non-covalent interactions, notably hydrogen bonding and $\pi\cdots\pi$ stacking. In contrast to the oligomeric and macrocyclic building modules, small acyclic tectons are fewer for constructing organic nanotubes.²⁸ Shimizu et al. have reported a crystal structure of macro cyclic bis-urea which self-assemble via N-H \cdots O H-bonding, an α -network of stacked rings. This strong H-bonded macrocyclic nano tube functions as zeolite and shows reversible guest uptake.²⁹ Perhydropyrene (PHTP) exhibits honeycomb network to form narrow tunnels of 5 Å diameter. In the absence of donor and acceptor group, the molecules stack at the nodes of hexagonal framework.²³ Weak H-bonded host network is exemplified by tetrahedral tecton tetrakis(4-nitrophenyl)methane which includes guest molecules in its channel. It also

undergoes structural transformation and exhibit pseudopolymorphism. The diamondoid networks are made exclusively with C–H \cdots O and $\pi\cdots\pi$ interactions.³



Scheme 1. Different possibilities of forming channel host architectures.

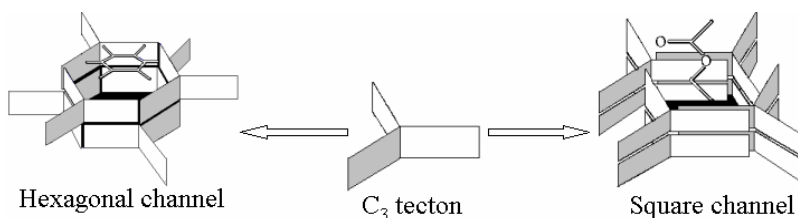
This chapter deals with channel and cage type of structures constructed by trigonal tectons, 2,4,6-tris(2-halo-3-pyridinoxy)-1,3,5-triazine 3X (X = chloro, bromo, iodo; Scheme 2). The host frameworks are built via weak H-bonds and $\pi\cdots\pi$ interactions. The importance of these weak interactions is suggested by the very different crystal structures of 2,4,6-tris(2-halophenoxy)-1,3,5-triazine 2X (X = fluoro, chloro, bromo, iodo) in which C–H \cdots N interactions are not possible, discussed in chapter 3. Crystal structures of 2X in $P\bar{1}$ space group are close-packed with no available voids for guest inclusion. The halogens do not engage in significant interactions and mainly play a space-filling role in the present structures 3.



Scheme 2. 3X crystal structures are studied in this chapter.

4.2 Channel Structure

2,4,6-Tris(4-chlorophenoxy)-1,3,5-triazine, 1Cl is an excellent hexagonal host to study the build up of hexagonal columnar structure from an exo-functional molecule.²⁶ We show in this chapter that the related molecule, 2,4,6-tris(2-chloro-3-pyridinoxy)-1,3,5-triazine 3Cl, organizes in a rectangular tubular structure for encapsulation of linear guest molecules (Scheme 3). The idea of replacing the phenoxy group by pyridinoxy on the triazine core was to promote specific C–H...N interactions along the aromatic channel wall. In contrast to hexagonal pores in host 1, pyridinoxy triazine 3Cl forms square channels stabilized by weak hydrogen bonds mainly and very weak halogen interactions but is robust enough to survive partial guest loss and exchange of solvent vapour without a change in structural integrity.



Scheme 3. Self-assembly of a trigonal tecton to square-shaped channel in host 3 whereas the expected hexagonal network is obtained in 1.

Crystallization of 3Cl from solvents like nitromethane, acetone, methylethyl ketone, ethyl acetate and acetylacetone afforded diffraction quality crystals whose isostructural structures were solved in the space group $P\bar{1}$ with one host molecule in the asymmetric unit. The host molecule adopts a pseudo- C_3 conformation of pyridinoxy rings in the solid state: whereas the pyridyl rings are oriented trigonal, C_3 symmetry is broken by N and Cl atoms pointing upward to the triazine plane for two rings and the third one is on down side. From the viewpoint of tecton 3Cl leading to a columnar self-assembled structure, it is notable that the pyridyl rings are almost orthogonal to the triazine plane in the solid state (Figure 2). This is due to the stable minimum energy conformation as calculated in chapter 3.

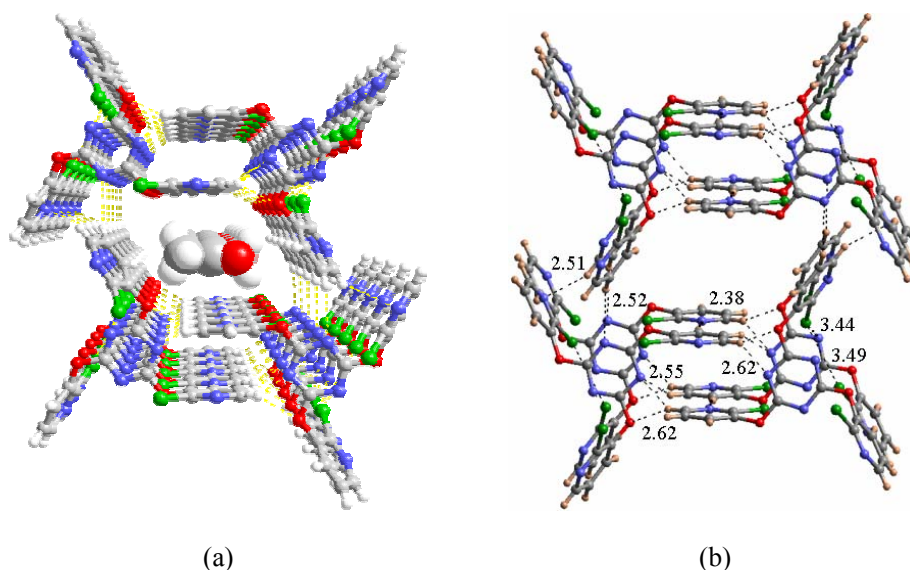


Figure 2. (a) Channel structure of 3Cl•methylethyl ketone. (b) C–H \cdots N, Cl \cdots Cl and Cl \cdots N interactions between eight molecules of 2 to show the intra- and inter-layer organization in 2-butanone inclusion structure.

Four molecules of 3Cl aggregate as dimers via C–H \cdots N_{triazine} interactions to form a rectangular grid with pyridyl rings aligned perpendicular to the triazine plane (Figure 2). Such panels stack with no offset through short, linear interlayer C–H \cdots N_{pyridine} interaction as well as longer, bifurcated and weak Cl \cdots N_{triazine} and Cl \cdots Cl halogen bonds.³⁰ Inclusion of guest species in the resulting porous tubular architecture with aromatic walls is reminiscent of molecular pens reported by Bishop and co-workers³¹ in a brominated isoquinoline host. We infer that the guests are aligned lengthwise along the channel wall (*a*-axis) of isostructural clathrates of 3Cl from the correlation between guest length and host–guest stoichiometry (Table 2). Guest molecules are disordered, even at 100 K, due to the mismatched periodicity of guest and host sub-structures except methylethyl ketone (MEK). MEK and the *a*-axis are of similar length, which causes one guest molecule residing per unit cell and commensurate relationship between host and guest molecules. The disorderness in MEK is due to the presence of inversion center in the cavity. This kind of incommensurate relationship is seen in urea channel inclusion clathrates.²² The guest species are tightly encapsulated in the nanotube because of perfect

size match and host–guest van der Waals interactions. The square channels of 3Cl do not include wider guests such as benzene, mesitylene and branched alkanones. The packing coefficient of 3Cl·MEK is 69.4% and 3Cl without guest is 61.9%.

Atwood and Barbour³² have highlighted the commercial significance of trapping methane and other volatile guests in organic solids, particularly calix[4]arenes. The available pore area in the square channel of 3Cl (~ 4.0 Å on each side) is of the correct dimensions for a kinetic fit of gas molecules (H_2 , $\text{CH}_4 = 3.8$ Å, freon, $\text{CO}_2 = 3.4 \times 5.2$ Å) in van der Waals confinement. This aromatic wall framework 3Cl with square channels complements the hexagonal cyclotriphosphazene apohost exploited by Sozzani²⁵ for gas storage. Relatively narrow channels with interacting walls provide greater stability and hence milder guest absorption conditions than those necessary for the widely reported metal–organic frameworks. The channels in 3Cl are continuous and of uniform dimension along the a -axis. The inclusion of long-chain guests with little branching makes host 3Cl an organic urea-inclusion compound analogue for further structural and spectroscopic studies.

This supramolecular channel structure mimics a cyclophane host.³³ The rectangular cyclic host molecules stack one above another to form tube like structure where the benzene guest molecules are enclosed between adjacent cyclophane species (Figure 3).

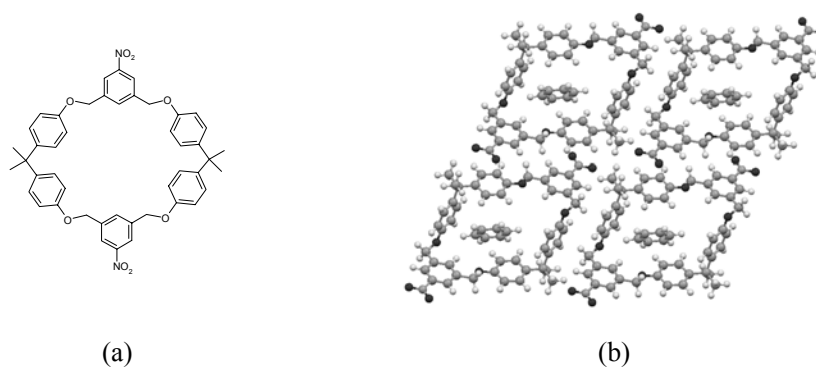


Figure 3. A cyclophane molecule (a) forms square channel structure, which includes benzene as guest (b).

An organic tubular structure with aromatic-ring walls was recently constructed using strong N–H \cdots O/ N–H \cdots N hydrogen bonds mediated self-assembly of a sheet-like molecule.³⁴ However, there are no available voids ($\pi\cdots\pi = 3.9 \text{ \AA} \approx$ van der Waals sum of 3.5 \AA) in the tubuland for guest inclusion. We demonstrate in this system the role of weak hydrogen bonds in the organization of a carbon nanotube like architecture 3Cl and van der Waals forces driven guest inclusion.

4.3 Self Host–guest Structure

The guest free form of 3Cl was obtained during the sublimation experiment at reduced pressure near its melting point. The non-sublimed material undergoes transformation from channel structure to guest free form. The molecules crystallize in chiral $P6_3$ space group with three $1/3$ molecule in the asymmetric unit. It maintains its trigonal symmetry in the solid state. Two of the three symmetry independent molecules form hexagonal channel wall via C–H \cdots N, C–H \cdots O, C–H \cdots Cl and $\pi\cdots\pi$ interactions residing alternately at the nodes to form D_3 -PU like dimer from opposite side of the Cl atoms. The $\pi\cdots\pi$ stacking distance between the triazine planes in the PU is 3.29 \AA . One of the symmetry independent molecule interacts with symmetry related molecules as well as second symmetry independent molecule to construct the wall, where as the second molecule interacts with the third symmetry independent guest-like molecule sitting in the channel (Figure 4). The guest-like molecules do not interact each other and only interact with host channel wall via C–H \cdots N H-bonds. The distance between the guest triazine rings is 6.01 \AA . The Cl atoms in these two molecules direct in $-c$ direction and opposite to the first molecule, resulting in non-centrosymmetry in the crystal. The pyridyl planes are tilted by 85.6° , 89.9° and 80.6° angles with the central triazine plane respectively for these three symmetry independent molecules. The packing coefficient of this guest free form (63.2%) is less than 3Cl•MEK (69.4%).

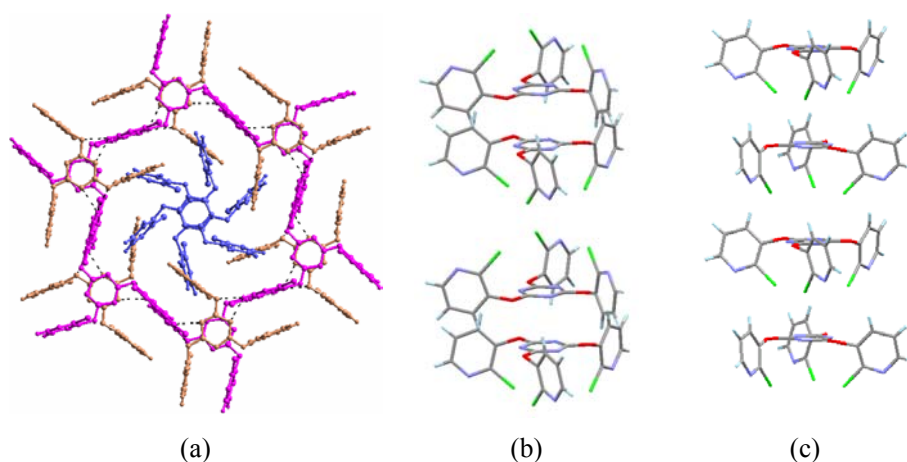


Figure 4. (a) View of the *ab*-layer in guest-free crystal structure 3Cl in $P6_3$ space group to show the self-inclusion channel network of symmetry independent molecules (colored differently). (b) The stacked D_3 -PUs along *c*-axis making the channel wall. (c) Molecules are hanging in the channel like guest.

4.4 High Z' and Examples of Self-inclusion Systems

The occurrence of $Z' > 1$ in crystal structure is an interesting phenomenon. It is the number of formula units in the unit cell divided by the number of independent general positions.³⁵ In general Z' represents number of molecules in asymmetric unit in a single component system. Only 10.8% crystal structures show this unusual behavior.³⁶ Though there is no hard-and-fast rule why some compounds crystallize with multiple molecules in asymmetric unit, the common belief is that when molecules cannot pack efficiently by crystallographic symmetry operations due to irregular shape or strong directional interaction, another symmetry independent unit/units fulfill the requirement. It has been noticed that molecules containing strong H-bonding functionalities, such as nucleotides, nucleosides, steroids and alcohols, are more prone to adopt higher Z' values in their crystal structures. Brock et al. have pointed out that monoalcohols^{37a} contain 40% of the structures with $Z' > 1$ and for vic-diols^{37b} it is 33%. Craven noted that ~50% of cholesterol have $Z' > 1$ in their crystal structures.^{37c} In a recent review Steed has pointed out the driving factors that promote higher Z' value:³⁵ (1) irregular and non-self complementary molecular shape; (2) Small number of strong interacting functional

groups distributed unevenly on molecular surface; (3) Competition between close-packing and strong directional synthon; (4) If strongly interacting self-complementary functionality and resolved chiral center are present together; (5) Mismatched length between the components in cocrystals or clathrates.

One prerequisite of self host–guest phenomenon is the crystal structure should have more than one symmetry independent molecule. One or some of the symmetry independent molecules form host architecture in usual sense and the remaining molecules fill up the cavities like guest. Herbstein and Marsh^{38a} first pointed out self-inclusion phenomenon in their work with trimesic acid (TMA). In the crystal structure of $\text{TMA} \cdot 5/6\text{H}_2\text{O}$ in *P1* space group, the asymmetric unit contain 12 TMA acid and 10 water molecules. Among them 10 TMA and the water molecules form stacked layers with rectangular channel, which is filled up by a molecular chain of remaining two TMA molecules via $\text{COOH} \cdots \text{COOH}$ dimer synthon. These two symmetry independent molecules behave like guest (Figure 5).

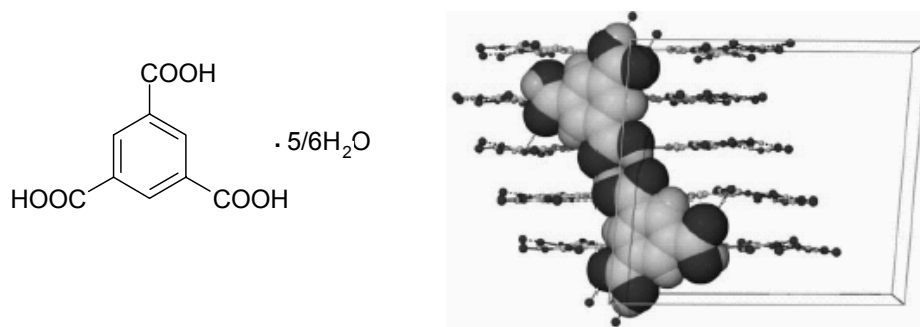


Figure 5. Guest like TMA shown in space-fill model sitting in the channel formed by layered host like TMA and water molecules.

In a recent thesis from our group, Aitipamula has reported a self host–guest system in the course of his studies on inclusion complexes of T-shaped, keto-bisphenol.^{38b} 4,4-Bis(4'-hydroxyphenyl)cyclohexanone crystallizes in space group *Cc* with two molecules in the asymmetric unit. They differ in the conformation of equatorial phenyl and hydroxy groups. One molecule form square grid network and the second one

fill up the channel in it (Figure 6).

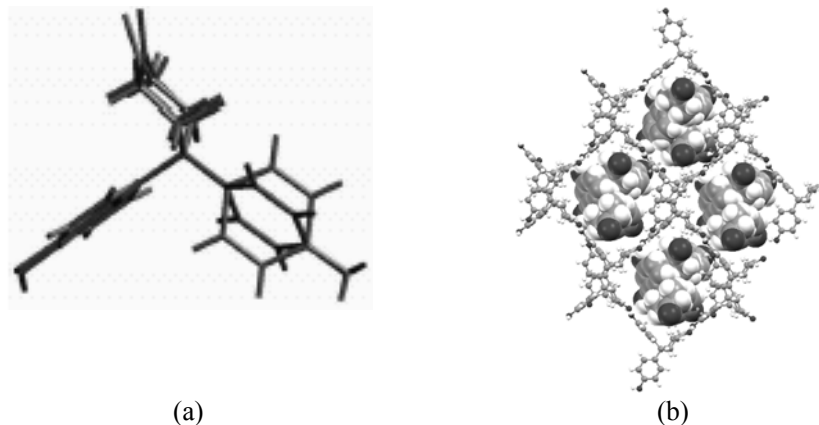


Figure 6. (a) Overlay of two symmetry independent molecules. (b) Self host-guest complex. Symmetry independent molecules with different colors make host and guest like appearance.

Bishop and co-workers observed self host-guest type of molecular arrangement in the crystal structure of a C_2 symmetric molecule, exo-2,exo-6-dihydroxy-2,6-dimethyl-9-oxabicyclo[3.3.1]nonane (DDON).^{38c} There are six molecules in the asymmetric unit. Four of them are ordered and encircle two other disordered molecules.

4.5 Guest Exchange and PXRD Experiment

In order to evaluate the strength of empty voids in 3Cl, the solvated crystal of acetone was heated to 65–70 °C at 0.2 Torr to get different solvent content by adjusting the time and powder XRDs were recorded (Figure 7). The 50% desolvated material matches with the original solid whereas there are changes in the structure at lower solvent content between 15–40%. Interestingly, the solvent-free apohost readily includes ethyl acetate vapor in 2 h to restore the original inclusion structure (PXRD). In contrast to facile guest uptake by the apohost, the guest-free hexagonal form appears to be stable to EtOAc vapor. This exhibits the difference in property in two forms of the solid. In competition experiments, the longer acetylacetone and ethyl acetate guests are able to

displace the shorter acetone solvent. The simulated PXRD pattern of guest-free form is different from the experimental PXRD plot. These observations clearly indicate that the apohost obtained after guest removal is a different form, not the guest free $P6_3$ form.

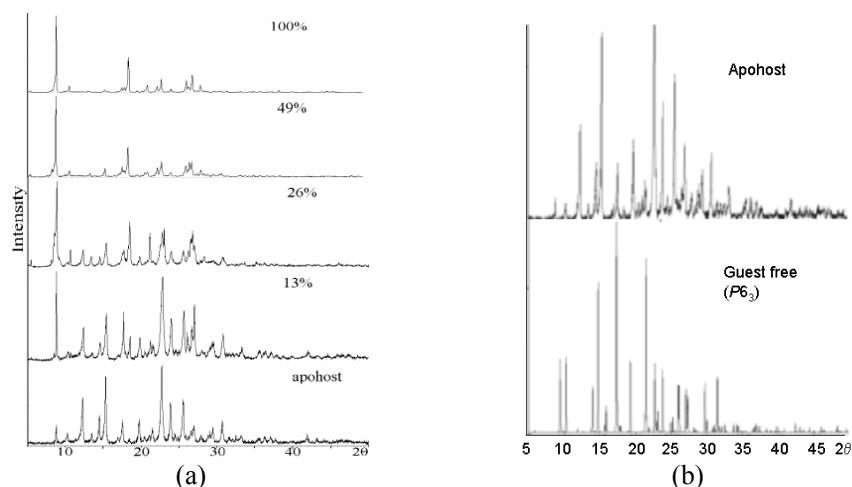


Figure 7. (a) Experimental PXRD of 2•acetone with different guest extent shows the gradual degradation of host architecture with respect to guest loss after 50% guest removal. (b) Comparison between apohost experimental and guest free simulated PXRD plots.

Shimizu and co-workers showed the reversible guest uptake by the channel structure of a bis-urea. NMR, TGA and PXRD experiments proved that this macromolecular organic zeolite release acetic acid guest molecules below 90°C without changing host architecture and reload the guest molecules upon exposure to solvent vapour.²⁹

4.6 Cage Structure

Inclusion adducts of bromo and iodo-derivatives, 3Br and 3I, are very different from 3Cl. The guest molecules are sandwiched in a hexagonal cavity instead of rectangular channel. The inter-layer C–H⋯N interaction in the channel structure of 3Br and 3I would be too long and the packing efficiency would be reduced because of the larger halogen atom.

X-ray diffraction showed the crystal structures of 3Br and 3I are isostructural and crystallize in $R\bar{3}$ space group with 1/3 molecule in asymmetric unit. Unlike 2 these molecules maintain their trigonal symmetry in the crystal. The host molecules self-assemble via the C_{3i} -PU in the ab -plane together with a helix of C–H \cdots N hydrogen bonds along the c -axis to generate a hexagonal host framework (Figure 8). The PUs are stabilized by C–H \cdots O, C–H \cdots N and $\pi\cdots\pi$ interactions. The guest molecules, such as mesitylene, collidine and diiodomethane are sandwiched in the hexagonal cavity with an effective diameter of ~ 11 Å between the C_{3i} -PU of host molecules. Only hexachlorobenzene guest molecule is ordered due to symmetry and size match. In contrast to 4-XPOT structures (discussed in chapter 2) with halogen trimer synthon, crystal structure 3Br/3I is stabilized by weak H-bonds.

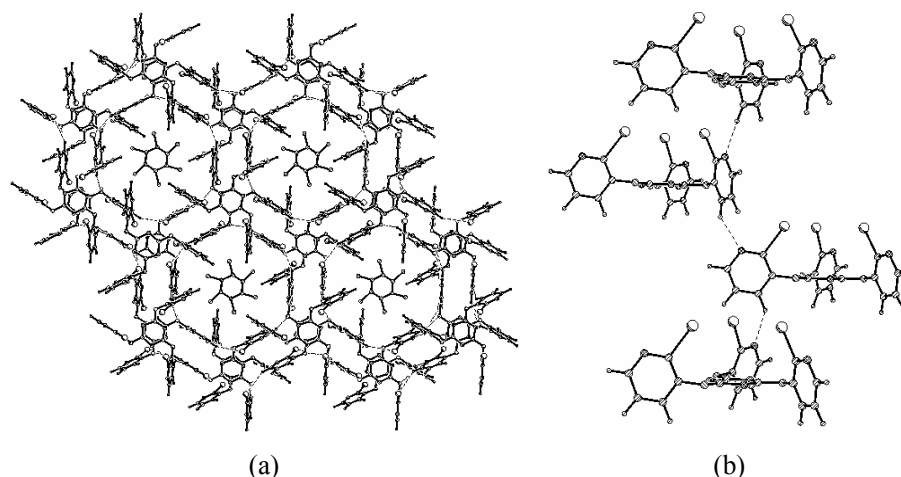


Figure 8. Crystal structure of 3I•mesitylene. (a) A view of the ab -layer to show the hexagonal cavity of 2 and the included guest (mesitylene) molecules. (b) Helix of C–H \cdots N interactions stabilizes the structure along the c -axis.

X-ray diffraction analysis shows that 3Br•mesitylene and 3Br•diiodomethane are isostructural to 3I•mesitylene and 3I•collidine. Interestingly 3Br•diiodomethane undergoes phase transition on temperature change. At room temperature, the structure is expected hexagonal cage framework ($R\bar{3}$) and at low temperature (100K), the structure adopts triclinic crystal system. The structure solves in $P\bar{1}$ space group with two

molecules in asymmetric unit and they differ in conformation, nevertheless the host framework maintains the pseudo hexagonal architecture. This phenomenon has been observed in the case of urea clathrates.²²

Recently Ripmeester and coworkers have reported polymorphism in inclusion structure of TATM with 1,3-dichloropropane guest molecule. Interestingly the host-guest ratio in all the five complexes is 2:1 and crystallize in monoclinic or triclinic crystal systems. The host as well as guest molecules differ in conformation in different complexes.³⁹

Table 1. Intermolecular interaction geometries in 3Cl•guest, 3Br•guest and 3I•guest crystal structures.

Complex	Interaction	d (Å)	D (Å)	θ (°)
3Cl•methylethyl ketone	C(5)–H···N(4)	2.55	3.553(3)	153.4
	C(6)–H···N(6)	2.56	3.583(3)	157.5
	C(10)–H···N(5)	2.38	3.464(3)	175.9
	C(11)–H···N(2)	2.54	3.481(3)	144.0
	C(12)–H···O(3)	2.62	3.617(3)	153.0
	C(12)–H···N(2)	2.62	3.543(3)	142.2
	C(15)–H···Cl(3)	2.92	3.627(3)	122.8
	C(16)–H···N(1)	2.52	3.434(4)	141.7
	C(17)–H···N(4)	2.51	3.471(4)	147.3
	Cl(1)···Cl(3)		3.488(1)	140.1, 120.0
	Cl(3)···N(3)		3.439(2)	149.4
3Cl•ethyl acetate	C(5)–H···N(4)	2.56	3.557(4)	152.5
	C(6)–H···N(6)	2.54	3.566(5)	158.0
	C(10)–H···N(5)	2.39	3.466(4)	174.5
	C(11)–H···N(2)	2.55	3.497(5)	145.3
	C(12)–H···O(3)	2.60	3.599(4)	152.8
	C(12)–H···N(2)	2.57	3.503(5)	142.9
	C(15)–H···Cl(3)	2.90	3.623(4)	124.0
	C(16)–H···N(1)	2.55	3.392(4)	133.8
	C(17)–H···N(4)	2.61	3.561(5)	145.8
	Cl(1)···Cl(3)		3.475(2)	139.7, 120.0
	Cl(3)···N(3)		3.416(3)	148.4
3Cl•acetone	C(5)–H···N(4)	2.56	3.555(3)	152.7
	C(6)–H···N(6)	2.56	3.585(3)	157.4
	C(10)–H···N(5)	2.38	3.463(3)	173.8
	C(11)–H···N(2)	2.53	3.481(3)	145.7

	C(12)–H···O(3)	2.65	3.629(2)	150.7
	C(12)–H···N(2)	2.64	3.560(3)	142.0
	C(15)–H···Cl(3)	2.91	3.599(2)	121.9
	C(16)–H···N(1)	2.55	3.407(3)	135.5
	C(17)–H···N(4)	2.55	3.494(3)	144.6
	Cl(1)···Cl(3)		3.474(1)	140.1, 121.7
	Cl(3)···N(3)		3.437(2)	150.8
3Cl•nitromethane	C(5)–H···N(4)	2.63	3.628(5)	152.2
	C(6)–H···N(6)	2.63	3.659(5)	158.6
	C(10)–H···N(5)	2.47	3.547(5)	171.1
	C(11)–H···N(2)	2.62	3.594(5)	149.1
	C(12)–H···O(3)	2.64	3.642(5)	153.8
	C(12)–H···N(2)	2.68	3.597(5)	142.5
	C(15)–H···Cl(3)	2.87	3.310(5)	104.7
	C(16)–H···N(1)	2.59	3.445(4)	135.4
	C(17)–H···N(4)	2.66	3.624(6)	147.6
	Cl(1)···Cl(3)		3.510(1)	139.1, 120.1
	Cl(3)···N(3)		3.447(3)	149.0
3Cl•acetylacetone	C(5)–H···N(4)	2.55	3.548(3)	152.5
	C(6)–H···N(6)	2.54	3.566(3)	158.2
	C(10)–H···N(5)	2.38	3.459(3)	174.0
	C(11)–H···N(2)	2.57	3.523(3)	146.4
	C(12)–H···O(3)	2.59	3.598(3)	153.8
	C(12)–H···N(2)	2.60	3.528(3)	142.80
	C(15)–H···Cl(3)	2.90	3.299(3)	101.89
	C(16)–H···N(1)	2.53	3.361(3)	132.81
	C(17)–H···N(4)	2.61	3.553(3)	145.36
	Cl(1)···Cl(3)		3.476(1)	139.9, 119.8
	Cl(3)···N(3)		3.411(2)	147.4
3Cl (guest free)	C(3)–H···N(4)	2.67	3.471(10)	130.1
	C(3)–H···O(3)	2.95	3.811(8)	136.4
	C(9)–H···N(2)	2.90	3.708(10)	131.6
	C(11)–H···O(3)	2.95	3.710(9)	127.4
	C(11)–H···N(5)	2.69	3.736(11)	162.9
	C(15)–H···N(6)	2.60	3.470(9)	137.1
	C(17)–H···N(1)	2.58	3.386(8)	130.6
	C(17)–H···O(1)	2.41	3.456(9)	163.1
3Br•mesitylene	C(5)–H···O(1)	2.60	3.531(9)	143.3
	C(3)–H···N(2)	2.43	3.303(7)	136.9
	C(5)–H···N(1)	2.81	3.648(9)	133.8
	$\pi \cdots \pi$		3.337	

3Br•diiodomethane (298K)	C(5)–H···O(1)	2.63	3.539(7)	141.1
	C(3)–H···N(2)	2.45	3.361(7)	141.0
	C(5)–H···N(1)	2.84	3.645(7)	130.9
	$\pi\cdots\pi$		3.332	
3Br•diiodomethane (100K)	C(8)–H···O(3)	2.53	3.396(8)	136.3
	C(13)–H···O(6)	2.63	3.418(8)	129.3
	C(18)–H···O(5)	2.56	3.358(8)	129.8
	C(27)–H···O(1)	2.68	3.573(8)	138.9
	C(32)–H···O(2)	2.52	3.472(10)	145.6
	C(37)–H···O(4)	2.58	3.483(9)	140.3
	C(6)–H···N(10)	2.34	3.216(9)	137.2
	C(13)–H···N(9)	2.37	3.285(9)	141.3
	C(16)–H···N(11)	2.66	3.478(9)	131.8
	C(18)–H···N(8)	2.58	3.407(9)	132.3
	C(25)–H···N(4)	2.31	3.261(9)	146.1
	C(30)–H···N(12)	2.37	3.263(9)	138.8
	C(35)–H···N(6)	2.37	3.334(9)	147.7
	$\pi\cdots\pi$		3.265	
	$\pi\cdots\pi$		3.275	
3I•collidine	C(5)–H···O(1)	2.59	3.494(7)	140.7
	C(3)–H···N(2)	2.39	3.278(9)	137.8
	C(5)–H···N(1)	2.74	3.580(8)	134.0
	$\pi\cdots\pi$		3.284	
3I•mesitylene	C(5)–H···O(1)	2.60	3.516(9)	137.6
	C(3)–H···N(2)	2.42	3.322(9)	142.4
	C(5)–H···N(1)	2.78	3.628(10)	149.0
	$\pi\cdots\pi$		3.304	

4.7 Isostructurality between 1X•guest and 3X•guest

3Br•guest and 3I•guest are quite interestingly isostructural with the cage structures of 1Br•guest and 1I•guest in $R\bar{3}$ space group. In 1X•guest (X=Br, I) crystal structures the host molecules self-assemble via X_3 synthon, where as in 3X•guest (X=Br, I) the molecules interact via weak H-bonds like C–H···N, C–H···O etc. It is quite unusual that in a small molecular system exchange of positions of three large halogens like I, Br produce similar crystal structures. Some important factors should be noted and they might be playing an important role for the isostructural behavior. (1) In both systems the molecules maintain trigonal symmetry and crystallize in hexagonal system. (2) The

halogens in $1X \cdot \text{guest}$ drive self-assembly process via the halogen trimer synthon and have a space-filling role. In $3X \cdot \text{guest}$ crystal structure the halogens are shifted from *para* to *ortho* position and contribute similar volume effect, but they do not form inter-halogen synthon. In the presence of pyridyl N atoms, the molecules assemble via C–H...N interactions. On the other hand, in the absence of these N atoms, the molecules in $2X \cdot \text{guest}$ crystallize differently (chapter 3). (3) In both the systems the trigonal tectons form similar PU dimer. In fact PU formation is a general criteria for aryloxytriazine molecules as observed in large number of cases. (4) The repeating unit in $1X \cdot \text{guest}$ crystal structure along *c*-axis is triazine ring–halogen trimer synthon–guest–halogen trimer synthon–triazine ring. In $3X \cdot \text{guest}$ crystal structures, the repeating unit along *c*-axis is triazine ring–intramolecular iodo trimer–guest– intramolecular iodo trimer–triazine ring. Thus intermolecular iodo trimer synthon has been replaced by intramolecular iodo trimer but the remaining parts are similar (Figure 9). Isostructurality of $1I \cdot \text{guest}$ and $3I \cdot \text{guest}$ would result from a combination of above factors. Some other unusual isostructural pair of systems reported in CSD were discussed in chapter 3.

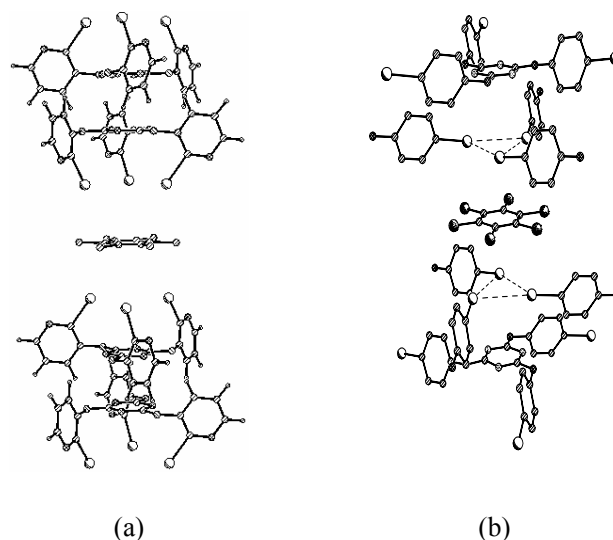


Figure 9. Comparison of repeating unit in $3I \cdot \text{mesitylene}$ (a) and $1I \cdot \text{mesitylene}$ (b). The intra molecular iodo trimer in $3I \cdot \text{mesitylene}$ has been replaced by intermolecular iodo trimer synthon in $1I \cdot \text{mesitylene}$.

4.8 Thermal Analysis

In addition to crystallographic characterisation of host–guest structures, thermochemical analysis provides valuable information about the strength of guest to host interactions. The parameter $T_{\text{on}} - T_{\text{bp}}$, the difference between the onset temperature for guest release from host lattice compared to the normal boiling point of the solvent, is a measure of how strongly the guest molecule is bound to the host architecture.⁴⁰

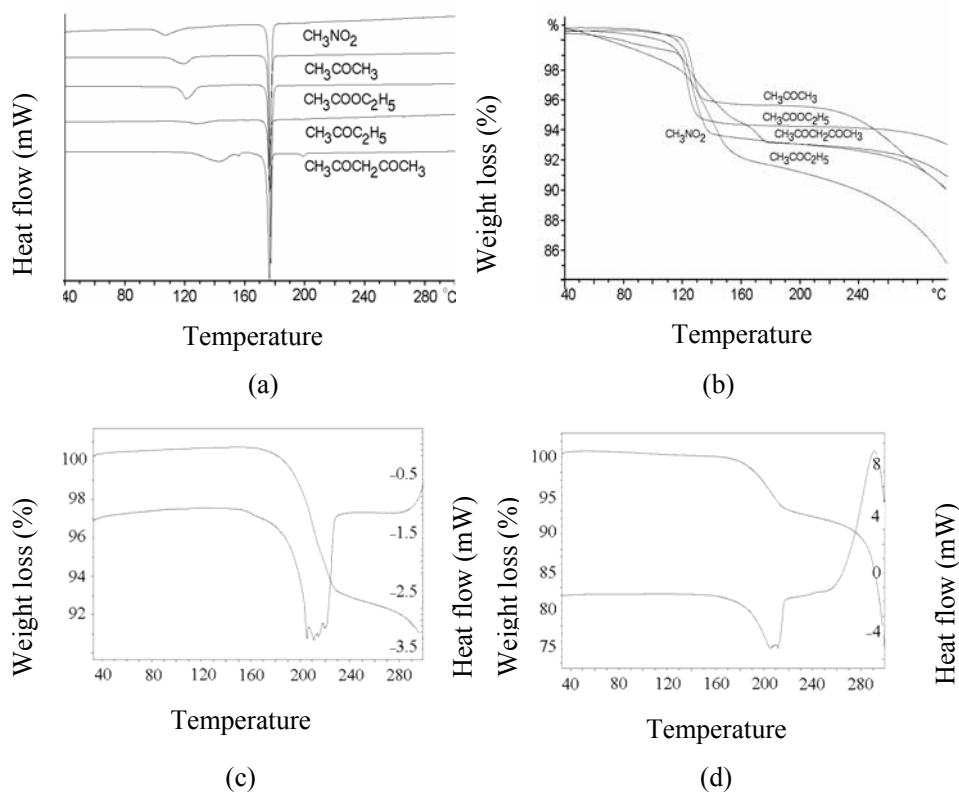


Figure 10. (a) DSC and (b) TGA plots of five solvates of 3Cl. DSC and TG plots of 3I•mesitylene (c) and 3I•collidine (d).

Examination of the host architecture suggests that the guest molecule can escape from the channel type host architecture of 1X ($P6_3/m$) with relative ease than the channel

structure in $P\bar{1}$ of 3Cl because the channel is narrower in the later case (Table 2). Guest molecules such as ethyl acetate, acetone are not stable in the hexagonal channel when the crystal is taken out from solution. On the other hand, the guest molecules are tightly held in the rectangular narrow channel of 3Cl host. Quite surprisingly higher boiling nitromethane escapes from the host lattice at lower temperature than low boiling acetone from the isostructural host framework. The host–guest interaction is of van der Waals type and thus larger van der Waals surface of acetone is attributed to its higher stability. In fact, longer guest molecules with larger surface area have higher T_{onset} value, is reflected through out the series of five host–guest complexes; ethylacetate and methylethyl ketone evolve at similar temperature.

Table 2. Thermal analysis (TG/DSC) on inclusion compounds of 3X.

Complex	Length Å	Host : guest ^a	host : guest ^b	T_{onset} (°C)
3Cl•CH ₃ NO ₂	5.2	1.0 : 0.55	1.0 : 0.60	99
3Cl•CH ₃ COCH ₃	6.7	1.0 : 0.53	1.0 : 0.43	109
3Cl•CH ₃ COC ₂ H ₅	7.8	1.0 : 0.50	1.0 : 0.50	118
3Cl•CH ₃ CO ₂ C ₂ H ₅	9.1	1.0 : 0.38	1.0 : 0.33	116
3Cl•CH ₃ COCH ₂ COCH ₃	9.2	1.0 : 0.25	1.0 : 0.34	126
3I•C ₉ H ₁₂		1.0 : 0.50	1.0 : 0.50	200
3I•C ₈ H ₁₁ N		1.0 : 0.50	1.0 : 0.50	197

^a Host : guest ratios have been determined from residual electron densities of disordered guest molecules. ^b Host : guest ratios calculated according to TGA.

Although the host···host and host···guest intermolecular interactions are weak in both cage type host architectures, the guest is released at a higher temperature from the 3I framework than 1I in TGA measurements (Table 3; Figure 10). Mesitylene, collidine are evolved from the 3I host cavity at about their boiling point and the observed weight loss is in good agreement with that calculated from the host:guest stoichiometry determined from the X-ray crystal structure. In contrast, the release of collidine and mesitylene from the cage lattice of iodo-pyridinoxy triazine 2 occurs at 50–70 °C higher temperature. The comparison of packing coefficients between mesitylene and collidine clathrates in two systems (1I and 3I) has been listed in table 3. Analysis shows that the

packing coefficient (C_k) values are higher and cavities are smaller for 1I host framework.

Table 3. Comparison of packing coefficients and T_{onset} between two cage systems.

Complex	C_k^a	Cavity size (\AA^3)	T_{onset} ($^{\circ}\text{C}$)
1I•mesitylene	57.0	302.9	200
3I•mesitylene	53.2	362.3	169
1I•collidine	57.7	293.5	197
3I•collidine	54.2	340.8	155

^a C_k calculated from Platon after removing disordered guest molecules.

Nevertheless 3I•guest is more stable to temperature albeit the melting point of the host material is less. This shows that even though the host architecture is assembled via weak H-bonds and van der Waals interactions, it is quite strong and thermally stable. Some of the highest recorded values of $T_{\text{on}} - T_{\text{bp}}$ are 320°C and 370°C for the release of CH_4 and CF_4 from the interstitial void of calix[4]arene host lattice.^{32a}

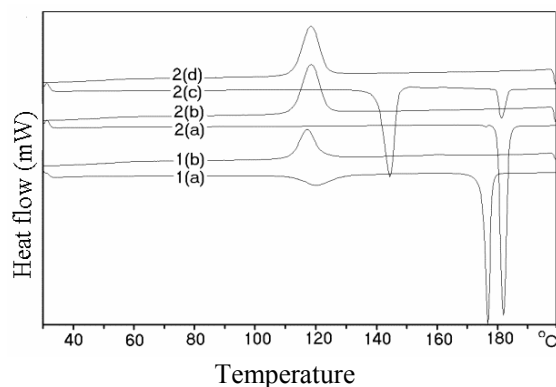


Figure 11. Heat-cool-heat DSC diagram of 3Cl. 1(a) Heating curve of 3Cl•acetone. 1(b) Cooling curve of 1(a). 2(a) Heating curve of guest free 3Cl. 2(b) Cooling curve of 2(a). Reheating 2(b) is presented by 2(c) and cooling of 2(c) gives the plot 2(d).

Heat-cool-heat DSC diagram clearly shows three different phases apart from channel clathrate structure (Figure 11). Heating 3Cl•acetone compound produces apohost after 120°C , which melts at 177°C and it solidifies while cooling at much less temperature 115°C . Heating $P6_3$ guest-free compound gives an endotherm at 182°C for

melting, higher than the apohost, which produces an exotherm at same cooling temperature. Reheating this resultant compound produces a broad endotherm at much less temperature 143°C indicative of amorphous phase and a small endotherm at 182°C corresponding to guest free form. Cooling curve mimics other two cooling experiments.

4.9 Conclusions

The high molecular symmetry and absence of strong hydrogen bonding groups means that inclusion of guest molecules in the voids is perhaps necessary to stabilize the crystal structure. We speculate that the reversible desolvation–solvation behavior of host 3Cl could be due to its ability to transform the porous channel framework to a close-packed structure by a change in molecular conformation and movement of pyridinoxy rings into the voids. The lower melting of the apohost in comparison to guest free form and easy resolution of apohost indicate that it is not efficiently close-packed after guest removal. The packing coefficient of the channel structure without guest (61.9%) is lower than guest-free close-packed structure (63.2%) and 3Cl•methylethyl ketone has higher packing fraction (69.4%). Characterization of apohost 3Cl by single crystal X-ray diffraction has so far been elusive.

The cage structures of 3Br and 3I hosts are assembled via C–H...N, C–H...O and $\pi\cdots\pi$ stacking interactions. The channel structure of 3Cl is not possible in 3Br and 3I because of the larger *ortho*-halogen atom. In spite of low packing capability 3I cage structure releases guest molecules (mesitylene and collidine) at very high temperature.

4.10 Experimental

Synthesis

2,4,6-Tris(2-halo-3-pyridinoxy)-1,3,5-triazine (3X): 2-halo-3-pyridinol and KOH (4.0 equiv each) were dissolved in acetone and stirred for 30 minutes. Cyanuric chloride (1.0 equiv) was added to the reaction mixture at 0 °C and stirred for 1 h. The reaction mixture was allowed to stir for 1 d at room temperature, poured into crushed ice, the resulting white precipitate was suction filtered and then washed with methanol. The product was purified by column chromatography and crystallized from the appropriate solvent.

2,4,6-Tris(2-chloro-3-pyridinoxy)-1,3,5-triazine (3Cl): $^1\text{H-NMR}$ (CDCl_3 , 400 MHz): δ 8.29 (d, J 4 Hz, 3 H), 7.53 (d, J 8 Hz, 3 H), 7.28 (dd, J 8, 4 Hz 3 H).

2,4,6-Tris(2-bromo-3-pyridinoxy)-1,3,5-triazine (3Br): $^1\text{H-NMR}$ (CDCl_3 , 400 MHz): δ 8.28 (d, J 4 Hz, 3 H), 7.45 (d, J 8 Hz, 3 H), 7.27 (dd, J 8, 4 Hz 3 H).

2,4,6-Tris(2-iodo-3-pyridinoxy)-1,3,5-triazine (3I): $^1\text{H-NMR}$ (CDCl_3 , 200 MHz) δ 8.27 (d, J 4 Hz, 3 H), 7.38 (d, J 8 Hz, 3 H), 7.28 (dd, J 8, 4 Hz 3 H).

X-Ray crystallography

Reflections were collected for the single crystal of 3I crystals on a Siemens SMART CCD area detector system and for 3Cl and 3Br crystals on a Bruker SMART APEX CCD area detector system (Mo-K α radiation, $\lambda = 0.71073 \text{ \AA}$). Empirical absorption correction was applied for 3I and multi-scan absorption correction was applied for 3Cl and 3Br using SADABS. Structure solution and refinement were performed with SHELXS-97 and SHELXL-97 packages. Hydrogen atoms were generated with idealised geometries and isotropically refined using Riding model. Refinement of coordinates and anisotropic thermal parameters of non-hydrogen atoms was carried out by the full-matrix least-squares method.

Thermal Analysis

Differential scanning calorimetry (DSC) was performed on a Mettler Toledo DSC 822e instrument and thermogravimetry (TGA) on a Mettler Toledo TGA=SDTA 851e, and data manipulated in the STAR software module. Crystals taken from the mother liquor were blotted dry on a filter paper and placed in open alumina pans for TGA measurements and in crimped aluminium but vented sample pans for DSC measurements. Sample size in each case was 5–7 mg. The temperature range was 30–300°C at a heating rate of 10°C/min. The samples were purged with a stream of dry nitrogen at a flow rate of 150 ml/min for DSC and 50 ml/min for TGA.

PXRD

Powder XRD of all samples were recorded on a PANalytical 1830 (Philips Analytical) diffractometer using Cu-K α X-radiation at 35 kV and 25 mA. Diffraction patterns were collected over 2θ range of 5-50° at scan rate of 2 °/min.

4.11 References

1. (a) J. W. Steed and J. L. Atwood, *Supramolecular Chemistry*; John Wiley: Chichester, **2000**. (b) *Encyclopedia of Supramolecular Chemistry*; Eds. J. W. Steed and J. L. Atwood, Marcel Dekker: New York, **2004**. (c) *Nanoporous Materials: Science and Engineering*; Eds. G. Q. Max Lu and X. S. Zhao, World Scientific Press: Singapore, **2004**.
2. (a) J. D. Wuest, *Chem. Commun.*, **2005**, 5830. (b) A. Nangia, *Curr. Opin. Solid State Mater. Sci.*, **2001**, 5, 115. (c) G. R. Desiraju and T. Steiner, *The Weak Hydrogen Bond in Structural Chemistry and Biology*; Oxford University Press, **1999**.
3. R. Thaimattam, F. Xue, J. A. R. P. Sarma, T. C. W. Mak and G. R. Desiraju, *J. Am. Chem. Soc.*, **2001**, 123, 4432.
4. (a) F. C. Pigge, F. Ghasedi, Z. Zheng, N. P. Rath, G. Nichols and J. S. Chickos, *J. Chem. Soc., Perkin Trans. 2*, **2000**, 2458. (b) F. C. Pigge, Z. Zheng and N. P. Rath, *New J. Chem.*, **2000**, 24, 183. (c) V. S. S. Kumar, F. C. Pigge and N. P. Rath, *CrystEngComm*, **2004**, 6, 531.
5. (a) K. S. Suslick, P. Bhyrappa, J.-H. Chou, M. E. Kosal, S. Nakagaki, D. W. Smithenry and S. R. Wilson, *Acc. Chem. Res.*, **2005**, 38, 283. (b) M. P. Byrn, C. J. Curtis, Y. Hsiou, S. I. Khan, P. A. Sawin, S. K. Tendick, A. Terzis and C. E. Strouse, *J. Am. Chem. Soc.*, **1993**, 115, 9480. (c) M. P. Byrn, C. J. Curtis, Y. Hsiou, S. I. Khan, P. A. Sawin, S. K. Tendick, A. Terzis and C. E. Strouse, *J. Am. Chem. Soc.*, **1991**, 113, 6549.
6. (a) J. L. M. Dillen and H. M. Roos, *Acta Crystallogr.*, **1992**, C48, 2229. (b) H. M. Roos and J. L. M. Dillen, *Acta Crystallogr.*, **1992**, C48, 1882. (c) P. H. Van Rooyen and H. M. Roos, *Acta Crystallogr.*, **1991**, C47, 2718. (d) L. Pang, R. C. Hynes and M. A. Whitehead, *Acta Crystallogr.*, **1994**, C50, 615. (e) L. Pang and F. Brisse, *Acta*

- Crystallogr.*, **1994**, C50, 1947. (f) L. Pang and F. Brisse, *Can. J. Chem.*, **1994**, 72, 2318. (g) P. S. Sidhu and J. A. Ripmeester, *J. Supramol. Chem.*, **2001**, 1, 63. (h) P. S. Sidhu and J. A. Ripmeester, *Supramol. Chem.*, **2003**, 15, 433.
7. P. S. Sidhu, G. D. Enright, J. A. Ripmeester and G. H. Peener, *J. Phys. Chem.*, **2002**, B106, 8569.
 8. P. S. Sidhu, G. D. Enright, K. A. Udachin and J. A. Ripmeester, *Chem. Commun.*, **2005**, 2092.
 9. J. L. Atwood, L. J. Barbour and A. Jerga, *Science*, **2002**, 296, 2367.
 10. V. S. S. Kumar and A. Nangia, *Chem. Commun.*, **2001**, 2392.
 11. (a) D. T. Bong, T. D. Clark, J. R. Granja and M. R. Ghadiri, *Angew. Chem. Int. Ed.*, **2001**, 40, 988. (b) C. H. Görbitz, M. Nilsen, K. Szeto and L. W. Tangen, *Chem. Commun.*, **2005**, 4288. (c) C. H. Görbitz, *CrystEngComm*, **2005**, 7, 670.
 12. G. M. Preston, T. P. Carroll, W. B. Guggino and P. Agre, *Science*, **1992**, 256, 385.
 13. B. Eisenberg, *Acc. Chem. Res.*, **1998**, 31, 117.
 14. (a) P. B. Sigler, Z. Xu, H. S. Rye, S. G. Burston, W. A. Fenton and A. L. Horwich, *Annu. Rev. Biochem.*, **1998**, 67, 581. (b) A. L. Horwich, E. U. Weber-Ban and D. Finley, *Proc. Natl. Acad. Sci. USA*, **1999**, 96, 11033.
 15. (a) P. Zwicky, D. Voges and W. Baumeister, *Philos. Trans. Soc. London*, **1999**, B354, 1501. (b) D. Voges, P. Zwickl and W. Baumeister, *Annu. Rev. Biochem.*, **1999**, 68, 1015.
 16. G. Hummer, J. C. Rasaiah and J. P. Noworyta, *Nature*, **2001**, 414, 188.
 17. P. R. Ashton, S. J. Cantrill, G. Gattuso, S. Menzer, S. A. Nepogodiev, A. N. Shipway, J. F. Stoddart and D. J. Williams, *Chem. Eur. J.*, **1997**, 3, 1299.
 18. T. D. Clark and M. R. Ghadiri, *J. Am. Chem. Soc.*, **1995**, 117, 12364.
 19. M. Miyata and K. Sada, *Comprehensive Supramolecular Chemistry*; Eds. D. D. MacNicol, F. Toda, R. Bishop, Pergamon Press: Oxford, **1996**, 6, 147.
 20. F. Toda, K. Tanaka, T. Imai and S. A. Bourne, *Supramol. Chem.*, **1995**, 5, 289.
 21. D. Mentzafos, I. M. Mavridis, G. Le Bas and G. Tsoucaris, *Acta Crystallogr.*, **1990**, B46, 746.
 22. K. D. M. Harris, *Chem. Soc. Rev.*, **1997**, 26, 279.

23. M. Farina, *Inclusion Compounds*; Eds. J. L. Atwood, J. E. D. Davies and D. D. MacNicol, Academic Press: London, **1984**, 2, 69.
24. R. Gerdil, *Topics in Current Chemistry*; Ed. E. Weber, Springer: Berlin, **1986**, 140, 71.
25. P. Sozzani, S. Bracco, A. Comotti, L. Ferretti and R. Simonutti, *Angew. Chem. Int. Ed.*, **2005**, 44, 1816.
26. R. K. R. Jetti, P. K. Thallapally, F. Xue, T. C. W. Mak and A. Nangia, *Tetrahedron*, **2000**, 56, 6707.
27. R. Arad-Yellin, B. S. Green, M. Knossow and G. Tsoucaris, *Inclusion Compounds*; Eds. J. L. Atwood, J. E. D. Davies and D. D. MacNicol, Academic Press: London, **1984**, 3, 263.
28. (a) H. Fenniri, B. L. Deng and A. E. Ribbe, *J. Am. Chem. Soc.*, **2002**, 124, 11064. (b) H. Fenniri, P. Mathivanan, K. L. Vidale, D. M. Sherman, K. Hallenga, K. V. Wood and J. G. Stowell, *J. Am. Chem. Soc.*, **2001**, 123, 3854. (c) S. Ray, D. Haldar, M. G. B. Drew and A. Banerjee, *Org. Lett.*, **2004**, 6, 4463. (d) M. Mascal, N. M. Hext, R. Warmuth, J. R. Arnall-Culliford, M. H. Moore and J. P. Turkenburg, *J. Org. Chem.*, **1999**, 64, 8479. (e) A. Ranganathan, V. R. Pedireddi and C. N. R. Rao, *J. Am. Chem. Soc.*, **1999**, 121, 1752. (f) N. Kimizuka, T. Kawasaki, K. Hirata and T. Kunitake, *J. Am. Chem. Soc.*, **1995**, 117, 6360.
29. L. S. Shimizu, A. D. Hughes, M. D. Smith, M. J. Davis, B. P. Zhang, H.-C. Z. Loye and K. D. Shimizu, *J. Am. Chem. Soc.*, **2003**, 125, 14972.
30. J. P. M. Lommerse, A. J. Stone, R. Taylor and F. H. Allen, *J. Am. Chem. Soc.*, **1996**, 118, 3108.
31. A. N. M. M. Rahaman, R. Bishop, D. C. Craig and M. L. Scudder, *Chem. Commun.*, **1999**, 2389.
32. (a) J. L. Atwood, L. J. Barbour and A. Jerga, *Science*, **2002**, 296, 2367. (b) J. L. Atwood, L. J. Barbour, P. K. Thallapally and T. B. Wirsig, *Chem. Commun.*, **2005**, 51. (c) P. K. Thallapally, T. B. Wirsig, L. J. Barbour and J. L. Atwood, *Chem. Commun.*, **2005**, 4420.

33. K. Saigo, M. Kubo, R.-J. Lin, A. Youda and M. Hasegawa, *Tet. Lett.*, **1985**, 26, 1325.
34. Z.-Q. Hu and C.-F. Chen, *Chem. Commun.*, **2005**, 2445.
35. J. W. Steed, *CrystEngComm*, **2003**, 5, 169.
36. T. Steiner, *Acta Crystallogr.*, **2000**, B56, 673.
37. (a) C. P. Brock and L. L. Duncan, *Chem. Mater.*, **1994**, 6, 1307. (b) C. P. Brock, *Acta Crystallogr.*, **2002**, B58, 1025. (c) B. M. Craven, *Acta Crystallogr.*, **1979**, B35, 1123.
38. (a) F. H. Herbstein and R. E. Marsh, *Acta Crystallogr.*, **1977**, B33, 2358. (b) S. Aitipamula, G. R. Desiraju, M. Jaskolski, A. Nangia and R. Thaimattam, *CrystEngComm*, **2003**, 5, 447. (c) K. C. Pich, R. Bishop, D. C. Craig, I. G. Dance, A. D. Rae and M. L. Scudder, *Struct. Chem.*, **1993**, 4, 41.
39. P. S. Sidhu, G. D. Enright, K. A. Udachin and J. A. Ripmeester, *Cryst. Growth Des.*, **2004**, 4, 1249.
40. L. R. Nassimbeni, *Acc. Chem. Res.*, **2003**, 36, 631.

CHAPTER 5

WATER CLUSTERS IN HALOGENATED PHLOROGLUCINOL HOST

5.1 Introduction

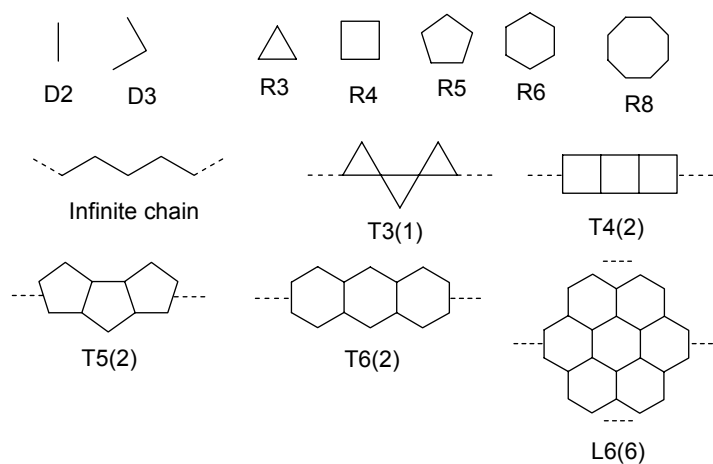
Water is the most studied and yet the least understood of chemical species.¹ In spite of the simple molecular structure it shows a lot of anomalous behavior like, high melting and boiling point, low density in solid phase, extensive H-bonding, high dielectric constant, etc.^{1a,2} Water has attracted considerable attention from structural chemists and biologists because of its importance in gas hydrates, its different topologies, and the important role of water in the structure, conformation and function of nucleotides and peptides as well as in protein–DNA binding. Clathrate structures of water can be divided into two classes. (a) Clathrate hydrates,³ in this class of compounds water forms hydrogen-bonded polyhedral cages where the guest molecules, generally hydrophobic, are trapped by nondirectional weak host–guest interactions. It is assumed that the empty hydrate lattice, which is metastable with respect to ice, is stabilized by the inclusion of guest molecules.⁴ Naturally occurring gas hydrates constitute a vast amount of untapped energy source. On the other hand water clusters cause numerous problems and challenges for oil and gas exploration. Another class of clathrate is (b) hydrated clathrates, where the water clusters are trapped in the cavity of organic or metal–organic host framework. This class of compounds shows a significant variation in their nature. The included water molecules can form discrete and extended motifs, e.g. finite and infinite chains, ring motifs of different topologies, e.g. 1D tapes, 2D sheets, and 3D networks. Recently this class of compounds has elicited interest for academic and practical reasons. Water is commonly regarded as the “solvent of life”, because our bodies are constituted of 70% water and it plays a structural as well as functional role in biomolecules. Due to the difficulties in studying macromolecules accurately, even using modern sophisticated instruments, it is easier to study trapped water clusters in small molecular host architectures by accurate X-ray diffraction. Such entrapment of water to

understand its nature in solid ice and liquid phases as well as structural and functional properties in biology has become a hot topic in supramolecular chemistry. The increase in frequency of water structures published in 2005 could be a consequence of studies on water being selected as one of the top 10 breakthroughs by the international journal *Science* in 2004.⁵

There are several studies on water in biological systems. Agre delivered his Nobel Lecture at Stockholm in 2004 about the aquaporin water channels.⁶ These membrane proteins explain how our brains secrete and absorb spinal fluid, how the eyes generate aqueous humor, how we can generate aqueous tears, saliva, sweat and bile and how our kidneys can concentrate urine so effectively. Water channel has been found in red blood cells and renal tubules where water rapidly and selectively crosses the plasma membrane.⁷ Water also plays an important role in protein–DNA recognition.⁸ Water molecules participate in H-bonding networks that link side chain and main chain atoms of proteins with the anionic oxygens of phosphodiester backbone and functional groups on DNA bases to stabilize the biological system.⁹ Structural analyses of the waters present at the interface in protein–DNA complexes indicate that the majority of these waters facilitate binding by screening electrostatic repulsions between like charges on the protein and the DNA. Thus water release from the interface, in general, is favored entropically but enthalpically unfavorable.⁹ Water also stabilizes the *B*-DNA dodecamer structure via minor groove hydration spine and its disruption transforms the structure to *A* form.¹⁰ Protein folding and defolding is connected to the role of water molecules, in the cases of fibrous proteins, water plays a more important structural role. The orientational ordering and thermodynamical study of “structural” waters have been made possible by small peptides in the solid state, which fold into standard polypeptide motifs containing waters of hydration which apparently stabilize the structure.¹¹

Infantes and co-workers reported that 6.6 % of organic compounds are hydrated and this value increases to 75 % for bioactive pharmaceutical compounds.¹² There is no easy answer to the question, when hydrates form. Some general ideas have been proposed to explain this important phenomenon. Molecules containing charged or strong H-bonding functional groups favor hydration for obvious reason. Infantes and co-

workers categorized and ranked different functional groups, which promote hydration. When the donor/acceptor ratio is imbalanced in a molecule, this causes entrapment of waters.¹³ Another argument is that the strong H-bonds are directional and when the groups are locked in a fixed position, they may lose directionality. By incorporating small and flexible water molecule it is possible to fulfill the geometric requirement. Water can play a space filling role also,¹⁴ though it has been seen that only 4 % of the crystal structures contain water molecules without H-bonding.¹⁵



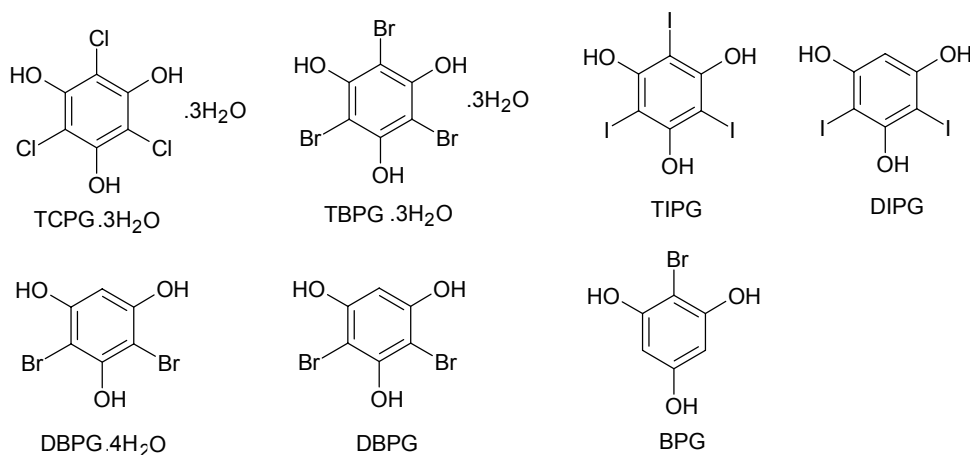
Scheme 1. Few examples of different water clusters found in host cavities.¹⁶

A large variety of water topologies have been trapped into the crystal lattice. They are discrete or extended in 1D, 2D or three dimensions. Infantes and Motherwell divided these topologies in different categories, e.g. discrete chains (D), discrete rings (R), infinite chains in 1D without ring (C), infinite tapes in 1D involving rings (T), infinite layers in 2D (L) (Scheme 1).¹⁶ One-dimensional water chain structures constitute a potentially important form of water but which is poorly understood.¹⁷ Many fundamental biological process depend on water chains.^{6,7,18} This motif is involved in proton transport in gramicidin A¹⁹ via the Grotthuss relay mechanism.²⁰ 1D chains are generally stabilized by strong H-bonding between neighboring waters along the chain and functional groups along the channel wall. Buchanan *et al.* have trapped water chains in the crystal structures of 4,4'-methylene-bis(2,5-dimethylimidazole) and 1-

methylimidazole-4-carboxaldehyde and showed that these water chains in the small molecular lattice channel can serve as a model for biological proton wires.²¹ Ripmeester *et al.* claimed that the water chain included in the channel of hydrophobic molecule tris(5-acetyl-3-thienyl)methane crystal is capable of water transport.²² Saykally and co-workers have carried out extensive measurements of vibration–rotation–tunneling (VRT) spectra for small water clusters to the hexamer W_6 level.²³ They have been able to confirm theoretical predictions of quasiplanar ring structures as the most stable form for W_2 – W_5 clusters but not for the W_6 hexamer, for which they have found, again in agreement with theoretical predictions, a three-dimensional cage structure as the lowest energy conformation. Theoretical calculations show small water clusters like trimer, tetramer, pentamer are stable in cyclic form but the larger water clusters like to form three dimensional structures. The six membered water clusters are intermediate which shows different local minima for three dimensional as well as cyclic hexamer.²⁴ Recently Steed and co-workers have reported cyclic water tetramer in the crystal structures of four isomorphous complexes, $[M(L)_4(H_2O)_2]SO_4 \cdot 2H_2O$ ($M = Co, Ni, Cu, Zn$, $L = N$ -4-tolyl- N' -3-pyridylurea). Here two metal bound waters donate H-bonds to two free water molecules.²⁵ Vittal and co-workers have reported cyclic water tetramer in hydrogen-bonded polyrotaxane-like crystal structure of $[Zn(OAc)_2(\mu\text{-bpe})] \cdot 2H_2O$. Very recently Zuhayra *et al.* have published a planar water tetramer with tetrahedrally coordinated water embedded in a hydrogen-bonded cubane like network of $[Tc_4(CO)_{12}-(\mu_3\text{-OH})_4] \cdot 4H_2O$.²⁶ Whereas the even-numbered water ring morphologies such as $(H_2O)_n$ ($n = 4, 6, 8, 10, 12$ and 18) in the solid state complexes are frequently observed, the odd-numbered water rings are rarely reported. Gao and co-workers have noticed puckered and edge sharing cyclic water pentamer tape in the crystal structure of *trans*-4,4'-azopyridine dioxide $\cdot 4H_2O$.²⁷ Datta *et al.* have found ribbons of edge sharing cyclic water pentamers in a metal–organic framework formed by $[Cu(DPA)(CO_3)] \cdot 3H_2O$.²⁸ Ye and co-workers have trapped discrete cyclic water hexamer in chair form in the crystal structures of $[M(H_2biim)_2(OH)_2](ina)_2 \cdot 4H_2O$ ($M = Zn$ and Co , $H_2biim = 2,2'$ -biimidazole, $ina =$ isoniconate), where two of the six water molecules are bonded to metal atom.²⁹ A 1D tape of water hexamer has been reported by Custelcean. This water

tape made of ice like chair hexamer is included in the channel of 2,4-dimethyl-5-aminobenzo[b]-1,8-naphthyridine crystal lattice.³⁰ When 1,4-phenylenediboronic acid was crystallized from water, Höpfl *et al.* have noticed that a 2D layer of water hexamer in boat as well as chair conformation is trapped in the layered crystal structure of the clathrate.³¹ Higher order water clusters such as octamer,^{32a,b} decamer,^{32c,d} dodecamer,^{32e} etc. also have been reported in the literature.

This chapter deals with the different halogenated phloroglucinols, which were synthesized and crystallized to trap water clusters of different topologies (Scheme 2). Since halogen and –OH groups play a similar role in H-bonding, they can act as donor and acceptor, we examined various halogenated phloroglucinols.



Scheme 2. Different hydrated and anhydrous halogenated phloroglucinol crystal structures are discussed in this chapter.

5.2 Results and Discussion

Among the six halogenated phloroglucinol compounds studied in this chapter, three are hydrated—trichlorophloroglucinol trihydrate (TCPG $\cdot 3\text{H}_2\text{O}$), tribromophloroglucinol trihydrate (TBPG $\cdot 3\text{H}_2\text{O}$) and dibromophloroglucinol tetrahydrate (DBPG $\cdot 4\text{H}_2\text{O}$). DBPG also crystallizes in anhydrous form. Other three compounds namely, triiodophloroglucinol (TIPG), diiodophloroglucinol (DIPG) and

bromophloroglucinol (BPG) crystallize without incorporating water in the lattice.

5.2.1 TCPG•3H₂O and TBPG•3H₂O

TCPG crystallizes as a trihydrate from ethyl acetate solvent. The X-ray crystal structure of TCPG•3H₂O in $P2_1/n$ space group has one host and three symmetry-independent water molecules. The heavy atoms are fully ordered whereas phenol OH and one of the water H atoms are disordered, even at 100 K. Inversion-related molecules of TCPG stack at van der Waals distance in a Piedfort Unit³³ assembly ($\pi\cdots\pi$ 3.28, 3.41 Å) to form a hexahost dimer with six phenolic –OH groups radiating outwards (Figure 1a). Three phenolic –OHs (O1, O2, O3) are hydrogen-bonded to crystallographically distinct water molecules (O4, O5, O6), which are in turn H-bonded to phenol acceptor groups (O1, O3, O2; O \cdots O 2.70–2.83 Å). The second donor hydrogen of the water molecule is used in H-bonding with itself to form a helical spine of O_w–H \cdots O_w hydrogen bonds between symmetry-independent waters (helix pitch = 6.93 Å = *a*-axis; Figure 1d). Six such helices of tetracoordinated water molecules surround a Piedfort stack of TCPG host molecules (Figure 1a). The almost flat *bc*-layer has a hexagonal arrangement of TCPG molecules mediated via phenol groups, water molecules, and Cl \cdots Cl contacts (3.38, 3.34 Å). The trigonal nanotube containing the 1D helical water polymer along the *a*-axis has a pore of ~4.6 Å on each side. The disorder of phenol H atoms in TCPG•3H₂O could be due to intramolecular O–H \cdots Cl interactions³⁴ with the flanking chlorine atoms.

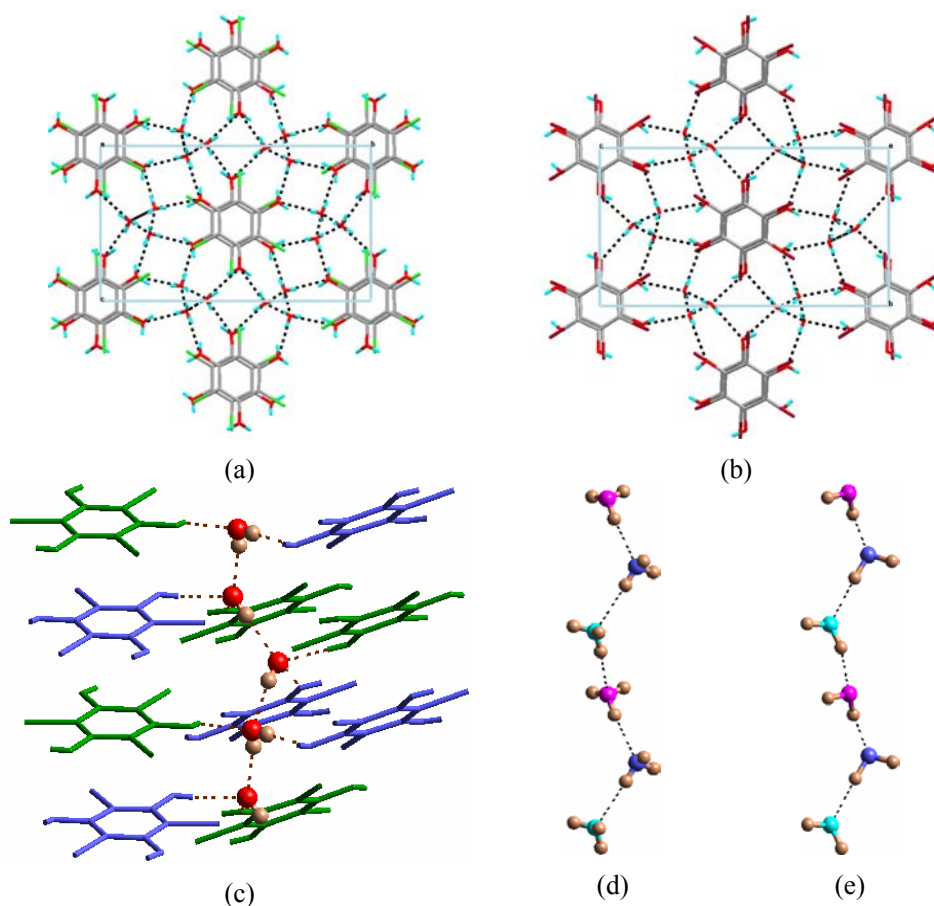


Figure 1. (a)/(b) Piedfort Unit of π -stacked TCPG/TBPG molecules to show six phenol OHs extending radially. Water helices are encircled in the triangular pores of three TCPG/TBPG stacks. Six water helices surround a rod of host molecules when viewed down the a -axis. (c) Spiral assembly of host molecules (green, blue) around the water helix in TBPG•3H₂O. (d) O_w–H...O_w hydrogen bonding in a water helix of TCPG•3H₂O (disordered protons are shown). (e) Homodromic H-bonds in the water helix of ordered TBPG•3H₂O. The hexagonal packing of host frameworks is similar but the water molecules are arranged differently.

However, the handedness of water helices (helix pitch = 7.10 Å = a -axis; Figure 1c,e) surrounding a Piedfort stack ($\pi \cdots \pi$ 3.30, 3.37 Å) of TBPG host molecules (Br...Br 3.29, 3.47 Å) is different (Figure 2). The six water helices (O_w–H...O_w) encircling a rod of TCPG host molecule are alternately right- and left-handed (PMPMPM; P = plus or

right-handed, M = minus or left-handed) whereas their alignment in TBPG trihydrate is, interestingly, three contiguous helices of the same chirality and the other three of opposite helicity (PPPM). The latter situation is novel among the known examples of helical water chains.³⁵ The water helix has homodromic chains of $O_w-H\cdots O_w$ hydrogen bonds (cooperative H-bonding)^{1d,36} in the fully ordered TBPG•3H₂O structure. Two factors should be considered to understand these differences: (1) The 1D water helix is the central self-assembly building unit in both hydrate host–guest structures; (2) Bromine is about 0.1 Å larger than chlorine (van der Waals radii: Cl 1.75 Å, Br 1.85 Å), and also more polarizable. There are small, yet structurally significant, differences in halogen⋯halogen interactions. While both Cl⋯Cl interactions are of about the same length (3.38, 3.44 Å) one of the Br⋯Br contacts is much shorter than the other (3.29, 3.47 Å).³⁷ Whereas TCPG host molecules are arranged in an almost flat *bc*-sheet, TBPG molecules lie in a corrugated layer because phenyl rings connected via the short Br⋯Br contact are tilted. This tilt in the phenolic –OH groups changes the position of hydrogen-bonded water molecules along the *a*-axis and, in turn, the helicity of the water chain. Water helices that are adjacent to the roughly coplanar host phenyl rings, and lie across longer inter-halogen contacts (Cl⋯Cl 3.387, 3.443 Å; Br⋯Br 3.473 Å), are of opposite handedness (PM), whereas 1D water chains that are adjacent to the tilted host phenyl rings, and are arranged across the short Br⋯Br contact of 3.291 Å, have the same handedness (PP or MM) (Figure 2). The present case is the first illustration on the role of weak halogen⋯halogen interactions in directing the helical twist of strong $O_w-H\cdots O_w$ chains in crystal structures.³⁸ Bromine is able to participate in shorter inter-halogen contacts than chlorine with respect to the van der Waals radius because of its better polarizability.

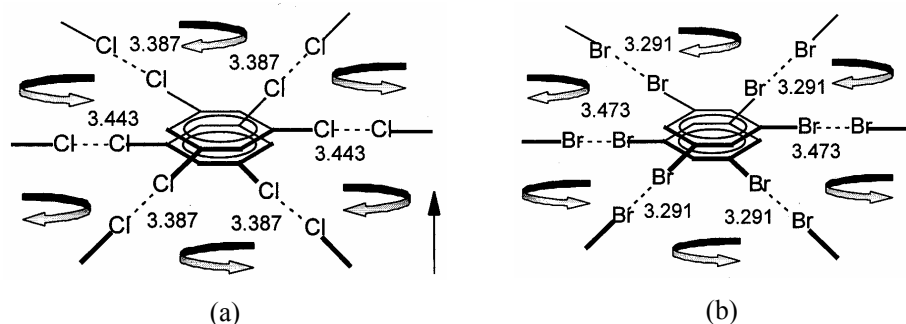


Figure 2. Six water helices surround the Piedfort dimer of (a) TCPG and (b) TBPG (phenolic $-\text{OH}$ groups are omitted for clarity). The handedness of water helices across longer inter-halogen contacts of ~ 3.4 Å is opposite whereas it is the same when the distance is ~ 3.3 Å. This is due to the tilt of phenyl ring.

There are some interesting reports on water helices enclathrated in small molecular lattice host channel. Birkedal *et al.* have noticed negative thermal expansion of the c -axis of dipeptide tryptophylglycine $\cdot\text{H}_2\text{O}$ (TrpGly $\cdot\text{H}_2\text{O}$) crystal, where the helical water chain was made responsible for this unusual behavior. Lowering the temperature increases the ordering of the water molecules, resembles water-ice nature (Figure 3a).^{35a} Two opposite single helices in the same channel has been reported by Chen *et al.* in the crystal structure of trimesic acid \cdot melamine trihydrate cocrystal (Figure 3b).³⁹ Vittal and Sreenivasulu have reported helical water chain inside coordination polymer helix of $[(\text{H}_2\text{O})_2\text{C}\{\text{Ni}(\text{Hsglu})(\text{H}_2\text{O})\}]\cdot\text{H}_2\text{O}$ ($\text{H}_3\text{suglu} = N$ -(2-hydroxybenzyl)-L-glutamic acid).⁴⁰

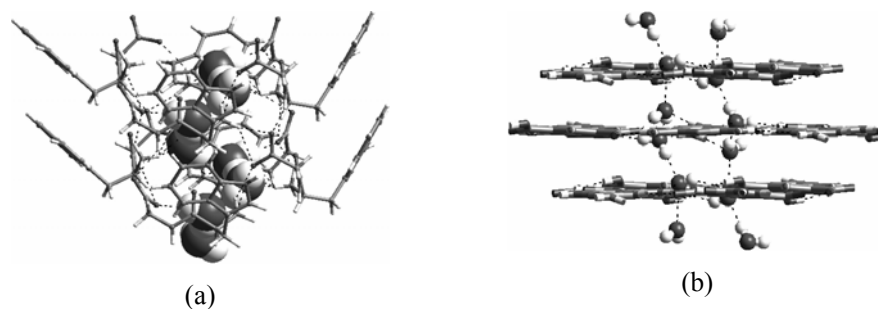


Figure 3. (a) Negative thermal expansion shown by the water helix in the crystal structure of TrpGly $\cdot\text{H}_2\text{O}$. (b) Two opposite handed single helices in the same channel of the complex of trimesic acid \cdot melamine trihydrate crystal structure.

5.2.2 DBPG•4H₂O and DBPG (anhydrous)

Crystals of the composition DBPG•4H₂O were obtained by slow evaporation of a solution of dibromophloroglucinol in aqueous methanol. The asymmetric unit (space group *C2/c*) contains 0.5 molecule of DBPG (with O1 phenol and C4 atoms residing on the 2-fold rotation axis) and two water molecules (O3 and O4). Four DBPG molecules are hydrogen-bonded via water molecules (O2–H···O3 2.67 Å, O3–H···O2 2.82 Å) and Br···Br contact (3.45 Å) to form a rectangular grid of 8.0×4.5 Å voids in the *ab*-plane (Figure 4a). Aromatic rings of adjacent layers stack with excellent π ··· π overlap at 3.42 Å inter-planar distance to make channels along the *c*-axis. Hydrogen-bonded water molecules reside in the tubular framework of DBPG host connected via water···phenol bonding. The H atom of phenol O1 is disordered over two locations by crystallographic 2-fold symmetry and one of the H atoms of water O4 has 0.5 occupancy (H4B, H4C). The intricate H-bond network of water molecules along [001] is shown in figure 4c,d. Three structural features of the water cluster deserve discussion. (1) O3 and O4 water molecules are H-bonded in a hexamer of boat cyclohexane conformation. The four O atoms that constitute the bottom of the boat are nearly planar, deviating by only 0.25 Å from the mean plane of O3–O4–O3–O4 atoms. (2) Such hexamers are connected at the O4–O4 bond to form a linear tape of tetra-coordinated water motif in boat cyclohexane conformation for the first time, similar to the H-bond network along the *c*-axis in hexagonal ice (*I_h*) (Figure 4e). (3) The edge O atoms pointing towards each other in the high-energy boat hexamer of water molecules are stabilized by cooperative H-bonds with the phenol host (O1–H···O4 2.77 Å).

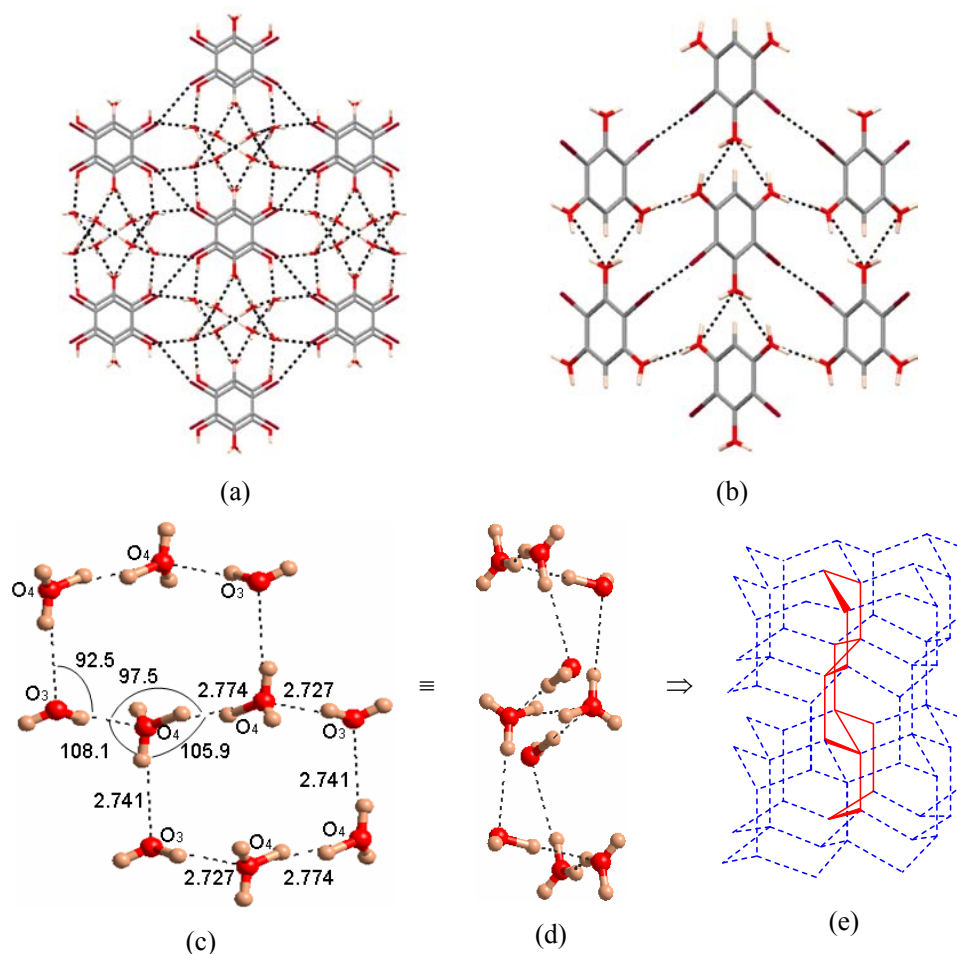
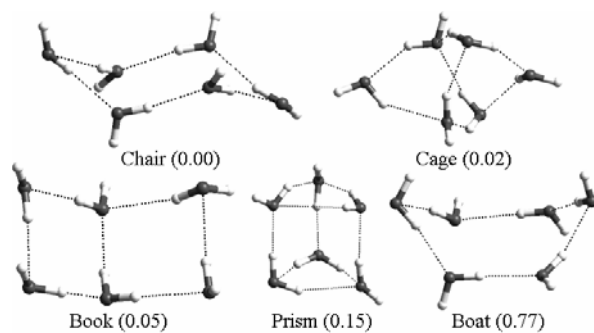


Figure 4. Rectangular grid of DBPG molecules in the ab -plane and stacking of aromatic rings with no offset generates channels down the c -axis. (b) Pseudo hexagonal packing of anhydrous DBPG molecules. (c) Hydrogen bonding between O3 and O4 water molecules in the water hexamer tape structure bonded to phenol O1 and O2 atoms along the tubular host framework. (d) Boat cyclohexane conformation of T6(2) water tape in DBPG·4H₂O. (e) T6(2) tape (red) highlighted in the structure of hexagonal ice I_h (blue). Water O atoms are located at the nodes and H-bonds are represented as lines in the 3D network.

In the past several decades, considerable attention has been drawn in experimental and theoretical studies of small water clusters, specially water hexamer because it is the building block of ice I_h and I_c and is relevant to bulk water as well. So

far, thirteen polymorphic phases of pure solid water have been characterized, denoted as I_h , I_c , and II to XI^{41a,b} and the recently described ice XII.^{41c,d} In addition, two amorphous ice polymorphs^{41e} (low- and high-density) have been detected. Losada and Leutwyler have showed that at the MP2/aVTZ level, among five low energy discrete water hexamers prism is lowest in energy, followed by cage which is 0.07 kcal/mol and book which is 0.48 kcal/mol higher. The two cyclic isomers chair and boat lie 1.03 and 2.11 kcal/mol above the prism. When zero-point vibrational energy change upon cluster formation is taken into account, the stability sequence of the isomeric clusters changes completely. Chair becomes the lowest-energy isomer, followed very closely by cage (+0.02 kcal/mol) and book (+0.05 kcal/mol) and then by prism (+0.15 kcal/mol), boat remains the highest-energy of these five isomers at +0.77 kcal/mol (Scheme 3).^{24a} The energy may not be the same when water molecules are four-coordinated.



Scheme 3. Computed energies (MP2/aVTZ level) of the five lowest energy (relative to chair, in kcal/mol) water hexamer structures.

The high energy boat conformation of water hexamer in 2D layer has been reported by Iwamoto *et al.* Puckered networks of $[\text{CdNi}(\text{CN})_4]_\infty$ and water layers are stacked alternately in the double layered crystal structure of $[\text{CdNi}(\text{CN})_4] \cdot 4\text{H}_2\text{O}$.⁴² A puckered discrete boat of water hexamer has been included in the crystal structure of polymeric $[\text{Cu}_2(\text{btc})(\text{Py})_4 \cdot 2\text{H}_2\text{O}] \cdot 4\text{H}_2\text{O}$.⁴³ This hexamer contains unsaturated H-bonded water molecules, which is present in bulk water.

Here we report a 1D tape of cyclic water hexamer in boat conformation. The

infinite tape motif in the present hydrate structure is constituted by boat cyclohexane rings and has the notation T6(2), namely a tape of 6-membered rings with 2 shared water molecules. The seven examples of T6(2) water topology reported in the 2002 version of the Cambridge Structural Database (CSD)⁴⁴ have chair cyclohexane conformation. However, a very recent (2005) critical evaluation of water oligomers by Mascal, Infantes and Chisholm shows that out of 31 examples of T6(2) clusters, 7 structures have water molecules in the boat conformation (CSD refcodes ODIMAP, BELFED, WUXLOQ, PIZPET, PIZPIX/01, PIZPOD).⁴⁵ Six of these hits are metal–organics and one is an organic host structure. We have collected reflections on DBPG•4H₂O crystal at 298 K and 100 K to confirm that there is no phase transition⁴⁶ and water H atom positions are assigned from difference electron density maps at 100 K. The T6(2) boat water tape in DBPG host is unique among the 7 CSD refcodes. (1) Our structure has tetra-coordinated water molecules, as in ices I_h and I_c, in contrast to mixture of 4-coordinated and 3/5-coordinated waters in the reported structures. The 1D water tape in ODIMAP is highly distorted compared to the tetrahedral geometry in I_h. Gillon *et al.*⁴⁷ surveyed the CSD for hydration motifs in molecular crystals: 3-coordinated water is the most common (38.40%) followed by 4-coordinated water (27.45%), or the so-called Walrafen pentamer.^{1a} (2) Whereas the T6(2) tapes are coordinated to other water molecules in CSD structures, only water molecules that are part of the boat cyclohexane cluster propagate the tape motif in DBPG tetrahydrate. The water cluster boat geometry shows the expected variation with temperature. The mean O...O distance of 2.74 Å at 100 K (2.77 Å at 298 K) is closer to the distance in hexagonal ice (2.75 Å) than liquid water (2.85 Å), whereas O–O–O angles vary from 92–105° compared to the mean value of 109.5° in the tetrahedral arrangement of water neighbors in ice.

When DBPG was dissolved in ethyl acetate and the solution was layered with chloroform, the anhydrous form (space group *Pbcn*) crystallized with 0.5 molecule in the asymmetric unit, exhibiting a pseudo-hexagonal arrangement of molecules (Figure 4b) via phenolic O–H...O H-bonds (2.92, 3.12 Å) and Br...Br interaction (3.49 Å). There is no significant π – π stacking (Piedfort Unit). Here too, the molecule resides on the 2-fold rotation axis and phenol protons are disordered over two sites with 0.5 occupancy. The

packing fraction of DBPG•4H₂O is 68.3% with water occupying 35.8% of the crystal volume and the DBPG packing fraction is 73.7%.

5.2.3 TIPG

TIPG was crystallized from ethyl acetate and chloroform mixed solvent to afford X-ray diffraction quality single crystals in the space group $P2_12_12_1$ with one molecule in the asymmetric unit. The OH groups are surrounded by bulky iodo groups and hence cannot participate in any significant hydrogen bonding. The inability of H-bond formation by the OH groups has been reflected by the larger O...O distances (3.21 and 3.27 Å) among the neighboring –OH groups. On the other hand larger and polarizable iodo groups form shorter I...I contacts (3.78 Å, 164.2°, 103.9° and 3.90 Å, 145.8°, 82.6°).

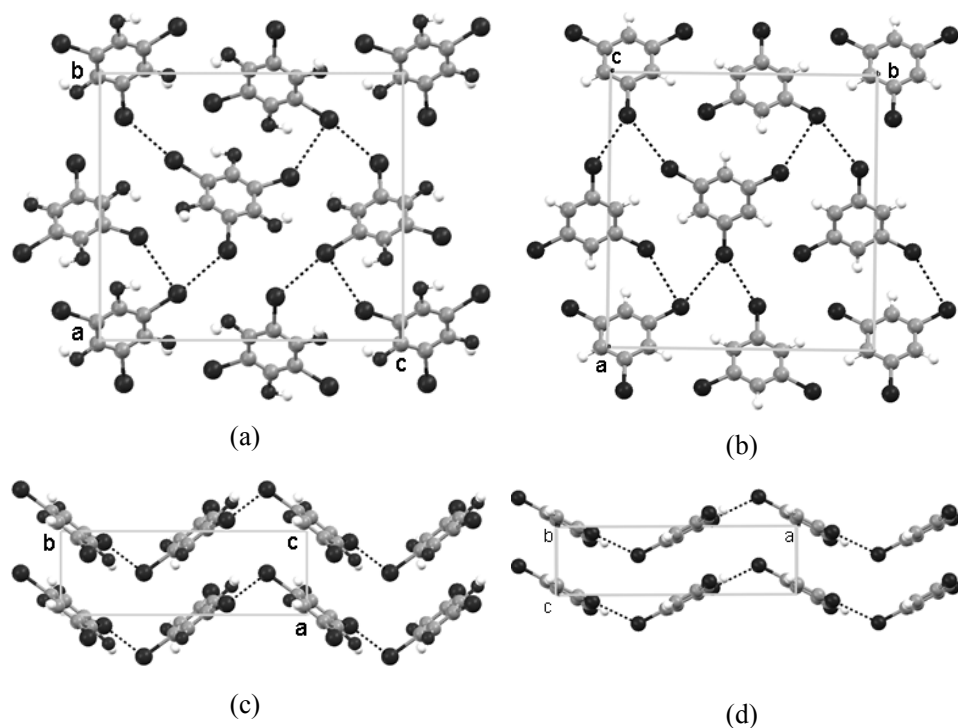


Figure 5. Structural similarity between TIPG and TBB. View perpendicular to corrugated sheet (a) and (b), parallel to the sheet (c) and (d) of TIPG and TBB crystal structures.

The molecules form corrugated sheet like structure in the *bc*-plane mediated by very weak O–H...O hydrogen bonds (*D* 3.21 Å) along *a*-axis and short I...I interactions (Figure 5a,c). Further evidence of the steric crowding around the –OH groups is the structural similarity of TIPG with the crystal structure of tribromobenzene (space group $P2_12_12_1$; Figure 5b,d), i.e. –OH group is like H atom and does not make any hydrogen bond.

5.2.4. DIPG

DIPG was crystallized from ethyl acetate in $P\bar{1}$ space group with two symmetry independent molecules. The relatively less hindered OH groups compared to TIPG, form hydrogen bonds (*D* 2.81, 2.85 and 3.00 Å) and the iodo groups are involved in I...I (3.82 Å, 165.5° and 93.7°), I...O (3.12 Å, 158.8°) and I... π (3.32 Å, 169.0° and 3.42 Å, 179.0°) interactions. The molecules form square network via O–H...O hydrogen bonds and I...O halogen bonds (Figure 6a). The different kinds of interactions made by the iodo groups in this structure are shown in figure 6b.

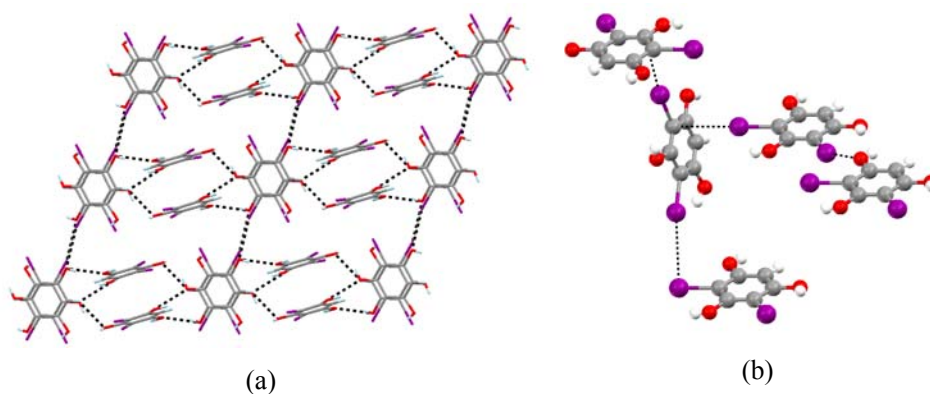


Figure 6. (a) Square network made by the DIPG molecules mediated via O–H...O hydrogen bonds and I...O halogen bonds. (b) Three different kinds of interactions such as I...I, I...O and I... π , made by the iodo groups in this structure.

5.2.5 BPG

X-ray quality single crystals of BPG were obtained from ethyl acetate solution. It

crystallizes in $P2_1$ space group with one molecule in the asymmetric unit. Comparatively free OH groups in this molecule form stronger hydrogen bonds (D 2.76, 2.77 and 2.78 Å) than in the crystal structures of DBPG, TIPG and DIPG. All the three OH groups act as a donor as well as an acceptor in the infinite, zig-zag and helical chains of $O-H\cdots O$ hydrogen bonds propagate along the b -axis. In this structure Br is involved in $Br\cdots O$ (3.33 Å, 157.2°) and weak $Br\cdots Br$ (type II, 3.79 Å, 157.2° and 92.5°) interactions (Figure 7).

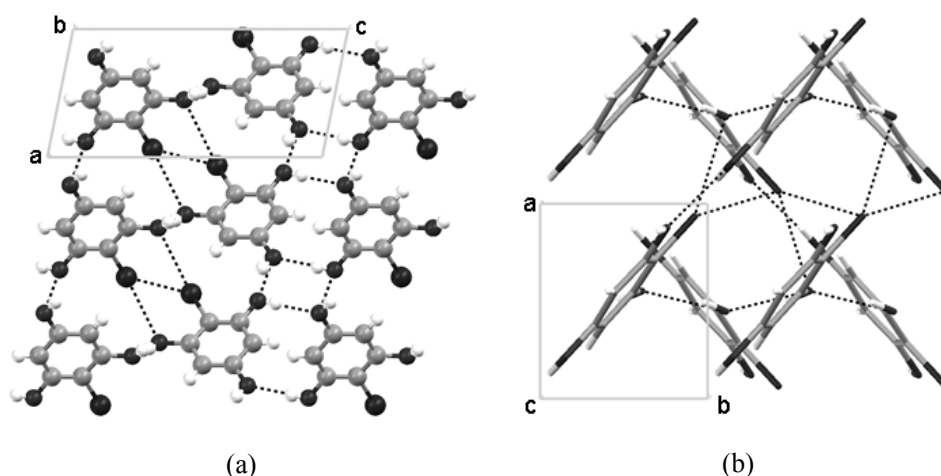


Figure 7. Infinite $O-H\cdots O$ mediated architecture in the crystal structures of BPG molecules, stabilized further by $Br\cdots O$ and $Br\cdots Br$ interactions, view down the b -axis (a) and c -axis (b).

Table 1. Interaction geometries in TCPG•3H₂O, TBPG•3H₂O, DBPG•4H₂O, DBPG, TIPG, DIPG and BPG. O–H distance is neutron-normalized to 0.983 Å.

Compound	Interaction	d (Å)	D (Å)	θ (°)
TCPG•3H ₂ O	O(1)–H(1A)⋯O(4)	1.79	2.711(2)	154.0
	O(1)–H(1B)⋯O(4)	1.93	2.832(2)	150.9
	O(2)–H(2A)⋯O(5)	1.83	2.737(3)	152.6
	O(2)–H(2B)⋯O(6)	1.89	2.798(3)	151.5
	O(3)–H(3B)⋯O(5)	1.88	2.782(3)	151.5
	O(3)–H(3A)⋯O(6)	1.81	2.699(3)	148.2
	O(4)–H(4C)⋯O(1)	1.76	2.711(2)	161.0

	O(4)–H(4B)···O(1)	1.87	2.832(2)	164.5
	O(6)–H(6B)···O(2)	1.83	2.798(3)	167.4
	O(5)–H(5C)···O(2)	1.78	2.737(3)	163.8
	O(5)–H(5B)···O(3)	1.82	2.782(3)	166.1
	O(6)–H(6C)···O(3)	1.73	2.699(3)	168.2
	O(4)–H(4A)···O(6)	1.81	2.787(3)	169.8
	O(6)–H(6A)···O(5)	1.81	2.773(3)	166.3
	O(5)–H(5A)···O(4)	1.81	2.785(3)	170.5
	Cl(1)···Cl(3)		3.387(1)	173.3, 155.9
	Cl(2)···Cl(2)		3.443(1)	149.4, 149.4
	$\pi\cdots\pi$		3.28, 3.41	
TBPG•3H ₂ O	O(1)–H(1)···O(6)	1.84	2.743(3)	151.6
	O(2)–H(2)···O(4)	2.01	2.772(3)	132.5
	O(3)–H(3)···O(5)	1.83	2.724(3)	148.8
	O(4)–H(4A)···O(6)	1.88	2.844(4)	166.4
	O(4)–H(4B)···O(1)	1.88	2.860(3)	172.6
	O(5)–H(5A)···O(3)	2.04	2.976(3)	159.3
	O(5)–H(5B)···O(4)	1.85	2.826(3)	168.9
	O(6)–H(6A)···O(2)	1.97	2.882(3)	154.0
	O(6)–H(6B)···O(5)	1.88	2.843(3)	164.3
	Br(2)···Br(3)		3.291(0)	162.2, 144.2
	Br(1)···Br(1)		3.473(1)	167.2, 167.2
	$\pi\cdots\pi$		3.30, 3.37	
DBPG•4H ₂ O	O(1)–H(1)···O(4)	1.84	2.770(3)	157.2
	O(2)–H(2)···O(3)	1.69	2.669(2)	172.4
	O(3)–H(3A)···O(2)	1.85	2.806(3)	164.4
	O(3)–H(3B)···O(4)	1.76	2.727(3)	167.6
	O(4)–H(4A)···O(3)	1.78	2.741(3)	164.3
	O(4)–H(4B)···O(4)	1.81	2.774(3)	167.4
	O(4)–H(4C)···O(1)	1.85	2.770(3)	154.9
	Br···Br		3.452(4)	140.5, 140.5
DBPG	O(1)–H(1)···O(2)	2.11	2.916(5)	138.0
	O(2)–H(2A)···O(2)	2.21	3.123(6)	153.4
	O(2)–H(2B)···O(1)	2.07	2.916(5)	142.7
	Br···Br		3.491(1)	170.0, 87.5
TIPG	O(1)–H(1)···O(3)	2.37	3.214(4)	143.6
	I(1)···I(2)		3.897(1)	145.8, 82.6
	I(2)···I(3)		3.779(1)	103.9, 164.2
	I(3)···I(3)		4.120(1)	140.2, 140.2

DIPG	O(1)–H(1)···O(5)	1.93	2.849(6)	154.8
	O(2)–H(2)···O(6)	2.39	3.145(6)	133.1
	O(5)–H(5)···O(2)	2.18	3.004(7)	140.0
	O(4)–H(4)···O(3)	1.86	2.812(6)	161.9
	I(2)···I(3)		3.825(1)	165.5, 93.7
	I(4)···O(1)		3.125(4)	158.8
	I(3)··· π		3.421(6)	179.0
	I··· π		3.320(5)	169.0
BPG	O(1)–H(1)···O(1)	1.81	2.763(6)	162.6
	O(2)–H(2)···O(3)	1.80	2.770(7)	169.0
	O(3)–H(3)···O(2)	1.90	2.779(7)	147.3
	Br(1)···O(1)		3.326(5)	157.2

5.2.6 Thermal Analysis

Water loss in thermal gravimetric analysis (TGA; Figure 8b) matches with the trihydrate stoichiometry of TCPG•3H₂O (obsd. 18.8%, calc. 19.0%) and TBPG•3H₂O (obsd. 12.5%, calc. 12.9%). The endotherm for water evolution from TCPG is at 103 °C and from TBPG at 77 °C (major) and 94 °C (minor) in DSC (differential scanning calorimetry; Figure 8a). The normalized enthalpy for water transit (–656 and –332 J/g) and strength of O–H···O hydrogen bonds in TCPG•3H₂O and TBPG•3H₂O are 62 and 46 kJ/mol per water molecule (21 and 15 kJ per H-bond). The stronger H-bond energy, higher onset temperature, and higher enthalpy for water release from TCPG compared to TBPG channel is due to the stronger (shorter) hydrogen bonds in the former structure (O···O 2.70–2.83 Å vs. 2.72–2.98 Å).

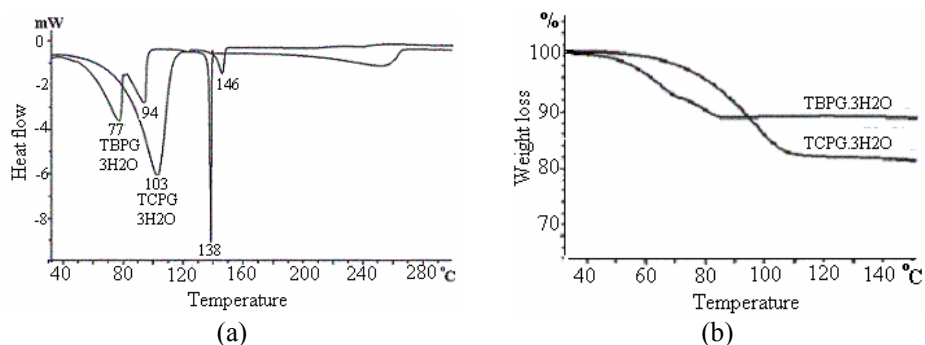


Figure 8. DSC (a) and TGA (b) plot of TCPG•3H₂O and TBPG•3H₂O.

The evolution of water from the channel structure of DBPG host was analyzed by thermal gravimetric analysis and differential scanning calorimetry (TGA, DSC; Figure 9). There is 19.5% weight loss between 40–90 °C in DBPG•4H₂O (calc. = 20.2%) consistent with the broad endotherm peak at 81.6 °C. The enthalpy for water release is 29.7 kJ/mol, which means 10.8 kJ/mol per hydrogen bond. This value is about half that in crystalline ice polymorphs (~22 kJ/mol).⁴⁸ The second endotherm at 97.7 °C is phase transition of the channel structure to the anhydrous form since this thermal event in DSC is not concomitant with weight loss in TGA. DBPG melts at 170–171 °C.

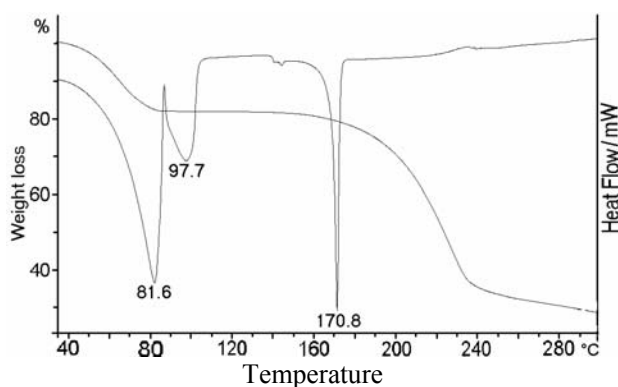


Figure 9. DSC and TGA thermograms of DBPG•4H₂O. The major endotherm peak at 81.6 °C is due to water loss consistent with TGA. The endotherm at 97.7 °C is phase transition of the water-filled channel structure to the anhydrous apohost, which completely melts at 170.8 °C.

5.2.7 PXRD and IR Analysis

Powder X-ray diffraction (PXRD) of the hydrate and anhydrous material showed differences in dehydration/rehydration behavior. Dehydration of TCPG•3H₂O at 115 °C for 2 h under vacuum afforded material whose PXRD is identical to the original powder pattern, showing that this hydrogen-bonded host lattice is robust enough to the loss of interstitial water (Figure 10a,b). The dehydrated material regained about two-third of its water from atmospheric moisture within 4 h and gained the original water stoichiometry (19% weight increase) after 24 h (TGA). Thus, TCPG•3H₂O exhibits “organic zeolite” like behavior through reversible water loss and uptake. On the other hand, PXRD trace

of $\text{TBPG} \cdot 3\text{H}_2\text{O}$ after dehydration is significantly different (Figure 10c,d). Thus, there are structural and functional differences between these hydrate channel inclusion structures.

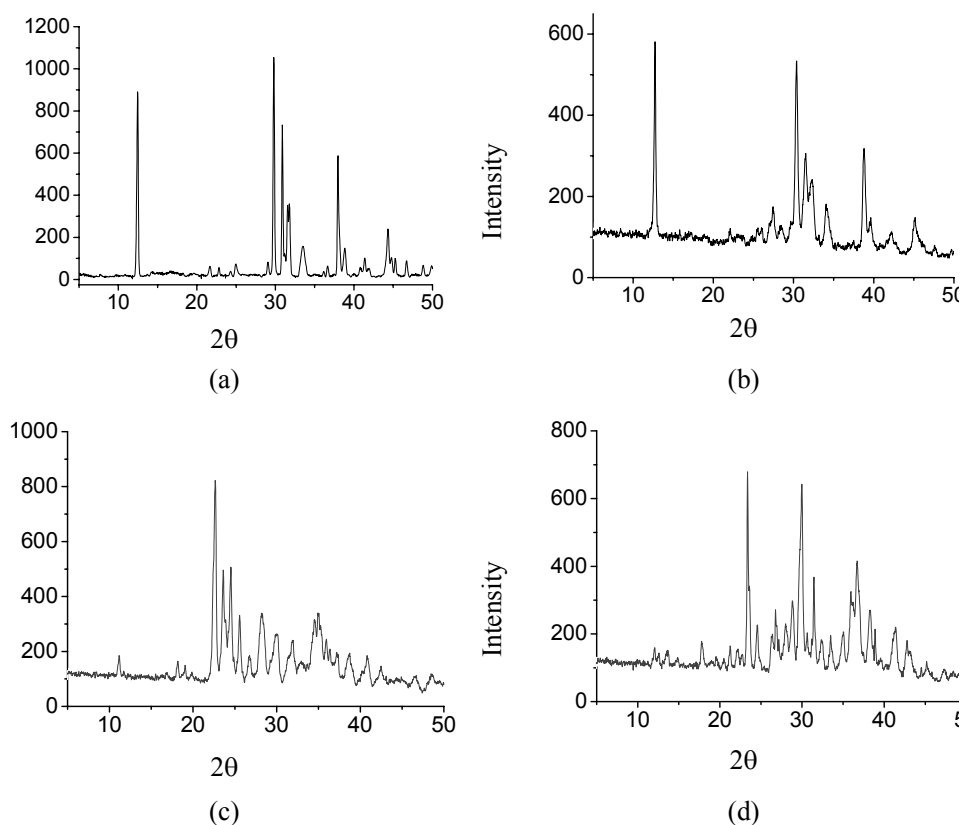


Figure 10. Powder X-ray diffraction of hydrated and dehydrated/rehydrated samples. $\text{TCPCG} \cdot 3\text{H}_2\text{O}$: (a) original trihydrate powder; (b) dehydrated powder reabsorbs the water content of trihydrate. $\text{TBPG} \cdot 3\text{H}_2\text{O}$: (c) original trihydrate powder; (d) dehydrated powder, (c) and (d) have different PXRDs. The material in (b) shows partial uptake of water from the atmosphere in a few hours and completely rehydrates after 1-2 days, as measured by TG analysis.

Dehydration of the water-filled channel of $\text{DBPG} \cdot 4\text{H}_2\text{O}$ at 90°C for 30 min at 0.2 Torr gave a microcrystalline solid whose powder XRD matches with simulated peaks from the *Pbcn* X-ray crystal structure. When the dehydrated material was left overnight in a chamber saturated with water vapour it completely converts to the tetrahydrate form

(PXRD, TGA; Figure 11). Thus, the organic host DBPG functions like a supramolecular sponge:⁴⁹ it readily uptakes moisture and releases the guest under relatively mild conditions ($<100\text{ }^{\circ}\text{C}$). The IR spectrum (KBr) of anhydrous and hydrate DBPG show similar broad peaks for OH stretch in the range $3000\text{--}3500\text{ cm}^{-1}$ due to H-bonded phenol and water aggregates, making it difficult to identify the peaks from water clusters (compare with hexagonal ice at 3220 cm^{-1} and liquid water at 3280 cm^{-1}).

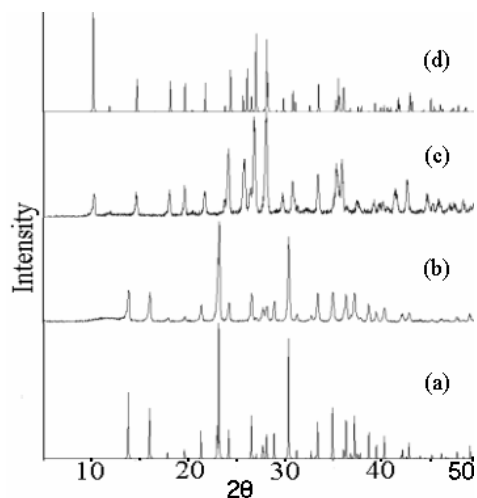


Figure 11. Powder X-ray diffraction plots. (a) anhydrous DBPG (simulated). (b) Expulsion of water from the tetrahydrate (experimental). (c) Rehydration of the anhydrous form with water vapor (experimental). (d) $\text{DBPG}\cdot 4\text{H}_2\text{O}$ (simulated).

5.3 Conclusions

Two crystal structures of unsubstituted phloroglucinol are reported as anhydrous and dihydrate form.⁵⁰ Interestingly substitution on phloroglucinol by halogen groups increases the hydration in $\text{TCPG}\cdot 3\text{H}_2\text{O}$, $\text{TBPG}\cdot 3\text{H}_2\text{O}$ and $\text{DBPG}\cdot 4\text{H}_2\text{O}$ compounds. Moreover TBPG easily forms hydrate from chloroform–ethyl solvent mixture, whereas DBPG hydration occurs from aqueous methanol and the anhydrous crystal structure is easily formed from chloroform–ethyl acetate solvent mixture and monosubstituted phloroglucinol (BPG) crystallize as anhydrous form. On the other hand TIPG and DIPG crystallize without inclusion of water. Thus the result indicates that with increase in

halogenation the hydration capacity of phloroglucinol increases, on the other hand with increase in bulkiness of the halogen the hydration affinity decreases. Hydrogen bond strengths weaken from TCPG•3H₂O to TBPG•3H₂O crystal structure due to the increase in bulkiness of the halogen groups (O...O distances and DSC/TGA) and in TIPG crystal structure, the very large iodo groups mask –OH groups to prevent from any significant H-bond formation. Bulky groups around strong H-bonding functional group –OH, avert two –OH groups to come closer to interact. Thus small water molecules, which are capable of forming strong H-bond, interact with phenolic –OH groups and stabilize the crystal lattice.

In this context it is important to mention the observation by Infantes and co-workers on the affinity to water of 36 chemical groups, which are most frequent in the crystal structures.¹² The crystal structures containing ionic groups are predictably highly hydrated. Neutral strong H-bonding groups, such as OH, NH₂, CO, COOH, etc. are also popular in the hydrate structures. But weak H-bonding groups, such as terminal halogens, CF₃, CCl₃, ether (–O–), CN and NO₂ have very low affinity toward water. This is not surprising because O–H...halogen (or other weak acceptors) H-bond strength is not comparable to O–H...O H-bond and they are unlikely to disturb the H-bonding network in bulk water. They have further shown that with increase in the number of halogens in a molecule, the hydration probability decreases.

Strong O–H...O hydrogen bonds force both the systems TCPG•3H₂O and TBPG•3H₂O to adopt near identical packing, which brings large, polarizable bromo groups at very short distance. It causes phenyl groups to tilt around short Br...Br contact resulting in different helicity of the water chain.

Stronger H-bonding in the tetrahydrate structure compared to the anhydrous form is the reason for water inclusion despite a lower packing fraction of the hydrate crystal. Whereas inter-halogen interactions are type I in the hydrate structure, they are the polarization induced type II contact in the anhydrous form. Cyclic water hexamers are prototypical structural motifs in ice polymorphs I_c, I_h, proton-disordered ice II, and bulk water. Cubic ice is stable below –120 °C but undergoes phase transition to normal hexagonal ice above –80 °C. The absence of phase transition in DBPG•4H₂O between

100–298 K provides a 1D ice-like structural motif for variable-temperature diffraction and spectroscopy experiments.

5.4 Experimental

Synthesis

TCPG: Phloroglucinol dihydrate (6.2 mmol, 781 mg) was dissolved in MeOH (10 mL). 4% NaOCl (32 g) added drop wise during 2 hrs. at 0°C and stirrer for another 1 hour. The solution was neutralized with dil. HCl. Excess chlorine was removed by sodium thiosulphate. The Compound was extracted using EtOAc.

TBPG and TIPG have been synthesised according to the reported procedure.⁵¹

DBPG and BPG: 25 mL water solution of KBrO₃ (3.3 mmol, 551 mg) and KBr (6.7 mmol, 440 mg) was added to water solution of phloroglucinol (10 mmol, 1260 mg, 15 mL) and 0.85 mL of conc. HCl at 0 °C slowly. Then the mixture was stirred for over night at room temperature. It was then extracted by diethyl ether and the two compounds separated and purified by column chromatography.

DIPG: 25 mL water solution of KIO₃ (3.3 mmol, 706 mg) and KI (6.7 mmol, 1112 mg) was added to water solution of phloroglucinol (10 mmol, 1260 mg, 15 mL) and 0.85 ml of conc. HCl at 0 °C slowly. Then the mixture was stirred for over night at room temperature. It was then extracted by diethyl ether and purified by column chromatography.

TCPG: ¹H-NMR (DMSO-d₆, 400 MHz) δ 9.91 (s).

TBPG: ¹H-NMR (CDCl₃, 400 MHz) δ 6.01 (s).

TIPG: ¹H-NMR (CDCl₃, 400 MHz) δ 5.97 (s).

DBPG: ¹H-NMR (CDCl₃, 400 MHz) δ 6.42 (s, 1H), 5.77 (s, 1H), 5.51 (s, 2H).

DIPG: ¹H-NMR (CDCl₃, 400 MHz) δ 6.38 (s, 1H), 5.77 (s, 1H), 5.57 (s, 2H).

BPG: ¹H-NMR (CDCl₃, 400 MHz) δ 6.15 (s, 2H), 5.38 (s, 2H), 4.94 (s, 1H).

X-ray Crystallography

Reflections were collected for the single crystal of TIPG on a KUMA CCD area detector system and for TCPG, TBPG, DBPG, DIPG, BPG on a Bruker SMART APEX CCD area detector system (Mo-K α radiation, $\lambda = 0.71073$ Å). Multi-scan absorption correction was applied for TIPG using XEMP⁵² and for TCPG, TBPG, DBPG, DIPG, BPG using SADABS. Structure solution and refinement were performed with SHELXS-97 and SHELXL-97 packages. C–H hydrogen atoms were generated with idealised geometries and isotropically refined using Riding model. O–H hydrogen atoms were located and refined isotropically from difference electron density map. Refinement of coordinates and anisotropic thermal parameters of non-hydrogen atoms was carried out by the full-matrix least-squares method.

H atoms of three phenol groups (O1, O2, O3) in TCPG are oriented in two positions (A and B) in the electron density map. H atoms of water molecules (O4, O5, O6) are present in three positions (A, B and C). The occupancy of these H atoms was refined to get a good *R*-factor of 2.89%.

All non-hydrogen atoms were refined anisotropically and H atoms connected to oxygens were located from difference electron density maps. For DBPG•4H₂O at 298 K, seven restraints are due to fixing seven O–H distances at 0.82 Å and four restraints are due to fixing four H–O–H angles at 105°. In both the tetrahydrate structures one phenolic hydrogen H1 is disordered over two positions due to symmetry and one water hydrogen is also disordered over two positions H4B and H4C with 0.5 occupancy each. In anhydrous DBPG three restraints are due to fixing the three O–H distances at 0.82 Å. Each phenolic hydrogen is disordered over two positions with 0.5 occupancy.

PXRD

Powder XRD of all samples were recorded on a PANalytical 1830 (Philips Analytical) diffractometer using Cu-K α X-radiation at 35 kV and 25 mA. Diffraction patterns were collected over 2θ range of 5–50° at scan rate of 2 °/min.

5.5 References

1. (a) R. Ludwig, *Angew. Chem. Int. Ed.*, **2001**, 40, 1808. (b) R. Ludwig, *Angew. Chem. Int. Ed.*, **2003**, 42, 258. (c) J. M. Ugalde, I. Alkorta and J. Elguero, *Angew. Chem. Int. Ed.*, **2000**, 39, 717. (d) G. A. Jeffrey, in *An Introduction to Hydrogen Bonding*; OUP: Oxford, **1997**.
2. L. Pauling, *J. Am. Chem. Soc.*, **1935**, 57, 2680.
3. C. I. Ratcliffe and J. A. Ripmeester, *Encyclopedia of supramolecular chemistry*, **2004**, 281.
4. J. H. van der Waals and J. C. Platteeuw, *Adv. Chem. Phys.*, **1959**, 2, 1.
5. *Science*, **2004**, 306, 2017.
6. P. Agre, *Angew. Chem. Int. Ed.* **2004**, 43, 4278.
7. G. M. Preston, T. P. Carroll, W. B. Guggino and P. Agre, *Science*, **1992**, 256, 385.
8. B. Jayaram and T. Jain, *Annu. Rev. Biophys. Biomol. Struct.*, **2004**, 33, 343.
9. N. C. Seeman, J. M. Rosenberg and A. Rich, *Proc. Natl. Acad. Sci. USA*, **1976**, 73, 804.
10. H. R. Drew and R. E. Dickerson, *J. Mol. Biol.*, **1981**, 151, 535.
11. R. Parthasarathy, S. Chaturvedi and K. Go, *Proc. Natl. Acad. Sci. U.S.A.*, **1990**, 871.
12. L. Infantes, J. Chisholm and S. Motherwell, *CrystEngComm*, **2003**, 5, 480.
13. G. R. Desiraju, *J. Chem. Soc., Chem. Commun.*, **1991**, 426.
14. R. Custelcean, C. Afloroaei, M. Vlassa and M. Polverejan, *Angew. Chem. Int. Ed.*, **2000**, 39, 3094.
15. T. Steiner, *Acta Crystallogr.*, **1995**, D51, 93.
16. L. Infantes and S. Motherwell, *CrystEngComm*, **2002**, 4, 454.
17. G. Hummer and J. C. Noworyta, *Nature*, **2001**, 414, 181.
18. (a) S. Cukierman, *Biophys. J.*, **2000**, 78, 1825. (b) K. Mitsuoka, K. Murata, T. Walz, T. Hirai, P. Agre, J. B. Heymann, A. Engel and Y. Fujiyoshi, *J. Struct. Biol.*, **1999**, 128, 34.
19. S. Cukierman, *Biophys. J.*, **2000**, 78, 1825.
20. C. J. T. de Grotthuss, *Ann. Chim.*, **1806**, 58, 54.

21. L. E. Cheruzel, M. S. Pometun, M. R. Cecil, M. S. Mashuta, R. J. Wittebort and R. M. Buchanan, *Angew. Chem. Int. Ed.*, **2003**, *42*, 5452.
22. P. S. Sidhu, K. A. Udachin and J. A. Ripmeester, *Chem. Commun.*, **2004**, 1358.
23. K. Liu, J. D. Cruzan and R. J. Saykally, *Science*, **1996**, *271*, 929.
24. (a) M. Losada and S. Leutwyler, *J. Chem. Phys.*, **2002**, *117*, 2003. (b) D. M. Upadhyay, M. K. Shukla and P. C. Mishra, *Quantum Chem.* **2001**, *81*, 90. (c) S. S. Xantheas, C. J. Burnham and R. Harrison, *J. Chem. Phys.*, **2002**, *116*, 1493.
25. D. R. Turner, M. Henry, C. Wilkinson, G. J. McIntyre, S. A. Mason, A. E. Goeta and J. W. Steed, *J. Am. Chem. Soc.*, **2005**, *127*, 11063.
26. M. Zuhayra, W. U. Kampen, E. Henze, Z. Soti, L. Zsolnai, G. Huttner and F. Oberdorfers, *J. Am. Chem. Soc.*, **2006**, *128*, 424.
27. B.-Q. Ma, H.-L. Sun and S. Gao, *Chem. Commun.*, **2004**, 2220.
28. J. P. Naskar, M. G. B. Drew, A. Hulme, D. A. Tocher and D. Datta, *CrystEngComm*, **2005**, *7*, 67.
29. B.-H. Ye, B.-B. Ding, Y.-Q. Weng and X.-M. Chen, *Inorg. Chem.*, **2004**, *43*, 6866.
30. R. Custelcean, C. Afloroaei, M. Vlassa and M. Polverejan, *Angew. Chem. Int. Ed.*, **2000**, *39*, 3094.
31. P. Rodriguez-Cuamatzi, G. Vargas-Diaz and H. Höpfl, *Angew. Chem. Int. Ed.*, **2004**, *43*, 3041.
32. (a) J. L. Atwood, L. J. Barbour, T. J. Ness, C. L. Raston and P. L. Raston, *J. Am. Chem. Soc.*, **2001**, *123*, 7192. (b) B.-Q. Ma, H.-L. Sun and S. Gao, *Chem. Commun.*, **2005**, 2336. (c) L. J. Barbour, G. W. Orr and J. L. Atwood, *Nature*, **1998**, *393*, 671. (d) L. J. barbour, G. W. Orr and J. L. Atwood, *Chem. Commun.*, **2000**, 859. (e) B.-Q. Ma, H.-L. Sun and S. Gao, *Angew. Chem. Int. Ed.*, **2004**, *43*, 1374.
33. D. D. MacNicol and G. A. Downing, in *Comprehensive Supramolecular Chemistry*, Vol.6, *Solid-State Supramolecular Chemistry, Crystal Engineering*, Eds. D. D. MacNicol, F. Toda and R. Bishop, Pergamon, Oxford, **1996**, pp. 421-464.
34. R. Banerjee, G. R. Desiraju, R. Mondal and J. A. K. Howard, *Chem. Eur. J.*, **2004**, *10*, 3373.

35. (a) H. Birkedal, D. Schwarzenbach and P. Pattison, *Angew. Chem. Int. Ed.*, **2002**, *41*, 754. (b) A. Mukherjee, M. K. Saha, M. Nethaji and A. R. Chakravarty, *Chem. Commun.*, **2004**, 716. (c) B. Sreenivasulu and J. J. Vittal, *Angew. Chem. Int. Ed.*, **2004**, *43*, 5769. (d) X.-L. Zhang and X.-M. Cheng, *Cryst. Growth Des.*, **2005**, *5*, 617.
36. (a) T. Steiner, *Angew. Chem. Int. Ed.*, **2002**, *41*, 48. (b) G. R. Desiraju and T. Steiner, in *The Weak Hydrogen Bond In Structural Chemistry and Biology*; Oxford University Press: New York, **1999**.
37. The Br \cdots Br contact of 3.29 Å is quite short. There are only 16 structures (DBRDOX, FEWDAN, GUGXOV, GUJSIN, JUBNAV, POXZOR, QAKBUA, QALWOQ, QIQCUO, TPHMBR02, XACXEE, XAJPII, YAGYIP, TOZLII, DANZIC, QAQLUQ) in the Cambridge Structural Database (CSD, www.ccdc.cam.ac.uk, Jan 2006 > 350000 entries, R factor \leq 0.1) with Br \cdots Br < 3.30 Å.
38. Two recent examples of weak halogen \cdots halogen and halogen \cdots oxygen interactions directing self-assembly in strongly hydrogen-bonded systems are: (a) J. N. Moorthy, R. Natarajan, P. Mal and P. Venugopalan, *J. Am. Chem. Soc.*, **2002**, *124*, 6530. (b) S. George, A. Nangia, C.-K. Lam, T. C. W. Mak and J.-F. Nicoud, *Chem. Commun.*, **2004**, 1202.
39. X.-L. Zhang and X.-M. Chen, *Cryst. Growth Des.*, **2005**, *5*, 617.
40. B. Sreenivasulu and J. J. Vittal, *Angew. Chem. Int. Ed.*, **2004**, *43*, 5769.
41. (a) D. Eisenberg and W. Kauzmann, *The Structure and Properties of Water*, Oxford University Press, Oxford, **1969**. (b) N. H. Fletcher, *The Chemical Physics of Ice*, Cambridge University Press, Cambridge, **1970**. (c) C. Loban, J. J. Finney and W. F. Kuhs, *Nature*, **1998**, *391*, 268. (d) M. Koza, H. Shober, A. Tölle, F. Fujara and T. Hansen, *Nature*, **1999**, *397*, 660. (e) O. Mishima and H. E. Stanley, *Nature*, **1998**, *396*, 329.
42. K.-M. Park, R. Kuroda and T. Iwamoto, *Angew. Chem. Int. Ed.*, **1993**, *32*, 884.
43. S. K. Ghosh and P. K. Bharadwaj, *Inorg. Chem.*, **2004**, *43*, 5180.
44. F. H. Allen, *Acta Crystallogr.*, **2002**, *B58*, 380.
45. M. Mascal, L. Infantes and J. Chisholm, *Angew. Chem., Int. Ed.*, **2006**, *45*, 32.
46. C. Janiak and T. G. Scharmann, *J. Am. Chem. Soc.*, **2002**, *124*, 14010.

47. A. L. Gillon, N. Feeder, R. J. Davey and R. Storey, *Cryst. Growth Des.*, **2003**, *3*, 663.
48. M. Henry, *Chem. Phys. Chem.*, **2002**, *3*, 607.
49. The word ‘sponge’ has been used previously for host lattice. M. P. Byrn, C. J. Curtis, Y. Hsiou, S. I. Khan, P. A. Sawin, R. Tsurumi and C. E. Strouse, *J. Am. Chem. Soc.*, **1990**, *112*, 1865.
50. (a) K. Maartmann-Moe, *Acta Crystallogr*, **1965**, *19*, 155. (b) S. C. Wallwork and H. M. Powell, *Acta Crystallogr*, **1957**, *10*, 48.
51. (a) W. Francis and A. J. Hill, *J. Am. Chem. Soc.*, **1924**, *46*, 2498. (b) F. L. Weitzl, *J. Org. Chem.*, **1976**, *41*, 2044.
52. XEMP (Version 4.2): Siemens Analytical X-ray Instruments Inc., Madison, Wisconsin, USA. Siemens (**1994**).

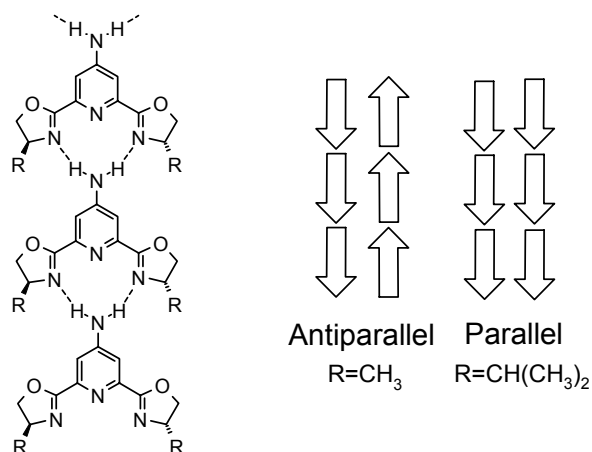
CHAPTER 6

HALOGEN...HALOGEN INTERACTION TO INDUCE SUPRAMOLECULAR NON-CENTROSYMMETRY

6.1 Introduction

Crystal structures with non-centrosymmetric packing of molecules are important as electro-optic and nonlinear optical materials, useful in asymmetric synthesis and provide insight into the evolution of chirality in nature.¹ Design of molecular materials for quadratic nonlinear optical (NLO) applications, such as second harmonic generation (SHG), require molecular engineering as well as crystal engineering. Bulk NLO susceptibility depends on the molecular hyperpolarizability (β) and the orientation and organization of molecular dipoles.² An essential condition for even-order NLO processes is that the structure must be non-centrosymmetric; however, optimal molecular orientations are required to achieve appreciable SHG effects.³ Crystallisation of achiral and racemic molecules in space groups that lack the inversion center has been a challenge since the early days of crystal engineering. Organic molecular crystals show a strong preference toward centrosymmetric packing. Centro symmetric organisation is favored for typical organic molecules because of the anti-parallel alignment of dipoles (charge cancellation in neighboring domains) and the universality of close-packing (bumps fit into hollows). Even though no direct correlation was found between the ground-state dipole moment of molecules and the preference for centrosymmetric packing,⁴ it is generally believed that electrostatic interactions would promote anti-parallel organization of dipolar molecules. Almost always molecules with an inversion center crystallize in centrosymmetric space group⁵ and carboxylic acid dimer crystallize in centrosymmetric space groups.⁶ Only 10–15% of achiral organic molecules crystallize in non-centrosymmetric space groups such as $P2_1$, $P2_12_12_1$, $Pca2_1$, $Pna2_1$, $Fdd2$, etc.⁷ Several approaches have been developed to assemble molecules in non-centrosymmetric lattices. Octupolar molecules provide one strategy toward non-centrosymmetric crystals,

because there is no ground state dipole moment.⁸ Some other strategies are incorporation of bulky substituents,⁹ vanishing dipole moment (POM),¹⁰ exploitation of H-bond interactions,¹¹ host-guest complexation in channel structure,¹² diamondoid network¹³ and using molecular chirality.¹⁴ The probability for non-centrosymmetric crystal structure is almost 40% in *meta*-substituted benzenes because of their dissymmetrical shape.¹⁵ A guaranteed method to produce non-centrosymmetric lattice is the use of chiral molecules but it does not necessarily mean optimal molecular orientations and SHG efficiency. Recently Parquette and co-workers have demonstrated the influence of steric effect on the formation of polar 1D hydrogen-bonded networks. They have shown that the methyl substituted chiral, 4-amino-2,6-bis(oxazoliny)pyridine (ampybox) align anti-parallel where as isopropyl-substituted ampybox pack in a parallel arrangement (Scheme 1).¹⁶ Despite the immense utility of chiral/polar crystals in supramolecular materials there is no general solution to avoiding the above difficulty. A better understanding of the factors that promote polar self-assembly of molecules in the solid-state is therefore of fundamental interest in crystal engineering and nanotechnology.



Scheme 1. Formation of a 1D network *via* intermolecular hydrogen bonding between adjacent ampybox molecules. Methyl substituted ampybox pack in anti-parallel arrangement and isopropyl substituted ampybox pack in parallel arrangement.

Halogen...halogen interactions are of two types (Scheme 1a, X = Cl, Br, I). Type I interactions generally occur across the inversion center whereas type II interactions are optimized between molecules related by screw axis and glide plane.¹⁷ The tendency of halogens to participate in type II interaction increases as Cl<Br<I (Figure 1) because (1) the heavier, more polarizable halogen has greater elliptical charge distribution and (2) heavier halogen...halogen interactions are stabilized by electrophile–nucleophile pairing.

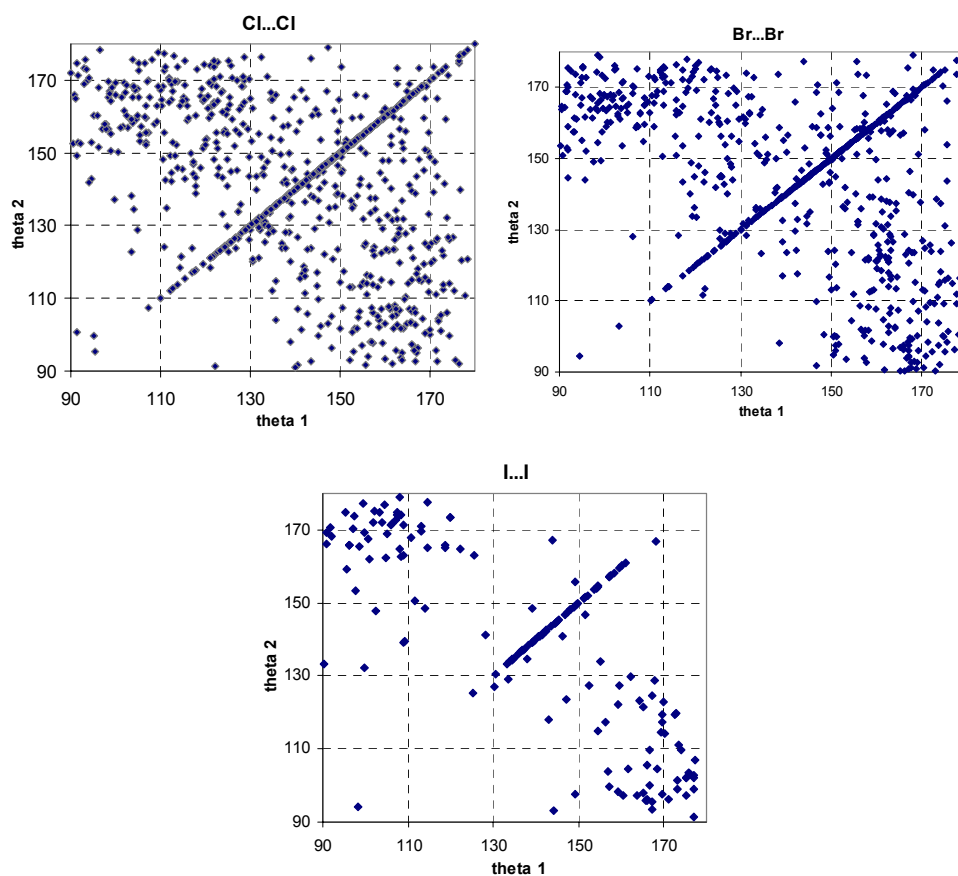
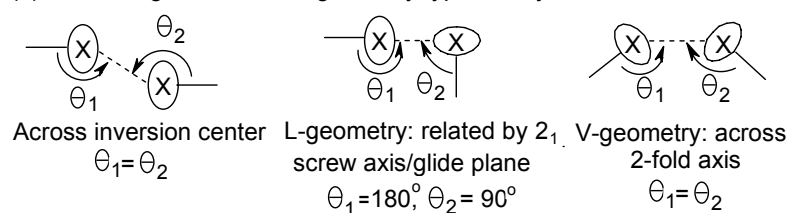


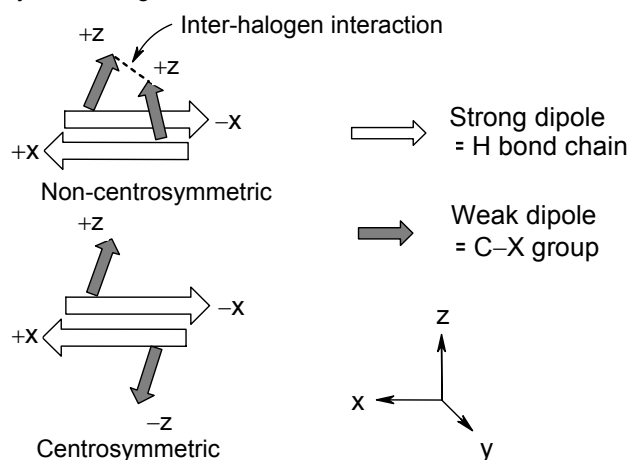
Figure 1. Geometrical parameters of halogen...halogen interactions (C–X...X–C fragment) in accurate (3D coordinates determined, no disorder, no ions, no errors, no powder structures, not polymeric) organic crystal structures extracted from the Cambridge Structural Database (ConQuest 1.8, January 2006 update): (a) Cl...Cl, 3.0–3.5 Å, $R \leq 0.05$; (b) Br...Br, 3.0–3.7 Å, $R \leq 0.10$; (c) I...I, 3.0–2.98 Å, $R \leq 0.10$.

Moorthy et al. showed that $X\cdots X$ interactions direct helical chains of $O-H\cdots O$ hydrogen bonds in mesitoic acids instead of the common carboxylic acid dimer. When the halogen is replaced by isosteric methyl group, the carboxylic acid dimer reform.¹⁸ Our approach to inducing non-centrosymmetric crystallization of dipolar molecules is summarized in scheme 2. We assume that the strong hydrogen bonding functional groups (strong dipole) will align anti-parallel. If a halogen atom is placed in the molecule (weak dipole) at a specific position that would optimize L- or V-shaped $X\cdots X$ interaction, then the overall crystal structure will have non-centrosymmetric packing without changing the strong H-bond pattern.

(a) Inter-halogen interaction geometry types in crystals

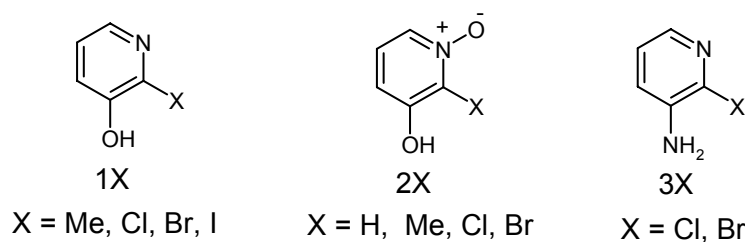


(b) Model for non-centrosymmetric crystallization via L- or V-geometry inter-halogen interactions



Scheme 2. (a) Inter-halogen interaction types. (b) Non-centrosymmetric alignment of H-bond chains due to L- or V-geometry of $X\cdots X$ interactions.

To test this hypothesis, we have chosen molecules containing strong donor and acceptor groups *meta* to each other in the aryl ring and halogen is in between them. To check the influence of the halogen group, it was replaced by hydrogen and methyl groups. Ten crystal structures in three series of molecules, namely 2-halo-3-hydroxypyridine 1X, 2-halo-3-hydroxypyridine *N*-oxide, 2X and 2-halo-3-aminopyridine, 3X were determined (Scheme 3). The hydrogen bond metrics and space group are given in table 1 and 2.



Scheme 3. Compounds studied in this chapter to test the hypothesis of scheme 2.

6.2. Crystal Structures of 1X

There are four crystal structures in this series of compounds—2-chloro-3-hydroxypyridine (1Cl), 2-Bromo-3-hydroxypyridine (1Br), 2-iodo-3-hydroxypyridine (1I) and 2-methyl-3-hydroxypyridine (1Me) are reported in this chapter. The parent compound 3-hydroxypyridine (1H) is already reported in CSD.

6.2.1. 3-Hydroxypyridine

The crystal structure of parent compound 3-hydroxypyridine (1H) is reported by Ohms et al.¹⁹ It crystallizes in the centrosymmetric space group $P2_1/c$ with two molecules in the asymmetric unit. Alternate symmetry independent molecules are linked by strong O—H...N hydrogen bonds to form molecular chain. These chains run in opposite directions to maintain the center of symmetry (Figure 2) and the molecular planes are near perpendicular to the next molecule in the chain.

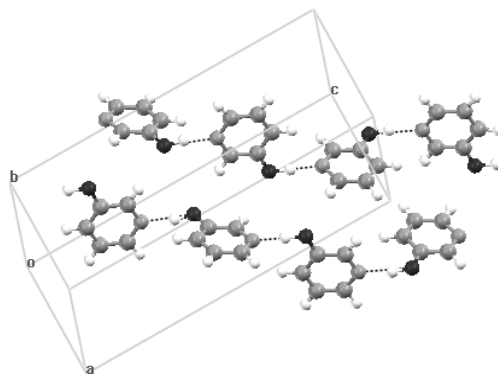


Figure 2. Chains of 3-hydroxypyridine molecules are running anti-parallel. Molecules are connected via strong O–H···N H-bonds.

6.2.2 2-Chloro-3-hydroxypyridine, 1Cl

Single crystals of good quality for X-ray data collection were obtained from ethyl acetate. Replacing *ortho*-H by Cl, the molecule (1Cl) crystallizes in polar space group *Fdd2* with one molecule in the asymmetric unit. Anti-parallel chains of O–H···N hydrogen-bonded glide related molecules run along $[101]$ and $[-101]$. Four such molecular chains pass across the unit cell and so the distance between such two chains is $b/4$ Å. The crossing point of these chains has type I Cl···Cl contact. This Cl···Cl type I interaction (3.35 Å, 158.9°, 158.9°) is related by the less common 2-fold symmetry instead of frequently occurring inversion center. A view down the chain direction shows X-shaped geometry where the four arms of ‘X’ contain two Cl atoms in same side and two aryl rings. The ‘X’ junction is glued by O–H···N interaction. Though the strong H-bond functionalities run in opposite direction, the Cl atoms are directed on same side of ‘X’ in all chains resulting in non-centrosymmetric crystal structure (Figure 3).

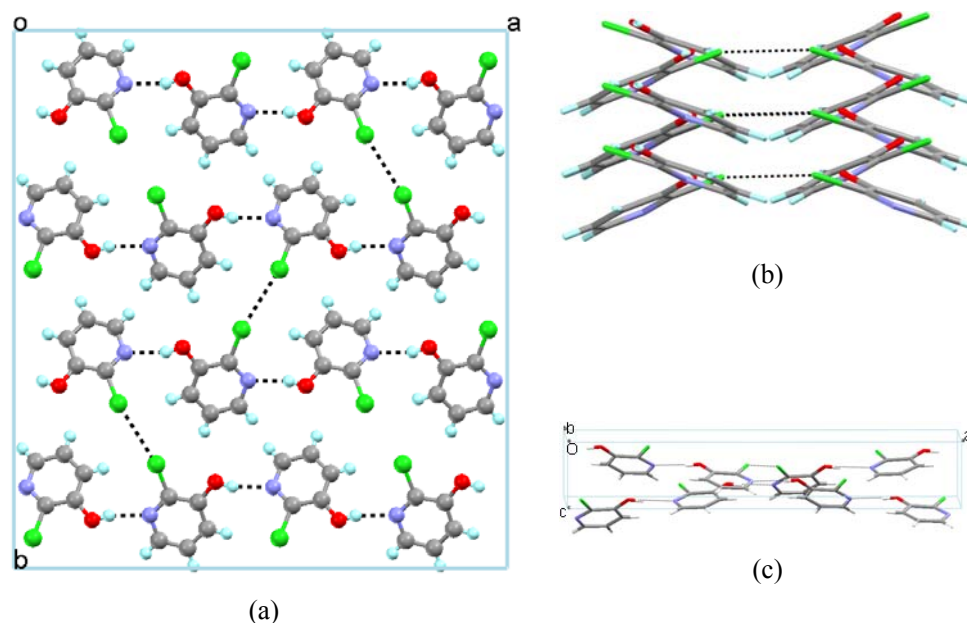


Figure 3. (a) View down the *b*-axis. Four molecular chains are running anti-parallel. (b) View down the *a*-axis. Adjacent chains contact via two-fold symmetry related Cl...Cl interactions. (c) Molecular chains are crossing each other and make Cl...Cl interaction in the contact zone.

6.2.3 2-Bromo-3-hydroxypyridine, 1Br and 2-Iodo-3-hydroxypyridine, 1I

1Br was crystallized from ethyl acetate. The crystal adopts non-centrosymmetric space group in orthorhombic system ($Pna2_1$) with one molecule in the asymmetric unit. 1I was crystallized from ethyl acetate and is isostructural to 1Br. The molecules form molecular chains via strong O-H...N H-bonds and these chains run anti-parallel along the *a*-axis. Two such chains pass across the unit cell but do not cross like 1Cl. The halogen...halogen interaction is the polarization-induced type II contact across the two-fold screw axis. Br...Br interaction geometry is 3.64 Å, 170.2°, 121.2° and I...I interaction geometry is 3.74 Å, 174.4°, 114.5°. 1Br and 1I also have similar X-shaped geometry of the chains like 1Cl (Figure 4).

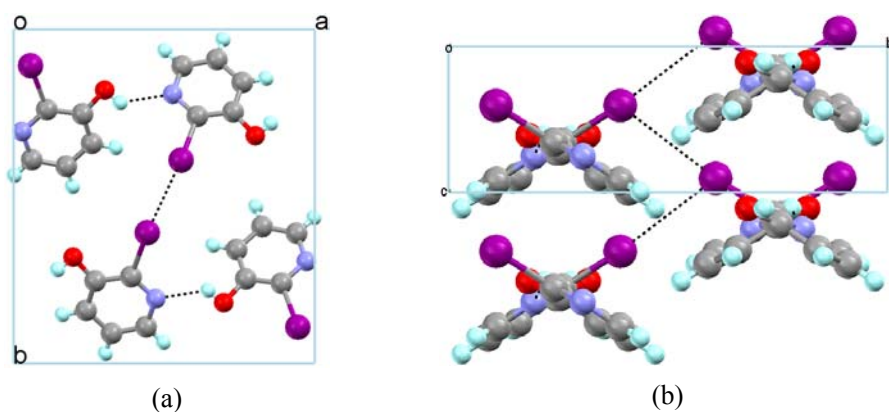


Figure 4. (a) Anti-parallel molecular chains of 1I along c direction and (b) non-centrosymmetric orientation of the X-shaped chains, viewed down the c -axis. The iodo groups in X-geometric chain are all upward ($-c$).

6.2.4 2-Methyl-3-hydroxypyridine, 1Me

1Me was crystallized from acetone. It crystallizes in centrosymmetric space group $C2/c$ and the asymmetric unit contains one molecule. Here also the description of the strong $O-H\cdots N$ hydrogen bond is similar to halo compounds. They run anti-parallel and do not cross each other like 1Br and 1I. It also maintains the X-geometry but the relative orientation of the chains or 'X's are different from halo compounds. In the absence of specific halogen \cdots halogen interaction the chains are related by center of inversion. The methyl groups in two adjacent 'X's are oriented in opposite direction unlike halogens where they are on the same side (Figure 5).

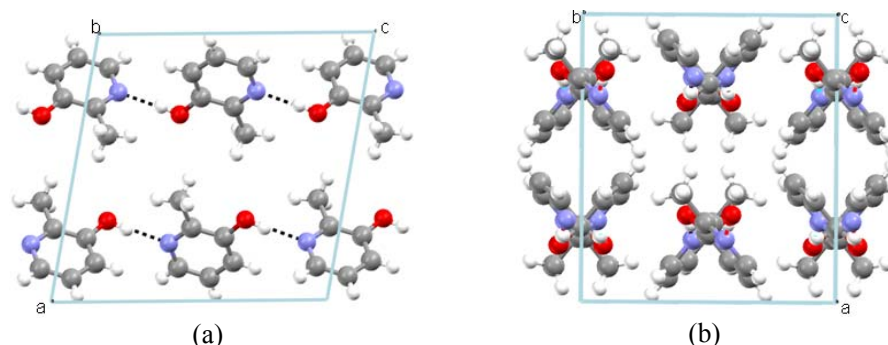


Figure 5. (a) Anti-parallel molecular chains of 1Me along c direction and (b) centrosymmetric orientation of the X-shaped chains down the c -axis.

Inspired by the result obtained from 2-halo-3-hydroxypyridine, two more series of compounds were investigated by changing acceptor group from pyridine to pyridine *N*-oxide and donor group from OH to NH₂. These two new families of compounds are 2-substituted-3-hydroxypyridine *N*-oxide and 2-substituted-3-aminopyridine.

6.3 Crystal Structures of 2X

This family of compounds contain four molecules, namely 3-hydroxypyridine *N*-oxide (2H), 2-chloro-3-hydroxypyridine *N*-oxide (2Cl), 2-bromo-3-hydroxypyridine *N*-oxide (2Br) and 2-methyl-3-hydroxypyridine *N*-oxide (2Me). Due to synthetic problem the iodo derivative could not be prepared.

6.3.1 3-hydroxypyridine *N*-oxide, 2H

Crystals were obtained from methanol solution for single crystal X-ray diffraction. 2H crystallize in centrosymmetric space group $P\bar{1}$ with one molecule in the asymmetric unit. The inversion center is sitting between the oxygen atoms of two molecules. As a result the molecule is disordered in the positions of C–OH and N–O with 0.5 occupancy each. The molecules form expected molecular chain along [201] via O–H...O H-bonds.

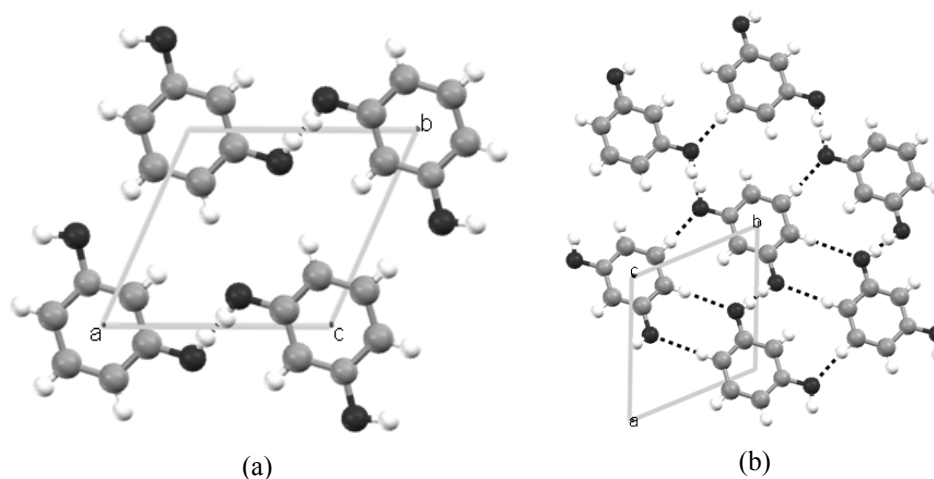


Figure 6. (a) Molecular chain along [201] via O–H...O H-bonds and (b) pseudo hexagonal layer via strong O–H...O and weak C–H...O hydrogen bonds in (–102) plane.

But in this case the molecules are coplanar rather than forming X-shaped junction. The tectons form pseudo hexagonal 2D layer in (-102) plane via $\text{O-H}\cdots\text{O}$ and $\text{C-H}\cdots\text{O}$ H-bonds (Figure 6).

6.3.2 2-Chloro-3-hydroxypyridine *N*-oxide, 2Cl

Crystals of 2Cl were obtained from methanol solution for single crystal X-ray diffraction. It crystallizes in non-centrosymmetric space group $Pna2_1$. The $\text{O-H}\cdots\text{O}$ H-bond mediated molecular chains run along $[011]$ and $[0\bar{1}1]$. Similar to 1Cl, the chains cross each other and make $\text{Cl}\cdots\text{Cl}$ contact around 2 fold screw axis with intermediate geometry of type I and type II (3.51 \AA , 133.0° and 101.4°). It also adopt X-geometry along chain axis like 1Cl and infinite $\text{Cl}\cdots\text{Cl}$ interactions propagate along c -axis (Figure 7).

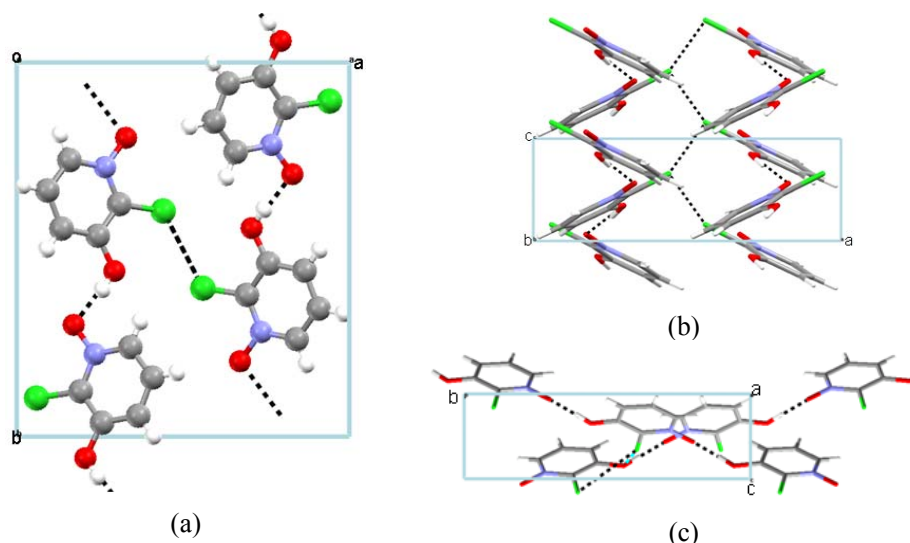


Figure 7. (a) $\text{O-H}\cdots\text{O}$ H-bond mediated molecular chains propagate in opposite direction. (b) Infinite $\text{Cl}\cdots\text{Cl}$ interactions along c -axis and (c) molecular chains cross with $\text{Cl}\cdots\text{Cl}$ interaction at the junction.

6.3.3 2-Bromo-3-hydroxypyridine *N*-oxide, 2Br

2Br was crystallized from methanol solution to produce diffraction quality single crystals. It crystallizes in non-centrosymmetric $P2_12_12_1$ space group and the asymmetric

unit contains one molecule. The usual O—H...O H-bond mediated and 2-fold screw related molecular chains run along the *c* direction without crossing, unlike 2Cl. But it does not form X-geometry across the molecular chains. The infinite Br...Br interactions propagate along the *a*-axis and adopt border line type II geometry (3.93 Å, 171.5°, 126.1°; Figure 8).

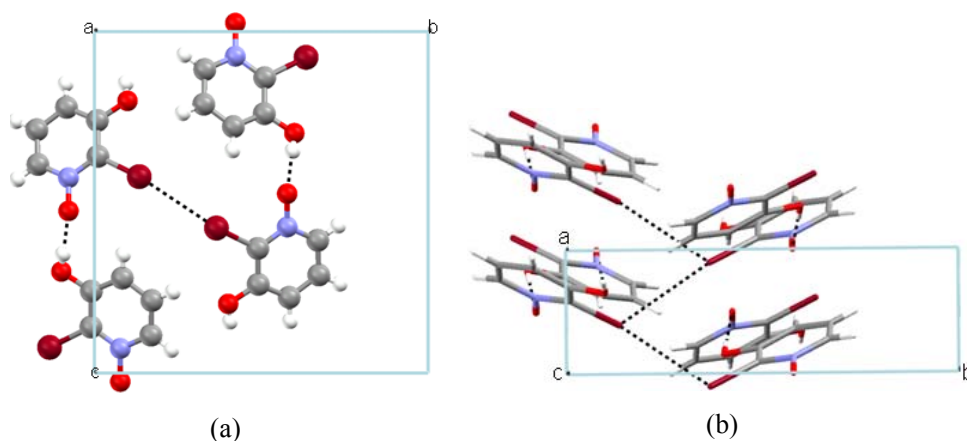


Figure 8. (a) Anti-parallel O—H...O H-bonded molecular chains proliferate along [001] direction. (b) Infinite Br...Br interactions propagate along *a*-axis.

6.3.4 2-Methyl-3-hydroxypyridine *N*-oxide, 2Me

X-ray diffraction quality crystals of 2Me were obtained from methanol. It crystallizes in centrosymmetric space group $P2_1/c$ with one molecule in asymmetric unit. The anti-parallel molecular chains mediated via O—H...O H-bonds disseminate parallel to the *c*-axis and adopt X-geometry. Within a layer in *ac*-plane the packing of 'X' chains is non-centrosymmetric like 1Br and 1I, but the next layer is related by the inversion center (Figure 9).

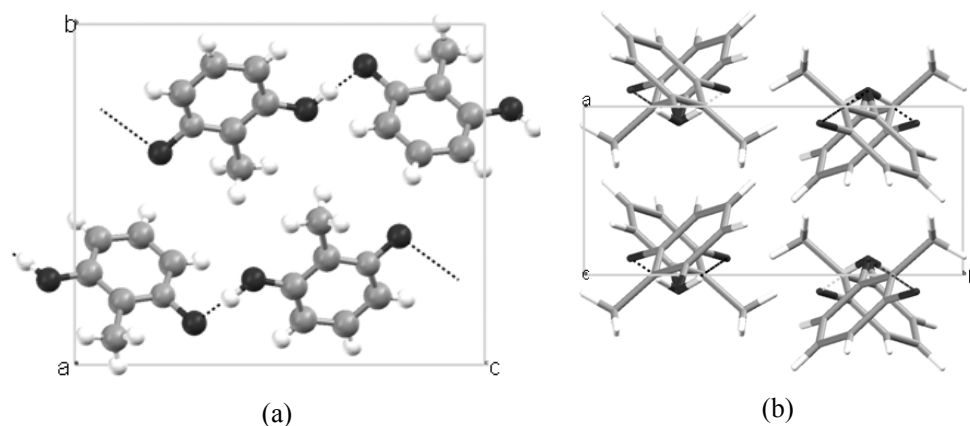


Figure 9. (a) Anti-parallel molecular chains run along the *c*-axis mediated by O–H···O hydrogen bonds. (b) Centrosymmetric arrangement of X-shaped chains.

6.4 Crystal structures of 3X

Crystal structures of molecules 2-chloro-3-aminopyridine (3Cl) and 2-bromo-3-aminopyridine (3Br) are discussed in this series.

6.4.1 2-Chloro-3-aminopyridine, 3Cl

3Cl was crystallized from dichloromethane solution for single crystal X-ray diffraction. It crystallizes in centrosymmetric space group $P2_1/n$ and contains one symmetry independent molecule. The best donor N–H bonds with best acceptor pyridine N and forms N–H···N hydrogen bond linked glide related molecular chain along [101]. The left over N–H is directed to intramolecular Cl atom. These chains show X-shaped geometry, similar to 1Cl and 2Cl. However 3Cl molecular chains propagate parallel without crossing. Another difference is that there is no Cl···Cl interaction in 3Cl compared to 1Cl and 2Cl (Figure 10).

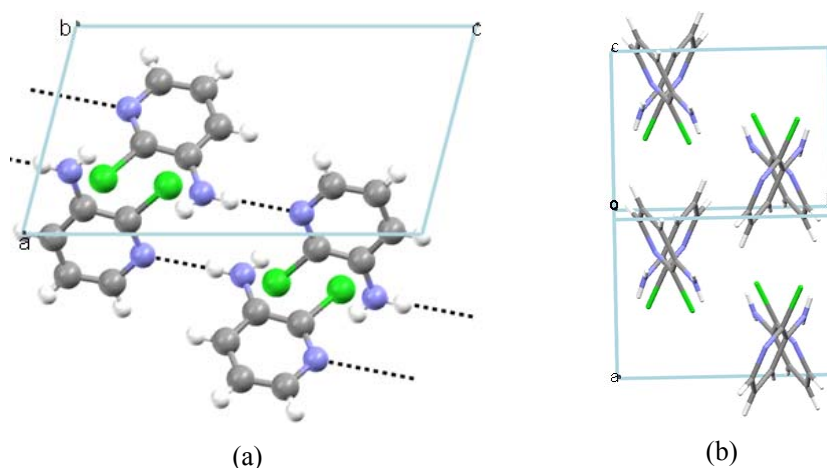


Figure 10. (a) N-H...N hydrogen bond mediated anti-parallel molecular chains along [101]. (b) Centrosymmetric X-shaped molecular chains without Cl...Cl interaction.

6.4.2 2-Bromo-3-aminopyridine, 3Br

3Br was crystallized from dichloromethane to obtain X-ray quality single crystals. The crystal structure is slightly complicated due to the presence of four molecules in asymmetric unit in space group $P2_1$. These four molecules form tetrameric unit via N-H...N H-bonds and this unit repeats to construct the infinite molecular chain along [102]. The Br...Br interaction (3.63 Å, 148.1°, 102.5° and 3.64 Å, 177.7°, 102.6°) occurs between two pairs of symmetry-independent molecules (Figure 11).

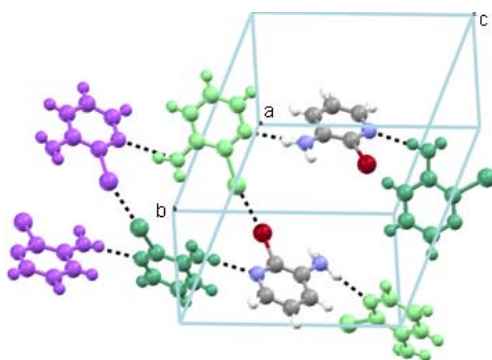


Figure 11. Four symmetry independent molecules (different colors) form the tetrameric repeating unit of the molecular chains. Symmetry independent molecules are further connected via Br...Br interactions.

Table 1. O–H···N, O–H···O, N–H···N and X···X interaction geometry.

Compound	Interaction	d (Å)	D (Å)	θ°
1H	O–H···N	1.63	2.678	178.6
		1.68	2.670	166.1
1Cl	O–H···N	1.92	2.719(2)	164
	Cl···Cl		3.350(1)	158.9, 158.9
1Br	O–H···N	2.06	2.676(3)	151
	Br···Br		3.637(1)	170.2, 121.2
1I	O–H···N	2.12	2.676(4)	130
	I···I		3.738(1)	174.4, 114.5
1Me	O–H···N	1.85	2.691(6)	173
2H	O–H···O	1.61	2.548(2)	164
		1.72	2.546(2)	174
	C–H···O	2.58	3.455(2)	157
		2.46	3.384	173
2Cl	O–H···O	1.69	2.538(2)	174
	Cl···Cl		3.510(1)	132.9, 101.4
2Br	O–H···O	1.88	2.618(4)	176
	Br···Br		3.930(1)	171.5, 126.1
2Me	O–H···O	1.54	2.539(2)	175
3Cl	N–H···N	2.23	3.088(4)	174
	Cl···Cl		absent	
3Br	N–H···N	2.11	3.011(5)	159
		2.13	3.071(5)	172
		2.19	3.019(5)	173
		2.31	3.077(5)	171
	Br···Br		3.634(1)	148.1, 102.5
			3.636(1)	177.8, 102.6
			3.964(1)	107.4, 103.1

6.5 Discussion

In the crystal structure of 1Br, molecules in adjacent chains participate in type II Br···Br interaction shorter than the van der Waals sum. The molecules lie in (011) and (01–1) planes with the C–Br bonds generating a net dipole along the $-c$ vector. 1I has an

identical polar arrangement of O–H...N chains directed by I...I interaction. In contrast to type II halogen...halogen interaction in bromo and iodo structures, halogen atoms participate in type I geometry in 1Cl between hydrogen-bonded chains related by two-fold axis. A view down the H-bond chain axis shows that the angle at which the molecular planes intersect is different in Cl, Br and I derivatives (Figure 12). If the intersection of molecules is viewed as a hinge, the halogen...halogen interactions are supramolecular handles to modify the hinge angle.

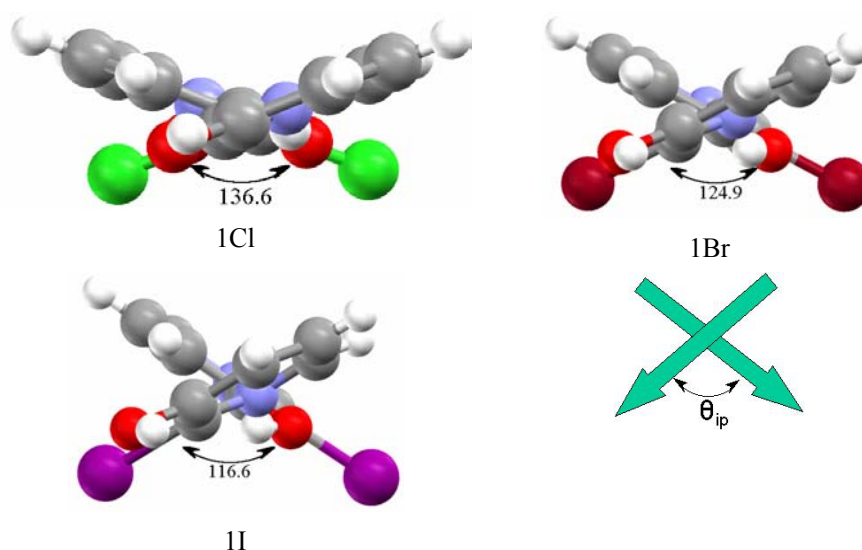


Figure 12. Halogen...halogen interactions modulate the inter-planar hinge angle (θ_{ip}) in O–H...N hydrogen-bonded chains of 1Cl, 1Br and 1I.

There are several factors that suggest a specific, structure-directing effect of X...X interactions. (1) The halogen bonding becomes more significant for iodo than bromo or chloro. (2) The type II interaction tends more towards the ideal L-shaped geometry in iodo than bromo compounds where chloro compound has type I interaction with V-shaped geometry. (3) The higher dipole moment of the iodo compound and optimal polar alignment of chromophores in the solid, 1I should have the highest optical response. SHG values in table 2 bear out these molecular and crystal structure trends. The iodo derivative has the highest SHG response (\approx urea) whereas bromo and chloro

pyridinolols are $<U$. While the absolute values are no doubt modest, because there is no extended conjugation in the molecule, the role of halogens as steering groups for non-centrosymmetric crystallization is unprecedented. The importance of halogen...halogen interaction has been tested by replacing the halogen by methyl group. The crystal structures of 1Me and 2Me adopt centrosymmetric space group, which indicates the universal preference for centrosymmetric packing dominates in the absence of specific halogen...halogen interactions. A situation similar to scheme 2 should also prevail in the corresponding pyridine *N*-oxides 2X. Crystal structure of its bromo derivative 2Br has O-H...O chains (1.88 Å, 175.7°) running along [001] and bromine atoms of adjacent chains engage in type II interaction. The Cl...Cl interaction in chloro compound 2Cl, takes intermediate geometry between V and L and is weakly SHG active. Though the crystal structure of 3Br is non-centrosymmetric in the presence of Br...Br interaction, the 3Cl crystallize in centrosymmetric space group, because it lacks halogen...halogen interaction. This result is consistent with statistical database analysis.¹⁷ The crystal structure of 3Cl is quite similar to 2Me meaning that the Cl group is acting as space filler.

6.6 Dipole Moment Comparison

The general belief is that with increase in dipole moment, molecules prefer centro symmetric arrangement to cancel out dipolar charges. On the other hand, Whitesell, Davis and co-workers stated that molecular dipole moment is not the reason for global preference of centrosymmetric structures.⁴ Though they did not ignore the influence of local electrostatic forces, they came to the conclusion from an analysis of dipole moment distribution in non-centrosymmetric space groups $P1$, $P2_1$ and centrosymmetric space group $P\bar{1}$. Based on a recent statistical analysis of diphenyl ethers, it has been shown that molecules with dipole moment < 4 have a 3:7 preference for non-centrosymmetry where as molecules with dipole moment > 4 crystallize in centrosymmetric space groups.²⁰ The molecules selected in the present study are typical organic molecules, which have dipole moment 2.5–5.5 D (Table 2). In spite of the higher dipole moment in the present families of halogenated molecules, they adopt non-

centrosymmetric crystal structure. Most interesting observation is that the 1X and 2X (X = halogen group) compounds have higher dipole moment than 1H, 1Me, 2H and 2Me compounds, but the former crystallize in non-centrosymmetric space groups where as latter structures are centrosymmetric. This study shows that by further optimizing inter-halogen interactions for supramolecular self-assembly, the chances of non-centrosymmetric crystallization are significantly improved to almost cent percent in a sub-set of carefully designed molecules.

Table 2. Molecular dipole moment (μ , calculated in AM1) and SHG efficiency (measured using Nd³⁺-YAG laser at 1064 nm) of crystals 1X, 2X and 3X.

Compound	Space group	SHG activity	μ (Debye)
1H	$P2_1/c$	nil	2.96
1Me	$C2/c$	nil	2.62
1Cl	$Fdd2$	<urea	3.88
1Br	$Pna2_1$	<urea	3.94
1I	$Pna2_1$	\approx urea	3.88
2H	$P\bar{1}$	nil	4.88
2Me	$P2_1/c$	nil	4.54
2Cl	$Pna2_1$	<urea	5.28
2Br	$P2_12_12_1$	very weak	5.23
3Cl	$P2_1/n$	nil	3.49
3Br	$P2_1$	<urea	3.61

6.7 Conclusions

Non-centrosymmetric space group is the first of many conditions for SHG activity because other factors like phase-matching, transparency/efficiency trade-off and thermal stability must also be optimized. The best space group for NLO materials is $P2_1$ followed by $Pca2_1$, $Pna2_1$ and the least useful is $P2_12_12_1$ (the dipole moments are mutually orthogonal in this arrangement and hence cancel out).²¹ Exploiting halogen...halogen interaction with appropriate symmetry operators in the L/V-geometry in inducing non-centrosymmetry favors the likelihood of crystallization in the more efficient SHG space groups. The major difficulty in molecular and crystal engineering of

SHG solids is that increasing molecular hyperpolarizability (β) in NLO-phores through push–pull conjugation also favors centrosymmetric alignment of the strong dipoles. The molecules studied do not have high β values to produce strong SHG effect but their shape and synthons offer a novel strategy to design new non-centrosymmetric solids.

6.8 Experimental Section

Synthesis

2-Methyl-3-hydroxypyridine, 2-chloro-3-hydroxypyridine, 2-bromo-3-hydroxypyridine, 2-chloro-3-aminopyridine and 2-bromo-3-aminopyridine were purchased from Lancaster and/or Acros Chemicals and used as such for crystallization.

2-Iodo-3-hydroxypyridine (1I): 3-Hydroxypyridine, KOH and NaI (1.0 equiv each) were dissolved in MeOH (15 mL), 4% NaOCl solution (1.0 equiv) was slowly added at 0 °C. The solution was neutralised after 2 h and the solid product was separated by filtration.

3-Hydroxypyridine *N*-oxide (2H): 3-Hydroxypyridine and *m*-CPBA (1.0 equiv each) were dissolved in EtOAc (10 mL) and stirred at room temperature for 2 h. The precipitated solid product was collected by filtration. The other *N*-oxides were prepared by the same procedure.

2-Iodo-3-hydroxypyridine (1I): ¹H-NMR (CDCl₃, 200 MHz) δ 7.98 (d, J 5 Hz, 1H), 7.22 (d, J 8 Hz, 1H), 7.16 (dd, J 8, 5 Hz, 1H), 5.49 (s, 1H).

3-Hydroxypyridine *N*-oxide (2H): ¹H-NMR (DMSO-d₆, 200 MHz) δ 10.49 (s, 1H), 7.75 (s, 1H), 7.73 (d, J 6 Hz, 1H), 7.21 (dd, J 8, 6 Hz, 1H), 6.81 (d, J 8 Hz, 1H).

2-Methyl-3-hydroxypyridine *N*-oxide (2Me): ¹H-NMR (DMSO-d₆, 400MHz) δ 10.46 (s, 1H), 7.81 (d, J 6 Hz, 1H), 7.06 (dd, J 8, 6 Hz, 1H), 6.81 (d, J 8 Hz, 1H), 2.24 (s, 3H).

2-Chloro-3-hydroxypyridine *N*-oxide (2Cl): ¹H-NMR (DMSO-d₆, 400MHz) δ 11.36 (s, 1H), 8.00 (d, J 6 Hz, 1H), 7.20 (dd, J 8, 6 Hz, 1H), 6.94 (d, J 8 Hz, 1H).

2-Bromo-3-hydroxypyridine *N*-oxide (2Br): ¹H-NMR (DMSO-d₆, 200MHz) δ 10.90 (s, 1H), 7.85 (d, J 5 Hz, 1H), 6.99 (dd, J 7, 5 Hz, 1H), 6.81 (d, J 7 Hz, 1H).

X-Ray crystallography

Reflections were collected for the single crystal on a Bruker SMART APEX CCD area detector system (Mo-K α radiation, $\lambda = 0.71073$ Å). Multi-scan absorption correction was applied for 4-XPOT using SADABS. Structure solution and refinement were performed with SHELXS-97 and SHELXL-97 packages. All non-hydrogen atoms were refined anisotropically. H atoms connected to C were generated by riding model and H atoms connected to oxygen were located in difference electron density maps.

6.9 References

1. (a) D. Y. Curtin and I. C. Paul, *Chem. Rev.*, **1981**, 81, 525. (b) *Non-linear Optical Properties of Organic Molecules and Crystals*; Eds. J. Zyss and D. S. Chemla, Academic Press: New York, **1987**, vols. 1 and 2.
2. (a) J. Zyss and I. Ledoux, *Chem. Rev.* **1994**, 94, 77. (b) N. J. Long, *Angew. Chem., Int. Ed.*, **1995**, 34, 21. (c) J. J. Wolff, F. Siegler, R. Matschiner and R. Wortmann, *Angew. Chem. Int. Ed.*, **2000**, 39, 1436.
3. (a) W. Nie, *Adv. Mater.*, **1993**, 5, 520. (b) D. R. Kanis, M. A. Ratner and T. J. Marks, *Chem. Rev.*, **1994**, 94, 195. (c) T. J. Marks and M. A. Ratner, *Angew. Chem. Int. Ed.*, **1995**, 34, 155. (d) J. Zyss and J. F. Nicoud, *Curr. Opin. Solid State Mater. Sci.*, **1996**, 1, 533.
4. J. K. Whitesell, R. E. Davis, L. L. Saunders, J. R. Wilson and J. P. Feagins, *J. Am. Chem. Soc.*, **1991**, 113, 3267.
5. E. Pidcock, W. D. S. Motherwell and J. C. Cole, *Acta Crystallogr.*, **2003**, B59, 634.
6. (a) G. M. Frankenbach and M. C. Etter, *Chem. Mater.*, **1992**, 4, 272. (b) T. Steiner, *Acta Crystallogr.*, **2001**, B57, 103.
7. (a) E. Pidcock, *Chem. Commun.*, **2005**, 3457. (b) M. C. Etter and K.-S. Huang, *Chem. Mater.*, **1992**, 4, 824. (c) C. P. Brock and J. D. Dunitz, *Chem. Mater.*, **1994**, 6, 1118. (d) M. S. Hendi, P. Hooter, R. E. Davis, V. M. Lynch and K. A. Wheeler, *Cryst. Growth Des.*, **2004**, 4, 95.

8. (a) V. R. Thalladi, S. Brasselet, H.-C. Weiss, D. Bläser, A. K. Katz, H. L. Carrell, R. Boese, J. Zyss, A. Nangia and G. R. Desiraju, *J. Am. Chem. Soc.*, **1998**, *120*, 2563. (b) G. Alcaraz, L. Euzenat, O. Mongin, C. kanat, I. Ledoux, J. Zyss, M. Blanchard-Desce and M. Vaultier, *Chem. Commun.*, **2003**, 2766. (c) C. Dhenaut, I. Leudox, I. D. W. Samuel, J. Zyss, M. Bourgault and H. L. Bozec, *Nature*, **1995**, *374*, 339. (d) B. R. Chow, S. J. Lee, S. H. Lee, K. H. Son, Y. H. Kim, J.-Y. Doo, G. J. Lee, T. I. Kang, Y. K. Lee, M. Cho and S.-J. Jeon, *Chem. Mater.*, **2001**, *13*, 1438.
9. (a) B. F. Levine, C. G. Bethea, C. D. Thurmond, R. T. Lynch and J. L. Bernstein, *J. Appl. Phys.*, **1979**, *50*, 2523. (b) J. Zyss, *J. Phys.*, **1993**, *D26*, B198. (c) G. F. Lipscomb, A. F. Garito and R. S. Narang, *J. Chem. Phys.*, **1981**, *75*, 1509.
10. J. Zyss, D. S. Chemla and J. F. Nicoud, *J. Chem. Phys.*, **1981**, *74*, 4800.
11. (a) T. Tsunekawa, T. Gotoh and M. Iwamoto, *Chem. Phys. Lett.*, **1990**, *166*, 353. (b) W. Tam, B. Guerin, J. C. Calabrese and S. H. Stevenson, *Chem. Phys. Lett.*, **1989**, *154*, 93.
12. (a) M. D. Hollingsworth, U. Werner-Zwanzinger, M. E. Brown, J. D. Chaney, J. C. Huffman, K. D. M. Harris and S. P. J. Smart, *J. Am. Chem. Soc.*, **1999**, *121*, 9732. (b) J. Hulliger, P. Rogin, A. Quintel, P. Rechsteiner, O. König and M. Wübbenhorst, *Adv. Mater.*, **1997**, *9*, 662.
13. (a) O. R. Evans and W. Lin, *Acc. Chem. Res.*, **2002**, *35*, 511. (b) O. R. Evans, R.-G. Xiong, Z. Wang, G. K. Wong and W. Lin, *Angew. Chem. Int. Ed.*, **1999**, *38*, 536. (c) O. R. Evans and W. Lin, *Chem. Mater.*, **2001**, *13*, 2705. (d) W. Lin, L. Ma and O. R. Evans, *Chem. Commun.*, **2000**, 2263.
14. (a) J. Zyss, J.-F. Nicoud and M. Coquillay, *J. Chem. Phys.*, **1984**, *81*, 4160. (b) T. Ueniya, N. Uenishi, Y. Shimizu, T. Yoneyama and K. Nakatsu, *Mol. Cryst. Liq. Cryst.*, **1990**, *A182*, 51.
15. G. R. Desiraju and T. S. R. Krishna, *Mol. Cryst. Liq. Cryst.*, **1988**, *159*, 277.
16. A. J. Preston, J. C. Gallucci and J. R. Parquette, *Chem. Commun.*, **2005**, 3280.
17. G. R. Desiraju and R. Parthasarathy, *J. Am. Chem. Soc.*, **1989**, *111*, 8725.
18. J. N. Moorthy, R. Natarajan, P. Mal and P. Venugopalan, *J. Am. Chem. Soc.*, **2002**, *124*, 6530.

19. U. Ohms, H. Guth and W. Z. Treutmann, *Kristallogr., Kristalloggeom., Kristallphys., Kristallchem.*, **1983**, 162, 299.
20. A. Dey and G. R. Desiraju, *Chem. Commun.*, **2005**, 2486.
21. J. Zyss and J. L. Oudar, *Phy. Rev.*, **1982**, A26, 2028.

CHAPTER 7

HALOGEN BONDING AND HYDROGEN BONDING IN CRYSTAL PACKING

7.1 Introduction

Crystal of an organic compound is the perfect supermolecule, “a supermolecule par excellence”¹ and intermolecular forces are responsible for the extraordinary precision in which molecules can interact to form a highly ordered crystalline materials.² These interactions can be controlled by the designed placement of functional groups in the tecton to generate supramolecular synthon,³ crucial structural unit within supermolecules. Interactions, such as C–H \cdots π , C–H \cdots O, C–H \cdots N etc. are energetically weak, less specific and weakly directional. These interactions are difficult to control and exploit for designing supramolecular architectures. On the other hand, strong interactions such as O–H \cdots O, O–H \cdots N, acid \cdots acid, amide \cdots amide etc. are more useful, because of their specificity and directionality.

A proper understanding of hydrogen bonding and supramolecular synthons is important in the design of solid-state architectures with new functional groups, or new combinations of known functional groups. Early studies in crystal engineering focused on exploiting hydrogen bonding between the same functional groups, or homosynthons, e.g. COOH \cdots COOH, CONH₂ \cdots CONH₂, OH \cdots OH, etc. Several supramolecular architectures have been engineered by the strategy of molecular tectonics using appropriate robust functional groups in the periphery of the building blocks.⁵ Trigonal symmetric molecule, such as trimesic acid, form hexagonal network via carboxylic acid dimer synthon by three symmetrically disposed COOH groups. This hexagonal network can include guest molecules^{6a} (Figure 1a) or may undergo interpenetration^{6b} to avoid free space. Wuest et al. used pyridone and other strong H-bonding functional groups in the tetrahedral tecton to engineer diamondoid network (Figure 1b).⁷

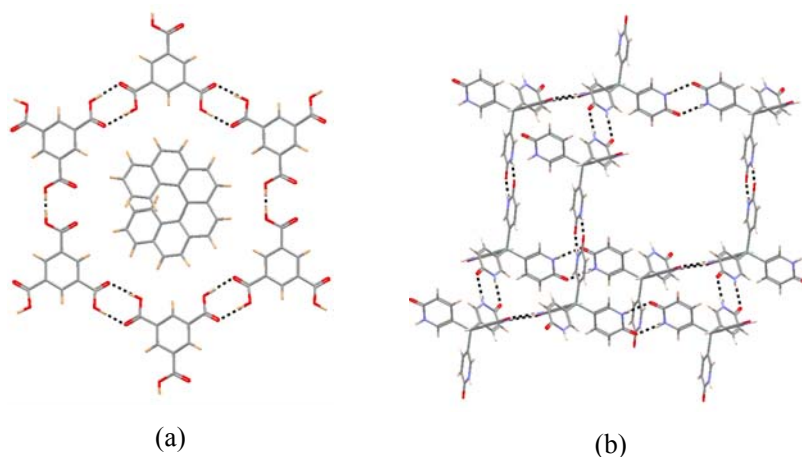


Figure 1. (a) Hexagonal framework formed by trimesic acid via acid dimer homosynthon, which include guest molecules such as phenanthrophenanthrene. In the absence of suitable guest molecule it undergoes interpenetration. (b) Diamondoid network formed by tetrakis(1,2-dihydro-2-oxo-5-pyridyl)silane via pyridone dimer homosynthon.

A recent trend is to utilize complementary functional groups for controlling the organization of molecules in the target architecture. Some common heterosynthons⁸ i.e. between unlike functional groups are acid...pyridine,⁹ phenol...pyridine,¹⁰ acid...amide,¹¹ hydroxy...amine,¹² amide...pyridine *N*-oxide¹³ etc. Generally these synthons are more robust, at the same time it increases the diversity and increasingly being used to design materials as well as pharmaceutical cocrystals.¹⁴ Coppens et al. have shown hexagonal network made of two trigonal molecules, trimesic acid and 1,3,5-tris(4-pyridyl)-2,4,6-triazine cocrystal via acid...pyridine heterosynthon, where pyrene guest molecules reside as nano-rod (Figure 3a).¹⁵ Ermer and Eling noticed diamondoid network in the crystal structure of 4-aminophenol. Molecules form 3D network via OH...NH₂ hydrogen bonds, where synthons form infinite 2D hexagonal layer and the phenyl rings connect these layers in third direction (Figure 2b).¹⁶

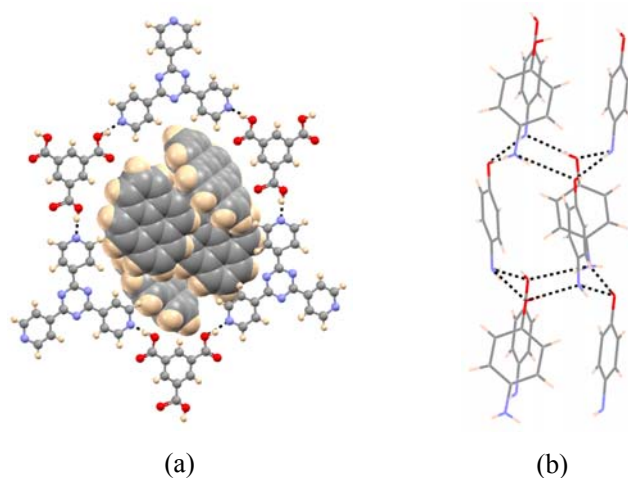


Figure 2. (a) Pyrene guest molecules fill up the hexagonal channel created by the complex of trimesic acid and tripyridyl triazine connected by acid...pyridine heterosynthon. (b) Diamondoid 3D network formed by saturated OH...NH₂ heterosynthon in the crystal structure of 4-aminophenol.

Recently halogen bond synthons have attracted a special attention to the crystal engineers. Under favorable conditions it can be energetically as strong as classical H-bonds. Allen and co-workers and more recently Resnati *et al.* showed that electron deficient iodo compounds can form very strong halogen bonds with pyridyl group, pyridyl *N*-oxide, nitrile groups, nitro groups, etc.¹⁷ 2,4,6-Trichloro-1,3,5-triazine crystallize as layered structure. These 2D layers are constructed by hexagonal packing of the trigonal tecton via short Cl...N interactions (Figure 3a).¹⁸ Desiraju and co-workers have designed diamondoid network mediated via halogen bonding between hexamethylenetetramine and tetrabromomethane. The tertiary amine N atom interacts with bromo group to build the 2-fold interpenetrated diamondoid network (Figure 3b).¹⁹ Thalladi *et al.* combined strong H-bond with halogen bond to obtain infinite 1D chain. They cocrystallized 1,4-dinitrobenzene and 4-iodocinnamic acid where acid group form expected dimer homosynthon and iodo group form halogen bond with nitro group.²⁰

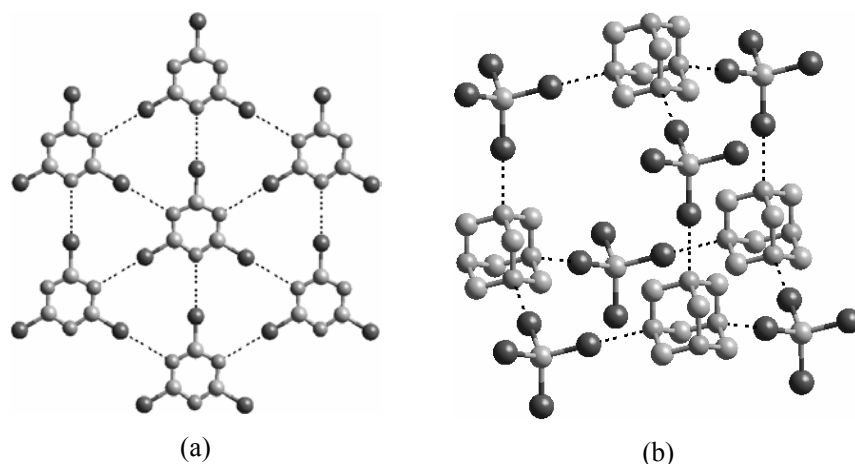
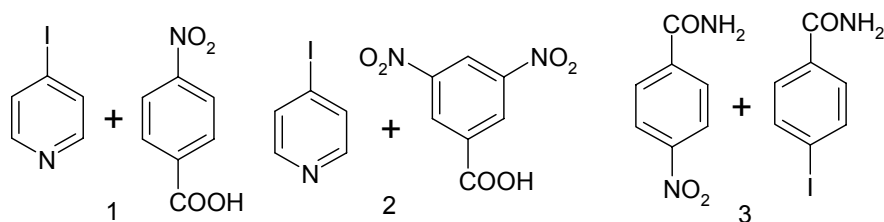


Figure 3. Hexagonal 2D layer structure of 2,4,6-trichloro-1,3,5-triazine via Cl...N halogen bond. (b) Diamondoid network mediated via Br...N halogen bond in the crystal structure of hexamethylenetetramine and tetrabromo methane binary system.

In this chapter we show the combination of robust hydrogen bonding heterosynthon with halogen bond in 1D tape and strong hydrogen bonding homosynthon with halogen bond in 2D layer. We have chosen the binary 1:1 systems of 4-nitrobenzoic acid•4-iodopyridine, 1, 3,5-dinitrobenzoic acid•4-iodopyridine, 2, and 4-nitrobenzamide•4-iodobenzamide, 3 to perform the experiment (Scheme 1). The interaction geometries in 1, 2 and 3 are listed in table 1.



Scheme 1. Cocrystals of the binary systems have been studied in this chapter.

7.2 Results and Discussions

7.2.1 4-Nitrobenzoic Acid•4-Iodopyridine, 1

Cocrystal 1 was obtained upon mixing equimolar quantities of the molecular

components in EtOAc/THF solvent mixture at room temperature after a few days. The crystal structure solves in $P\bar{1}$ space group with one molecule each in the asymmetric unit. The crystal structure of **1** shows the expected acid \cdots pyridine and iodo \cdots nitro recognition in linear tapes of molecules (Figure 1a). The O–H \cdots N hydrogen bond (1.64 Å, 2.61 Å, 172.2°) is fortified by auxiliary C–H \cdots O interaction and the iodine forms a bifurcated interaction with both O atoms of the nitro group (I \cdots O₂N, 3.41 Å, 3.44 Å, 158.8°, 162.2°). Both the molecular components including the COOH and NO₂ groups lie in the plane defined by the aromatic rings. These tapes stack one over other without offset and one tape is surrounded by six others (Figure 4b).

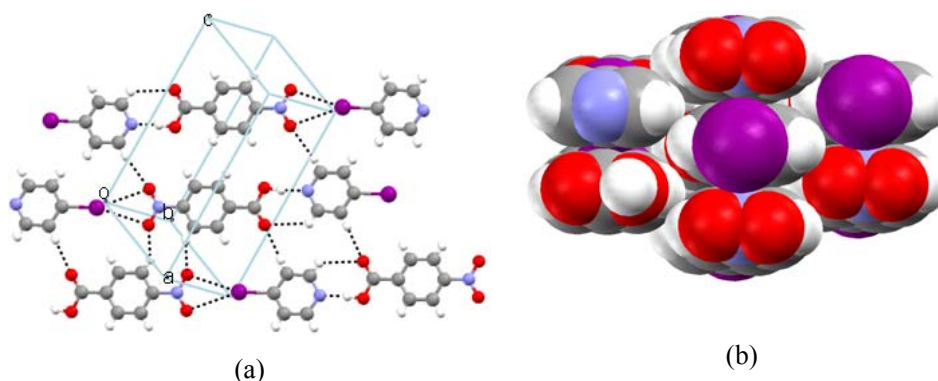


Figure 4. (a) One dimensional tape via acid \cdots pyridine heterosynthon and iodo \cdots nitro halogen bond made of binary compounds in **1**. These tapes are connected by weak C–H \cdots O H-bonds. (b) View down the tape, one tape is surrounded by six neighboring tapes.

7.2.2 3,5-Dinitrobenzoic Acid•4-Iodopyridine, **2**

Encouraged by the high degree of selectivity in O–H \cdots N and C–I \cdots O bonding in stabilizing the structure of **1**, we examined the structure of **2** which has an extra nitro acceptor for competition with donor groups. Diffraction quality single crystals of **2** were obtained upon mixing equimolar quantities of the molecular components in EtOAc/THF solvent mixture. The cocrystal **2** crystallizes in $P2_1/c$ space group and the asymmetric unit contains one each of the molecular components. Similar to **1**, it also forms molecular tape via acid \cdots pyridine and iodo \cdots nitro recognition. The O–H \cdots N interaction involving the stronger O–H donor acid is shorter in **2** (1.62 Å, 2.56 Å, 158.2°). The iodine bonds to

one of the nitro groups in a single interaction ($\text{C}\cdots\text{I}\cdots\text{O}$, 3.40 Å, 157.1 °) to form zigzag tapes of molecules. In contrast to coplanar geometry in 1, acid and pyridine molecular planes of 2 are twisted out by 60° and there is no auxiliary support from $\text{C}\cdots\text{H}\cdots\text{O}$ interaction to the acid···pyridine heterosynthon. The tapes are connected by weak $\text{C}\cdots\text{H}\cdots\text{O}$ interactions.

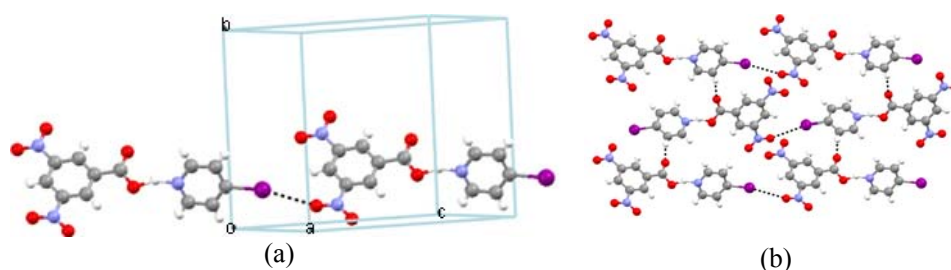


Figure 5. (a) One dimensional tape via acid···pyridine heterosynthon and iodo···nitro halogen bond between two non-planar compounds in 2. (b) These tapes are connected by $\text{C}\cdots\text{H}\cdots\text{O}$ weak H-bonds.

7.2.3 4-Nitrobenzamide•4-Iodobenzamide, 3

To extend the 1D tape motif of 1 and 2 to a 2D sheet, and also to explore related structures with hydrogen and halogen bonding interactions, cocrystal 3 was studied which was obtained from ethyl acetate. The binary system is solved in $P\bar{1}$ space group with one molecule in the asymmetric unit, each 0.5 occupancy of the two components.

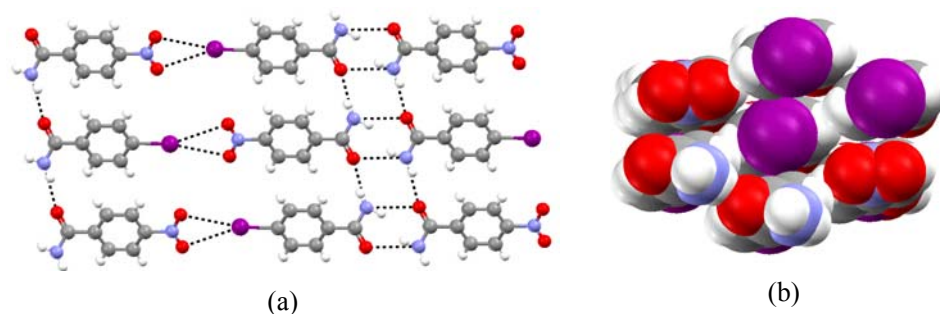


Figure 6. (a) 2D sheet like structure in cocrystal 3, controlled by amide···amide tape homosynthon and iodo···nitro halogen bonding (disorderness is not shown). (b) One tape is surrounded by another six neighboring tapes with slight offset stacking.

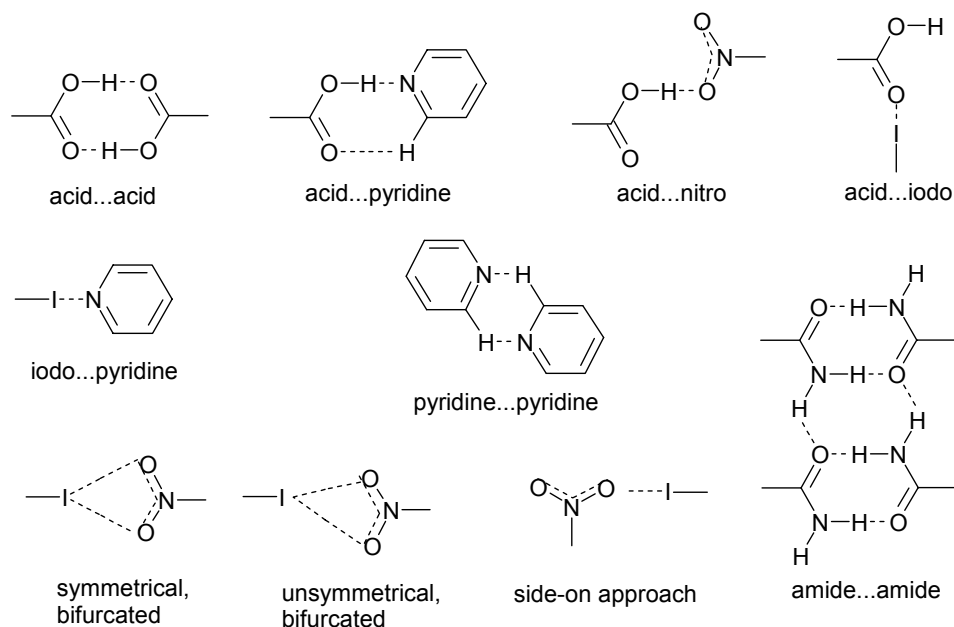
The iodo and nitro groups are disordered. The carboxamide groups are engaged in the 5.1 Å axis tape synthon²¹ via N–H···O H-bonds (2.03 Å, 2.93 Å, 148.1° and 1.91 Å, 2.90 Å, 166.5°) and the iodo···nitro groups engage in a bifurcated interaction (3.41 Å, 165.5°; 3.42 Å, 158.8°), similar to 1, connecting the molecular components in a sheet-like structure (Figure 6a). View down the tape axis, one tape is surrounded by six other (similar to 1), but with slight offset in the stacking (Figure 6b). The iodo···nitro interaction is postulated between these disordered groups (50% s.o.f.) compared to I···I or NO₂···NO₂ interactions because the distance is reasonable in the heterosynthon and it is also stabilized by I···O polarization.

Table 1. Interaction geometries in cocrystals 1, 2 and 3 (neutron normalized values).

Compound	Interaction	d (Å)	D (Å)	θ (°)
1	O (1)–H···N (2)	1.64	2.614(3)	172.2
	C (8)–H···O (3)	2.47	3.397(4)	142.3
	C (9)–H···O (4)	2.43	3.381(4)	145.3
	C (11)–H···O (2)	2.40	3.314(4)	141.2
	C (12)–H···O (2)	2.57	3.285(4)	122.9
	C (10)–I···O (3)		3.411(2)	158.8
	C (10)–I···O (4)		3.439(3)	162.2
2	O (6)–H···N (3)	1.62	2.560	158.2
	C (4)–H···O (5)	2.26	3.317(4)	163.6
	C (1)–H···O (2)	2.45	3.507(4)	163.8
	C (12)–H···O (2)	2.44	3.444(3)	154.1
	C (3)–I···O (4)		3.404(2)	157.1
3	N(1)–H···O (1)	1.91	2.902(8)	165.5
	N(1)–H···O (1)	2.03	2.932(9)	148.1
	C (2)–H···O (3)	2.39	3.465(18)	170.5
	C (4)–I···O (2)		3.416	158.8
	C (4)–I···O (3)		3.410	165.5

A natural question that arises when several functional groups are present during crystallization is: to what extent they will form the expected heterosynthon, or whether they will interfere to form diverse and unpredictable packing motifs. The ideal situation in crystal engineering would be to use those combinations of heterosynthons which

exhibit specific recognition for a particular hydrogen bond pairing and almost no bonding with other functional groups that are present in the self-assembly milieu. A case in point is crystal structures with acid...pyridine and iodo...nitro heterosynthons. While both these synthons independently show excellent structural control, the presence of all four functional groups in the same system can also lead to $\text{COOH}\cdots\text{O}_{\text{nitro}}$, $\text{C-H}\cdots\text{O}_{\text{nitro}}$, iodo...pyridine and iodo... O_{acid} bonding, among other possibilities (Scheme 2). For example, it has been observed that when urea, nitro and halogen functional groups are present then both urea...urea and urea...nitro hydrogen bonding take place depending on the halogen atom.²² There is thus a need to understand recognition and synthon selectivity in multi-functional crystal structures for the present phase of crystal engineering.²³



Scheme 2. Different possibilities of the interactions in the present binary systems 1, 2 and 3.

The high degree of selectivity in the present system may be contrasted with the crystal structure of 4-iodoanilinium 3-nitrophthalate.²⁴ Here, carboxylate...ammonium ionic hydrogen bonding is consistent with strongest-donor to strongest-acceptor

recognition.²⁵ However, among the weaker interactions instead of iodo...nitro bonding there is a short iodo...iodo interaction (3.54 Å) while the nitro group is engaged in a C–H...O interaction (2.49 Å). Similarly, when the halogen atom is chloro instead of iodo, acid...pyridine hydrogen bonding is persistent but there is no recurring halogen bonding pattern between Cl and NO₂ groups.²⁶ That the strength and specificity of iodo...nitro interaction is necessary for structural control is also noted in crystal structures which contain COOH, iodo and nitro functional groups: these structures are stabilized by COOH...COOH and iodo...nitro bonding.²⁷ There are no examples in the Cambridge Structural Database (CSD)²⁸ of the four functional groups, acid, pyridine, iodine and nitro, being present in the same crystal structure.

Structures of both the cocrystals 1 and 2 are stabilized by acid...pyridine and iodo...nitro synthons. This shows that when these four functional groups are competing during crystallization there is preference for selective pairing of hydrogen bonding and halogen bonding groups. While heterosynthons such as acid...pyridine, halogen...pyridine and iodo...nitro have been successfully used for crystal design, the competition of these functional groups has not been examined so far. This preliminary result shows the potential of simultaneously using several functional groups for solid-state design. In a recent result on N–H...O urea tape and I...O₂N synthons in iodophenyl-nitrophenylurea,²² Nangia and co-workers showed hydrogen bonding and halogen bonding may be utilized to control supramolecular aggregation in different regions of the crystal structure with negligible or no interference. Such modularity in self-assembly, or orthogonality in interaction pairing, is a prerequisite for crystal engineering of multi-functional crystals.

The energy of acid...acid homodimer (energy 7.8 kcal/mol per O–H...O bond)²⁹ and iodo...pyridine interaction (energy 3.4 kcal/mol)³⁰ in their respective crystal structures. Where as the energy of acid...pyridine heterosynthon²⁹ is 9.9 kcal/mol and that of I...O₂N interaction³¹ is 2.5 kcal/mol. This explains the ready formation of cocrystals 1 and 2.

7.3 Conclusions

Crystal engineering has been likened with covalent synthesis in recent papers.³² However, an important difference between molecular and supramolecular synthesis is that while the former can be carried out in a stepwise fashion, self-assembly occurs in a single step. It is therefore not possible to employ protection-deprotection protocols in crystallization, the way a synthetic chemist would use them in reactions on complex multi-functional molecules.³³ The idea that hydrogen bonding and halogen bonding interactions show selectivity and specificity in supramolecular recognition within each category and, furthermore, have little preference for bonding between the two categories means that crystal engineers can exploit this property for modular build-up of structures. This selectivity can be compared with the result of Aakeröy³⁴ and co-workers, who used the ‘Etters Rule’³⁵ on H-bonding in cocrystallization experiment, that is best donor bonds with best acceptor, second best donor bonds with second best acceptor and so on. Hydrogen bonding involves hard and electronegative donor and acceptor groups (OH, NH) whereas in halogen bonding the soft and polarizable iodine donor atom approaches O, N acceptors.³⁶ To conclude, strong hydrogen bonding groups together with weak halogen bonding interactions with iodine is the preferred combination for crystal engineering of multi-functional systems.

7.4 Experimental Section

X-Ray Crystallography

Reflections were collected for the single crystal of 1 and 2 on a KUMA CCD area detector system and for 3 on a Bruker SMART APEX CCD area detector system (Mo-K α radiation, $\lambda = 0.71073$ Å). Multi-scan absorption correction was applied for 1 and 2 using XEMP and for 3 using SADABS. Structure solution and refinement were performed with SHELXS-97 and SHELXL-97 packages. C–H hydrogen atoms were generated with idealised geometries and isotropically refined using Riding model. O–H and N–H hydrogen atoms were located and refined isotropically from difference electron density map. Refinement of coordinates and anisotropic thermal parameters of non-

hydrogen atoms was carried out by the full-matrix least-squares method (O2 was refined isotropically). In 3, the components occupy same place and the iodo and nitro group have 0.5 occupancy each.

7.5 References

1. J. D. Dunitz, *Pure Appl. Chem.*, **1991**, 63, 177.
2. G. R. Desiraju, *Crystal Engineering: The Design of Organic Solids*; Elsevier: Amsterdam. **1989**.
3. G. R. Desiraju, *Angew. Chem. Int. Ed.*, **1995**, 34, 2311.
4. (a) M. Nishio, *CrystEngComm*, **2004**, 6, 130. (b) G. R. Desiraju, T. Steiner, *The Weak Hydrogen bond in Structural Chemistry and Biology*; Oxford University Press: Oxford, **1999**. (c) G. R. Desiraju, *Acc. Chem. Res.*, **2002**, 35, 565.
5. J. D. Wuest, *Chem. Commun.*, **2005**, 5830.
6. (a) O. Ermer and J. Neudorfl, *Helv. Chim. Acta.*, **2001**, 84, 1268. (b) D. J. duchamp and R. E. Marsh, *Acta Crystallogr.*, **1969**, B25, 5.
7. (a) M. Simard, D. Su and J. D. Wuest, *J. Am. Chem. Soc.*, **1991**, 113, 4696. (b) X. Wang, M. Simard and J. D. Wuest, *J. Am. Chem. Soc.*, **1994**, 116, 12119.
8. C. B. Aakeroy, A. M. beatty and B. A. Helfrich, *J. Am. Chem. Soc.*, **2002**, 124, 14425.
9. (a) B. R. Bhogala, P. Vishweshwar and A. Nangia, *Cryst. Growth Des.*, **2002**, 2, 325. (b) B. R. Bhogala and A. Nangia, *Cryst. Growth Des.*, **2003**, 3, 547.
10. P. Vishweshwar, A. Nangia and V. M. Lynch, *CrystEngComm*, **2003**, 5, 164.
11. P. Vishweshwar, A. Nangia and V. M. Lynch, *Cryst. Growth. Des.*, **2003**, 3, 783.
12. (a) A. Dey, M. T. Kirchner, V. R. Vangala, G. R. Desiraju, R. Mondal and J. A. K. Howard, *J. Am. Chem. Soc.*, **2005**, 127, 10545. (b) V. R. Vangala, B. R. Bhogala, A. Dey, G. R. Desiraju, C. K. Broder, P. S. Smith, R. Mondal, J. A. K. Howard and C. C. Wilson, *J. Am. Chem. Soc.*, **2003**, 125, 14495.
13. L. S. Reddy, N. J. Babu and A. Nangia, *Chem. Commun.*, **2006**, 1369.
14. (a) S. G. Fleischman, S. S. Kuduva, J. A. McMahon, B. Moulton, R. D. Bailey, N. Rodríguez-Hornedo and M. J. Zaworotko, *Cryst. Growth Des.*, **2003**, 3, 909. (b) P.

- M. Bhatt, N. V. Ravindra, R. Banerjee and G. R. Desiraju, *Chem. Commun.*, **2005**, 1073.
15. B.-Q. Ma and P. Coppens, *Chem. Commun.*, **2003**, 2290.
16. O. Ermer and A. Eling, *J. Chem. Soc., Perkin Trans. 2*, **1994**, 925.
17. (a) E. Corradi, S. V. Meille, M. T. Messina, P. Metrangolo and G. Resnati, *Angew. Chem. Int. Ed.*, **2000**, 39, 1782. (b) P. Metrangolo, H. Neukirchi, T. Pilati and G. Resnati, *Acc. Chem. Res.*, **2005**, 38, 386. (c) J. P. M. Lommerse, A. J. Stone, R. Taylor and F. H. Allen., *J. Am. Chem. Soc.*, **1996**, 118, 3108.
18. K. Xu, D. M. Ho and R. A. P. Junior, *J. Am. Chem. Soc.*, **1994**, 116, 105.
19. D. S. Reddy, D. C. Craig, A. D. Rae and G. R. Desiraju, *J. Chem. Soc., Chem. Commun.*, **1993**, 1737.
20. V. R. Thalladi, B. S. Goud, V. J. Hoy, F. H. Allen, J. A. K. Howard and G. R. Desiraju, *Chem. Commun.*, **1996**, 401.
21. (a) G. T. R. Palmore and J. C. MacDonald, in *The Amide Linkage: Selected Structural Aspects in Chemistry, Biochemistry, and Materials Science*; Eds. A. Greenberg, C. M. Breneman and J. F. Liebman, John Wiley: Chichester, **2000**, pp. 291. (b) C. M. Reddy, L. S. Reddy, S. Aitipamula, A. Nangia, C.-K. Lam and T. C. W. Mak, *CrystEngComm*, **2005**, 7, 44.
22. S. George, A. Nangia, C.-K. Lam, T. C. W. Mak and J.-F. Nicoud, *Chem. Commun.*, **2004**, 1202.
23. (a) G. R. Desiraju, *Nature*, **2001**, 412, 397. (b) D. Braga, *Chem. Commun.*, **2003**, 2751.
24. C. Glidewell, J. N. Low, J. M. S. Skakle and J. L. Wardell, *Acta Crystallogr.*, **2003**, C59, o509.
25. M. C. Etter, *J. Phys. Chem.*, **1991**, 95, 4601.
26. (a) H. Ishida, T. Fukunaga and S. Kashino, *Acta Crystallogr.*, **2002**, E58, o1081 and o1083. (b) H. Ishida, B. Rahman and S. Kashino, *Acta Crystallogr.*, **2001**, C57, 876. (c) T. Sugiyama, J. Meng and T. Matsuura, *J. Mol. Struct.*, **2002**, 611, 53.

27. (a) V. R. Thalladi, B. S. Goud, V. J. Hoy, F. H. Allen, J. A. K. Howard and G. R. Desiraju, *Chem. Commun.*, **1996**, 401. (b) A. Ranganathan and V. R. Pedireddi, *Tetrahedron Lett.*, **1998**, 39, 1803.
28. Cambridge Crystallographic Data Centre, July **2004** update.
29. P. Vishweshwar, A. Nangia and V. M. Lynch, *J. Org. Chem.*, **2002**, 67, 556.
30. R. B. Walsh, C. W. Padgett, P. Metrangolo, G. Resnati, T. W. Hanks and W. T. Pennington, *Cryst. Growth Des.*, **2001**, 1, 165.
31. F. H. Allen, J. P. M. Lommerse, V. J. Hoy, J. A. K. Howard and G. R. Desiraju, *Acta Crystallogr.*, **1997**, B53, 1006.
32. (a) C. B. Aakeröy, A. M. Beatty and B. A. Helfrich, *J. Am. Chem. Soc.*, **2002**, 124, 14425. (b) D. Braga, G. R. Desiraju, J. S. Miller, A. G. Orpen and S. L. Price, *CrystEngComm*, **2002**, 4, 500.
33. (a) E. J. Corey and X.-M. Cheng, in *The Logic of Chemical Synthesis*; Wiley: New York, **1989**. (b) K. C. Nicolaou and E. J. Sorensen, in *Classics in Total Synthesis*, Wiley-VCH: Weinheim, **1996**.
34. (a) C. R. Aakeröy, J. Desper and J. F. Urbina, *Chem. Commun.*, **2005**, 2820. (b) C. R. Aakeröy, J. Desper and B. M. T. Scott, *Chem. Commun.*, **2006**, 1445.
35. (a) M. C. Etter, *Acc. Chem. Res.*, **1990**, 23, 120. (b) M. C. Etter, *J. Phys. Chem.*, **1991**, 95, 4601.
36. (a) R. Liantonio, P. Metrangolo, T. Pilati and G. Resnati, *Cryst. Growth Des.*, **2003**, 3, 355. (b) C. J. Kelly, J. M. S. Skakle, J. L. Wardell, S. M. S. V. Wardell, J. N. Low and C. Glidewell, *Acta Crystallogr.*, **2002**, B58, 94.

CHAPTER 8

CONCLUSIONS AND FUTURE PROSPECTS

From the studies reported in this thesis, the following conclusions and future implications can be drawn.

8.1 Halogen is a Sticky Group

There are some controversies on inter-halogen interactions, whether it is attractive in nature or just a result of close packing. The halogens are believed to be elliptical in shape and the ellipticity increases for heavier halogens the with van der Waals radius along C–X bond (polar region) being shorter than in the perpendicular direction (equatorial region). Because of non-spherical shape halogens can form contacts of less than van der Waals radius sum. On the other hand, the attractive nature has been explained by the model as the polar C–X region is electro positive and the equatorial region is negatively polarized and the polarization increases with increase in size of the halogen. As a result the tendency to form type II interaction ($\theta_1 \cong 180^\circ$, $\theta_2 \cong 90^\circ$) increases in the order $\text{Cl} < \text{Br} < \text{I}$. Type I geometry ($\theta_1 \cong \theta_2$) is believed to be a consequence of close packing whereas type II interaction is due to polarization induced electrophile–nucleophile pairing. Halogen bonding of donor halogens with acceptors containing lone pairs, e.g. N, O, P, S, Br^- , I^- is strong and directional, similar to traditional hydrogen bonds. In halogen bonding the lone pair is directed to the polar halogen region of partial electro positive character. Naturally the interaction becomes stronger as electron-withdrawing capacity of the halogen and electron-donating capacity around the lone pair group increases. Carbon bound neutral halogen can participate in H-bond as a weak acceptor.

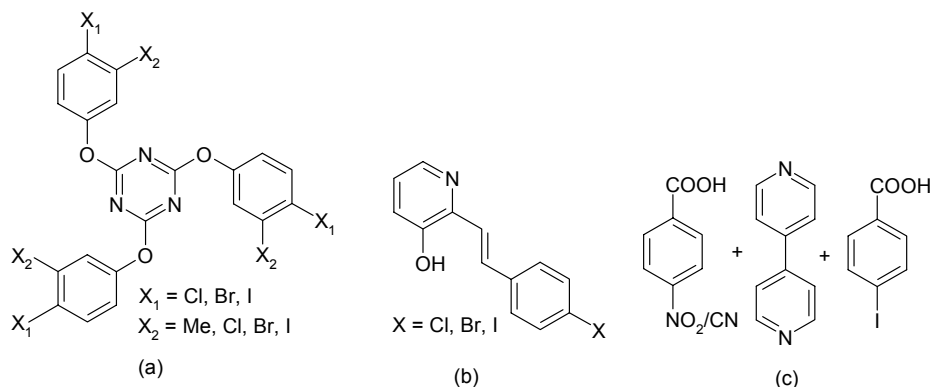
In the 4-XPOT series of crystal structures we have shown that the trigonal tectons assemble via halogen trimer synthon in the hexagonal crystal systems (Chapter 2). The halogen···halogen interaction adopts type II geometry with $\theta_1 \cong 162$ and $\theta_2 \cong 105^\circ$

and could be strengthened by cooperativity. The unsubstituted compound does not form similar packing (space group *Ia*) in the absence of halogen sticky group. Even isosteric methyl group at the 4-position (4-MePOT) cannot reform the trimer synthon and crystallize in *R3c* columnar structure, because methyl trimer would not be a stabilizing synthon except universal van der Waals interaction. Similarly 4-FPOT also crystallize (space group *P2₁/c*) in a completely different packing arrangement. Moreover with increase in polarizability of the halogens, the interaction becomes shorter with respect to van der Waals radii sum and more significant. All these evidences support the attractive nature (type II) of larger halogens and the directing role as sticky group. We have further shown similarity between halogens and ethynyl group in organic supramolecular chemistry (chapter 2). Due to the similarity in charge distribution and size they can play similar structure directing role in organic solid state chemistry, in spite of the shape differences. Halogen groups are elliptical whereas ethynyl group is cylindrical in shape. 4-EPOT assembles via ethynyl trimer synthon, mimic the halogen trimer synthon and produce isostructural crystal to 4-IPOT cage structure (Chapter 2).

In the crystal structures of 2-halo-3-pyridinol and the corresponding *N*-oxide series also we have proved the similar point (Chapter 6). In the presence of halogen group in the appropriate position the molecules adopt non-centrosymmetric packing, whereas absence of halogen groups results in center of symmetry in the crystal structure. Furthermore the attractive nature of the halogens has been tested by putting methyl group in the place of halogen. The centrosymmetric structure does not show any methyl...methyl contact. In this family also the I...I (3.74 Å) contact in 2-iodo-3-pyridinol crystal structure, is shorter and more significant (type II) than Br...Br (3.64 Å) contact in the isostructural crystal structure of 2-bromo-3-pyridinol, with respect to their van der Waals radii sum.

The 4-XPOT series can be further extended to obtain some more interesting results and to understand the nature of halogens. In the cage structure the 3-H is pointing towards the cavity, including guest molecules. Thus substitution the 3-H by methyl or other halogen groups can reduce the cavity size, which can produce guest free

isostructural crystal structure or include small size guest (Scheme 1a). This strategy may also convert channel structure of 4-CIPOT to cage structure.



Scheme 1

In the series of 2-halo-3-pyridinol and corresponding *N*-oxide crystal structures, packing is non-centrosymmetric. The bulk materials show SHG activity though very weak, \leq urea, because there is no push-pull NLO phore in the compound skeleton. Thus placing a conjugated spacer between halogen and aryl group may enhance the SHG activity of the compounds (Scheme 1b).

The idea of combining hydrogen bonding and halogen bonding used in cocrystal experiments in chapter 7, can be extended from binary to ternary complex by choosing proper combination of substrates shown in scheme 1c.

8.2 Halogen Exchange and Isostructurality

There are only a handful of functional groups which can be exchanged without change in crystal structures. C, quadrivalent Si, Ge, Sn and Pb atoms are generally inner core atoms and their exchange show isostructurality on few occasions. Phenyl-thiophene exchange has also been possible in some cases because of their similarity in size and shape. Chloro-methyl exchange is well known and recently Allen and co-workers have shown that bromo-methyl exchange is also equally favorable (26% and 25% respectively).

In chapter 3 we have shown from CSD search that the Cl/Br/I exchange probability is 30% to produce similar packing arrangements and Cl/Br exchange rate (66%) is higher than the Br/I (50%) exchange. Expectedly F behaves quite differently as shown by the low exchange probability (F/Cl 19%), because of small size (1.47 Å) and high electronegativity (3.98) of F.

In periodic table the halogen family, namely Cl, Br and I have van der Waals radii 1.75 Å, 1.85 Å and 1.98 Å respectively and the electronegativity of these three atoms are 3.16, 2.96 and 2.66 respectively in Pauling scale. Thus the geometric and chemical natures change slowly and gradually for halogens. In addition they are monovalent and hence the bond angle remains constant. On the other hand in chalcogen family, there is a sudden jump in size (van der Waals radii 1.52 Å and 1.80 Å respectively) and electronegativity (3.44 and 2.58) from O to S. Furthermore they differ considerably in the divalent geometry: Desiraju and co-workers showed from statistical analysis that in general the C–O–C angle in ether is $\sim 120^\circ$ and for C–S–C is $\sim 100^\circ$ in thioether. For these reasons the halogen exchange rate is so high in comparison to other groups or atoms in isostructurality of organic supramolecular chemistry.

In 4-XPOT•guest series of crystal structures 4-BrPOT is isostructural to 4-CIPOT or 4-IPOT depending upon guest molecule (Chapter 2). 4-IPOT is only 2D isostructural to 4-CIPOT, in the third dimension there is sliding of the layers in the cage structure of 4-IPOT, though the halogen trimer synthons have not been disturbed. It can be compared to acid dimer and amide dimer, where dimer motifs are the same. However in the perpendicular direction amide forms strong N–H \cdots O tape, which is absent in acid dimer and the crystal structures differ in that direction.

In the 3-XPOT series of crystal structures 3-MePOT, 3-CIPOT and 3-BrPOT are isostructural and do not contain any inter halogen interaction, indicate that the chemical nature of the halogen groups is not so important in these packings. But the more polarizable iodo groups make type II inter-halogen interaction in 3-IPOT crystal structure (Chapter 3). For the 2-XPOT series, the inter-halogen interactions in 2-FPOT and 2-CIPOT crystal structures are mainly driven by close packing and are 2D isostructural, but for isostructural 2-BrPOT and 2-IPOT pair, the polarizability factor

comes into play and type II interaction is formed (Chapter 3). There is no example so far in XPOT series where Cl/I exchange produces isostructural crystal structure.

In the series of 2,4,6-tris(2-halo-3-pyridinoxy)-1,3,5-triazine (3X, X = Cl, Br, I) clathrate crystal structures, 3Cl compound produce square channel type architecture, which is different from isostructural pair 3Br and 3I cage structures (Chapter 4). Here halogens mainly play space filling role as they do not participate in any considerable interaction.

Polarizability as well as geometry of the halogens, both played a key role behind these observations and crystal structures of bromo compounds have followed either Cl or I derivatives as expected.

8.3 Weak Interactions are Important in Crystal Packing

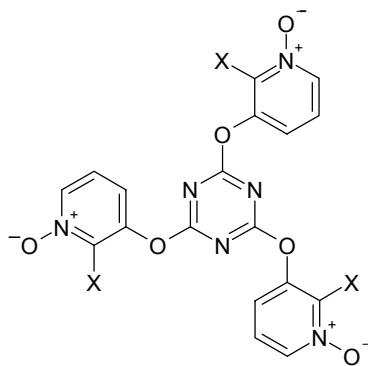
Crystal engineering is difficult when the interactions are weak H-bonds or similar less specific and weakly directional. On the other hand, due to the weakness of interactions, the frameworks are not very much rigid like strong H-bonded systems. This lability allow them to incorporate different guest molecules in adjustable cavities.

4-XPOT (X=Cl, Br, I, C≡C-H) trigonal tectons assemble in hexagonal crystal systems via weak halogen or ethynyl trimer synthons, assisted by weak C-H...O and C-H...N interactions (Chapter 2). The importance of these interactions have been proved by replacing the halogens by isosteric methyl group and the hydrogens by fluorine. In both the experiments the compounds crystallize in different arrangements. 4-IPOT and 4-EPOT produce isostructural cage structures with common guest molecules, but the 4-EPOT•guest systems are less vulnerable to temperature than the corresponding 4-IPOT•guest systems, as has been observed in thermal experiments. This stability is attributed to the better packing coefficient as well as stronger C-H...O and C-H...N interactions in comparison to 4-IPOT crystal structures.

The powder XRD and melting points show that the apohost obtained after complete guest loss from 3Cl host is different from the guest-free form as well as the channel structure (Chapter 4). Though the channel structure constructed by weak interactions, cannot survive complete guest loss, but strong enough up to 50% guest

removal and then it slowly starts decomposing with further loss of guest molecules. The narrow channel walls confine the linear guest molecules quite tightly via van der Waals interaction, as reflected by higher T_{onset} value for low boiling acetone guest in the TG and DSC experiments. Interestingly the acetone guest molecules evolve from the isostructural channel at higher temperature than the high boiling nitromethane because of the larger van der Waals surface area. The cage structures of 3Br and 3I hosts are mainly build up of C–H \cdots N, C–H \cdots O and $\pi\cdots\pi$ stack. Due to the weakening of interactions, the larger halogens cannot adopt the channel structure developed by 3Cl. In spite of low packing capability of the 3I cage structures than the similar 4-IPOT crystal structures, release of guest molecules (mesitylene and collidine) occurs at very high temperature.

Extension of the 3X series on replacing pyridyl groups by pyridine *N*-oxide can produce interesting result. It can moderate the channel or cage cavities by fine tuning of the cavity sizes and even can stabilize the system by strengthening the interactions as well (Scheme 2).



X = Me, Cl, Br, I

Scheme 2

8.4 Halogen and Hydration

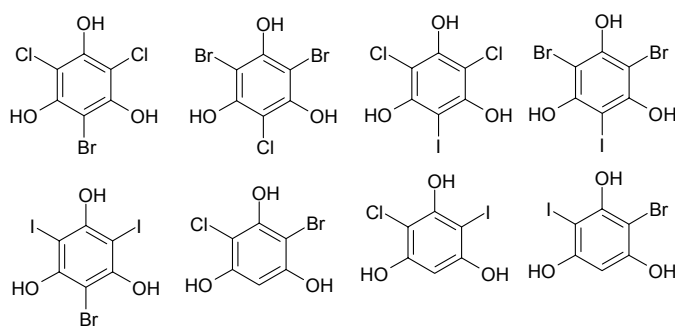
It is not easy to answer the reasons for hydration, though some general ideas have been proposed to explain this important phenomenon. Infantes and co-workers classified 36 chemical groups and their influences on hydration. They have reported that

molecules containing groups or atoms with ionic charges have more chances to be hydrated. Other strong H-bonding groups also show some tendency to include water in the crystal. Some other groups such as $-\text{CF}_3$, $-\text{CCl}_3$, $-\text{O}-$, $-\text{CN}$, $-\text{NO}_2$ etc. are less prone to hydration and the terminal bound halogens have the lowest affinity. They have further shown that with increase in the number of $-\text{COO}^-$ groups in a molecule, the hydration possibility increases steeply. For $-\text{OH}$ group the increase in hydration possibility is much less than $-\text{COO}^-$, where as for ether and halogen groups, it is flat or rather decreases. Halogens are weak acceptors and unsuitable for strong H-bonding to disrupt $\text{O}-\text{H}\cdots\text{O}$ H-bonded networks in bulk water. They have hypothesized that when the molecules are locked in fixed positions in the lattice, the strong H-bonding groups cannot satisfy the ideal H-bond geometry and hence uptake small, flexible water molecules to fulfill the requirements. If the donor and acceptor are not balanced then also it may cause hydration in the crystal. The void filling role of water molecules also has been proposed, though it has been seen quite expectedly that very less number (only 4%) of the crystal structures contain water molecules without H-bonding.

Anhydrous phloroglucinol and phloroglucinol dihydrate crystal structures are reported in the CSD. Interestingly substitution on phloroglucinol by halogen groups increases the hydration in $\text{TCPG}\cdot 3\text{H}_2\text{O}$, $\text{TBPG}\cdot 3\text{H}_2\text{O}$ and $\text{DBPG}\cdot 4\text{H}_2\text{O}$ compounds (Chapter 5). Furthermore TBPG easily forms hydrate from chloroform–ethyl acetate solvent mixture, whereas DBPG forms anhydrous crystal structure from chloroform–ethyl acetate solvent mixture and hydration occurs from aqueous methanol. Less halogenated phloroglucinol, such as bromophloroglucinol (BPG) crystallize as anhydrate from ethyl acetate, while TIPG and DIPG also crystallize as anhydrous materials. Thus the observations show that with increase in halogenations the hydration capacity increases of the halogenated phloroglucinol molecules, but with increase in the bulkiness of the halogens hydration affinity decreases. Hydrogen bonds become weaker with increase in the bulkiness of the halogens, evident in $\text{TCPG}\cdot 3\text{H}_2\text{O}$ and $\text{TBPG}\cdot 3\text{H}_2\text{O}$ crystal structures ($\text{O}\cdots\text{O}$ distances and DSC/TGA) and in TIPG, the very large iodo groups mask $-\text{OH}$ groups to prevent significant H-bond formation. Stronger H-bonding in the tetrahydrate structure compared to the anhydrous form explains the water inclusion

despite a lower packing fraction of the hydrate crystal structure. Bulky groups around strong H-bonding functional group -OH , prevent two phenolic -OH groups to come closer to make significant interaction. But the small water molecule, which is capable of forming strong H-bond, can approach phenolic -OH group and stabilizes the system. Interestingly the inter-halogen interactions are type I in the hydrate structure, but they are the polarization induced type II contact in the anhydrous form, indicates the importance of inter-halogen interaction increases with decrease in the influence of strong H-bonds.

Mixed halogenated phloroglucinols (Scheme 3) may be very good candidates to analyze the properties in the series of structures and also capture new water clusters in the organic crystal lattices.



Scheme 3

APPENDIX

Table 1. Crystallographic data for the structures discussed in this thesis.

<i>Chapter 2</i>			
	4-IPOT•MES	4-IPOT•COL	4-IPOT•TBM
Empirical formula	2(C ₂₁ H ₁₂ I ₃ N ₃ O ₃)· C ₉ H ₁₂	2(C ₂₁ H ₁₂ I ₃ N ₃ O ₃)· C ₈ H ₁₁ N	2(C ₂₁ H ₁₂ I ₃ N ₃ O ₃)· C ₉ H ₉ Br ₃
Formula wt.	1590.26	1591.25	1826.96
Crystal system	Hexagonal	Hexagonal	Hexagonal
Space group	$R\bar{3}$	$R\bar{3}$	$R\bar{3}$
T [K]	183(2)	123(2)	145(2)
a [Å]	15.668(3)	15.619(2)	15.7356(8)
b [Å]	15.668(3)	15.619(2)	15.7356(8)
c [Å]	18.475(5)	18.361(4)	18.3863(13)
α [deg]	90.00	90.00	90.00
β [deg]	90.00	90.00	90.00
γ [deg]	120.00	120.00	120.00
Z	3	3	3
Volume [Å ³]	3928.0(14)	3879.2(11)	3942.7(4)
D_{calc} [g/cm ³]	2.017	2.043	2.308
$F(000)$	2250	2250	2556
μ [mm ⁻¹]	3.613	3.659	5.882
θ_{max}	2.60–28.39	1.87–28.46	1.86–28.31
Range h	–20 to 15	–20 to 20	–20 to 20
Range k	–20 to 14	–20 to 20	–20 to 20
Range l	–24 to 18	–24 to 24	–24 to 24
N-total	6004	15471	16813
N-independent	2162	2177	2182
N-observed	1783	1974	2037
R_1 [$I > 2\sigma(I)$]	0.0489	0.0377	0.0482
wR_2	0.1237	0.0945	0.1160
GOF	1.057	1.109	1.080

Table 1. *Continued...*

<i>Chapter 2</i>			
4-IPOT•TIM	4-IPOT•HCB	4-IPOT•HFB	4-IPOT•MNP
2(C ₂₁ H ₁₂ I ₃ N ₃ O ₃)· C ₉ H ₉ I ₃ 1967.93 Hexagonal <i>R</i> $\bar{3}$ 100(2) 15.9236(9) 15.9236(9) 18.425(2) 90.00 90.00 120.00 3 4046.1(6) 2.423 2718 5.227 2.60–28.39 –19 to 20 –21 to 18 –23 to 23 8954 2124 1937 0.0239 0.0629 1.092	2(C ₂₁ H ₁₂ I ₃ N ₃ O ₃)· C ₆ Cl ₆ 1754.83 Hexagonal <i>R</i> $\bar{3}$ 223(2) 15.686(4) 15.686(4) 18.583(7) 90.00 90.00 120.00 3 3960(2) 2.208 2466 3.888 1.86–28.39 –14 to 20 –20 to 20 –20 to 23 5354 2142 1947 0.0307 0.0847 1.064	2(C ₂₁ H ₁₂ I ₃ N ₃ O ₃)· C ₆ F ₆ 1656.13 Hexagonal <i>R</i> $\bar{3}$ 100(2) 15.5466(4) 15.5466(4) 15.5466(4) 90.00 90.00 120.00 3 3799.3(3) 2.172 2322 3.756 1.88–28.16 –20 to 20 –19 to 15 –23 to 22 5718 1997 1954 0.0212 0.0589 1.106	2(C ₂₁ H ₁₂ I ₃ N ₃ O ₃)· C ₁₁ H ₁₀ 1612.26 Hexagonal <i>R</i> $\bar{3}$ 100(2) 15.5830(6) 15.5830(6) 18.3563(14) 90.00 90.00 120.00 3 3860.3(4) 2.081 2280 3.678 1.87–28.26 –19 to 18 –17 to 18 –24 to 24 8891 2073 2000 0.0210 0.0553 1.149

Table 1. Continued...

Chapter 2			
4-IPOT•DCM ^a	4-IPOT•DBM ^a	4-IPOT•DIM	4-BrPOT•HFB
2(C ₂₁ H ₁₂ I ₃ N ₃ O ₃)· CH ₂ Cl ₂	2(C ₂₁ H ₁₂ I ₃ N ₃ O ₃)· 3(CH ₂ Br ₂)	C ₂₁ H ₁₂ I ₃ N ₃ O ₃ · CH ₂ I ₂	2(C ₂₁ H ₁₂ I ₃ N ₃ O ₃)· C ₆ F ₆
1554.57	1751.88	1002.86	1374.13
Hexagonal	Hexagonal	Hexagonal	Hexagonal
$R\bar{3}$	$R\bar{3}$	$R\bar{3}$	$R\bar{3}$
293(2)	203(2)	145(2)	100(2)
15.7177(5)	15.6595(13)	15.6962(10)	15.1070(9)
15.7177(5)	15.6595(13)	15.6962(10)	15.1070(9)
18.9157(9)	18.681(2)	18.9478(18)	18.019(2)
90.00	90.00	90.00	90.00
90.00	90.00	90.00	90.00
120.00	120.00	120.00	120.00
3	3	6	6
4047.0(3)	3967.2(7)	4042.8(5)	3561.4(5)
1.914	2.200	2.472	1.922
2178	2439	2736	1998
3.600	5.840	5.798	5.154
1.84–27.98	2.60–28.32	1.84–27.00	1.92–26.01
–19 to 20	–20 to 18	–20 to 19	–16 to 18
–21 to 18	–20 to 15	–19 to 20	–16 to 11
–23 to 23	–12 to 24	–24 to 24	–22 to 22
9521	5706	12845	5932
2179	2170	1947	1562
1768	1639	1749	1454
0.0527	0.0682	0.0623	0.0246
0.1803	0.2017	0.1505	0.0632
1.109	1.056	1.056	1.035

^a The host:guest (highly disordered) stoichiometry from X-ray and TGA is different.

Table 1. *Continued...*

<i>Chapter 2</i>			
4-EPOT•HCB	4-EPOT•HFB	4-EPOT•HMB	4-EPOT•HMB
2(C ₂₇ H ₁₅ N ₃ O ₃)· C ₆ Cl ₆	2(C ₂₇ H ₁₅ N ₃ O ₃)· C ₆ F ₆	2(C ₂₇ H ₁₅ N ₃ O ₃)· C ₁₂ H ₁₈	2(C ₂₇ H ₁₅ N ₃ O ₃)· C ₁₂ H ₁₈
1143.60	1044.90	1021.10	1021.10
Hexagonal	Hexagonal	Hexagonal	Hexagonal
$R\bar{3}$	$R\bar{3}$	$R\bar{3}$	$R\bar{3}$
100(2)	100(2)	100(2)	200(2)
15.5522(8)	15.4470(7)	15.6256(8)	15.6556(10)
15.5522(8)	15.4470(7)	15.6256(8)	15.6556(10)
17.7308(17)	17.8145(16)	17.7141(18)	17.955(2)
90.00	90.00	90.00	90.00
90.00	90.00	90.00	90.00
120.00	120.00	120.00	120.00
3	3	3	3
3714.0(4)	3681.2(4)	3745.6(5)	3811.2(6)
1.534	1.414	1.358	1.335
1746	1602	1602	1602
0.411	0.108	0.088	0.087
1.90–25.49	1.90–25.50	1.89–25.49	1.88–26.36
–16 to 16	–18 to 18	–13 to 18	–19 to 19
–18 to 18	–15 to 18	–10 to 18	–16 to 19
–21 to 17	–21 to 21	–21 to 21	–20 to 22
4376	5434	4393	4845
1536	1522	1545	1747
1373	1369	1362	1233
0.0808	0.0525	0.0645	0.0788
0.2715	0.1549	0.2105	0.2297
1.096	1.083	1.095	1.086

Table 1. Continued...

Chapter 2			
4-EPOT•HMB	4-EPOT•MES	4-EPOT•COL	4-EPOT•DCM ^b
2(C ₂₇ H ₁₅ N ₃ O ₃)· C ₁₂ H ₁₈ 1021.10 Hexagonal <i>R</i> $\bar{3}$ 298(2) 15.6883(15) 15.6883(15) 18.205(3) 90.00 90.00 120.00 3 3880.4(9) 1.311 1602 0.085 1.87–25.48 –12 to 18 –16 to 18 –22 to 19 4567 1599 1083 0.0852 0.2442 1.113	2(C ₂₇ H ₁₅ N ₃ O ₃)· C ₉ H ₁₂ 979.03 Hexagonal <i>R</i> $\bar{3}$ 100(2) 15.6045(8) 15.6045(8) 17.7783(17) 90.00 90.00 120.00 3 3880.4(9) 1.301 1530 0.085 1.89–25.45 –17 to 13 –14 to 18 –21 to 22 5536 1542 1352 0.0485 0.1357 1.049	2(C ₂₇ H ₁₅ N ₃ O ₃)· C ₈ H ₁₁ N 980.02 Hexagonal <i>R</i> $\bar{3}$ 100(2) 15.5644(8) 15.5644(8) 17.7754(19) 90.00 90.00 120.00 3 3729.2(5) 1.309 1530 0.086 1.90–28.19 –16 to 19 –20 to 18 –23 to 23 7771 1997 1753 0.0951 0.2879 1.065	C ₂₇ H ₁₅ N ₃ O ₃ · CH ₂ Cl ₂ 514.35 Hexagonal <i>R</i> $\bar{3}$ 100(2) 15.5034(11) 15.5034(11) 17.905(3) 90.00 90.00 120.00 6 3727.1(7) 1.375 1584 0.297 1.90–25.50 –15 to 17 –18 to 18 –21 to 21 4164 1545 1155 0.0511 0.1332 1.081

Table 1. *Continued...*

<i>Chapter 2</i>			
4-EPOT•DBM^b	4-EPOT•DIM^b	4-EPOT•BEN	4-EPOT•DEE^b
C ₂₇ H ₁₅ N ₃ O ₃ ·	C ₂₁ H ₁₂ I ₃ N ₃ O ₃ ·	C ₂₁ H ₁₂ I ₃ N ₃ O ₃ ·	C ₂₁ H ₁₂ I ₃ N ₃ O ₃ ·
CH ₂ Br ₂	CH ₂ I ₂	0.5C ₆ H ₆	C ₄ H ₁₀ O
603.27	697.25	468.47	503.54
Hexagonal	Hexagonal	Hexagonal	Hexagonal
$R\bar{3}$	$R\bar{3}$	$R\bar{3}$	$R\bar{3}$
298(2)	100(2)	100(2)	100(2)
15.460(2)	15.507(2)	15.4807(14)	15.4965(14)
15.460(2)	15.507(2)	15.4807(14)	15.4965(14)
18.191(4)	18.506(4)	17.913(4)	17.877(3)
90.00	90.00	90.00	90.00
90.00	90.00	90.00	90.00
120.00	120.00	120.00	120.00
6	6	6	6
3765.6(11)	3853.9(11)	3717.7(9)	3717.9(8)
1.596	1.803	1.255	1.349
1800	2016	1458	1584
3.265	2.483	0.083	0.091
1.89–25.49	1.87–25.49	1.87–25.49	1.90–26.30
–18 to 18	–18 to 18	–19 to 10	–19 to 17
–18 to 18	–18 to 18	–13 to 19	–18 to 17
–21 to 21	–22 to 21	–22 to 22	–22 to 21
6590	6714	5868	4706
1563	1601	1697	1697
1097	1113	1317	1339
0.0661	0.0585	0.0518	0.0553
0.1832	0.1604	0.1420	0.1213
1.037	1.056	1.055	1.064

Table 1. Continued...

Chapter 2	Chapter 3		
4-EPOT•TCM	3-IPOT	2-FPOT	2-CIPOT
$C_{27}H_{15}N_3O_3 \cdot$ CCl_4	$C_{21}H_{12}I_3N_3O_3$	$C_{21}H_{12}F_3N_3O_3$	$C_{21}H_{12}Cl_3N_3O_3$
583.23	735.04	411.34	460.69
Hexagonal	Hexagonal	Triclinic	Triclinic
$P6_3/m$	$R\bar{3}$	$P\bar{1}$	$P\bar{1}$
298(2)	223(2)	298(2)	100(2)
14.2601(3)	23.421(3)	10.2873(14)	10.5719(9)
14.2601(3)	23.421(3)	10.4290(14)	10.8569(10)
7.9185(5)	7.3005(16)	10.8937(15)	20.0712(18)
90.00	90.00	61.934(2)	99.9270(10)
90.00	90.00	70.098(2)	90.8230(10)
120.00	120.00	72.723(2)	115.8400(10)
2	6	2	4
1394.50(10)	3468.2(10)	956.4(2)	2031.9(3)
1.389	2.112	1.428	1.506
592	2052	420	936
0.459	4.082	0.117	0.480
1.65–25.50	2.97–28.27	2.13–26.04	2.07–25.50
–17 to 9	–18 to 30	–12 to 12	–12 to 12
–14 to 17	–21 to 22	–11 to 12	–12 to 13
–9 to 9	–9 to 9	–13 to 13	–24 to 24
7210	4640	6860	15603
940	1894	3602	7512
658	1512	2505	6584
0.0799	0.0576	0.0429	0.0327
0.2479	0.1655	0.1172	0.0864
1.068	1.068	1.021	1.035

Table 1. Continued...

<i>Chapter 3</i>		<i>Chapter 4</i>	
2-BrPOT	2-IPOT	3Cl•methylethyl ketone	3Cl•ethyl acetate^b
C ₂₁ H ₁₂ Br ₃ N ₃ O ₃	C ₂₁ H ₁₂ I ₃ N ₃ O ₃	C ₁₈ H ₉ N ₆ O ₃ Cl ₃ · 0.5(C ₄ H ₈ O)	C ₁₈ H ₉ N ₆ O ₃ Cl ₃ · 0.38(C ₄ H ₈ O ₂)
594.07	735.04	498.71	496.94
Triclinic	Triclinic	Triclinic	Triclinic
<i>P</i> $\bar{1}$	<i>P</i> $\bar{1}$	<i>P</i> $\bar{1}$	<i>P</i> $\bar{1}$
298(2)	100(2)	100(2)	100(2)
12.6081(7)	12.6396(8)	6.2589(5)	6.2474(13)
12.9537(7)	13.1959(9)	10.1316(8)	10.134(2)
15.6797(9)	15.7765(10)	16.8663(13)	16.828(4)
72.3010(10)	71.4550(10)	86.0240(10)	93.843(3)
69.5760(10)	68.9180(10)	87.5270(10)	92.715(3)
67.1300(10)	66.9950(10)	88.2010(10)	90.321(3)
4	4	2	2
2168.7(2)	2211.2(2)	1065.54(15)	1061.8(4)
1.819	2.208	1.554	1.554
1152	1368	506	468
5.608	4.268	0.470	0.464
1.41–25.50	1.71–25.50	1.21–26.02	1.21–26.00
–15 to 15	–15 to 15	–7 to 7	–7 to 7
–15 to 14	–15 to 15	–12 to 12	–7 to 12
–18 to 18	–19 to 19	–20 to 20	–20 to 20
16946	25999	7788	8293
8064	8229	4190	4161
4797	7810	3259	2950
0.0489	0.0217	0.0455	0.0569
0.1327	0.0525	0.1168	0.1411
1.042	1.089	1.022	1.045

Table 1. Continued...

Chapter 4			
3Cl•acetone ^b	3Cl•nitromethane ^b	3Cl•acetylacetone ^b	3Cl (guest free)
C ₁₈ H ₉ N ₆ O ₃ Cl ₃ · 0.53(C ₃ H ₆ O)	C ₁₈ H ₉ N ₆ O ₃ Cl ₃ · 0.55(CH ₃ NO ₂)	C ₁₈ H ₉ N ₆ O ₃ Cl ₃ · 0.25(C ₅ H ₈ O ₂)	C ₁₈ H ₉ N ₆ O ₃ Cl ₃
494.45	497.05	488.70	463.66
Triclinic	Triclinic	Triclinic	Hexagonal
<i>P</i> $\bar{1}$	<i>P</i> $\bar{1}$	<i>P</i> $\bar{1}$	<i>P</i> 6 ₃
100(2)	298(2)	100(2)	298(2)
6.2482(7)	6.3045(7)	6.2453(6)	17.2490(9)
10.1684(12)	10.1891(11)	10.1233(10)	17.2490(9)
16.8235(19)	17.0142(19)	16.8774(17)	12.0227(12)
86.796(2)	93.247(2)	93.037(2)	90.00
87.072(2)	92.607(2)	92.521(2)	90.00
89.309(2)	90.350(2)	90.826(2)	120.00
2	2	2	6
1065.8(2)	1090.0(2)	1064.36(18)	3097.9(4)
1.541	1.514	1.525	1.491
468	468	468	1404
0.462	0.452	0.463	0.477
1.21–26.38	1.20–26.08	2.01–26.40	1.36–25.48
–7 to 7	–7 to 5	–7 to 7	–20 to 20
–12 to 12	–12 to 12	–12 to 12	–20 to 20
–19 to 20	–20 to 20	–20 to 21	–14 to 14
13401	7576	7939	29302
4339	4293	4314	3657
3578	2051	3489	2767
0.0420	0.0586	0.0429	0.0663
0.1023	0.1229	0.1027	0.1910
1.045	0.882	1.059	1.036

Table 1. *Continued...*

<i>Chapter 4</i>			
3Br•mesitylene	3Br•diiodomethane^b	3Br•diiodomethane^b	3I•collidine
C ₁₈ H ₉ Br ₃ N ₆ O ₃ ·	C ₁₈ H ₉ Br ₃ N ₆ O ₃ ·	C ₁₈ H ₉ Br ₃ N ₆ O ₃ ·	2(C ₁₈ H ₉ I ₃ N ₆ O)·
0.5(C ₉ H ₁₂)	CH ₂ I ₂	CH ₂ I ₂	C ₈ H ₁₁ N
657.14	864.87	864.87	1597.20
Hexagonal	Hexagonal	Triclinic	Hexagonal
$R\bar{3}$	$R\bar{3}$	$P\bar{1}$	$R\bar{3}$
298(2)	298(2)	100(2)	123(2)
16.730(2)	16.660(2)	11.060(2)	16.655(2)
16.730(2)	16.660(2)	14.514(3)	16.655(2)
16.631(3)	16.897(3)	16.482(3)	16.601(3)
90.00	90.00	89.38(3)	90.00
90.00	90.00	89.39(3)	90.00
120.00	120.00	80.32(3)	120.00
6	6	4	3
4031.5(11)	4061.6(12)	2607.9(9)	3987.9(11)
1.624	2.122	2.203	1.995
1926	2412	1608	2250
4.537	6.781	7.040	3.562
1.86–26.03	1.86–26.02	1.24–26.11	1.87–28.47
–20 to 19	–19 to 20	–13 to 13	–22 to 22
–20 to 20	–20 to 20	–17 to 17	–18 to 20
–20 to 18	–20 to 20	–20 to 20	–22 to 22
7479	7546	27104	14163
1777	1787	10244	2238
1021	1078	6653	1554
0.0532	0.0507	0.0671	0.0504
0.1745	0.1570	0.1826	0.1465
1.033	1.080	0.974	1.061

^b Structures refined after removing electron densities due to highly disordered guest molecules using SQUEEZE programme.

Table 1. Continued...

Chapter 4	Chapter 5		
3I•mesitylene	TCPG•3(H ₂ O)	TBPG•3(H ₂ O)	DBPG•4(H ₂ O)
2(C ₁₈ H ₉ I ₃ N ₆ O ₃)· C ₉ H ₁₂	C ₆ H ₃ Cl ₃ O ₃ · 3(H ₂ O)	C ₆ H ₃ Br ₃ O ₃ · 3(H ₂ O)	C ₆ H ₄ Br ₂ O ₃ · 4(H ₂ O)
1596.21	283.48	416.86	355.98
Hexagonal	Monoclinic	Monoclinic	Monoclinic
<i>R</i> 3̄	<i>P</i> 2 ₁ / <i>n</i>	<i>P</i> 2 ₁ / <i>c</i>	<i>C</i> 2/ <i>c</i>
183(2)	100(2)	100(2)	100(2)
16.750(2)	6.9261(10)	7.1076(5)	16.0309(12)
16.750(2)	16.057(2)	9.1708(7)	10.6848(8)
16.800(3)	9.9510(15)	16.7599(12)	7.3246(5)
90.00	90.00	90.00	90.00
90.00	109.923(2)	93.9930(10)	111.4500(10)
120.00	90.00	90.00	90.00
3	4	4	4
4082.1(12)	1040.4(3)	1089.80(14)	1167.71(15)
1.948	1.810	2.541	2.025
2250	576	792	696
3.480	0.886	11.110	6.955
1.85–28.44	2.52–25.50	2.44–26.37	2.34–26.01
–22 to 22	–8 to 8	–8 to 8	–19 to 19
–22 to 22	–19 to 17	–10 to 11	–8 to 13
–22 to 22	–12 to 12	–20 to 20	–9 to 8
16471	8941	8509	3137
2278	1926	2218	1151
1341	1769	2083	1071
0.0574	0.0289	0.0193	0.0198
0.1433	0.0725	0.0490	0.0502
1.023	1.048	1.127	1.081

Table 1. *Continued...*

<i>Chapter 5</i>			
DBPG•4(H₂O)	DBPG	TIPG	DIPG
C ₆ H ₄ Br ₂ O ₃ · 4(H ₂ O)	C ₆ H ₄ Br ₂ O ₃	C ₆ H ₃ I ₃ O ₃	C ₆ H ₄ I ₂ O ₃
355.98	283.91	503.78	377.89
Monoclinic	Orthorhombic	Orthorhombic	Triclinic
<i>C2/c</i>	<i>Pbcn</i>	<i>P2₁2₁2₁</i>	<i>P1̄</i>
298(2)	298(2)	130(2)	100(2)
16.135(4)	5.4011(5)	4.6341(2)	8.6725(7)
10.740(2)	12.8974(13)	13.5632(4)	9.1836(7)
7.4390(17)	10.9478(11)	15.3796(4)	11.8436(10)
90.00	90.00	90.00	106.0050(10)
111.354(3)	90.00	90.00	111.1790(10)
90.00	90.00	90.00	97.1080(10)
4	4	4	4
1200.5(5)	762.63(13)	966.66(6)	818.80(11)
1.970	2.473	3.462	3.065
696	536	888	680
6.765	10.579	9.666	7.635
2.33–25.50	3.16–25.89	3.05– 25.48	1.97– 26.05
–19 to 19	–6 to 6	–3 to 5	–10 to 10
–12 to 12	–12 to 15	–16 to 16	–10 to 11
–9 to 9	–9 to 13	–18 to 18	–13 to 14
5188	3093	10669	8795
1117	741	1805	3229
992	664	1804	3046
0.0253	0.0298	0.0171	0.0264
0.0667	0.0794	0.0431	0.0650
1.101	1.114	1.220	1.062

Table 1. Continued...

Chapter 5	Chapter 6		
BPG	1Cl	1Br	1I
C ₆ H ₅ BrO ₃	C ₅ H ₄ ClNO	C ₅ H ₄ BrNO	C ₅ H ₄ INO
205.01	129.54	174.00	220.99
Monoclinic	Orthorhombic	Orthorhombic	Orthorhombic
<i>P</i> 2 ₁	<i>Fdd</i> 2	<i>Pna</i> 2 ₁	<i>Pna</i> 2 ₁
298(2)	298(2)	100(2)	100(2)
5.700(2)	23.069(4)	11.5563(12)	11.5329(11)
4.8582(19)	25.231(4)	12.7285(13)	12.8331(12)
11.972(5)	3.8429(6)	3.8875(4)	4.2475(4)
90.00	90.00	90.00	90.00
101.434(6)	90.00	90.00	90.00
90.00	90.00	90.00	90.00
2	16	4	4
325.0(2)	2236.8(6)	571.83(10)	628.64(10)
2.095	1.539	2.021	2.335
200	1056	336	335
6.259	0.565	7.074	4.990
1.74–26.00	2.39–26.29	2.38–26.01	2.37–26.38
–7 to 7	–17 to 28	–9 to 14	–14 to 12
–5 to 5	–17 to 30	–15 to 14	–14 to 16
–14 to 14	–4 to 4	–3 to 4	–5 to 3
3308	2039	1950	2213
1258	1103	833	927
1130	1049	797	920
0.0435	0.0295	0.0198	0.0172
0.0943	0.0764	0.0507	0.0457
1.057	1.096	1.041	1.231

Table 1. *Continued...*

<i>Chapter 6</i>			
1Me	2H	2Cl	2Br
C ₆ H ₇ NO	C ₅ H ₅ NO ₂	C ₅ H ₄ ClNO ₂	C ₅ H ₄ BrNO ₂
109.13	111.10	145.54	190.00
Monoclinic	Triclinic	Orthorhombic	Orthorhombic
<i>C2/c</i>	<i>P</i> $\bar{1}$	<i>Pna2</i> ₁	<i>P2</i> ₁ <i>2</i> ₁ <i>2</i> ₁
100(2)	298(2)	100	298(2)
11.053(2)	6.3536(8)	11.2712(14)	3.8571(5)
9.6151(19)	6.5014(8)	12.7754(16)	12.3235(15)
11.316(2)	6.9499(8)	3.7794(5)	12.5884(15)
90.00	113.794(2)	90.00	90.00
100.64(3)	99.650(2)	90.00	90.00
90.00	106.930(2)	90.00	90.00
8	2	4	4
1181.9(4)	237.59(5)	544.21(12)	598.36(13)
1.227	1.553	1.776	2.109
464	116	296	368
0.085	0.122	0.605	6.782
2.83–26.12	3.39–26.02	2.41–25.99	2.31–26.00
–13 to 13	–7 to 7	–6 to 13	–4 to 4
0 to 11	–7 to 8	–13 to 15	–15 to 13
0 to 13	–8 to 5	–4 to 4	–14 to 15
1165	1737	2329	2146
1165	941	1012	1168
770	889	940	1100
0.1495	0.0398	0.0266	0.0252
0.3050	0.1055	0.0617	0.0589
1.323	1.115	1.058	1.041

Table 1. Continued...

Chapter 6			Chapter 7
2Me	3Cl	3Br	1
C ₆ H ₇ NO ₂	C ₅ H ₅ ClN ₂	C ₅ H ₅ BrN ₂	C ₇ H ₅ NO ₄ ·C ₅ H ₄ IN
125.13	128.56	173.02	372.11
Monoclinic	Monoclinic	Monoclinic	Triclinic
<i>P</i> 2 ₁ / <i>c</i>	<i>P</i> 2 ₁ / <i>n</i>	<i>P</i> 2 ₁	<i>P</i> 1̄
298(2)	298(2)	100(2)	130(2)
4.6258(9)	6.446(5)	7.9689(5)	6.6732(13)
10.3353(19)	8.022(6)	13.1908(8)	7.5224(15)
12.677(2)	11.991(8)	11.6096(7)	12.876(3)
90.00	90.00	90.00	93.51(3)
99.270(3)	104.510(11)	104.6860(10)	102.41(3)
90.00	90.00	90.00	91.90(3)
4	4	8	2
598.18(19)	600.3(7)	1180.49(13)	629.4(2)
1.389	1.423	1.947	1.964
264	264	672	360
0.106	0.518	6.845	2.556
2.56–26.04	3.09–26.19	1.81–26.37	3.07–25.00
–5 to 5	–7 to 7	–7 to 9	–7 to 7
–12 to 5	–9 to 9	–16 to 14	–8 to 6
–15 to 15	–14 to 14	–14 to 14	–15 to 15
3183	4239	6730	5906
1179	1186	4274	2181
768	922	4146	2123
0.0487	0.0429	0.0243	0.0247
0.1346	0.1222	0.0588	0.0618
1.036	1.045	1.036	1.062

Table 1. *Continued...*

<i>Chapter 7</i>	
2	3
C ₇ H ₄ N ₂ O ₆ ·	C ₇ H ₆ N ₂ O ₃ ·
C ₅ H ₄ IN	C ₇ H ₆ INO
417.11	413.17
Monoclinic	Triclinic
<i>P</i> 2 ₁ / <i>c</i>	<i>P</i> 1̄
130(2)	100(2)
9.1696(18)	5.0300(5)
11.260(2)	7.3023(7)
13.760(3)	10.7542(10)
90.00	103.577(2)
92.16(3)	94.9900(10)
90.00	103.585(2)
4	1
1419.8(5)	368.98(6)
1.951	1.859
808	202
2.290	2.192
2.87–25.50	1.97–26.36
–10 to 11	–6 to 6
–11 to 13	–9 to 8
–16 to 16	–13 to 13
15151	2766
2638	1509
2517	1495
0.0229	0.0740
0.0906	0.1802
1.380	1.428

ABOUT THE AUTHOR

Binoy Krishna Saha, son of Baidyanath Saha and Bela Saha, was born on 08 January 1978 in Raniganj, a town in Burdwan District of West Bengal, India. He received his elementary and secondary school education in Egara and Raniganj. After the completion of B. Sc. degree from Triveni Devi Bhalotia College, Raniganj, he joined the Department of Chemistry, University of Burdwan for M. Sc. in 1998. He joined the School of Chemistry, University of Hyderabad for Ph. D. in 2001. He was awarded research fellowship by the Council of Scientific and Industrial Research (JRF and SRF) for 2001-2006. He also qualified GATE exam with rank 20.

List of publications

1. Hexagonal host framework of *sym*-aryloxytriazines stabilised by weak intermolecular interactions.
B. K. Saha, S. Aitipamula, R. Banerjee, A. Nangia, R. K. R. Jetti, R. Boese, C-. K. Lam and T. C. W. Mak
Mol. Cryst. Liq. Cryst., **2005**, *440*, 295-316.
2. Halogen trimer-mediated hexagonal host framework of 2,4,6-tris(4-halophenoxy)-1,3,5-triazine. Supramolecular isomerism from hexagonal channel (X = Cl, Br) to cage structure (X = I).
B. K. Saha, R. K. R. Jetti, L. S. Reddy, S. Aitipamula and A. Nangia
Cryst. Growth Des., **2005**, *5*, 887-899.
3. Crystal engineering with hydrogen bonds and halogen bonds.
B. K. Saha, A. Nangia and M. Jaskólski
CrysstEngComm, **2005**, *7*, 355-358.
4. Helical water chains in aquapores of organic hexahost:remarkable halogen-substitution effect on the handedness of water helix.
B. K. Saha and A. Nangia
Chem. Commun., **2005**, 3024-3026.
5. First example of an ice-like water hexamer boat tape structure in a supramolecular organic host.
B. K. Saha and A. Nangia
Chem. Commun., **2006**, 1825-1827.
6. Using halogen...halogen interactions to direct non-centrosymmetric crystal packing in dipolar organic molecules.
B. K. Saha, A. Nangia and J.-F. Nicoud
Cryst. Growth Des., **2006** (In press).
7. A self-assembled organic tubular structure for van der Waals guest inclusion.
B. K. Saha and A. Nangia
(Communicated)
8. Ethynyl trimer-mediated hexagonal host framework of 2,4,6-tris(4-ethynylphenoxy)-1,3,5-triazine with strong van der Waals enclathration of organic guests.
B. K. Saha and A. Nangia
(Manuscript under preparation)
10. 2,4,6-Tris(halophenoxy)-1,3,5-triazine and isostructurality on halogen exchange.
B. K. Saha and A. Nangia
(Manuscript under preparation)